Distribution of arsenic in surficial deposits in the Cold Lake area of Alberta, Canada

by

Muhammad Babar Javed

A thesis submitted in partial fulfillment of the requirements for the degree of

Doctor of Philosophy

in

Soil Science

Department of Renewable Resources
University of Alberta

Abstract

Arsenic (As) concentration above the Health Canada and WHO drinking water guidelines of 10 μg L^{-1} in the Cold Lake area, Alberta is an issue of concern for environmental and human health. The source of groundwater As is ambiguous. This study was initiated to characterize the surficial deposits (sediments) drilled up to ~300 m depth from five different locations in the area to determine distribution and fractionation of As in sediments so that the potential source(s) of groundwater As could be inferred.

Total As concentration in sediments (n = 135) ranged from 0.8 to ~35 μg g^{-1}, but no significant correlation was found between As and sediments depth, lithology or geological formation. Maximum average As (~32 μg g^{-1}; n = 2) was found in sediments derived from shale. In addition, 20-25 μg g^{-1} As was also found in glacial till of Bonnyville, Grand Centre and Empress formations at some depths, might be due to mixing of underlying shale during glaciation.

To study the association of As with different inorganic and organic phases in sediments, a modified sequential extraction method was developed and employed on selected sediments (n = 22). Around 6-46 % of the total As was exchangeable and specifically adsorbed in all the sediments. Sediments having 7-35 μg g^{-1} As also contained significant sulfide bound As (11-34 % of total As). XRD and SEM-EDX analyses confirmed the presence of pyrite (FeS_2), and μ-XRD analysis signaled the presence of arsenopyrite (FeAsS) in high As sediments

(~20 $\mu g\ g^{-1}$ As). XANES spectroscopy showed dominance of arsenite (As^{III}; ~60-90 % of total As) in all the sediments.

In addition, effect of heat on As release from sediments was also studied to simulate the condition in the sediments near the steam injection wells that are installed for bitumen extraction. Effect of thermal treatment (~200^{o} C heat) on As release from sediments exhibited significant increase in the dissolved As concentrations (from 120 $\mu g\ L^{-1}$ to ~1400 $\mu g\ L^{-1}$) in the synthetic aquifer water. These findings may help understand the effect of in-situ oil extraction technique such as cyclic steam stimulation (CSS) on As and other metal mobilization in aquifers/groundwater.

A detailed speciation method for As^{III}, As^{V} and DMAA was also optimized, so that if a fresh core would acquire from the area As speciation could reliably be studied to infer the mobility and toxicity of As.

Preface

This thesis is an original work conducted by Muhammad Babar Javed. All the experimental work, chemical and mineralogical analysis described in the thesis performed by myself. The statistical analysis and the conclusions are also my own work.

A version of the chapter 2 in the thesis combined with arsenic data presented in chapter 4 has been published as Javed M. B., Kachanoski G., and Siddique T., "Arsenic fractionation and mineralogical characterization in sediments in the Cold Lake Region of Alberta , Canada," *Sci Total Environ*, 2014; 500-501:181–190. I was responsible for all the experimental work, data analysis and manuscript composition.

A version of chapter 3 in the thesis has also been published as Javed, M. B., Kachanoski, G., and Siddique, T., "A modified sequential extraction method for arsenic fractionation in sediments," *Anal Chim Acta*, 2013, 787, 102–110. All the experimental work, data analysis and manuscript preparation was done by me.

Versions of chapter 5 and 6 are in preparation to publish in peer reviewed journals.

Muhammad Babar Javed

ACKNOWLEDGEMENTS

I would like to express my sincere gratitude to Dr. Tariq Siddique, my supervisor, for guiding me through my PhD project. His enthusiasm in research has motivated me to complete my graduate study. I believe he has conveyed the spirit of scientific research with his timely advice about research, work ethics and life in general. I greatly appreciate his comments and suggestion for thesis drafts. I also want to thank, Dr. Gary Kachanoski and Dr. Bill Shotyk, who helped in providing me valuable comments and suggestions about my thesis research. I am also thankful to Laurence Andriashek (Alberta Geological Survey, Alberta Energy Regulator) for providing geological core sediments and technical assistance for result interpretation.

I would like to acknowledge and say thanks to Dr. Alsu Kuznetsova, Dr. Petr Kuznetsov and all the fellows of Soil Chemistry and Environmental Microbiology Research Laboratory who have been helpful for the completion of this project. The help extended by supporting staff of the Department of Renewable Resources is also gratefully acknowledged.

I would like to acknowledge the financial support from Higher Education Commission (HEC), The Islamia University Bahawalpur, Pakistan, Natural Sciences and Engineering Research Council of Canada (NSERC), Canadian Water Network (CWN) and the School of Energy and the Environment (SEE).

Finally, I am very grateful to my parents, brothers, sister, wife and daughter for their love, sacrifice, encouragement and patience during my studies.

Table of Contents

Chapter 1. Introduction

Chapter 3. Development of a sequential extraction method for arsenic fractionation in sediments

Chapter 4. Fractionation of arsenic and other trace elements in sediments

List of Tables

List of Figures

Chapter 1. Introduction

1.1 Arsenic contamination

Arsenic (As) is one of the ubiquitous trace elements present in the environment that has received global attention in recent years for its groundwater contamination and subsequent serious health effects. It is estimated that 40 to 100 million people in the world have been at risk of consuming As contaminated water (Páez-Espino et al., 2009; De Mora et al., 2011). Arsenic in drinking water seriously affects human health and is considered to be one of the main environmental causes of cancer mortality in the world (Rosen, 1971; Páez-Espino et al., 2009). The biggest poisoning outbreak of the 20th century is also attributed to As groundwater contamination in Bangladesh, where 30 to 77 million people are at risk due to excessive As in drinking water (Smith et al., 2000; Smedley and Kinniburgh, 2002). Arsenic can be found in both inorganic and organic forms in natural water, soil and sediments (Smedley and Kinniburgh, 2002). Inorganic As forms are more toxic, more mobile and are generally present in two oxidation states: arsenate ($H_nAsO_4^{n-3}$; n = 1, 2, 3) and arsenite ($H_nAsO_3^{n-3}$; n = 1, 2, 3) (Wang and Mulligan, 2006). The prevalence of a particular oxidation state of inorganic As is a function of pH and redox potential (Eh), both of which predict its mobility and toxicity in the environment (Sadiq, 1997; Katsoyiannis and Zouboulis, 2002; Smedley and Kinniburgh, 2002).

It is agreed that As in groundwater usually originates geogenically from sediments (Nickson et al., 2000). Arsenic is naturally enriched in shale containing pyrite (FeS_2, which is considered the principle carrier of As in rocks) and other minerals such as arsenopyrite (FeAsS), enargite (Cu_3AsS_4), scorodite ($FeAsO_4.2H_2O$) and annabergite $[(Ni)_3(AsO_4)_2]$ (Boyle and Jonasson, 1973). Weathering and biological transformation of these As containing minerals in sediments under natural conditions mobilize As in the environment (Smedley and Kinniburgh, 2002; Muloin and Dudas, 2005).

Distribution and chemical association of As with various inorganic and organic phases in sediments, rather than its total concentration, affect As mobility in sediment and its transport to water bodies. Sorption of As on solid constituents is one of the most important processes that immobilizes As (Sadiq, 1997). Arsenic can adsorb on the surfaces of a variety of materials, especially oxides of iron (Fe), Aluminum (Al) and manganese (Mn) (Smith et al., 1998). Co-precipitation of As with Fe oxyhydroxides has also been defined as the major mechanism that strongly retains As in sediments (Larios et al., 2012), but As-bearing Fe oxyhydroxides may act as a source of As during reductive dissolution of both amorphous and crystalline oxyhydroxides (Sadiq, 1997). Arsenic associated with hydrous Mn oxides (easily reducible oxides) is relatively more labile than Fe oxyhydroxides (Tessier et al., 1979). Carbonate minerals and organic matter in sediment can also act as sources of As contamination in aquatic ecosystems through the processes of acidification (low pH) and oxidation, respectively (Huang and Kretzschmar, 2010). Other more stable forms of As are naturally occurring As-bearing sulfide and silicate minerals; and weathering of these sulfides and silicate minerals can release As into the environment and/or may cause formation of other thermodynamically metastable new secondary minerals such as $FeAsO_4.2H_2O$ (Sadiq 1997; Larios et al., 2012).

Arsenic mobility in the sediment pore water and its transport to the water bodies is principally controlled by adsorption-desorption and solid phase precipitation-dissolution reactions. Important geochemical factors affecting these reactions in sediment are pore water chemistry, pH, redox conditions, soil solid composition and As-bearing minerals (Sadiq, 1997). To predict the fate of As in soil or sediment and its transport to ground or surface water, it is important to understand the nature of As association with different phases in sediments.

1.2 Research background and rationale

In northern Alberta, Canada relatively higher concentrations of As have been found in soil and groundwater. Dudas (1987) characterized Boundary and Josephine acid sulfate soils in northwestern Alberta and reported about 10 times higher As concentrations in these soils compared to the background As concentrations (~5 $\mu g\ g^{-1}$) found in Alberta soils (Dudas and Pawluk, 1980). These acid sulfate soils are derived from weathered shale rich in pyrite (FeS_2) (Dudas, 1987). Pyrite was believed to be the source of the elevated levels of As in the acid sulfate soils while secondary iron oxides in the soils formed from the weathering of pyrite were reported as the scavengers of As (Dudas, 1987). Brost (2002) also reported that most of the acid sulfate soils in northwestern Alberta contained naturally high level of As which was suspected to move to the groundwater.

High As concentration (>10 $\mu g\ L^{-1}$) in groundwater of Alberta is of great concern from environmental and human health perspectives. In 2000, Alberta Health and Wellness conducted a survey to assess the occurrence of As in groundwater from domestic wells in three Regional Health Authority (RHA): Lakeland, Aspen, and Keeweetinok in northern Alberta. According to the survey, annual average As concentrations exceeded 25 $\mu g\ L^{-1}$ (Canadian Drinking Water Guideline for As in 2000) in 22% water samples from Lakeland RHA, 4% from Aspen RHA and 20% from Keeweetinok RHA (Health Surveillance, 2000). Since the revision of water quality guidelines in 2006, about 50% domestic well water in the Lakeland RHA fell in the category that had As levels exceeding 10 $\mu g\ L^{-1}$ (current maximum acceptable concentration in drinking water; Health Canada, 2006). The higher concentrations of As in groundwater were correlated with bedrock geological formations containing marine shale (Health Surveillance, 2000). The Cold Lake area that is situated within the Lakeland RHA also contained elevated levels of dissolved As in well water (Stein et al., 2000), which is used extensively for household, agriculture and industrial purposes (Lemay et al., 2005). To understand the As groundwater issue in the Cold Lake area, Alberta Environment conducted a study to understand the hydrogeology of the area and the chemical characteristics of groundwater in order to elucidate conditions that may account for the higher levels of As (Stein et al., 2000). They reported that high As (>10 $\mu g\ L^{-1}$) in the shallow wells was of localized origin and related to low redox conditions but the cause of the low redox conditions was not identified. Another study was conducted by Alberta Geological Survey (AGS) to obtain the background geological information necessary to explain the elevated As levels in groundwater sourced from glacial aquifers in the Cold Lake area. They reported that As was present in both glacial and bedrock sediments (Andriashek, 2000). However, they did not correlate the chemical composition of sediments and the composition of groundwater in the area. In 2011, Alberta Innovates conducted a mineralogical study to determine the source of uranium (U) and As in shallow groundwater near Bonnyville, Alberta. They reported the presence of small framboidal pyrite containing ~1550 $\mu g\ g^{-1}$ As in un-weathered clay-till sediments (Moncur, 2011). Significant oxidation features such as brownish color due to presence of Fe oxyhydroxide in the unoxidized clay-till units were also observed where pyrite minerals were not found. However, the oxidized clay-till sediments contained spheroidal iron (Fe) oxyhydroxide that contained minor sulfur (S) and variable As, suggesting that these Fe oxyhydroxide represented former framboidal pyrite that could easily be oxidized (Moncur, 2011).

In addition to natural sources of groundwater contamination, anthropogenic activities may also enhance trace metal contamination in groundwater. Alberta has one of the richest oil (bitumen) deposits in the world, which lie beneath 140,200 km^2 of land in the Athabasca, Cold Lake and Peace River areas in northern Alberta (Mech, 2011). The major oil sands deposits (80 to 85 %) are located at greater depth (~400 m deep), requiring the use of *in situ* techniques to enhance the bitumen recovery process (Fennell, 2008). Because the bitumen is very viscous at normal temperature, heat is required to decrease the viscosity so that it can be collected and piped to the surface. Cyclic steam stimulation (CSS) bitumen extraction process is commonly used technique in the Cold Lake area, which is the largest *in situ* thermal oil operation in the world (Imperial Oil, 2014). The propagation of heat by injection wells can affect the geochemical behaviour of sediments (Fennell, 2008), which may subsequently increase As release from the solid surfaces by desorption or by the breakdown of As containing minerals in sediments. Fennel (2008) conducted a field study in the Cold Lake area to determine the effect of localized heating on solution chemistry of a fresh water aquifer. He also conducted a laboratory experiment to assess As release at high temperature (50 to 200 ^{o}C) from sediments collected form the aquifer. It was found that even low temperature (50 ^{o}C) initiated the release of As from sediments.

Previous research conducted in the Cold Lake area has described the detailed geological framework of the bedrock topography and glacial stratigraphy of the region to understand the hydrogeology of the area in order to elucidate conditions that may account for the higher groundwater As. Though the detailed geological characterization of the surficial deposits in the area has been completed, still research needs to be done on detailed investigation of the natural distribution of As in sediments with respect to different geochemical factors to find out the potential source of high As in groundwater. Important factors that can affect the distribution of As in sediments and its release into the groundwater are: geological formation, lithology (physical characteristics of the rock), redox condition, mineralogy, and As fractionation in the sediments. In addition to the natural distribution of As, investigation of the effect of elevated temperature (~200^o C) on As release from different sediment constituents is also inevitable to predict the impact of anthropogenic activity on As groundwater contamination. The study of distribution of other elements such as chalcophile, siderophile and lithophile in sediments of the Cold Lake area is also important to determine potential groundwater contamination and to help understand the potential source of As in sediments.

1.3 Research objectives

The overall objective of this research was to characterize surficial deposits to understand the potential source of As in the Cold Lake area. Therefore, this thesis addressed the following three specific objectives to: 1) determine the natural distribution of As in different geological formations in the area; 2) determine As fractionation and mineralogy of the sediments in different geological formations; 3) determine the effect of elevated temperature (~200^o C) on As release from different host phase in sediments.

1.4 Characteristics of the experimental sediments

The sediments (surficial deposits) used in this study were collected from the cores drilled at five different locations up to ~300 m depth in the Cold Lake area, which comprise the southeast part of the Athabasca Oil Sands. The sediment cores [four cores drilled in 1999-2000 namely WR99-1 (Dominion Land Survey (DLS) location: 07-36-77-15-W4), WEPA99-1 (03-08-77-14-W4), WEPA99-2 (13-12-74-17-W4), and WEPA00-1 (06-33-74-09-W4), and one core drilled in 2009 namely 14-01w (14-01-67-03-W4)] used for sample collection were selected based on stratigraphic units and their proximity to buried channel aquifers. The geological stratification in the area consists of eight glacial and non-glacial formations (Shale, Empress, Bronson, Bonnyville, Ethel Lake, Marie Creek, Grand Centre and Holocene; from oldest to youngest) that are located at different depths at different locations. A geological cross section of the area representing 3 cores (WEPA99-1, WEPA99-2 and WR99-1) is shown in Figure 1-1. The detail of the stratigraphy within the core is provided in section 2.2.2. Because of different geological formations and lithological heterogeneity in sediment cores, great variation in the sediment texture and redox zone was found among the sediment samples within each core. Each core did not have strata from all the geological formations; therefore, the number of samples taken from each geological formation varied.

Sediment samples were taken along the whole core depth to represent each stratum (based on visual observation) in the cores. Sediments were also collected from the zones of surficial (<75 m deep) and buried (75-150 m deep) channel aquifers to correlate sediment As concentrations with groundwater As. In addition, sub-samples were also collected from the depths that represented oxidized (brownish sediment due to Fe oxyhydroxide) and reduced [grayish zones due to high iron sulfide (FeS)] in the sediments (Figure 1-2).

1.5 Outline of the thesis

The seven chapters that make up this thesis include the pertinent background summarized in this introduction (chapter 1) followed by five chapters presented as a series of manuscripts addressing the specific objectives (chapter 2, 4 and 5) and the development of methods for metal fractionation and speciation (chapter 3 and 6), and a final concluding chapter (chapter 7). The second chapter is a study that reveals the overall distribution of total As and other elements (chalcophile, siderophile and lithophile) in surficial deposits. The third chapter is on the development of a sequential extraction method for complete metal fractionation of As and other metals (>90% of total metals) in surficial deposits. Chapter four is comprised of As fractionation and mineralogical investigation of As in sediments. Chapter five describes the effect of thermal treatment (~200^{o} C) on As fractionation and its release from sediments. Chapter six is a method development study for the speciation of arsenite (As^{III}), arsenate (As^{V}) and dimethylarsenic acid (DMAA) in river water and sediments. Though our core sediments were not analyzed for redox speciation because they were old and were not preserved for speciation analysis, it was inevitable to develop a simple and robust speciation method for As that could reliably be employed for the future research if newly drilled core are acquired from the area. Finally, the concluding chapter (chapter 7) contains an overall synthesis of the results and the research limitations.

Literature cited

Andriashek L. D. Geochemistry of selected glacial and bedrock geologic units, Cold Lake Area, Alberta. 2000. http://ags.gov.ab.ca/publications/ESR/PDF/ESR_2000_10.pdf

Andriashek L. D. Quaternary geological setting of the Athabasca Oil Sands (in situ) area, Northeast Alberta. 2003. http://www.ags.gov.ab.ca/publications/ESR/PDF/ESR_2002_03.pdf

Brost P. Redistribution of arsenic and iron in an acid sulphate soil, Alberta, Canada. MSc Thesis. University of Alberta. 2002.

De Mora K., Joshi N., Balint B. L., Ward F. B., Elfick A., French C. E. A pH-based biosensor for detection of arsenic in drinking water. Anal Bioanal Chem 2011;400:1031–1039.

Dudas M. Accumulation of native arsenic in acid sulphate soils in Alberta. Can J soil Sci. 1987;67:317–31.

Dudas M., Pawluk S. Natural abundances and mineralogical partitioning of trace elements in selected Alberta soils. Can J Soil Sci. 1980;60:763–71.

Fennell J. W. Effects of aquifer heating on groundwater chemistry with a review of arsenic and its mobility. 2008.

Health Canada (2006), Guidelines for Canadian drinking water quality: Guideline technical document-Arsenic. Water Quality and Health Bureau, Healthy Environments and Consumer Safety Branch, Health Canada, Ottawa, Ontario.

Health Surveillance, Alberta Health and Wellness. Arsenic in groundwaer from domestic wells in three areas of northern Alberta. 2000.

Huang J-H., Kretzschmar R. Sequential extraction method for speciation of arsenate and arsenite in mineral soils. Anal Chem 2010;82(13):5534–5540.

Imperial Oil, Cold Lake Operations. http://www.imperialoil.ca/Canada-English/operations_sands_cold.aspx (Accessed December 9, 2014).

Katsoyiannis I. A., Zouboulis A. I. Removal of arsenic from contaminated water sources by sorption onto iron-oxide-coated polymeric materials. Water Res. 2002; 36(20):5141–55.

Lemay T., Parks K., Andriashek L. D., Michael K., Jean G., Kempin E., Stewart S. Regional Groundwater Quality Appraisal , Cold Lake-Beaver River Drainage Basin , Alberta. 2005.

Mech. M. A Comprehensive Guide to the Alberta Oil Sands. 2011.

Moncur A. Uranium and Arsenic Sources in Shallow Groundwater Near Bonnyville , Alberta : A Mineralogy Study. Alberta Innovates Technology Futures 2011.

Páez-Espino D., Tamames J., De Lorenzo V., Cánovas D. Microbial responses to environmental arsenic. Biometals 2009;22:117–30.

Rosen P. Theoretical significance of arsenic as a carcinogen. J Theor Biol. 1971;32(2):425–426.

Sadiq M. Arsenic chemistry in soils: an overview of thermodynamic predictions and field observations. 1997;93:117-136.

Smedley P. L., Kinniburgh D. G. A review of the source, behaviour and distribution of arsenic in natural waters. Appl Geochem 2002;17:517–568.

Smith A. H., Lingas E. O., Rahman M. Contamination of drinking-water by arsenic in Bangladesh: a public health emergency. Bull World Health Organ 2000;78(9):1093–1103.

Stein R., Dudas M., Klebek M. Occurrence of arsenic in groundwater near Cold Lake, Alberta. 2000.

Wang S., Mulligan C. N. Occurrence of arsenic contamination in Canada: sources, behavior and distribution. Sci Total Environ 2006;366:701–721.

Figures

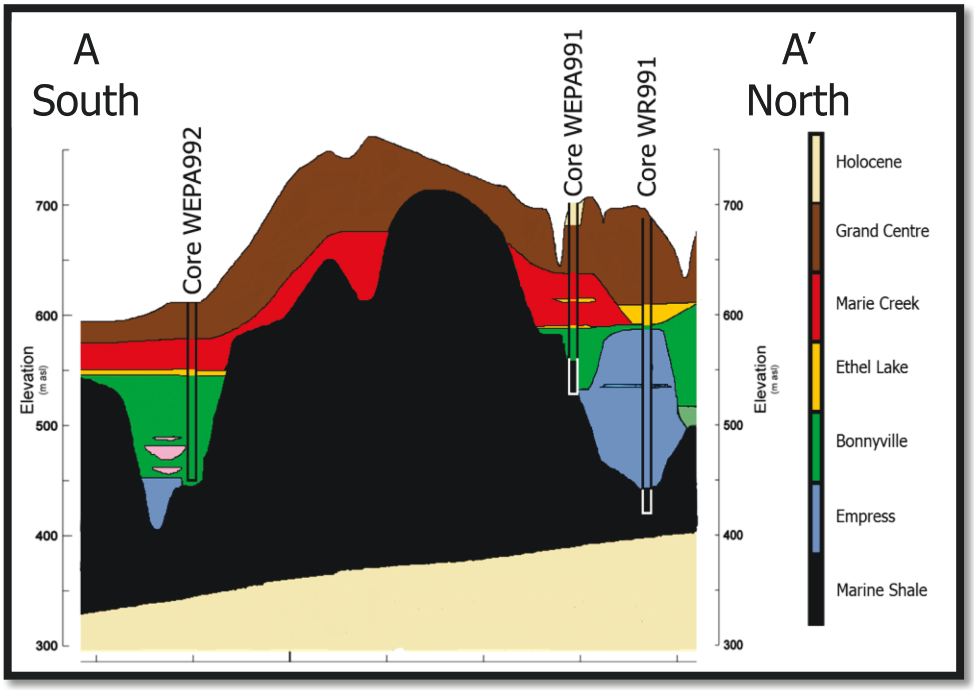

Figure 1- 1. Geological cross section of part (A-A´; shown in Figure 2-1) of study area that is showing three cores taken for our study and stratification of different formations within the cores.

In this cross section Bronson Lake formation is not present. The information to construct this figure was obtained from Andriashek, 2003.

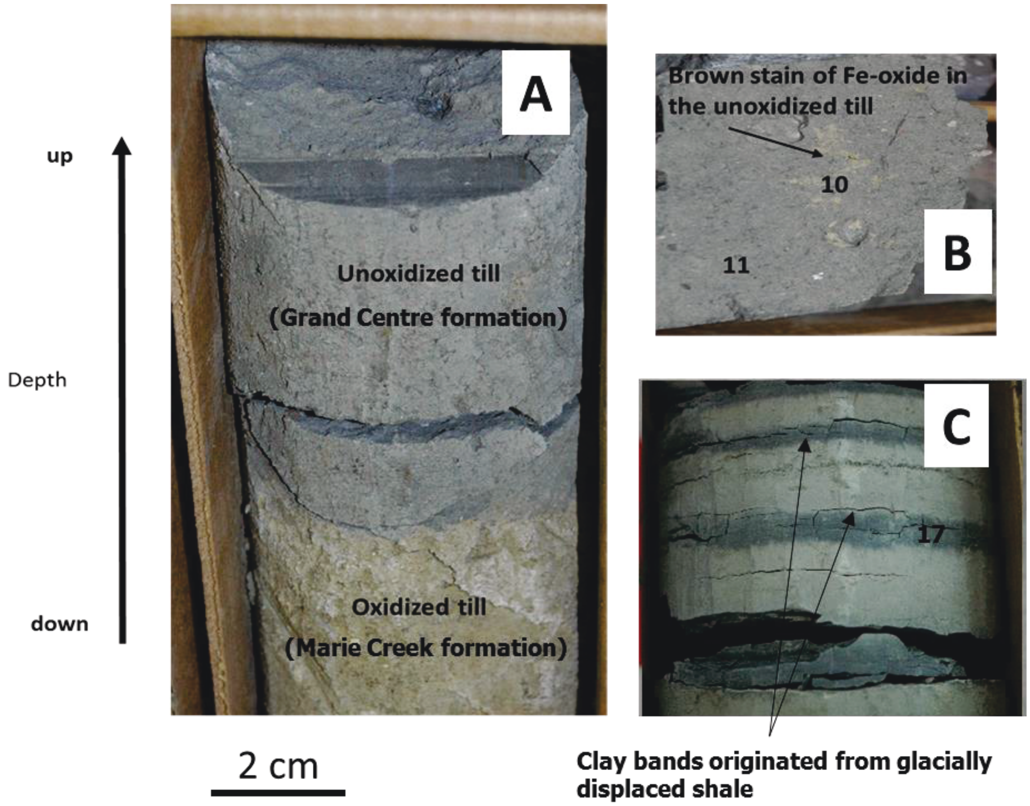

Figure 1- 2. Photos of sediments taken from cores WEPA99-1 and WR99-1 showing characteristic features of the core sediments.

A) Sediments taken from core WEPA99-1 at ~62 m depth from surface which show oxidized till underlying the unoxidized till, **B)** mottles of Fe oxides within the unoxidized till, **C)** sediment taken form core WR99-1 at ~114 m depth from surface which shows clear bands of clay originated from glacially displaced shale.

Different numbers correspond to the sample numbers shown in Figure 2-2.

Chapter 2. Distribution of arsenic and other trace elements in sediments[1]

2.1 Introduction

Arsenic (As) is a ubiquitous metalloid with some of its chemical forms being extremely toxic. It has received global attention in recent years for its groundwater contamination and subsequent serious health effects. Arsenic concentrations >10 µg L^{-1} (the maximum acceptable concentration in Canada; Health Canada, 2006) have been found in groundwater in the Lakeland health region where ~50% drinking water wells contained As that exceeded maximum acceptable concentration (Health Surveillance, 2000; Fitzgerald et al., 2001). The Cold Lake area that is situated within the Lakeland health region also contained elevated levels (>10 µg L^{-1}) of dissolved As in the well water (Stein et al., 2000), which is extensively used for household, agriculture and industrial purposes (Lemay et al., 2005). Generally, high levels of As in groundwater are attributed to the sulfide-rich high As aquifers (Wang and Mulligan, 2006).

It is agreed that As in groundwater usually originates geogenically from sediments (Nickson et al., 2000). Arsenic is naturally enriched in shale containing pyrite (FeS_2, which is considered the principle carrier of As in rocks) and other minerals such as arsenopyrite (FeAsS), enargite (Cu_3AsS_4), scorodite ($FeAsO_4.2H_2O$) and annabergite [$(Ni)_3(AsO_4)_2$] (Boyle and Jonasson, 1973).

---

[1] A version of this chapter combined with arsenic data presented in chapter 4 has been published in "Science of the total environment" journal. Copy is annexed at the end of this thesis.

Weathering and biological transformation of As containing minerals such as FeS_2 and FeAsS in sediments under natural conditions mobilize As in the environment (Smedley and Kinniburgh, 2002; Muloin and Dudas, 2005). Alberta Health and Wellness (Health Surveillance, 2000) and Alberta Environment (Stein et al., 2000) conducted studies in the Cold Lake area to determine the source of groundwater As, they correlated naturally occurring higher groundwater As with bedrock geological formations containing marine shale. Marine shale inclusions or enrichment within Quaternary (glacial) sediments are one of the important sources of groundwater As (Andriashek, 2000).

Because the potential source(s) responsible for As-laden groundwater in the Cold Lake area of Alberta are still unknown, a comprehensive investigation of the sediments collected from cores drilled from five different locations up to ~300 m depth in the Cold Lake area was performed to gain insight into the distribution of As in sediments. Distribution of chalcophile, siderophile and lithophile elements were also studied to better understand the source of As in the sediments.

2.2 Experimental section

2.2.1 Reagents

Trace metal grade nitric acid (HNO_3), calcium chloride ($CaCl_2$) and chromium (Cr) powder were purchased from Sigma-Aldrich (Ontario, Canada) to perform the chemical analyses. All solutions were prepared using nanopure water (Barnstead nanopure, Thermo Scientific). The reagent blanks of all the chemical solutions were analyzed along with the experimental samples. Concentrations of all the elements in the blanks were below the limits of detection [LODs, $\leq$0.075 µg L^{-1}; LOD was determined using 3 × standard deviation (σ) of intensities of 7 blanks + average of the 7 blank intensities] using quadrupole inductively coupled plasma mass spectrometry (ICP-MS; Perkin-Elmer ELAN 9000 and iCap Q-Thermo scientific). All laboratory glass-and plastic-ware was cleaned by soaking in 5% (v/v) HNO_3 overnight and then repeatedly rinsed with nanopure water. A multi-elemental river water reference material (SLRS-5) to determine the analytical accuracy and a multi-elemental sediment certified reference material (HISS-1) to determine the efficiency and accuracy of the digestion and quantification methods were purchased from National Research Council Canada.

2.2.2 Sediments collection and their physicochemical characterization

The Alberta Geological Survey-Alberta Energy Regulator (AGS-AER) drilled surficial deposits (100 to 300 m-thick sediments overlying bedrock) at eight different locations in the Cold Lake area (southeast part of the Athabasca Oil Sands) to explore the hydrogeology and hydrogeochemistry of the region. The cores were stored in wooden boxes at the AGS Mineral Core Research Facility in Edmonton, Alberta, Canada under ambient conditions. To investigate large area in the region, these already drilled cores were used for studying As distribution in the sediments. For this study, five sediment cores (four cores drilled in 1999-2000 namely WEPA99-1, WEPA99-2, WR99-1, and WEPA00-1, and one core drilled in 2009 namely 14-01w) were selected based on geological formations and their proximity to buried channel aquifers (Figure 2-1). The stratigraphy of the area consists of eight glacial and non-glacial formations (Figure 1-1), and the nature and distribution of geological sediments are well described by Andriashek, 2003.

Some significant geological characteristics of the cores are briefly described here. The sediments within the core WEPA99-1 (Dominion Land Survey (DLS) location: 03-08-77-14-W4) included the following features: the upper 20 m sediments were composed of glaciofluvial outwash sand of the upper terrace of the House River, a tributary of Athabasca River (Figure 2-2). The till at 20 m (Grand Centre formation) contained higher amounts of clay in the matrix with depth, including more shale clasts (chunks of pre-existing rock) in the pebble fraction (2-64 mm). Enrichment of clay and shale clasts attributed to glacial erosion and incorporation of bedrock material in Grand Centre till (Andraishek, 2003). At a depth of ~62 m, there was a sharp contact between unoxidized till of Grand Centre formation and the highly weathered oxidized till of Marie Creek formation as shown in Figure 1-2A. The oxidized profile on the surface of Marie Creek till extended for a depth of ~5 m where iron (Fe) mottles were visible (Figure 1-2B). The till between 95 and 154.5 m mainly composed of Bonnyville formation containing abundant clasts of shale, which imparted an overall more clayey composition to the till (Andraishek, 2003). The shale sediments particularly of LaBiche formation were present at the bottom (~155 m depth) of the core.

Some significant aspects of the core WEPA99-2 (Dominion Land Survey (DLS) location: 13-12-74-17-W4) geology included the following: the entire 158 m of surficial deposits at that site composed of till, with the exception of ~4 m of silt and clay at a depth of ~60 m, and ~18 m of silt at a depth of ~137 m (Figure 2-2). Unlike core WEPA99-1, no buried oxidized horizon was found in this core. A strata of relatively high-carbonate till and sand was found at a depth between 30 and 58 m. That high carbonate till was correlated with the high-carbonate Marie Creek till at depths below 62 m in WEPA99-1.

The surficial deposits of core WR99-1 (Dominion Land Survey (DLS) location: 07-36-77-15-W4) included the following features: The total depth of the core was ~235 m where the uppermost one-third (~75 m) of the sediments was comprised of till only. The bottom two-thirds of the sediments (~160 m) were composed of two sediment sequences, each of which grades from gravel to silt and clay. These sequences were interpreted to be of fluvial origin (Andraishek, 2003). In the lower sediment sequence huge amount of pebbles were found and their composition showed a clast lithology (physical characteristics of the rock) that indicated a source from the local bedrock (Andraishek, 2003). The upper sediment sequence was comprised of gravel and sand that contained granite and gneiss clasts (Andraishek, 2003). The layers of clay were also found in the interval between 100 and 122 m, however, the origin of the clay was not certain (Andraishek, 2003). Lithologs of core at 105 m described the clay as black, highly broken, and deformed with slickensides, which indicated that it was a block of glacially displaced shale (Figure 1-2C). A change in the drill method at a depth of ~162 m, from core barrel to tricone rock bit, resulted in poor sample recovery and poor descriptions of lithology in the interval from 165 to 190 m.

The geology within core WEPA00-1 (Dominion Land Survey (DLS) location: 06-33-74-09-W4) included the following characteristics: the surficial deposits of ~174 m depth contained ~35 m of till overlying ~45 m of sand and gravel, which covered more than 94 m of till with interbeds of sand. The upper 20 m of till was characterized by a higher matrix carbonate content of Marie Creek formation. The carbonate values decreased abruptly beneath a 2 m thick silt and clay bed, which was present on top of a buried, weakly oxidized till. Oxidation of the till was shown as rust coloured iron staining along fractures and joints. The lithology changed from till to sand at ~35.5 m depth, to sand and gravel at a depth of ~80 m (Figure 2-2).

The geological information of the core 14-01w (Dominion Land Survey (DLS) location: 14-01-67-03-W4) was taken from the geophysical log of Matrix Solution Inc. that drilled the core 14-01w. Significant aspects of the geology within the core included the following: the top ~74 m of the sediments consisted of clay (Figure 2-2), with small layers of sand at ~16.5 m and ~23 m depths. From 74 to 87 m, the lithology of the sediments was sand with some clay, and a clay layer was also present from 87 to 91 m depth. At the bottom of the core, the sediments were derived from shale of the Lea Park formation.

Because of the lithological heterogeneity in each sediment core, sub-samples were taken along the whole core depth to represent each stratum (based on visual observation) in the cores. In addition, sub-samples were also collected from the depths that represented oxidized (brownish sediment due to Fe oxyhydroxide) and reduced [grayish sediment due to high iron sulfide (FeS)] zones as well as the zones of surficial (<75 m deep) and buried (75-150 m deep) channel aquifers to correlate sediment redox conditions with groundwater As concentration.

Sediment cores were already air dried when sub-samples were taken in 2010, which might have changed oxidation state of As in the sediments. Therefore, chemical speciation of As was not performed using these sediments. Arsenic concentrations determined in the sediments taken from outer and inner portions of the cores were compared to the As concentration determined at the time of cores collection by Andriashek, (2003). No significant difference was found in As concentrations between outer and inner sediments and the As determined in sediments at the time of core collection. However, sediments taken from the inner portion of the cores were used in this study. The sediment samples were ground with agate mortar and pestle and passed through 125 μm sieve before all analyses. The pH of sediment slurry prepared with 0.05 M $CaCl_2$ solution (1:5 ratio; Sumner, 1994) was measured using accumet® AR20 pH meter. The pH ranged between 4.7 and 9.1, but most sediments had pH ~7. Total organic carbon (TOC) contents in sediments determined by the loss on ignition method (LOI; Ball, 1964) were <1% in most sediments but a few had TOC up to 2.8±0.2 %. The information about particle size distribution (PSD) and texture of the sediments was obtained from elsewhere (Andriashek, 2003). In general, ~50% of the PSD was in the range of 50-63 μm size. Total As and other elements concentrations were determined using the methods described in section 2.2.3. Chromium reducible sulfur method (Hsieh and Shieh, 1997) was employed to determine the reduced inorganic sulfur. The physicochemical properties of selected (n = 22) sediments are provided in Table 2-1.

2.2.3 Total arsenic and other elements concentration in sediments

For total concentrations of As and 15 other elements including chalcophile (Pb, Cd, Cu and Se), siderophile (Mo, Co and Ni) and lithophile (V, Cr, B, Be, U, Ba, Sr and Rb) in sediments, sediment samples were digested with concentrated HNO_3 (1:20 sediment: acid ratio) in a microwave digestion unit (MARS6, CEM) at 180±10 ºC for 10 min using a modified EPA method (3050B, 1996). After cooling, the digested samples were diluted with nanopure water (final HNO_3 concentration ~1% in solution), filtered through 0.45-µm PTFE filters (033911C, Fisher Scientific) and analyzed using quadrupole ICP-MS (Perkin-Elmer ELAN 9000 and iCap Q- Thermo scientific).

To maintain quality assurance and quality control (QA/QC) for experimental procedure and equipment operation, duplicate experimental blanks and duplicate sediments (n = 6) were included in the microwave digestion for the determination of total elemental concentrations in sediment samples. The variation in duplicate samples were below 10% for total elemental concentrations quantified using quadrupole ICP-MS. In all the experimental blanks, As was below the limit of detection (LOD; 0.01 µg L^{-1} As) of quadrupole ICP-MS, and insignificant concentrations of other elements were found in the blanks that were account for during calculation of the elemental concentrations in experimental sediments. Multi-elemental external standards (CLMS-2N, CLMO9-2Y, and ISOT-B11; SPEX Certi Prep) in the range of 2 to 50 µg L^{-1} prepared in 1% HNO_3

were used to calibrate the quadrupole ICP-MS. Immediately after calibration standards, six initial calibration blanks (ICB) were analyzed to ensure that instrument was clean. During the analysis of experimental samples, continuous calibration blanks (CCB) to check any metal contamination in the instrument and continuous calibration verification (CCV) multi-elemental standards of 2 and 20 $\mu g\ L^{-1}$ to assure the validity of the initial calibration of the instrument were also included after every 10 samples. All the blanks (ICB and CCB) showed elemental concentrations lower than the LOD of quadrupole ICP-MS, and all the elemental concentrations in all the CCVs were within ±10% of their actual values (2 and 20 $\mu g\ L^{-1}$). The multi-elemental river water certified reference material (SLRS-5) and multi-elemental marine sediment certified reference material for trace elements (HISS-1) were also analyzed to determine the efficacy and accuracy of the digestion and quantification methods. All the elemental concentrations were within $\pm$ 15% of the certified values in both the reference materials. In addition, scandium (Sc), yttrium (Y) and terbium (Tb) internal standards were used in the quantification of all the external standards, ICB, CCB, CCV and experimental samples to account for any instrumental drift.

2.2.4 Statistical analysis

Comparison of all the means of elemental concentrations in sediments and Pearson correlation analysis were performed using SAS 9.3. To determine the relevance in elemental distribution in sediments, two dimensional ordination principle component analysis (PCA) was performed using XLSTAT 2014.

2.3 Results

2.3.1 Arsenic distribution in sediments

Arsenic distribution in sediments with respect to depth, geological formations, lithology, TOC, pH and redox conditions is shown in Figure 2-2 and Table 2-1 (different numbers 1 to 22 shown in Figure 2-2 and Table 2-1 are the sediments selected for detailed As characterization). Generally, arsenic concentrations in sediments at different depths did not significantly ($P > 0.05$) vary with geological formations, lithologies, pH and TOC of sediments. Quadrupole ICP-MS analysis showed that As concentrations were up to 35 $\mu g\ g^{-1}$ in sediments. However, higher As concentrations were detected in unoxidized clayey zones in the Grand Centre (24.9±4.2 $\mu g\ g^{-1}$ As) and Bonnyville (19.9±1.8 $\mu g\ g^{-1}$ As) formations, particularly in core WEPA99-1 compared to the average As concentration (~5 $\mu g\ g^{-1}$) measured in all sediments (n = 135) collected from all the geological formations with different lithologies and redox zones (Figure 2-2 and Table A-1). Higher As concentration (22.5±2.1 $\mu g\ g^{-1}$ As) was also found in localized unoxidized sediment in the Empress Formation (core WR99-1). The marine shale sediments clearly exhibited higher concentrations of As (~13 $\mu g\ g^{-1}$; n = 14) in the cores (WR99-1, WEPA99-1 and 14-01w). Among all the sediments, the highest average concentration of As (32 $\mu g\ g^{-1}$; n = 2) was also determined in shale samples (core 14-01w).

2.3.2 Distribution of other elements in sediments

The distribution of chalcophile (Cd, Se, Pb and Cu), siderophile (Mo, Co and Ni) and lithophile (Be, U, Rb, Sr, Cr, B, V and Ba) elements in the sediments is shown in Appendix A (Figures A1-A3). Among the chalcophile elements, Cd, Se and Pb concentrations in the sediments were higher than their natural abundance in the earth crust and average concentrations in the shale sediments particularly at those depths where As concentrations were higher, which was clearly evident in core WR99-1 (Figure A-1). Among the siderophile elements, only Mo concentration was higher than its natural abundance and average concentration in shale in the sediments where As concentration was higher (Figure A-2), which might suggest the presence of shale sediments at that depths. Sediments derived from shale contained high Mo concentrations (Mao et al., 2002; Orberger et al., 2005). All the lithophile elements in our sediments were lower than their natural abundance in earth crust and average concentrations in shale except Cr, V and B (Figure A-3). Higher concentration of B was clearly evident in cores WR99-1 and WEPA99-2. The results of all these elemental concentrations in sediments showed that only the distribution of most of chalcophile elements (Cd, Se and Pb) and Mo were similar to the As in the sediments, which suggested that sulfide minerals present in the shale sediments might be the potential source of As in sediments. The detailed association of these elements with different solid constituents in sediments are discussed in chapter 4.

2.3.3 Principle component analysis (PCA)

After determination of total elemental concentrations, a PCA was performed using total concentrations of the selected elements in sediments to determine the relevance in elemental distribution. Overall observing the positions of all the elements in the PCA 2-dimensional ordination, most of the chalcophile elements such as Se, Cd and Pb were clustered together with As in one quadrant (Figure 2-3). The elements enriched in shale such as Mo, U and Ba were also classified in the same quadrant. Silicates and carbonates were present in different quadrant of PCA showing their irrelevance with the distribution of As in sediments.

2.4 Discussion

Elevated As in domestic well water in the Cold Lake area of Alberta, Canada is a health concern that warrants detailed geochemical characterization of the glacial till surficial deposits (sediments) that feed the aquifers in the region. The groundwater is surrounded with surficial deposits of varying geochemical characteristics originated from different sources such as marine shale and glacial till (Lemay et al., 2005). These sediments contain different As and other elemental concentrations that can become mobile in sediments pore water and a fraction of their total concentration can leach to groundwater (Santona et al., 2006). Arsenic-laden groundwater is also attributed to the sediment's As concentration through which the water passes (Wang and Mulligan, 2006). Therefore, this study was conducted to comprehensively investigate As distribution in sediments collected from different locations (up to ~300 m depth) in the Cold Lake area and to correlate it with As concentrations in surficial (<75 m deep) and buried (75-150 m deep) aquifer water. Elemental concentrations in aquifer water from the same study area was reported by Lemay, 2003.

In our study, we found that As concentrations were up to ~35 μg g^{-1} in sediments without exhibiting any significant relationship with geochemical parameters such as lithology, pH, TOC and redox zones along the depth profiles of collected sediment cores. However, some pattern of As distribution in different geological formations could be established (Figures 1-1 and 2-2). Higher As concentrations (7 to 35 μg g^{-1}; average: ~13 μg g^{-1}; n = 14) were found in sediments derived from marine shale that constituted the bottom portions of core holes WR99-1, WEPA99-1 and 14-01w. These As concentrations were similar to the average As concentration (~15 μg g^{-1}) in the shale reported by Boyle and Jonasson, (1973), which is commonly found in various parts of Canada including east- and west-central Alberta (Muloin and Dudas, 2005). Shale of marine origin often contains elevated levels of As that is concentrated in sulfide minerals such as FeS_2 and FeAsS (Muloin and Dudas, 2005). In general, the average As concentration in shale is an order of magnitude greater than other geological materials such as carbonates (Smedley and Kinniburgh, 2002). High As concentrations were also found in some sediments taken from the Grand Centre (24.9±4.2 μg g^{-1} As), Bonnyville (19.9±1.8 μg g^{-1} As) and Empress formations (~15 μg g^{-1} average As; n= 2). If we see the locations of collected cores with respect to geological setting of all the formations present in the region (Figure 1-1), the Bonnyville and Empress formations were directly overlying the shale that might be mixed with these formation during deposition, and high As concentrations in these formations were found mostly in unoxidized horizons. The Bonnyville formation features the abundance of diamicton (non-sorted sediments; Andriashek and Fenton, 1989) and directly overlies the shale in cores WEPA99-1 and WEPA99-2. The Empress formation is of fluvial origin and directly overlies marine cretaceous and non-marine tertiary bedrock (Andriashek and Fenton, 1989). Though the Grand Centre formation did not have any direct contact with shale (core WEPA99-1), a higher concentration of As was probably due to the glacial thrust that displaced and mixed older deposits (such as shale) during the deposition of Grand Centre formation (Andriashek and Fenton, 1989; Andriashek, 1998). Our results are in conformity with the findings of Andriashek, 2000 who studied As in glacial till farther to the south in the Cold Lake area and reported high As in Grand Center and Bonnyville formations. In our study, other formations in the region such as Marie Creek, Ethel Lake, and Bronson Lake as well as Holocene (recently deposited material) showed lower concentrations of As at different depths in the collected cores. In contrast, Andriashek and Geol (2003) reported a high As concentration in the oxidized zone of the Marie Creek formation in the core WEPA99-1. However in our study, higher As concentrations were found in the unoxidized sediments from Grand Center, Bonyville and Empress formations. Few brown Fe oxides mottles were found within the unoxidized Grand Center formation (Figure 1-2B) but upon analyses lower As concentrations were found in these mottles compared to the adjacent unoxidized sediments. The high As in unoxidized sediments could be due to the inclusion of marine shale.

After total As determination to further characterize the sediments, 22 sediments were chosen from different cores representing different lithologies and grouped under low (As <7 μg g^{-1}; samples 1 to 9) and high As sediments (As >7 μg g^{-1}; samples 10 to 22) for further investigations (Table 1). Shale is considered a source of high As in sediments that contains an average As of 10 to 15 μg g^{-1} (Krauskopf, 1979; Boyle and Jonasson, 1973). The lowest As concentration (~7 μg g^{-1}) found in our shale sediments was used for demarcation between designated low and high As sediments. High As sediments (~20 μg g^{-1} As) were relatively darker (unoxidized) in color than low As sediments (<7 μg g^{-1} As). For example in core WEPA99-1, a few occurrences of brown-coloured Fe oxides were observed within the unoxidized dark gray sediments taken from the Grand Center formation (Figure 1-2B). We separated the oxidized sediment (sample 10) from the unoxidized sediment (sample 11) for As determination. High As concentration (24.9±4.2 μg g^{-1} As) was found in unoxidized sediment, which also contained high sulfide minerals (2.8±0.2 %), as compared to the oxidized sediment (7.5±0.1 μg g^{-1} As) in which only 0.8±0.1 % sulfides were present. Sediments obtained from the Bonnyville formation in core WEPA99-1 showed a darker gray color with depth and corresponding increase in As concentrations (Figure 2-2). We found ~20 μg g^{-1} As in sediment 13 at deepest depth in the Bonnyville formation where sulfide minerals were ~2%. Another high As sediment (sample 17; 22.5±2.1 μg g^{-1} As) sampled from Empress formation, was also very dark gray to black coloured and it too contained relatively high sulfide minerals (1.2%). Overall, sediments (11, 13 and 17) containing higher As (20 to 25 $\mu g\ g^{-1}$) among high As sediments from different formations also contained relatively higher sulfide minerals (1.2-2.8 %; Table 2-1).

We also compared other elemental concentrations in sediments with the sediments As by applying Pearson correlation analysis to determine the association of elemental distribution in sediments. A good correlation found between As and U, Mo, Pb and Ba ($r = 0.80$, $r = 0.76$, $r = 0.76$ and $r = 0.66$, respectively) suggested that presence of marine shale might attribute high As in the sediments. Marine shale is 10 to 100 times enriched in As, U, Mo and Ba compared to other sedimentary rock (Mao et al., 2002; Orberger et al., 2005). These correlation results are also in conformity with the findings of Andriashek (2000), who reported similar distribution of As, Ba and Pb in sediments in glacial till farther to the south in the Cold Lake area.

Generally sediments impart the metals to aquifers water (Muloin and Dudas, 2005). Lemay (2003) reported elemental concentrations in different Quaternary drift and Quaternary-Tertiary buried channel aquifers from the same locations where our sediment cores were taken. Comparing our sediment As concentrations to the aquifer-water As values reported by Lemay 2003, we observed that generally sediment total As concentrations were lower than the average As concentration (5 $\mu g\ g^{-1}$) where aquifer As was <10 $\mu g\ L^{-1}$. We also observed that sediment As concentrations were directly related with the aquifer water As. For example two surficial aquifers present at 39.5 m and 74 m depths

(Lemay, 2003) in core WEPA00-1 had As concentrations <10 $\mu g\ L^{-1}$ in water where the surrounding sediments had ~3 $\mu g\ g^{-1}$ As. In core WR99-1, a sand and gravel aquifer in the drift sediments at ~229 m depth with ~20 $\mu g\ L^{-1}$ As (Lemay, 2003) corresponded to relatively higher As concentration (average ~11 $\mu g\ g^{-1}$) in the sediments at that depth. Comparison of the sediments As to the aquifer water As might suggest that occurrence of As in aquifer water is of localized origin and proximity of the As-bearing sediment to aquifer water might be one of the possible causes of high As in the groundwater. This finding also suggest that sediment As might attribute the localized high As in porewater that can migrate to contaminate the aquifer water.

Different geochemical conditions including presence of competing anions such as phosphate (PO_4^{3-}) and carbonate (CO_3^{2-}) ions in pore water that can desorb the exchangeable As in sediments, and oxidative breakdown of FeS_2 and FeAsS minerals in sediments that can release the minerals bound As into groundwater could be important processes in As groundwater contamination (Keon et al., 2001; Javed et al., 2013). Though natural geochemical conditions slowly release As, anthropogenic activities such as Cyclic Steam Stimulation (CSS) that is currently operating in the Cold Lake region (Andriashek, 2003; Fennell, 2008) to extract the bitumen could enhance the As release by the breakdown and/or desorption of As from these minerals in sediments. The results provide insights into the distribution of As in sediments of different geological formations that can be used to predict As availability and transport to groundwater.

Literature cited

Andriashek L. D. Geochemistry of selected glacial and bedrock geological units, Cold Lake Area, Alberta. Alberta Geological Survey open file report. 1998.

Andriashek L. D. Geochemistry of selected glacial and bedrock geologic units, Cold Lake Area, Alberta. 2000. http://ags.gov.ab.ca/publications/ESR/PDF/ESR_2000_10.pdf

Andriashek L. D. Quaternary geological setting of the Athabasca Oil Sands (in situ) area, Northeast Alberta. 2003. http://www.ags.gov.ab.ca/publications/ESR/PDF/ESR_2002_03.pdf

Andriashek L. D., Fenton M. M. Quaternary stratigraphy and surficial geology of the Sand River area 73L. 1989. http://www.ags.gov.ab.ca/publications/BUL/PDF/BUL_057.pdf

Ball D. F. Loss-on-ignition as an estimate of organic matter and organic carbon in non-calcareous soils. J soil Sci 1964;15(1):86-92.

Boyle R. W., Jonasson I. R. The geochemistry of arsenic and its use as an indicatior element in geochemical prospecting. J Geochemical Explor 1973;2:251–296.

Fennell J. W. Effects of aquifer heating on groundwater chemistry with a review of arsenic and its mobility. PhD thesis 2008, Universiyt of Calgary.

Fitzgerald D., Chanasyk D. S., Neilson R. D., Kiely D., Audette R. Farm well water quality in Alberta. Water Qual Res 2001;36(3):565–588.

Health Canada (2006), Guidelines for Canadian drinking water quality: Guideline technical document-Arsenic. Water Quality and Health Bureau, Healthy Environments and Consumer Safety Branch, Health Canada, Ottawa, Ontario.

Health Surveillance, Alberta Health and Wellness. Arsenic in groundwaer from domestic wells in three areas of northern Alberta. 2000. http://www.health.alberta.ca/documents/Arsenic-Groundwater-Wells-2000.pdf

Hsieh Y. P., Shieh Y. N. Analysis of reduced inorganic sulfur by diffusion methods: improved apparatus and evaluation for sulfur isotopic studies. Chem Geol 1997;137(3-4):255–261.

Javed M. B., Kachanoski G., Siddique T. A modified sequential extraction method for arsenic fractionation in sediments. Anal Chim Acta 2013;787:102–110.

Javed M. B., Kachanoski G., Siddique T. Arsenic fractionation and mineralogical characterization of sediments in the Cold Lake area of Alberta, Canada. Sci Total Environ 2014;500-501:181–190.

Keon N. E., Swartz C. H., Brabander D. J., Harvey C., Hemond H. F. Validation of an arsenic sequential extraction method for evaluating mobility in sediments. Environ Sci Technol 2001;35(13):2778–2784.

Krauskopf K. B. Introduction to geochemistry. 1979; McGraw-Hill Book Company.

Lemay T. G. Arsenic concentration in quaternary drift and quaternary-tertiary buried channel aquifer in the Athabasca Oil Sands (In Situ) area, Alberta. 2003. http://www.ags.gov.ab.ca/publications/GEO/PDF/GEO_2002_04.pdf

Lemay T. G., Parks K., Andriashek L. D., Michael K., Jean G. M., Stewart S. A., Kempin E. Regional groundwater quality appraisal , Cold Lake-Beaver River Drainage Basin , Alberta. 2005. http://www.ags.gov.ab.ca/publications/SPE/PDF/SPE_073.pdf

Mao J., Lehmann B., Du A., Zhang G., Ma D., Wang Y., Zeng M., Kerrich R. Re-Os Dating of Polymetallic Ni-Mo-PGE-Au Mineralization in Lower Cambrian Black Shales of South China and Its Geologic Significance. Econ Geol 2002;97:1051–1061.

Muloin T., Dudas M. J. Aqueous phase arsenic in weathered shale enriched in native arsenic. J Environ Eng 2005;4(6):461–468.

Nickson R. T., McArthur J. M., Ravenscroft P., Burgess W. G., Ahmed K. M. Mechanism of arsenic release to groundwater, Bangladesh and West Bengal. Appl Geochem 2000;15:403–413.

Orberger B., Wagner, C., Vymazalova, A. Rare metal sequestration and mobility in mineralized black shales from the Zunyi region, South China. Mineral Deposit 2005: 167-170.

Raj S. M., Jayaprakash M. Distribution and enrichment of trace metals in marine sediments of Bay of Bengal, off Ennore, south-east coast of India. Environ Geol 2008;56:207–217.

Rodrigues M. L. K., Formoso M. L. A. Geochemical distribution of selected heavy metals in stream sediments affected by tannery activities. Water Air Soil Pollut 2006;169:167–184.

Santona L., Castaldi P., Melis P. Evaluation of the interaction mechanisms between red muds and heavy metals. 2006;136(2):324–329.

Smedley P. L., Kinniburgh D. G. A review of the source, behaviour and distribution of arsenic in natural waters. 2002;17(5):517–568.

Stein R., Dudas M., Klebek M. Occurrence of arsenic in groundwater near Cold Lake, Alberta. 2000.

Stockdale A., Davison W., Zhang H., Hamilton-Taylor J. The association of cobalt with iron and manganese (Oxyhydr)oxides in marine sediment. Aquat Geochemistry. 2010;16(4):575–85.

Sumner M. E. Measurement of soil pH: Problems and solutions. Commun Soil Sci Plant Anal 1994; 25(7-8):859–879.

Tessier A., Campbell P. G. C., Bisson M. Sequential extraction procedure for the speciation of particulate trace metals. Anal Chem 1979;51(7):844–851.

US EPA. Method 3050B acid digestion of sediments, sludges, and soils. Washington, D.C.: U.S. Environmental Protection Agency; 1996.

Wang S., Mulligan C. N. Occurrence of arsenic contamination in Canada: sources, behavior and distribution. Sci Total Environ 2006;366:701–721.

Tables and figures

Table 2- 1. Physicochemical characteristics of the selected sediments used for detailed investigation.

Sedime ID[a]	Core Name	Texture[b]	Geological Formation	pH[c]	TOC (%)	As $_{total}$ (µg g^{-1})	Sulfide (%)	Fe $_{total}$ (%)
Low As samples (<7 µg g^{-1})								
1	14-01w	Sandy Clay	Bonnyville	7.2	0.5±0.1	6.5±0.8	0.2±0.1	2.8±0.4
2	14-01w	Sandy Clay	Bonnyville	7.0	0.3±0.1	4.9±0.7	0.1±0	1.7±0.2
3	WEPA99-1	Sand	Grand Centre	4.7	0.1±0.1	5.3±0.5	0.1±0	1.4±0.2
4	WEPA99-1	Sand	Grand Centre	6.3	0.1±0.1	3.1±0.1	0.1±0.1	1.9±0.5
5	WEPA99-1	Till	Marie Creek	7.2	0.1±0.1	4.2±0.3	0.1±0.1	1.7±0.3
6	WEPA99-2	Till	Grand Centre	6.3	0.7±0.1	5.6±0.8	0.2±0.1	2.7±0.8
7	WEPA99-2	Mudstone	Bonnyville	7.3	1.2±0.1	0.8±0	0.1±0	ND
8	WR99-1	Clay	Empress	7.2	0.6±0.1	6.1±0.7	0.1±0	2.8±0.9
9	WR99-1	Clay and silt	Empress	7.3	0.6±0.1	3.5±0.1	0.1±0.1	2.2±0.5
High As samples (>7 µg g^{-1})								
10	WEPA99-1	Till	Grand Centre	7.5	0.6±0.1	7.5±0.1	0.8±0.1	2.9±0.7
11	WEPA99-1	Till	Grand Centre	6.8	0.6±0.1	24.9±4.2	2.8±0.2	2.7±0.4
12	WEPA99-1	Till	Marie Creek	7.0	0.1±0.1	9.9±0.4	0.2±0	3.2±0.2
13	WEPA99-1	Till	Bonnyville	6.2	2.8±0.2	19.9±1.8	1.9±0.1	4.0±0.2
14	WEPA99-2	Till	Grand Centre	6.3	0.5±0.1	12.4±0.8	0.3±0.1	4.2±0.9
15	WEPA99-2	silt and clay	Ethel Lake	6.6	0.7±0.1	10.5±1.1	0.6±0.1	2.4±0.7
16	WEPA99-2	Mudstone	Bonnyville	7.4	0.3±0.1	8.8±0.9	0.3±0.1	2.1±0.6
17	WR99-1	Clay and silt	Empress	6.8	1.3±0.4	22.5±2.1	1.2±0.1	3.8±0.3
18	WR99-1	Clay and silt	Empress	6.2	1.1±0.2	8.9±0.9	0.4±0.1	2.4±0.8
19	WR99-1	-	Marine Shale	8.9	0.6±0.2	8.6±0.3	0.3±0.1	2.1±0.4
20	WR99-1	-	Marine Shale	5.3	0.1±0.1	18.6±1.8	0.9±0.1	3.1±0.7
21	WR99-1	-	Marine Shale	9.1	0.6±0.1	7.1±0.7	0.7±0.1	3.2±0.9
22	14-01w	-	Marine Shale	7.0	ND	35.4±2.3	2.2±0.2	2.9±0.4

Values represent the mean from analysis of triplicate ± 1 standard deviation.

[a] Sample ID refers to the numbers in Figure 2-2, [b] information about texture was obtained from elsewhere (Andriashek, 2003), texture analysis was not performed for samples 19-22, [c] pH was measured in suspension of sediment:0.05 M $CaCl_2$ (1:5), TOC: total organic carbon; ND: not detected

Sediments taken from unoxidized zones/layers, samples 17 and 18 were taken from the localized reduced layers

---

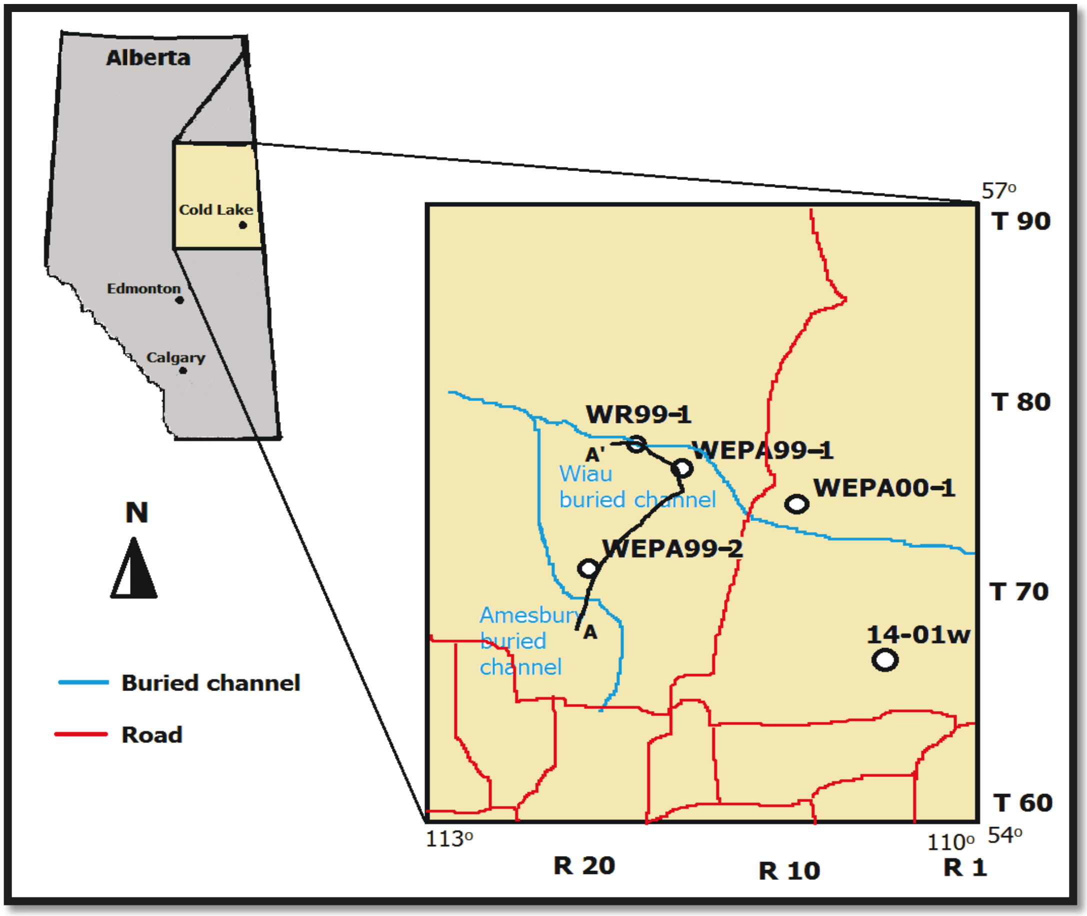

Figure 2- 1. Location of the five sediment cores taken for this study and two buried channel aquifers within the study area.

The information to construct this figure was obtained from Andriashek, 2003.

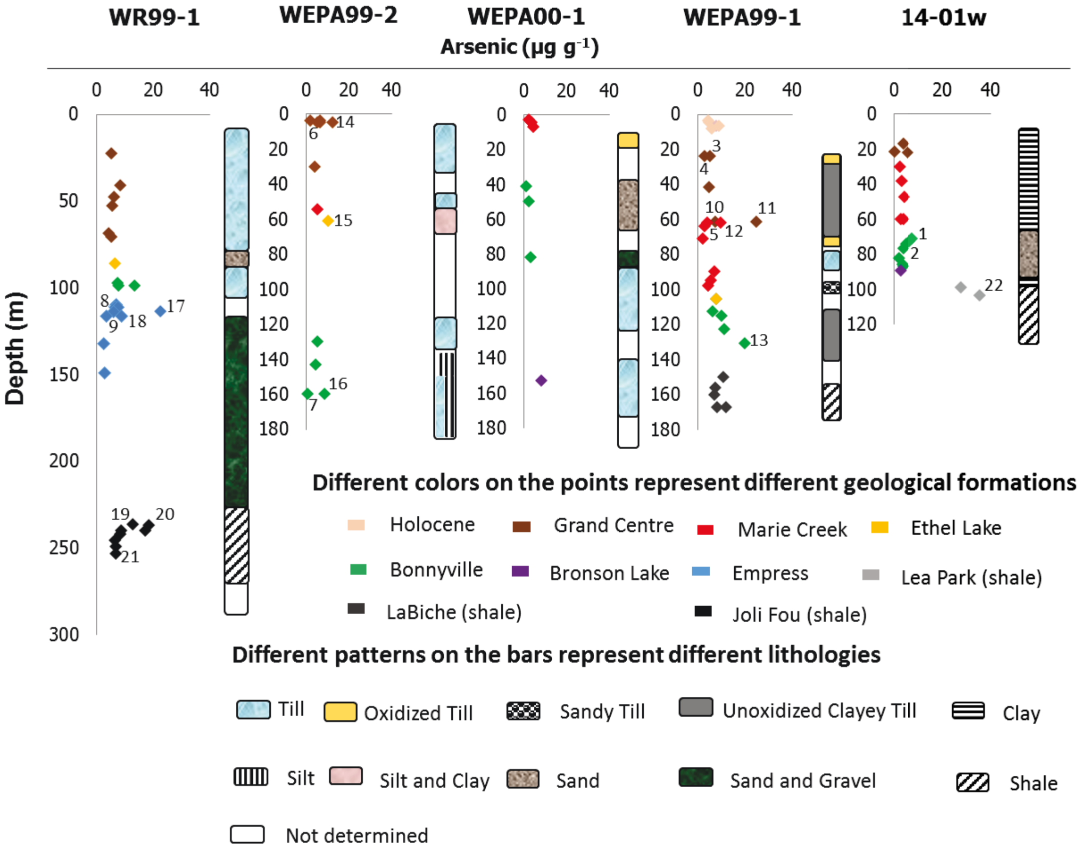

Figure 2- 2. Arsenic (As) distribution in sediment cores collected from five different locations in the Cold Lake area, Alberta.

The numbers (1-22) displayed on the data in the figure are the sediment samples selected for further As characterization. The information about the sediment texture and formation was obtained from Andriashek, 2003. The average As concentrations in earth crust and shale are 1.5 µg g^{-1} and 10 µg g^{-1}, respectively.

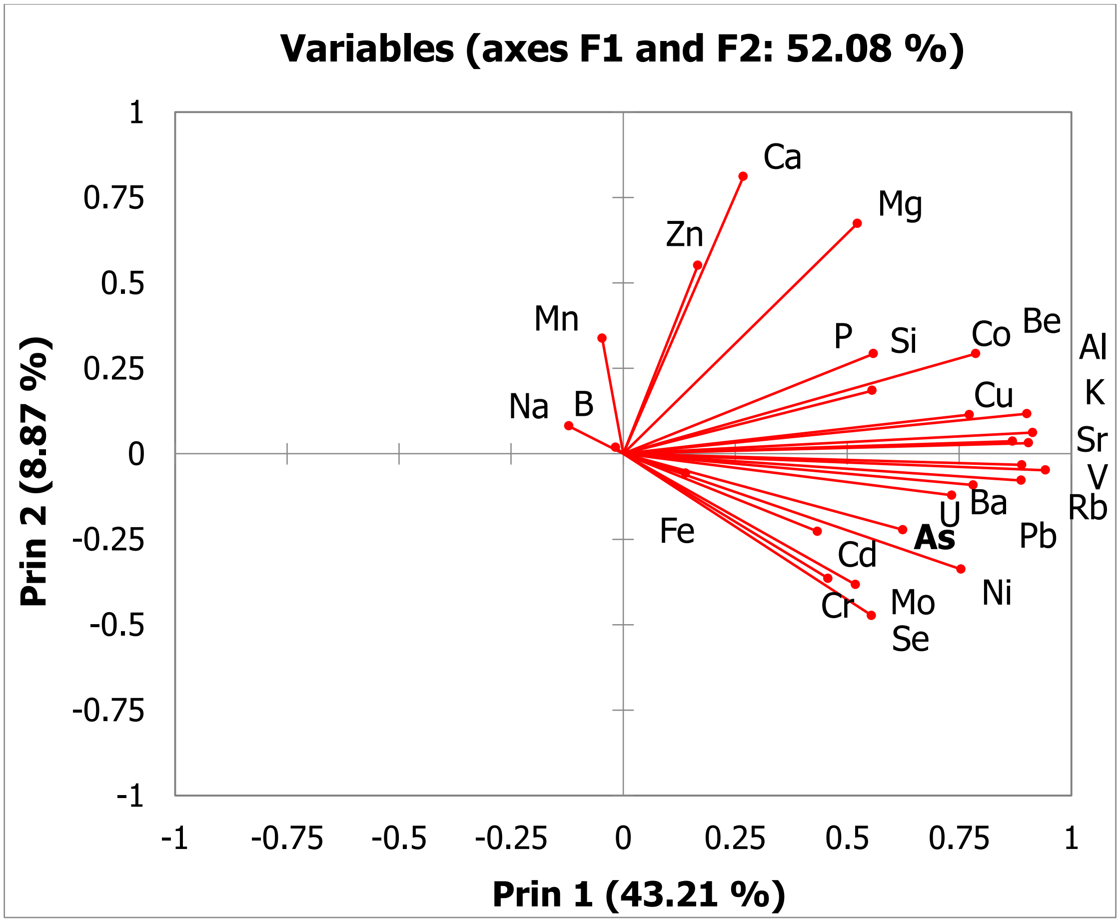

Figure 2- 3. Principle component analysis (PCA) of the total elemental concentrations to determine the relevance in elemental distribution in sediments.

The relationships between elements are represented by the angle between vectors drawn from origin to the element symbol. Higher correlations are represented by more acute angles (<90º) and no relationship is indicated by an orthogonal angle (90º). In addition, the extent to which the variability of element is captured in this two dimensional interpretation is indicated by the length of the vector. Two components (Prin 1 and Prin 2) used in this illustration explaining ~52% of the total variability controlling the elements distribution in sediments.

Chapter 3. Development of a sequential extraction method for arsenic fractionation in sediments[2]

3.1 Introduction

Arsenic (As) is a toxic trace element and its crustal abundance is ~0.0001% (Oremland and Stolz, 2003). However through geogenic processing of crustal materials, arsenic can concentrate in soils up to 57 to 110 $\mu g\ g^{-1}$ causing high concentrations of As in pore or surface water through desorption or dissolution processes (Mitchell and Barre, 1995; Alam and Sattar, 2000). High As concentration (>10 $\mu g\ L^{-1}$) in groundwater is of increasing concern due to its implications in human and ecological health (Dhar et al., 2004; Health Canada, 2006). Arsenic mobility is principally controlled by adsorption-desorption and solid phase precipitation-dissolution reactions. Important geochemical factors affecting these reactions in soils and sediments are pore water chemistry, pH, redox conditions, soil solid composition and As-bearing minerals (Sadiq, 1997). To predict the fate of As in soils or sediments and its transport to ground or surface water, it is important to understand nature of As association with different solid constituents.

Distribution and chemical association of As with various solid constituents, rather than its total concentration, affect As mobility in sediment and its transport to water bodies. Sorption of As on solid particles is one of the most

---

[2] A version of this chapter has been published.
Javed, M. B., Kachanoski, G., and Siddique, T. A modified sequential extraction method for arsenic fractionation in sediments. *Anal. Chim. Acta.* **2013**, *787*, 102–110. Copy is annexed at the end of this thesis.

important processes that immobilizes As (Sadiq, 1997). Arsenic can adsorb on the surfaces of a variety of materials, especially oxides of iron (Fe), Aluminum (Al) and manganese (Mn) (Smith et al., 1998). Coprecipitation of As with Fe oxyhydroxides has also been defined as the major mechanism that strongly retains As in sediments (Larios et al., 2012) but As-bearing Fe oxyhydroxides may act as a source of As during reductive dissolution of both amorphous and crystalline oxyhydroxides (Sadiq, 1997). Arsenic associated with hydrous Mn oxides (easily reducible oxides) is relatively more labile than Fe oxyhydroxides (Tessier et al., 1979). Arsenic adsorption on the edges of clay minerals and on the surface of calcite has also been observed (Larios et al., 2012). Other more stable forms of As are naturally occurring As-bearing sulfide ores and silicate minerals; and weathering of these sulfides and silicate minerals can release As into the environment and/or may cause formation of other thermodynamically metastable new secondary minerals (Sadiq, 1997).

Arsenic distribution in different solid constituents can be studied by sequential extraction procedure (SEP). Several SEP schemes have been developed by previous researchers to fractionate As in sediments (Tessier et al., 1979; Hall et al., 1996; Keon et al., 2001; Wenzel et al., 2001). These schemes vary in terms of number of fractions, extraction solutions and conditions and the sequence of extraction steps but the common feature is that the fractions are operationally defined. Different methods target different As phases in sediments and yield ~40 to 50 % of the total As in their final residual fractions. These unresolved residual fractions might contain As bound in silicates, pyrite and orpiment such as in

Tessier et al., 1979, Hall et al., 1996 and Wenzel et al., 2001 methods or As associated with organic and recalcitrant sulfides in Keon et al., 2001 method. Characterization of these residual fractions is important for comprehensive understanding of As fate in soils and sediments. Secondly, the common extractants used in the existing SEPs create interference during As determination if those extractants are analyzed by quadrupole inductively coupled plasma mass spectrometry (ICP-MS). Chloride (Cl^-)-containing extractants produce polyatomic ions (argon chloride; $^{40}Ar^{35}Cl$) when Cl^- reacts with argon (Ar) in ICP plasma. These polyatomic ions can interfere with ^{75}As due to same mass to charge ratio (m/z) (Goossens et al., 1993; Thomas, 2008) even if the quadrupole ICP-MS is equipped with a collision cell (Niemelä et al., 2003). Therefore, we developed a sequential extraction scheme by modifying the existing methods to (1) quantify As in maximum possible meaningful fractions and (2) choose only those extractants that can be analyzed by quadrupole ICP-MS without any polyatomic interference for As quantification. To check the applicability of the developed method, we compared it with the three existing sequential extraction methods described by Tessier et al., 1979, Keon et al., 2001 and Wenzel et al., 2001 using sediment samples. We also used the new scheme to test the specificity of the extractants to target pure mineral phases (calcite and dolomite) and natural minerals (arsenopyrite and orpiment). In addition, the developed method was also evaluated for the fractionation of other metals such as copper (Cu), cobalt (Co), chromium (Cr) and strontium (Sr).

3.2 Experimental section

3.2.1 Description of sediment samples used in sequential extraction protocol development

Sediment (surficial deposits) core samples used in the protocol development were obtained from Alberta Geological Survey (AGS) collected up to ~300 m depths from the Cold Lake area in Alberta, Canada, which is one of the As affected areas in northern Alberta. The air dried sediment samples were grounded with agate mortar and pestle and passed through 125 µm sieve. The particle size distribution of the sediments determined using laser particle size analyzer (Master sizer-Malvren 3000 Hydro®) are provided in Table B-1. The pH of the samples was determined by preparing a sediment slurry (sediment: 0.05 M $CaCl_2$; 1:5; Sumner, 1994) and measuring pH using Accumet® AR20 pH meter. Total organic carbon content of the sediments was determined by the loss on ignition method (LOI; Ball, 1964). The information about the texture of the sediments was obtained from the report published by the Alberta Energy Regulator-Alberta Geological Survey (AER-AGS; Andriashek, 2003). To determine the reduced inorganic sulfur, chromium reduction method (Hsieh and Shieh, 1997) was employed that was based on the conversion of reduced inorganic sulfur to H_2S by a hot acidic $CrCl_2$ solution. The evolved H_2S was trapped in a zinc acetate solution as ZnS. This ZnS was quantified by iodometric titration. The reduced inorganic sulfur compounds determined by this method were: (1) pyrite and other metal sulfides, (2) elemental sulfur, and (3) acid volatile sulfides. The sediments were also subjected to total elemental analysis particularly for iron (Fe), calcium (Ca) and As. The samples were digested with nitric acid (trace metal grade HNO_3) in the microwave digestion unit (3050B, 1996) and analyzed using quadrupole ICP-MS.

The total As concentrations in the core sediments ranged up to 35 µg g^{-1}. Five sediment samples with low As concentration (3.5 to 6.1 µg g^{-1}) and three sediment samples with high As concentration (19.9 to 35.4 µg g^{-1}) were selected for the development of sequential extraction method. Physico-chemical properties of the sediment samples used in this study are provided in Table 3-1.

3.2.2 Chemicals and minerals

To prepare the extraction solutions for As fractionation, trace metal grade hydrofluoric acid (HF), nitric acid (HNO_3), sodium acetate (CH_3COONa; abbreviated as NaOAc), sodium phosphate (NaH_2PO_4), ammonium oxalate [$(NH_4)_2C_2O_4.H_2O$], oxalic acid ($H_2C_2O_4$), titanium (Ti^{III}) sulfate [$Ti_2(SO_4)_3$], sodium citrate ($Na_3C_6H_5O_7.2H_2O$), sodium bicarbonate ($NaHCO_3$), and ethylene-diamine-tetra-acetic acid ($C_{10}H_{14}N_2Na_2O_2.2H_2O$; abbreviated as EDTA) were purchased from Sigma-Aldrich. The extraction solutions were prepared using nanopure water (Barnstead nanopure, Thermo Scientific). The pH of the extractants, if required, was adjusted with either sodium hydroxide (NaOH) or appropriate acid (CH_3COOH; abbreviated as HOAc, $H_2C_2O_4$, or HNO_3) to bring the pH to the desired values listed in Table 3-2. The reagent blanks from all the extraction solutions were also analyzed along with the experimental samples. To test the specificity of the extractants, pure minerals of calcite and dolomite were purchased from the Ward's scientific, and natural minerals of orpiment and arsenopyrite were collected from the Mineralogy Petrology Museum from the Department of Earth and Atmospheric Sciences, University of Alberta, Canada. These minerals were grounded with agate mortar and pestle, the particle size distribution of the grounded minerals determined using laser particle size analyzer are provided in Table B-1.

3.2.3 Development and use of sequential extraction protocol

A modified sequential extraction scheme was developed by combining the fractions reported in the existing methods (Tessier et al., 1979; Keon et al., 2001; Kreidie et al., 2010). We substituted Cl^--containing extractants by those solvents that eliminated formation of polyatomic ions ($^{40}Ar^{35}Cl$) and yielded same extraction efficiency in targeting As in different solid phase constituents. Table 3-2 summarizes the fractions, target solid phases, extractants, possible mechanisms to liberate the As and the source references for the extractants used in this proposed modified sequential extraction method.

In the sequential extraction, the sediment samples were treated with different extraction solutions in a sequence to collect the individual fraction from each extractant for As analysis. For the extraction of soluble fraction of As (F1), 0.4 g sediment was added to a 50-mL Nalgene (3118-0050, Fisher Scientific) centrifuge tube along with 40 mL of nanopure water. The sediment-extractant suspension was shaken for 30 min and then centrifuged to separate the supernatant. After that 1 M NaOAc (pH 8.2, adjusted with NaOH) was added and shaken for 2 h for the extraction of loosely adsorbed As (fraction F2). For strongly adsorbed As fraction (F3), 1 M NaH_2PO_4 (pH 5, adjusted with NaOH) was used and sediment suspension was shaken for 16h, centrifuges to separate supernatant. After that the same solid phase was subjected to second extraction for 24 h. Both the supernatants were pooled for As analysis. For the extraction of As bound to carbonate minerals (fraction F4), the sediment recovered from F3 was extracted with 1 M NaOAc (pH 5, adjusted with HOAc) for 5 h and supernatant was separated after centrifugation. The As coprecipitated with amorphous Fe, Al and Mn oxyhydroxides (fraction F5) was extracted with Tamm`s reagent (0.2 M ammonium oxalate at pH 3 adjusted with oxalic acid) in the dark (tubes were wrapped with aluminum foil) for 2 h. Extractant 0.05 M Ti-citrate-EDTA-bicarbonate (pH 7, adjusted with NaOH) was used for the removal of As coprecipitated with crystalline Fe, Al and Mn oxyhydroxides (fraction F6). The suspension was shaken for 2 h and repeated twice to completely extract the As from crystalline oxides. The As associated with As oxides and silicate clays (fraction F7) was extracted using 10 M HF for 1 and 24 h (5 g boric acid (H_3BO_3) was added at 16th h of 24 h extraction). By adding H_3BO_3, HF reacts with boron (B) to produce fluoroboric acid (HBF_4), which is equivalent to HNO_3 in strength and keep the liberated As in soluble form (Wu et al., 1996). For the extraction of pyrite and amorphous orpiment coprecipitated As (fraction F8), 16 N HNO_3 was used for 2 h extraction and the process was repeated twice. To determine the organic matter- and secondary sulfide-bound As (fraction F9), the recovered sediment from previous step was extracted with 30% H_2O_2 + 1 M NH_4OAc (1:2; pH 2, adjusted with HNO_3) for 16 h. Finally, the remaining sediment sample was digested with concentrated HNO_3 in a microwave assisted digestion unit to find the residual fraction of As.

In all the extraction steps, the sediment to extractant ratio (SER) of 1:100 as reported by Keon et al., 2001 was used to ensure complete reactivity of extractant with the solid phase. A minimum SER of 1:25 was recommended by Gleyzes et al., 2002 in the extraction process. The sediment-extractant suspensions were shaken for the specified duration, and then centrifuged (Sorvall® RC-5B Refrigerated Superspeed Centrifuge with Sorvall® HS-4 rotor) for 40 min at 6000*g* to separate the supernatant. The supernatant was decanted without removing any sediment particles and filtered through 0.45-µm PTFE filters (033911C, Fisher Scientific). The sediment sample was washed with nanopure water for 30 min after completion of each extraction and before the addition of the next extractant to the sediment sample. The washing solution after centrifugation was pooled with the decanted solution of the preceding fraction. The decanted extractants were acidified (at 1% final concentration of HNO_3) to prevent any precipitation before quadrupole ICP-MS analysis. In addition to As, the developed extraction method was also evaluated for the sequential extraction of Cu, Co, Cr and Sr from all the eight sediment samples.

3.2.4 Quadrupole ICP-MS analysis

The aliquot from each fraction was analyzed for As determination using quadrupole ICP-MS (Perkin-Elmer ELAN 9000). For the quantification of As, calibration curves were developed using multi-elemental external standards (CLMS-2N, SPEX Certi Prep) in the range from 0.2 to 500 µg L^{-1} in 1% HNO_3

that represented the matrix of extraction solutions. Scandium (Sc), yttrium (Y) and terbium (Tb) were used as internal standards to account for any instrumental drift over time. The limit of detection (LOD: determined using 3 × standard deviation (σ) of intensities of 7 blanks + average of the 7 blank intensities) of quadrupole ICP-MS for As was 0.01 μg L^{-1}. The detail of the ICP-MS analysis and QA/QC is provided in section 2.2.3.

3.2.5 Method verification and reproducibility

To compare the efficiency of the developed method to the existing source methods for the determination of As associated with different fractions of sediments, one sediment sample (S6; Table 3-1) was subjected to extraction using our proposed developed scheme as well as the existing source methods (Tessier et al., 1979; Keon et al., 2001; Wenzel et al., 2001). From now onward, we will be calling those methods by their first author names. This sample was chosen for the comparison because it was the only sample that contained As in all the fractions. Some extractants used in the source methods were replaced with their own alternatives mentioned in those methods to make the extractants compatible with quadrupole ICP-MS. For Tessier method, we used sodium acetate (NaOAc) and citrate-dithionite ($C_6H_5O_7^{3-}$-$S_2O_4^{2-}$) solutions instead of $MgCl_2$ and hydroxylamine hydrochloric acid ($NH_2OH.HCl$), respectively. This replacement of extractants was done to avoid the interference of ArCl with As using quadrupole ICP-MS. The Keon and Wenzel extraction methods were carried out exactly according to their original work. The supernatant solutions derived from this comparative study were analyzed using quadrupole ICP-MS.

To facilitate the comparison of different extraction steps among four sequential extraction methods, the extraction steps in the developed method were categorized into eight groups: G1, loosely adsorbed As (sum of fractions 1 and 2); G2, strongly adsorbed As; G3, arsenic bound to carbonates; G4, arsenic coprecipitated with Fe, Al and Mn oxyhydroxide (sum of fractions 5 and 6); G5, arsenic in As oxides (As_2O_3) and silicate clays; G6, arsenic coprecipitated with pyrite (FeS_2) and amorphous orpiment (As_2S_3); G7, arsenic bound to organic matter and secondary sulfides; and G8, as residual As.

We also tested the specificity of the extractants used in our developed scheme to dissolve four pure minerals such as calcite ($CaCO_3$), dolomite [$CaMg(CO_3)_2$], orpiment (As_2S_3) and arsenopyrite (FeAsS). The dissolution of calcite and dolomite was assessed using NaOAc (pH 5) in fraction F4 and orpiment and arsenopyrite using HNO_3 in fraction F8. After the extraction, the resulting solutions were subjected to quadrupole ICP-MS analysis to determine elemental composition, and the solid phase was examined using scanning electron microscope equipped with energy dispersive x-ray spectrometer (SEM-EDX) and x-ray diffractometer (XRD). We oven dried the solid phase of pure minerals after F3 and F7 and of S6 sample after F3, F4, F7 and F8 at 105^oC. For SEM-EDX analysis, samples were mounted on a double sided carbon tape attached on the aluminum stub and then coated with carbon to prevent charging on sample surface to prevent the charging on sample surface due to the electron beam. Zeiss EVO MA 15 SEM with LaB6 crystal source was used to get highly magnified (20-100000x) micromorphology images at ~5 nm resolution. SEM was also equipped with a Bruker silicon drift detector for EDX analysis with a peak resolution of ~125 eV. For XRD, oven dried solid phase were directly mounted on zero-background plates and analyzed via Rigaku Geigerflex powder diffractometer equipped with a cobalt x-ray source, graphite monochromator and scintillator detector. Samples were scanned using X-ray (Co Kα) from 5 to 80 2-theta in continuous mode. Rest of the sequential extraction steps for amorphous and crystalline oxides of Fe and Mn were already verified and used in the previous method (Keon et al., 2001). To analyse the difference among means while comparing different methods, t-test at 95% confidence interval was performed. SAS 9.3 was used for statistical comparisons and Pearson correlation analyses.

3.3 Results and discussion

3.3.1 Arsenic fractionation

To evaluate the performance of the developed sequential extraction method for As fractionation in sediment samples, eight samples (S1-S8) of different textures (till to silty clay) and As concentrations (3.5-35 µg g^{-1}) were used in this study (Table 3-1). Arsenic fractionation (Figure 3-1) revealed that soluble fraction (F1) of As was very low (~2% of the total As) in fine-textured sediment whereas 12% of the total As was extracted in the soluble fraction from coarse sediment (S2). This finding was in agreement with the observation of (Lombi et al., 2000) who found that sand- and silt-sized particles released typically equal or larger amounts of As in soluble fraction than the clay-sized particles. Also, the pH of the sample (S2) was low (pH, 4.67) which suggested the probable dominance of the soluble $H_2AsO_4^-$ and H_3AsO_3 forms of As at low pH as compared to other sparingly soluble forms of As ($HAsO_4^{2-}$, AsO_4^{3-}, $H_2AsO_3^-$ and $HAsO_3^{2-}$) (Muhammad Sadiq, 1997).

In ionically bound fraction (F2) where As is usually loosely adsorbed on the solid particles through outer-sphere complexes, relatively higher concentrations of As (7-14% of the total As) in samples S1, S4 and S5 are probably due to medium to fine textures. Third fraction (F3) represents strongly adsorbed (inner-sphere complexation) As in sediments. The amount of As in the analyzed samples varied from 13 to 29% of the total As in F3 fraction. Keon also found this fraction dominant (~50% of the total As) in samples having diverse chemical characteristics. After the first three fractions (F1-F3), it was assumed that the entire surface adsorbed As from all solid constituents (oxides of Fe, Al and Mn, carbonates, sulfides and silicates clays) was removed and only mineral coprecipitated As remained in the sediments. A little amount of carbonate bound As (~1% of the total As) was extracted in fraction F4 because we did not find appreciable amount of carbonates in the sediments. The results of fraction F5 showed clear relationship between As coprecipitated with amorphous Fe, Al and Mn oxyhydroxides and Fe content in the sediments. The least amount of As (<1% of the total As) was extracted from sediment S2 where total Fe concentration (1.36%) was minimum. Maximum As (22% of the total As) was extracted from sediment S7 that contained maximum total Fe (Table 3-1).

Arsenic coprecipitated with crystalline Fe, Al and Mn oxyhydroxides (F6) was the most dominant As pool (30-49% of the total As) in all the low-As sediments (S1-S5). Arsenic in F6 fraction ranged between 9 and 18 % of the total

As in high-As sediments containing higher sulfide minerals (Figure 3-1 and Table 3-1). A wide range of As (6-27% of the total As) associated with As oxides and silicate clays (fraction F7) was found in the sediments. In fraction F8, As coprecipitated with pyrite and amorphous orpiment significantly correlated ($r = 0.93$, $P < 0.05$) with sulfide minerals in the sediments. Maximum As (34% of the total As) was observed in sediment S8 that contained highest sulfide content (1.8%). Organic matter and secondary sulfide bound As (fraction F9) was low in all the sediments due to low (<1%) total organic carbon, except in sediment S6 where 9% of total As was extracted in F9 probably due to shale, which was a rich source of sulfide. Finally, the residual fraction (F10) contained less than 1% of the total As in all the sediments except S6 that contained ~3% As in F10 fraction.

The pooled amount of As recovered from all the fractions using the developed method matched (~83 to 122 %) the total As in sediments extracted by acid digestion. These results are in conformity with As recoveries of 80 to 120 % (Davidson et al., 1998) and 72 to 111 % (Villanueva-Estrada et al., 2013) when sum of As from all the fractions was compared to total As concentrations. Percent distribution of As among different fractions in the sediments using the developed method (Figure 3-1) was also supported by the physicochemical properties of the sediments reported in Table 3-1.

3.3.2 Applicability of the developed method to other metals' fractionation

The developed method was also evaluated for the fractionation of Cu, Cr, Co and Sr (Figure 3-2). In the sequential extraction of Cu, amorphous and crystalline Fe, Al and Mn oxyhydroxides bound Cu (F5 and F6) were the dominant fractions in most of the sediments (Figure 3-2). Pyrite and amorphous orpiment bound Cu fraction (F8) was also dominant in S5-S8 where higher concentration of sulfides were determined (Table 3-1). Similar results about Cu distribution were reported by Tessier et al., 1979 who found dominant fraction of Cu associated with sulfides, and Fe and Al oxides. For the sequential extraction of Co, ~50 % of total Co was released in soluble fraction (F1) from sediment S4, while strongly adsorbed fraction (F3) of Co was dominant (21-49% of the total Co) in rest of the samples. Amorphous Fe, Al and Mn oxides bound (F5) Co (6–31% of total Co) was also found in all the samples whereas pyrite bound (F8) Co (7-20% of total Co) was only observed in sediments S4-S8 that contained higher sulfides. The results are in accordance with the findings of Tessier et al., 1979 who found that maximum Co was bound to Fe oxides. Chromium (Cr) and Strontium (Sr) were dominantly present in the available forms (F1 and F2) and with silicates (F7). Overall, sum of all the fractions of sequential extraction for Cu, Co, Cr and Sr (Figure 3-2) showed 96 to 104 % recoveries compared to the total concentrations of Cu, Co, Cr and Sr in sediments obtained by acid digestion (Table 3-3), which suggested the applicability of the proposed extraction method for the fractionation of these metals.

3.3.3 Comparison of the developed method to the existing fractionation methods

To compare the developed method to other extraction methods described by Tessier et al., 1979, Keon et al., 2001 and Wenzel et al., 2001, one sediment sample (S6) was sequentially extracted with all the methods (Figure 3-3 and Table

B-2; Appendix B). A few previous sequential extraction methods (Kreidie et al., 2010; Larios et al., 2012) separated soluble As as first fraction, but most commonly used sequential extraction schemes (Tessier et al., 1979; Keon et al., 2001; Wenzel et al., 2001) skipped this first step and defined their first fractions as loosely adsorbed or exchangeable As fraction. Therefore for comparing our developed method to the other methods, we pooled the data of our first two fractions (water soluble and ionically adsorbed) and defined this pooled fraction as G1 (Figure 3-3). The concentration of As in G1 (0.033 ± 0.009 $\mu g\ g^{-1}$) of our developed method was similar to the As extracted in the first fractions obtained using Tessier (0.037 ± 0.011 $\mu g\ g^{-1}$) and Wenzel (0.031 ± 0.007 $\mu g\ g^{-1}$) methods (Appendix B; Table B-2). Therefore, the application of the proposed method is advantageous because it differentiates between the immediately available As fraction (soluble As) and a fraction potentially available as a result of desorption processes (loosely adsorbed As on mineral surfaces). In our scheme, we used 1 M NaOAc (pH 8.2) for loosely adsorbed fraction of As similar to the Tessier method but in Wenzel method, 0.05 M $(NH_4)_2SO_4$ was used, which showed almost the same extraction efficiency (90 % of the developed method).

For the extraction of strongly adsorbed As fraction (G2, Figure 3-3), we used 1 M NaH_2PO_4 extraction solution (used in the Keon method) while 0.05 M $(NH_4)H_2PO_4$ was used in the Wenzel method. Strongly adsorbed As extracted using the developed (8.29 ± 0.82 $\mu g\ g^{-1}$) and Keon (9.02 ± 0.97 $\mu g\ g^{-1}$) methods were similar ($P > 0.05$) due to the same extractant and extraction conditions. Wenzel method extracted slightly less As in this fraction due to weak extractant

(0.05 M versus 1 M) and less extraction time (16h versus 40h). Tessier method did not describe extraction of strongly adsorbed As fraction.

For the determination of carbonate bound As fraction (G3, Figure 3-3 and Table B-2), we used 1 M NaOAc (pH 5) for carbonate dissolution according to the Tessier method with the only modification of using SER of 1:100 to ensure the extractant availability to target all the carbonate minerals. Wenzel method did not describe carbonate bound As fraction. Keon method used HCl but that extractant overestimated the carbonate bound As due to Cl^- contribution to polyatomic ion interference (Figure 3-3). Further, specificity of HCl for carbonate minerals is not very appropriate because it also dissolves some sulfides and overestimates carbonate bound fraction of As (Keon et al., 2001). Using the developed and Tessier methods, we extracted <1% carbonate bound As (of the total As) because carbonates in the sediments were ~1% (LOD~0.1%). Extraction of As specifically bound to carbonates is also expected to occur in F3 fraction (strongly adsorbed As extracted by 1 M NaH_2PO_4) by competitive desorption with phosphate anions (Sadiq, 1997; Smith et al., 1998).

To extract As coprecipitated with amorphous and crystalline oxyhydroxides of Fe, Al and Mn, $NH_2OH.HCl$ with reducing properties is one of the most frequently used extraction solutions. The amount of As released by this reagent depends primarily on reaction temperature and acid concentration in $NH_2OH.HCl$ solution that helps to release As in the solution (Gleyzes et al., 2002). Tessier method used this reagent but Cl^- can interfere with As if samples are analyzed using quadrupole ICP-MS. Mihaljevic et al., (2003) also showed that the recovery of As was five times higher from the extraction of synthetic minerals by using $NH_2OH.HCl$ than the expected As concentrations due to the dissolution of non-targeted minerals. Therefore for comparing G4 fraction, a solution (commonly known as citrate-dithionite) containing 0.03 M sodium dithionite ($Na_2S_2O_4$), 0.175 M sodium citrate and 0.025 M citric acid ($C_6H_8O_7$) was used for Tessier method replacing $NH_2OH.HCl$ for the extraction of (amorphous and crystalline) oxyhydroxides of Fe, Al and Mn bound As in a single fraction. Both extraction solutions have been suggested in Tessier method. Additionally, Poulton and Canfield, (2005) compared the efficiency of $NH_2OH.HCl$ and citrate-dithionite for selective dissolution of iron oxyhydroxides and demonstrated that the citrate-dithionite extraction provided the most complete dissolution of iron minerals (ferrihydrite, lepidocrocite, goethite, and hematite), whereas $NH_2OH.HCl$ dissolved only (ferrihydrite and lepidocrocite). For Wenzel method, ammonium oxalate buffer was used for amorphous (fraction F5), and ammonium oxalate buffer and ascorbic acid ($C_6H_8O_6$) were used for crystalline oxyhydroxides of Fe, Al and Mn (fraction F6). We used Tamm's reagent (ammonium oxalate/oxalic acid buffer) and Ti-citrate-EDTA-bicarbonate in our developed method according to the Keon method for the extraction of amorphous (fraction F5) and crystalline (fraction F6) Fe oxyhydroxides coprecipitated As, respectively. Fractions F5 and F6 were combined into fraction G4 for comparison. In the Tamm's reagent, ammonium (NH_4^+) induces processes of protonation and oxalate causes complexation and reduction. In Ti-citrate-EDTA-bicarbonate, Ti causes reduction; citrate and EDTA are used for complexation; and bicarbonate maintains the pH around 7. In fraction G4, we found similar As extracted (10.89 ± 1.26-12.76 ± 1.57 µg g^{-1}; $P > 0.05$) using all the four methods (Figure 3-3), which also supported the accuracy of our developed method till this fraction. Arsenic co-precipitated with amorphous and crystalline iron oxyhydroxides (Fractions 5 and 6, Table B-2) was dominant in sediments extracted with either of the methods used in this study. But in Tessier method, co-precipitated As was extracted from both amorphous and crystalline oxyhydroxides as a single fraction unable to differentiate between amorphous or crystalline Fe bound As. In the developed method, presence of higher amount of crystalline oxyhydroxides bound As (18 % of the total As) signifies importance of separating crystalline oxyhydroxides bound As as a single fraction. Müller et al., (2007) reported a significant contribution of the crystalline Fe oxides to retain As (> 45 %) in river sediments. Similar observation was reported by Larios et al., (2012) where > 20 % of As was associated with crystalline Fe oxides in an industrially polluted damping site. Because these minerals (Fe, Al and Mn oxides) are regarded as important As scavengers in soils and sediments, sequential extraction of As from amorphous and crystalline Fe oxides is suggested (Xu et al., 1991).

Though Fe oxyhydroxides appear to dominate in As sorption process in soils, other constituents including such as silicate clay minerals (kaolinite and montmorillonite) are also capable of retaining or complexing As species (Goldberg and Glaubig, 1988). The type and quantity of silicate minerals present in soils or sediments also influence the retention of As. The degree of As sorption onto silicate minerals decreases in the order of kaolinite > vermiculite >

montmorillonite (Goldberg & Glaubig, 1988; BA Manning & Goldberg, 1997). Besides silicates bound As, arsenic oxides are also one of the major secondary As minerals formed by oxidation of arsenopyrite and native arsenic (Smedley & Kinniburgh, 2002a). For the extraction of As associated with As oxides and silicate clays (G5, Figure 3-3) in the developed method, 10 M HF was adopted as an extraction solution from the Keon method. HF has the ability to dissolve silicate minerals but it does not react with pyrite (Eghbalnia, 2012). Thus, it is appropriate to have 10 M HF extraction step before the extraction of pyrite and amorphous sulfide bound As. Arsenic extracted in this fraction by the developed (2.79 ± 0.07 $\mu g\ g^{-1}$) and Keon method (2.8 ± 0.11 $\mu g\ g^{-1}$) was in agreement. This fraction was not described in the Tessier and Wenzel methods (Table B-2).

Sulfide minerals are very insoluble and most of the methods (Tessier et al., 1979; Hall et al., 1996; Larios et al., 2012) relegate sulfide bound As to the residual fraction. But biogeochemical redox processes can release sulfide bound As (Eghbalnia, 2012). Therefore, As coprecipitated with pyrite and amorphous orpiment (fraction G6) was also extracted using 16 N HNO_3 according to Keon method. The results (Figure 3-3) reported similar As concentrations in G6 using both the developed (8.21 ± 0.47 $\mu g\ g^{-1}$) and Keon (7.72 ± 0.29$\mu g\ g^{-1}$) methods due to similar extraction conditions. Other methods did not describe this fraction. HNO_3 has the ability to react with uncoated or available pyrite only. If there is any recalcitrant sulfide covered with organic matter, HNO_3 cannot dissolve that sulfide minerals (Steel & Patrick, 2001). For this reason, arsenic co-precipitated with pyrite and amorphous orpiment was extracted first and then organic matter and secondary sulfide bound As was extracted in a separate fraction afterward.

For the extraction of organic matter and recalcitrant sulfide bound As (fraction G7), we used H_2O_2+NH_4OAc (pH 2) adopted from the method described by Kreidie et al., 2010 while Tessier method used H_2O_2+HNO_3 (pH 2) for the extraction of organic matter associated As. The strong oxidizing action of H_2O_2 in acidic medium is frequently employed for oxidation of organic material and refractory sulfides in sequential extraction. Arsenic extracted in this fraction was low in the developed method (2.91± 0.62 $\mu g\ g^{-1}$) compared to the Tessier method (9.63 ± 1.06 $\mu g\ g^{-1}$) because Tessier methods skipped some previous extraction steps (G2, G5 and G6, Figure 3-3). Tessier et al., (1979) also suggested separation of pyrite bound metals before the application of organic matter extraction step. Hall et al., (1996) used a combination of H_2O_2, NaOAc and HNO_3 for the extraction of As associated with sulfides and organic matter in spiked samples. They also compared their results with Tessier method which overestimated As due to the dissolution of sulfide minerals.

High concentrations of As were determined in the residual fractions extracted using Tessier (12.32 ± 1.58 $\mu g\ g^{-1}$) and Wenzel (16.24 ± 0.82 $\mu g\ g^{-1}$) methods compared to our developed method (0.9 ± 0.2 $\mu g\ g^{-1}$; G8, Figure 3-3). Because Tessier and Wenzel methods skipped previous extraction steps for silicate clay (G5) and sulfide bound (G6) As, the residual fractions in these methods might contain silicate and sulfide bound As. Tessier et al., (1979) defined their residual fraction as primary and secondary minerals including silicates and recalcitrant sulfides. The sum of G5 and G6 (~11.0 ± 0.4 μg g^{-1}) in our method corresponds to the As in residual fraction of Tessier method showing the advantage of our proposed scheme. Similarly, Mihaljevic et al., (2003) found elevated As concentrations in the residual fraction of spiked samples using Tessier method and attributed this higher concentration to arsenopyrite that was insufficiently extracted (oxidized) before As extraction in the residual fraction.

3.3.4 Assessment of the developed method for the dissolution of targeted minerals in pure phase and sediment

Four pure minerals such as calcite, dolomite, arsenopyrite and orpiment were sequentially extracted by applying the developed method. The dissolution of carbonate minerals (calcite and dolomite) were expected in fraction F4. Chemical analysis **(**data not shown**)** of the extraction solution revealed complete dissolution (~94%) of pure calcite in F4 using 1 M NaOAc (pH 5) as an extractant and no dissolution occurred in F3 (strongly adsorbed As). The SEM-EDX images (Figures 3-4 A-C) substantiated the persistence of calcite in F3. But F3 fraction might include some carbonate bound As particularly from dolomite because ~50% of the pure dolomite was dissolved in F3 fraction. Evidence of dolomite dissolution was also observed by SEM–EDX (Figures 3-4 D-F), where magnesium (Mg) intensity decreased after extraction with 1 M NaH_2PO_4 (F3). But in the S6 sediment (Figure B-1), similar Ca and Mg intensities of EDX were observed whether or not the sediment was extracted with 1 M NaH_2PO_4 though the intensities of these peaks were very small probably due to very low (<1%) carbonate minerals. These peaks were not detected after 1 M NaOAc (pH 5) extraction suggesting dissolution of carbonates in F4.

Fraction F8 in sequential extraction scheme determines As bound in sulfide minerals using 16 N HNO_3 as extractant. To evaluate if any dissolution of sulfide minerals (amorphous orpiment and arsenopyrite) occurs in F7, pure minerals (orpiment and pyrite) were extracted using 10 M HF. The SEM-EDX (Figures 3-5 and B-2) results suggested that these minerals were not dissolved in F7. SEM analysis revealed two mineral phases in untreated orpiment (Figures 3-5 A-B). Both the phases remained unaffected during 10 M HF extraction (Figures 3-5 C-F) which showed the stability of orpiment in 10 M HF. XRD diffractograms also showed the existence of these minerals when solid phase was analyzed by XRD before and after the extraction with 10 M HF (Figure B-3). Arsenopyrite did not dissolve in F7 as evident from SEM-EDX (Figure B-2) and XRD (Figures B-3 C-D) analyses. However, around 99 % amorphous orpiment and ~ 96 % arsenopyrite (determined by chemical analysis; data not shown) were only dissolved by 16 N HNO_3 in F8. Similar results were found in S6 sediment (Figure B-4), where no change in Fe:S ratio was observed before and after 10 M HF extraction.

3.4 Conclusions

The developed sequential extraction method can predict ~97% distribution or partitioning of total As in nine different meaningful pools associated with different solid constituents. The extractants used in the developed method are compatible with quadrupole ICP-MS eliminating interference from polyatomic ions during As analysis. This extraction scheme can also be employed for the fractionation of other metals such as Cu, Co, Cr and Sr. The applicability and utility of this method can further be augmented by testing this developed protocol for metal characterization in samples collected from different geo-environmental conditions.

Literature cited

Alam M. B., Sattar M. A. Assessment of arsenic contamination in soils andwaters in some areas of Bangladesh. Water Sci Technol. 2000;42:185–193.

Andriashek L. D. Quaternary geological setting of the Athabasca Oil Sands (in situ) area, Northeast Alberta. 2003. http://www.ags.gov.ab.ca/publications/ESR/PDF/ESR_2002_03.pdf

Ball D. F. Loss-on-ignition as an estimate of organic matter and organic carbon in non-calcareous soils. J soil Sci 1964;15(1):86-92.

Davidson C. M., Duncan A. L., Littlejohn D., Ure A. M., Garden L. M. A critical evaluation of the three-stage BCR sequential extraction procedure to assess the potential mobility and toxicity of heavy metals in industrially-contaminated land. Anal Chim Acta. 1998;363(1):45–55.

Dhar R. K., Zheng Y., Rubenstone J., Van-Geen A. A rapid colorimetric method for measuring arsenic concentrations in groundwater. Anal Chim Acta. 2004;526(2):203–209.

Eghbalnia M. Electrochemical and raman investigation of pyrite and chalcopyrite oxidation. Ph.D. Thesis. University of British Columbia. 2012.

Gleyzes C., Tellier S., Astruc M. Fractionation studies of trace elements in contaminated soils and sediments: a review of sequential extraction procedures. TrAC Trends Anal Chem. 2002;21(6-7):451–67.

Goldberg S., Glaubig R. Anion sorption on a calcareous, montmorillonitic soil—arsenic. Soil Sci Soc Am. 1988;52:1297–300.

Goossens J., Vanhaecke F., Moens L., Dams R. Elimination of interferences in the determination of arsenic and selenium in biological samples by inductively coupled plasma mass spectrometry. Anal Chim Acta. 1993;80:137–143.

Hall G. E. M., Vaive J. E., Beer R., Hoashi M. Selective leaches revisited, with emphasis on the amorphous Fe oxyhydroxide phase extraction. J Geochemical Explor. 1996;56(1):59–78.

Health Canada (2006), Guidelines for Canadian drinking water quality: Guideline technical document-Arsenic. Water Quality and Health Bureau, Healthy Environments and Consumer Safety Branch, Health Canada, Ottawa, Ontario.

Hsieh Y. P., Shieh Y. N. Analysis of reduced inorganic sulfur by diffusion methods: improved apparatus and evaluation for sulfur isotopic studies. Chem Geol 1997;137(3-4):255–261.

Keon N. E., Swartz C. H., Brabander D. J., Harvey C., Hemond H. F. Validation of an arsenic sequential extraction method for evaluating mobility in sediments. Environ Sci Technol 2001;35(13):2778–2784.

Kreidie N., Armiento G., Cibin G., Cinque G., Crovato C., Nardi E., Pacifico R., Cremisini C., Mottana, A. An integrated geochemical and mineralogical approach for the evaluation of arsenic mobility in mining soils. J Soils Sediments. 2010;11(1):37–52.

Larios R., Fernández-Martínez R., Rucandio I. Comparison of three sequential extraction procedures for fractionation of arsenic from highly polluted mining sediments. Anal Bioanal Chem. 2012;402(9):2909–21.

Lombi E., Sletten R., Wenzel W. Sequentially extracted arsenic from different size fractions of contaminated soils. Water Air Soil Pollut. 2000;1:319–332.

Manning B., Goldberg S. Adsorption and stability of arsenic (III) at the clay mineral-water interface. Environ Sci Technol. 1997;31(7):2005–2011.

Mihaljevic M., Ponavic M., Ettler V., Sebek O. A comparison of sequential extraction techniques for determining arsenic fractionation in synthetic mineral mixtures. Anal Bioanal Chem. 2003;377(4):723–9.

Mitchell P., Barre D. The nature and significance of public exposure to arsenic: a review of its relevance to South West England. Environ Geochem Health. 1995:57–82.

Müller K., Daus B., Morgenstern P., Wennrich R. Mobilization of antimony and arsenic in soil and sediment samples – evaluation of different leaching procedures. Water Air Soil Pollut. 2007;183(1-4):427–36.

Niemelä M., Perämäki P., Kola H., Piispanen J. Determination of arsenic, iron and selenium in moss samples using hexapole collision cell, inductively coupled plasma–mass spectrometry. Anal Chim Acta. 2003;493(1):3–12.

Oremland R. S., Stolz J. F. The ecology of arsenic. Science. 2003;300(5621):939–44.

Poulton S., Canfield D. Development of a sequential extraction procedure for iron: implications for iron partitioning in continentally derived particulates. Chem Geol. 2005;214(3-4):209–21.

Sadiq M. Arsenic chemistry in soils: an overview of thermodynamic predictions and field observations. 1997;93:117-136.

Smedley P. L., Kinniburgh D. G. A review of the source, behaviour and distribution of arsenic in natural waters. 2002;17(5):517–568.

Smith E., Naidu R., Alston A. Arsenic in the soil environment: a review. Adv Agron. 1998; 64: 149-195.

Steel K. M., Patrick J. W. The production of ultra clean coal by chemical demineralisation. Fuel. 2001;80(14):2019–23.

Sumner M. E. Measurement of soil pH: Problems and solutions. Commun Soil Sci Plant Anal 1994; 25(7-8):859–879.

Tessier A., Campbell P. G. C., Bisson M. Sequential extraction procedure for the speciation of particulate trace metals. Anal Chem 1979;51(7):844–851.

Thomas R. Practical guide to ICP-MS: A tutorial for beginners. 2008.

US EPA. Method 3050B acid digestion of sediments, sludges, and soils. Washington, D.C.: U.S. Environmental Protection Agency; 1996.

Villanueva-Estrada R. E., Prol-Ledesma R. M., Rodríguez-Díaz A. A., Canet C., Armienta M. A. Arsenic in hot springs of Bahía Concepción, Baja California Peninsula, México. Chem Geol. 2013;348:27–36.

Wenzel W. W., Kirchbaumer N., Prohaska T., Stingeder G., Lombi E., Adriano D. C. Arsenic fractionation in soils using an improved sequential extraction procedure. Anal Chim Acta. 2001;436(2):309–323.

Wu S., Zhao Y., Feng X., Wittmeier A. Spectrometry for total metal determination in silicon-containing solid samples using the microwave-assisted nitric acid–hydrofluoric acid–hydrogen peroxide–boric acid. Anal At Spectrom. 1996;11:287–96.

Xu H., Allard B., Grimvall A. Effects of acidification and natural organic materials on the mobility of arsenic in the environment. Water Air Soil Pollut. 1991;57-58:269–78.

Tables and figures

Table 3- 1. Selected physicochemical properties of the sediments used to develop the sequential extraction method for arsenic fractionation.

Sample	S1	S2	S3	S4	S5	S6	S7	S8
As(μg g^{-1})	4.9±0.7	5.4±0.5	4.2±0.1	6.1±0.6	3.6±0.8	35.5±5.8	19.9±4.2	24.4±6.2
Fe(%)	2.4±0.4	1.5±0.2	1.9±0.5	2.8±0.8	2.2±0.3	3.0±0.5	4.0 ±0.5	3.0±0.4
Ca(%)	1.9±0.4	0.1±0.1	0.3±0.2	1.1±0.2	0.9±0.4	0.8±0.2	0.8±0.4	0.4±0.1
Sulfide(%)	0.1±0	0.1±0	0.1±0.1	0.3±0.2	0.7±0.2	1.4±0.3	1.1±0.1	1.8±0.4
Texture[a]	Sandy clay	Till	Oxidized till	Silty clay	Silty clay	Shale	Clayey till	Clayey till
Sand(%)	- [b]	40	29	5	4	-	30	33
Silt(%)	-	42	46	75	77	-	43	45
Clay(%)	-	18	25	20	19	-	27	22
pH[c]	7.0	4.7	7.2	7.2	7.3	7.1	6.2	6.8
TOC(%)	0.3	0.1	ND	0.6	0.6	ND	0.8	0.6

Values represent the mean from analysis of triplicate ± 1 standard deviation.

[a] information about texture was obtained from a report ESR 2002-03 (Andriashek, 2003) [18]

[b] texture analysis was not performed

[c] pH was measured in suspension of sediment:0.05 M $CaCl_2$ (1:5)

TOC: total organic carbon; ND: not detected

Table 3- 2. Modified sequential extraction procedure for arsenic fractionation.

Fraction	Target phase	Extractant[¶]	Possible mechanism	Source ref.
F1	Soluble As	D.I water	dissolution with water	a
F2	Loosely adsorbed/ Exchangeable As	1 M NaOAc, pH 8.2	anion exchange of acetate for As	b
F3	Strongly/Specifically adsorbed As	1 M NaH_2PO_4, pH 5	anion exchange of PO_4^{3-} for $AsO_4^{3-}$and AsO_3^{3-}	c
F4	Carbonate bound As	1 M NaOAc, pH 5	dissolution of carbonate minerals to liberate As	b
F5	As co-precipitated with amorphous Fe, Al and Mn Oxyhydroxide	Tamm`s reagent (ammonium oxalate/ oxalic acid, pH 3)	ligand promoted complexation and dissolution of Fe, Al Mn oxyhydroxide	c
F6	As co-precipitated with crystalline Fe, Al and Mn oxyhydroxide	Ti-citrate-EDTA-bicarbonate, pH 7	Ti induced reduction of Fe^{3+} to Fe^{2+}	c
F7	As associated with As oxides and silicate clays	10 M HF	dissolution of silicate clays and As oxides	c
F8	As coprecipitated with pyrite and amorphous orpiment	16 N HNO_3	oxidation of pyrite and amorphous sulfides	c
F9	Organic matter and secondary sulfides	30% H_2O_2 + 1 M NH_4OAc (1:2), pH 2	oxidation of organic matter and secondary sulfides bound As	a
F10	Residual As	concentrated HNO_3	microwave assisted digestion	d

[¶] Extractants were added to sediments in sequential order (F1-F10) and the supernatant was removed after extraction and centrifugation. Sediments were washed with nanopure water by extraction for 30 min after removing each extractant. The water was separated by centrifugation and pooled with the decanted supernatant of the each preceding extractant.

a) Kreidie et al., (2010); b) Tessier et al., (1979); c) Keon et al., (2001); d) US EPA

Table 3- 3. Total concentrations of Cu, Co, Cr and Sr in the sediments.

Sample	Cu (μg g^{-1})	Co (μg g^{-1})	Cr (μg g^{-1})	Sr (μg g^{-1})
S1	15.6±0.8	8.1±0.3	42.0±2.7	46.0±1.6
S2	15.0±0.4	2.6±0.1	38.6±1.8	21.0±1.0
S3	13.1±0.1	5.9±0.4	20.1±0.7	29.0±0.8
S4	23.1±0.7	9.9±0.1	74.7±4.9	79.0±2.0
S5	27.0±0.3	7.7±0.3	32.8±1.8	45.0±1.4
S6	22.3±5.1	11.6±0.4	46.8±1.0	81.0±3.2
S7	32.2±1.0	7.5±0.1	71.8±2.9	79.8±2.4
S8	17.9±0.7	9.1±0.2	127.4±6.5	64.0±1.8

Values represent the mean from analysis of triplicate ± 1 standard deviation.

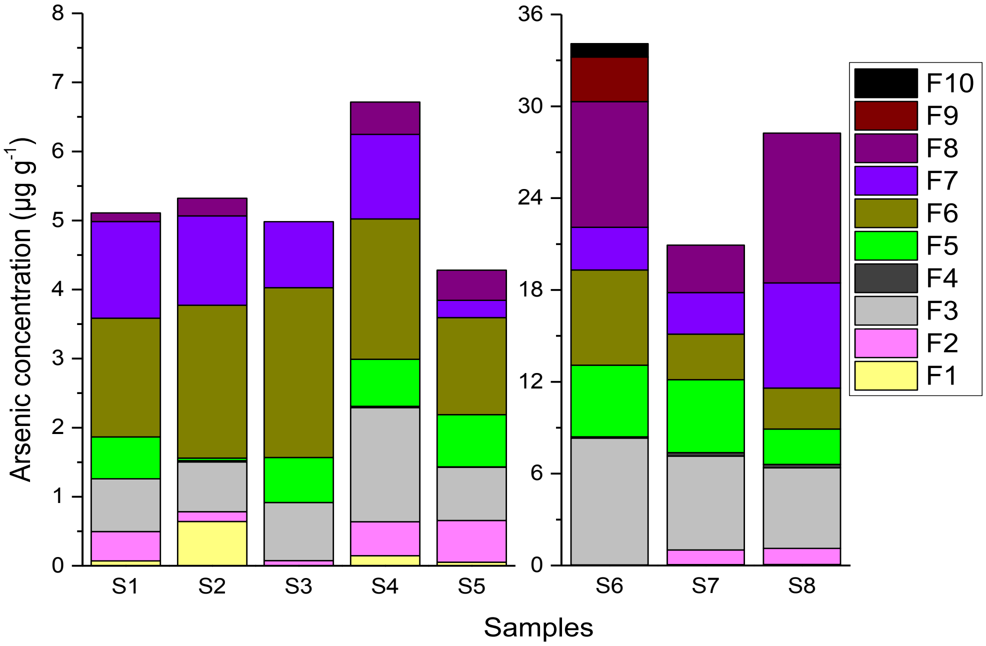

Figure 3- 1. Application of the developed sequential extraction method for arsenic fractionation in sediments.

F1, water soluble As; F2, ionically bound As; F3, strongly adsorbed As; F4; arsenic bound to carbonates; F5, arsenic coprecipitated with amorphous Fe, Al and Mn oxyhydroxides; F6, arsenic coprecipitated with crystalline Fe, Al and Mn oxyhydroxides; F7, arsenic associated with As oxides and silicate clays; F8, arsenic coprecipitated with pyrite and amorphous orpiment; F9, arsenic associated with organic matter and recalcitrant sulfides; F10, residual As.

Sum of As fractions extracted by the developed method varied from 83-122% of the total As extracted by the acid digestion in the sediments used in this study.

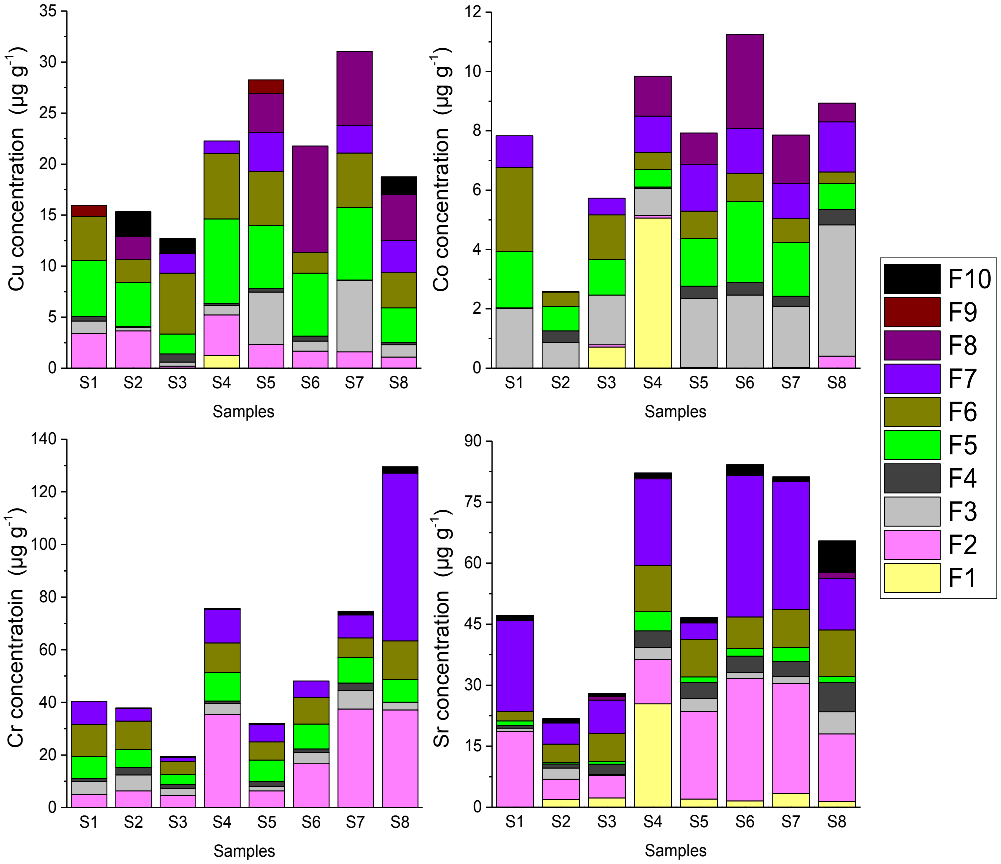

Figure 3- 2. Fractionation of Cu, Co, Cr and Sr by the developed method.

F1, water soluble metals; F2, ionically bound metals; F3, strongly adsorbed metals; F4; metals bound to carbonates; F5, metals coprecipitated with amorphous Fe, Al and Mn oxyhydroxides; F6, metals coprecipitated with crystalline Fe, Al and Mn oxyhydroxides; F7, metals associated with metal oxides and silicate clays; F8, metals coprecipitated with pyrite and amorphous orpiment; F9, metals associated with organic matter and recalcitrant sulfides; F10, residual metals.

Sum of all the sequential extraction fractions of all four elements in sediments varied from 96-104% as compared to the total elemental concentrations determined by the acid digestion.

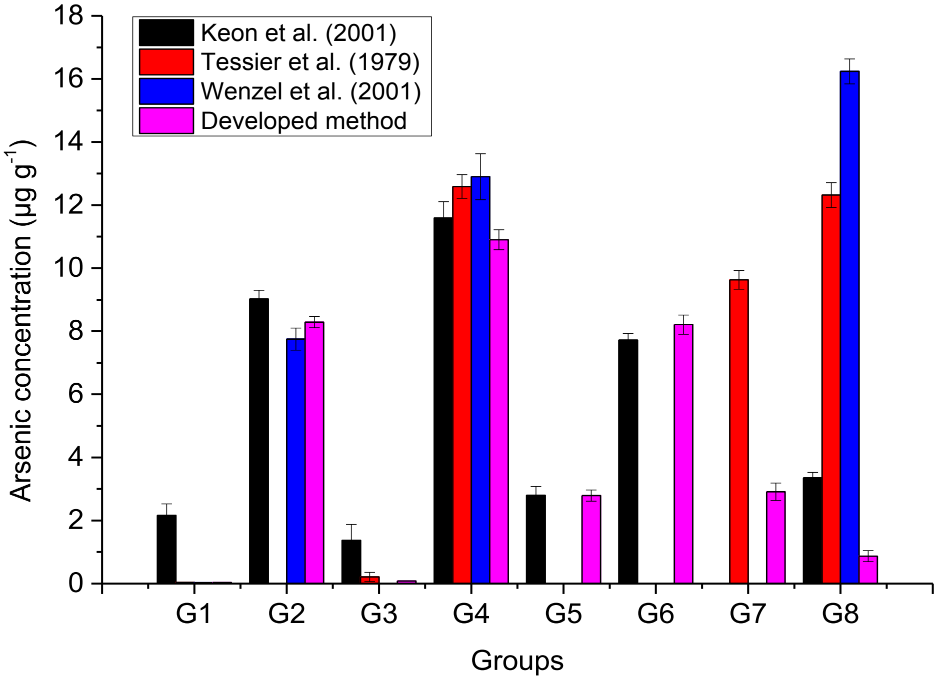

Figure 3- 3. Comparison of the developed sequential extraction method to the existing Keon et al., (2001), Tesseir et al., (1979) and Wenzel et al., (2001) methods for arsenic fractionation in sediment S6.

To facilitate the comparison of different extraction steps among four sequential extraction methods, the extraction steps were presented in eight groups: G1, loosely adsorbed As; G2, strongly adsorbed As; G3, arsenic bound to carbonates; G4, arsenic coprecipitated with Fe, Al and Mn oxyhydroxides; G5, arsenic associated with As oxides and silicate clays; G6, arsenic coprecipitated with pyrite and amorphous orpiment; G7, arsenic associated with organic matter and recalcitrant sulfides; G8, Residual As. For detailed comparison of the sequential extraction methods, see Table B-2.

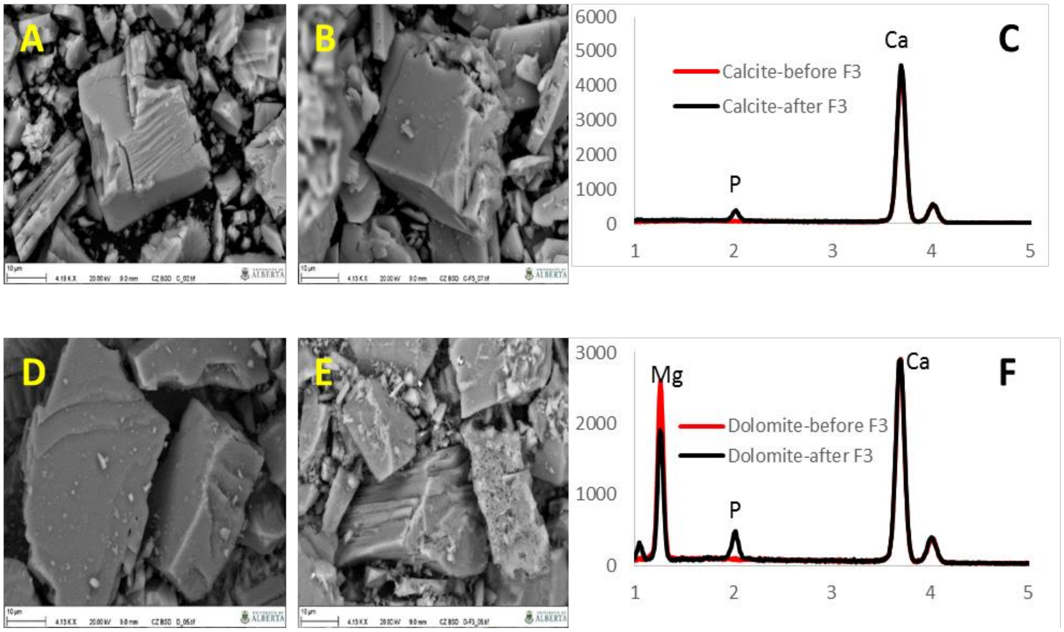

Figure 3- 4. SEM-EDX analysis of calcite (A-C) and dolomite (D-F) minerals to test their solubility using 1 M NaH_2PO_4 (pH 5) extraction.

(A) and (B) are SEM images of calcite mineral before and after 1 M NaH_2PO_4 (pH 5) extraction, respectively, along with EDX spectrum (C) which showed no evidence of calcite dissolution in F3. (D) and (E) are SEM images of dolomite mineral before and after 1 M NaH_2PO_4 (pH 5) extraction, respectively, along with EDX spectrum (F). These images showed sign of NaH_2PO_4 attack on dolomite mineral.

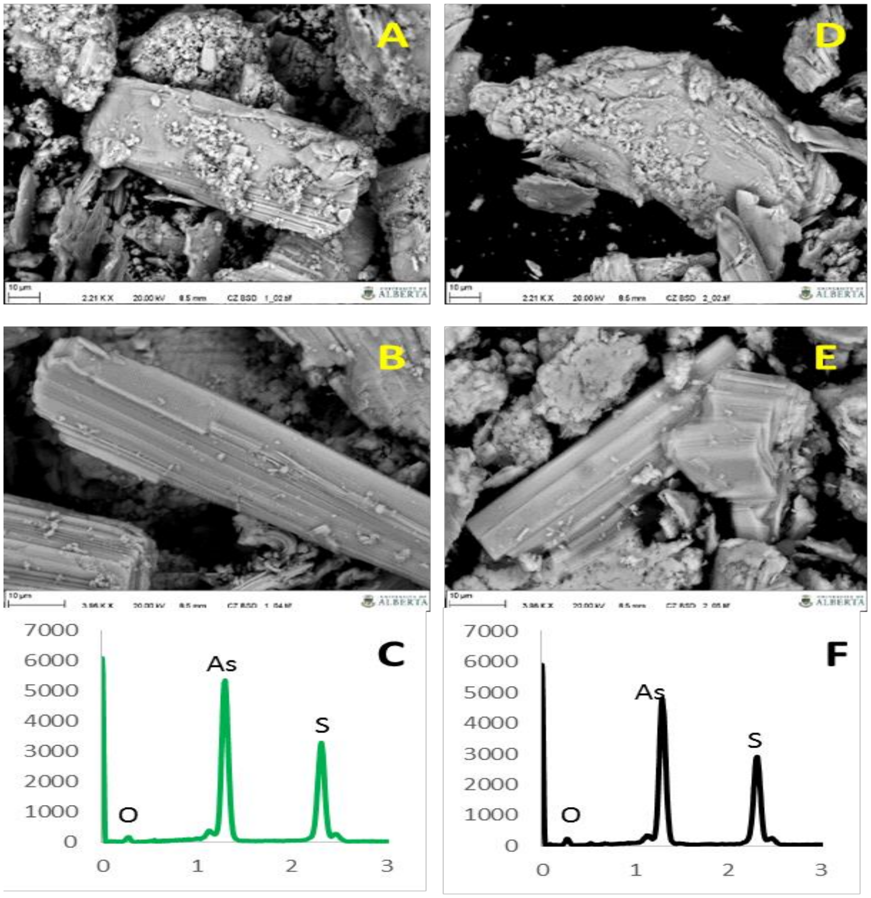

Figure 3- 5. SEM-EDX analysis of orpiment mineral to test the dissolution of orpiment in HF extraction.

In orpiment, two types of mineral phases were observed. SEM images (A) and (B) reveal two different phases in orpiment minerals along with EDX spectrum (C) before any extraction with 10 M HF. (D) and (E) are corresponding SEM images of those two phases (A) and (B), respectively after HF extraction. (F) shows EDX of HF extracted orpiment mineral. Both the phases were found after HF extraction, which showed the stability of orpiment in 10 M HF. After F8, all the solid phase was dissolved and there was not enough material for SEM analysis.

Chapter 4. Fractionation of arsenic and other trace elements in sediments[3]

4.1 Introduction

Arsenic (As) contamination in natural ecosystems such as soil, sediment, surface- and ground-water is a global concern because As persist and impart toxicity to the environment (He et al., 2005). High As concentrations >10 µg L^{-1} (the maximum acceptable concentration in Canada; Health Canada, 2006) have been found in groundwater in the Cold Lake area (Stein et al., 2000), which is extensively used for household, agriculture and industrial purposes (Lemay et al., 2005). It is agreed that As contamination in groundwater usually originates geogenically from sediments (Nickson et al., 2000). Generally, high levels of As in groundwater are attributed to the sulfide-rich high As aquifers (Wang and Mulligan, 2006). Arsenic is naturally enriched in shale containing pyrite (FeS_2, which is considered the principle carrier of elements in rocks) and other minerals such as arsenopyrite (FeAsS), enargite (Cu_3AsS_4), scorodite ($FeAsO_4.2H_2O$), galena (PbS) and annabergite [$(Ni)_3(AsO_4)_2$] (Boyle and Jonasson, 1973). Weathering and biological transformation of these As containing minerals in sediments under natural conditions mobilize As in the environment.(Smedley and Kinniburgh, 2002; Muloin and Dudas, 2005).

---

[3] A version of this chapter combined with chapter 2 comprised of arsenic data has been published in “Science of the total environment” journal.
Another version of this chapter combined with chapter 2 comprised of all the other elements data (excluding arsenic) is in preparation to submit for publication.

Traditional risk assessment of As contamination in surface- and groundwater is generally based on total As concentrations in soil and sediment (Murphy et al., 2000). However, the interaction of As with different solid constituents in soil and sediment is principal controlling factor of As contamination in water, particularly under the natural conditions. The distribution of As in soil or sediment, and its mobility in porewater and potential to contaminate groundwater are mostly related to iron (Fe), aluminum (Al) and (manganese) Mn oxides, carbonates, organic matter and sulfides with which metals are associated (Larios et al., 2012). Adsorption and coprecipitation of As with oxyhydroxides of Fe, Al and Mn are the most important processes that immobilize As under oxidized conditions (Larios et al., 2012; Javed et al., 2013). However under reducing conditions, reductive dissolution of these oxyhydroxides release sequestered As into the environment (Tessier et al., 1979). Carbonate minerals and organic matter in soil or sediment can also act as sources of As contamination in aquatic ecosystems through the processes of acidification (low pH) and oxidation, respectively (Huang and Kretzschmar, 2010). Sulfide minerals are a good scavenger of As under reduced conditions, but their oxidative breakdown can release the associated metals into the porewater (Larios et al., 2012). In addition to the natural process, anthropogenic activities such as mining and smelting can enhance metals release by exposing the unoxidized minerals to the atmosphere and make them vulnerable to weathering (Smedley and Kinniburgh, 2002). However, part or all of the released metals may occlude in the resulting metastable secondary minerals such as scorodite ($FeAsO_4.2H_2O$; Sadiq, 1997) for

As, and diminish the danger of groundwater contamination. Sequential extraction procedure can provide the information of the distribution of the metals in different solid phases of soil and sediment (Tessier et al., 1979).

Because the association of As with different solid constituents in sediments in the Cold Lake area of Alberta is still unknown, a comprehensive investigation was performed to gain insight into the As fractionation in surficial deposits (Quaternary glacial sediments). Mineralogical and spectroscopic techniques were also employed to validate the fractionation results.

4.2 Experimental section

4.2.1 Reagents and minerals

All the reagents used for the preparation of extraction solutions were trace metal grade purchased from Sigma-Aldrich (Ontario, Canada), and all the solutions were prepared using nanopure water (Barnstead nanopure, Thermo Scientific). The pH of the extractant solution, if required, was adjusted to the desired level with either sodium hydroxide (NaOH) or appropriate acid (HOAc, $H_2C_2O_4$ or HNO_3). The detail of the reagents are provided in sections 2.2.1 and 3.2.2. The reagent blanks from all the extraction solutions were also analyzed along with the experimental samples and concentrations of all the elements were lower than their detection limits (≤ 0.075 µg L^{-1}) in all solutions. All laboratory glass-and plastic-ware was cleaned by soaking in 5% (v/v) HNO_3 overnight and then repeatedly rinsed with nanopure water.

Pure phases of sodium arsenate [$Na_3As(V)O_4$], sodium arsenite [$Na_3As(III)O_3$] and arsenic oxide [$As_2(III)O_3$] were purchased from Sigma-Aldrich (Ontario, Canada). Natural minerals such as annabergite [$Ni_3(As(V)O_4)_2$], orpiment [$As_2(III)S_3$] and arsenopyrite [FeAs(III)S] were collected from the Mineralogy Petrology Museum in the Department of Earth and Atmospheric Sciences at the University of Alberta, Canada. These salts and minerals were used to obtain X-ray diffraction (XRD) patterns and X-ray absorption near edge structure (XANES) white line energy positions (As absorption edge energy) of arsenite (As^{III}) and arsenate (As^{V}) for comparison with the sediment As.

4.2.2 Sequential extraction of arsenic from sediments

After determination of total As concentrations, 22 sediments were chosen from different cores (shown in Figure 2-2) based on their As concentrations. We grouped the selected sediments in low As (<7 $\mu g\ g^{-1}$ As; samples 1-9) and high As sediments (>7 $\mu g\ g^{-1}$ As; samples 10-22). Shale is considered a source of high As in sediments that contains an average As of 10 to 15 $\mu g\ g^{-1}$ (Krauskopf, 1979; Boyle and Jonasson, 1973). The lowest As concentration (~7 $\mu g\ g^{-1}$) found in our shale sediments was used for demarcation between designated low and high As sediments. However, average As concentrations in different uncontaminated Canadian soils (4.8 to 13.6 $\mu g\ g^{-1}$ As) and sediments (6 to 100 $\mu g\ g^{-1}$ As) varies (Wang and Mulligan, 2006). Both low (As <7 $\mu g\ g^{-1}$; samples 1-9) and high As sediments (As >7 $\mu g\ g^{-1}$; samples 10-22) were selected for further chemical, mineralogical and spectroscopic investigation. Detailed information of the selected 22 sediments is provided in Table 2-1. To study different phases of As and other elements (soluble, exchangeable, bound to carbonates, associated with amorphous and crystalline Fe and Mn oxyhydroxides, associated with sulfides and organic matter; see detail in Table 3-2) in sediments, sequential extraction procedure (SEP; Javed et al., 2013) was applied to the selected sediments. Briefly, sediments (0.4 g) were sequentially extracted with 40 mL of the extractants for appropriate period of time as given in Table 3-2. The sediment-extractant suspensions were shaken for the specified duration, and then centrifuged (Sorvall® RC-5B Refrigerated Superspeed Centrifuge with Sorvall® HS-4 rotor) for 40 min at 6000*g* to separate the supernatants, which were decanted without removing any sediment particles and filtered through 0.45-µm PTFE filters. The sediments were washed with nanopure water for 30 min before adding the next extractant. After centrifugation, the washing solutions were pooled with their respective decanted solutions, acidified (1% final concentration of HNO_3), and analyzed for selected elements using quadrupole ICP-MS.

4.2.3 X-ray diffraction (XRD) of sediments

XRD (RIGAKU RU-200B) coupled with Cu X-ray source and scintillator detector was used to determine the bulk (silicate and non-silicate) mineralogy of sediments. Fine powdered samples of high (samples 11, 14 and 17) and low As sediments (samples 1, 2 and 9) were mounted on holder and scanned using Cu Kα X-ray from 4 to 100 2θ with a 0.05 2θ step-size and 4 seconds count-time per step. Because most As minerals such as FeAsS are very fine-grained (30-50 µm) and less abundant (<1 wt%) in natural sediments making them difficult to be determined using conventional XRD (Flemming, 2005). High energy synchrotron radiation (VESPER beam-line) at Canadian Light Source (CLS), University of Saskatchewan (Feng et al., 2010) was used to determine As minerals by applying micro (µ) XRD. For µ-XRD, standard minerals and sediments in Kapton tape were scanned under high energy radiation (~11.867 KeV). Diffracted X-rays were detected by 2D detector (GADDS) positioned at a distance of ~45 cm from the sample intersecting a 45° segment of diffraction space. Diffracted lines and spots from each lattice plane (*hkl*) of minerals produced an arc of radius 2θ (*hkl*) on GADDS image, and the intensity of diffracted lines and spots along each arc was integrated to create a plot of intensity versus 2θ. Jade and XMAS software were used for the analyses of XRD and µ-XRD data, respectively to identify the minerals.

4.2.4 X-ray absorption near edge structure spectroscopy (XANES) of sediments

To determine the dominant oxidation state of As in the sediments, arsenic K-edge XANES data was collected at the CLS. All the low (samples 1-9) and high As sediments (samples 10-22) were prepared in the same way as described for µ-XRD analysis. Six standards including sodium arsenate (As^{V}; absorption edge at 11874.2 eV), annabergite (As^{V}; 11874 eV), arsenic oxide (As^{III}; 11871 eV), sodium arsenite (As^{III}; 11870.5 eV), orpiment (As^{III}; 11868.4 eV) and arsenopyrite (As^{III}; 11868 eV) were analyzed to generate white line energy positions of As^{V} and As^{III} to compare with the sediment As white lines to determine the oxidation state of As in sediments. Most sediments generated white line energy position close to 11868 eV that corresponded well to As^{III} (Kachenko, 2010). Five scans from each standard and sediment sample were collected in the XANES region using a 4-element detector in fluorescence mode. Analysis of standards and sediments XANES spectra including smoothing, normalization and averaging the five raw spectra was carried out using Athena (Ifeffit, v.1.3) software. Athena was also used for linear combination fit (LCF) analysis (Shah et al., 2007) of sediments XANES spectra to determine the proportion of As^V and As^{III} present in the sediments. The goodness and quality of LCF of sediment among possible combinations of standards were assessed calculating the R-factor value that was equivalent to the normalized sum of the residuals (Manning, 2005).

4.2.5 X-ray fluorescence (XRF) and scanning electron microscopy (SEM) of sediments

To determine the spatial association of As and Fe, a 2×2 mm sample area of high As sediment (sediment 11; 24.9±4.2 μg As g^{-1}) prepared for μ-XRD was used for XRF mapping at VESPER beam-line using 0.2 mm step size and 5 seconds scan-time per step. To study the micromorphology of selected high As sediments, a high spatial resolution (~3 nm) JEOL (Field Emission) SEM equipped with energy dispersive X-ray spectrometer (EDX) was used at the University of Alberta. JEOL SEM was used to get high-resolution digital images of surface textures and microstructures, at magnifications ranging from 20x to 250,000x with a resolution of approximately ~3 nm. Powdered sediment samples were mounted on aluminum stub using a double-sided carbon tape, coated with carbon to prevent the charging on sample surface due to the electron beam and examined under SEM.

4.3 Results

4.3.1 Arsenic fractionation in sediments

Different As phases in selected low (samples 1-9; Figure C-1 A) and high As sediments (samples 10-22; Figures 4-1 A and C-2) were determined using sequential extraction approach. In high As sediments, greater As was found surface bound (exchangeable and specifically adsorbed fractions; F2 + F3: ~4.5 µg g^{-1} As; 32% of total As) on the solid phase (mineral and organic solid phases). Higher concentrations of As were also found coprecipitated with sulfide minerals such as FeS_2 and amorphous As_2S_3 (F8: ~3.4 µg g^{-1} As; 19% of total As). Around 17% of total As was extracted from each crystalline Fe, Al and Mn oxyhydroxides (F6), and silicate minerals and As oxides (F7). Arsenic associated with the amorphous Fe, Al and Mn oxyhydroxides (F5) contributed ~11% to the total As, and rest of the As phases produced <10% of the total As (Figure 4-1 A and C-2). In low As sediments, a significant proportion of total As was associated with the crystalline Fe, Al and Mn oxyhydroxides (F6: ~1.8 µg g^{-1} As; 40% of total As) and adsorbed on different solid phases (F2 + F3: ~1 µg g^{-1} As; ~20% of total As; Figure C-1 A). Arsenic associated with FeS_2 and amorphous As_2S_3 (F8) was only 0.2 µg g^{-1} (3.9% of total As), and rest of the sediment solid phases contained As similar to the high As sediments.

Total Fe concentrations and sulfide minerals also varied in sediments. In high As sediments, total Fe concentrations ranged from 2.1 to 4.2 % (Table 2-1). Sequential extraction of Fe revealed that ~60% of total Fe was associated with amorphous and crystalline Fe oxides. Silicate and sulfide minerals also contained significant amounts of Fe (21 and 12 % of total Fe, respectively; Figure 4-1 B). In low As samples, total Fe ranged between 1.4 and 2.8 %, and sequential extraction of Fe showed that ~80% of total Fe was associated with amorphous and crystalline Fe oxides. Around 12% of total Fe was associated with silicate minerals and only 1% of total Fe was found with sulfide minerals (Table 2-1; Figure C-1 B); because low As sediments contained small quantities of sulfide minerals (0.05 to 0.19 %) as compared to high As sediments (0.24 to 2.79 % sulfide minerals; Table 2-1). Generally, higher concentrations of As were found in the unoxidized sediments enriched in FeS minerals. In high As sediments, a significant positive correlation of sulfide minerals was found with total As (r = 0.83) and As associated with sulfide minerals (r = 0.90; Figure C-3 A) as compared to the low As sediments where we could not find good correlation between As (total and sulfide bound) and sulfide minerals (Figure C-3 B). As far as correlation between sulfide minerals and Fe concentrations in sediments is concerned, sulfide minerals in high As sediments showed higher correlation (r = 0.83) with Fe associated with sulfide minerals, but did not correlate well with total Fe in sediments (r = 0.18; Figure C-3 C). Fe and sulfide minerals did not show any correlation in low As sediments at all (Figure C-3 D).

4.3.2 Fractionation of other elements in sediments

After total elemental analyses, the selected sediment samples (n = 22) from different geological formations were sequentially extracted to determine the distribution of elements in different phases (such as soluble, exchangeable, bound to carbonates, associated with amorphous and crystalline Fe and Mn oxyhydroxides, associated with sulfides and organic matter; see detail in Table 3-2) of sediments. The overall results of the sequential extraction of sediments for 10 important elements are shown in Figure 4-2, and detailed sequential extraction results of individual elements are shown in Figure C-4. Overall three major phases containing these elements in the sediments were found. The maximum concentrations (36% median; 29.2 to 42.8% of total metal concentrations) of all the elements were associated with amorphous and crystalline Fe and Mn oxides (F5 and F6 of SEP; Figure 4-2), and a higher proportion of all the siderophile (Ni, 23% of total Ni and Co, 44% of total Co), lithophile (B, 30% of total B; V, 34% of total V; Cr, 29% of total Cr and U, 36% of total U) and chalcophile elements (Cu, 38% of total Cu; Se, 56% of total Se and Pb, 64% of total Pb) except Cd were found to be associated with Fe and Mn oxides (Figure C-4). Exchangeable and specifically adsorbed phase of the elements (F2 and F3) comprised ~27% (19 to 36 %) of the total concentrations of elements in sediments (Figure 4-2), and a significant proportion of all the chalcophile (Cu, 43% of total Cu; Se 32% of total Se and Cd 32% of total Cd), siderophile (Ni, 23% of total Ni and Co, 22% of total Co) and lithophile elements (B, 18% of total B; Cr, 37% of total Cr and U, 42% of total U) except Pb and V were found in the exchangeable phase (Figure C-4). Elements bound in silicate minerals (F7) also constituted a major pool of elements (~23%; 14 to 44 % of total metal concentrations), with the greatest proportion of the lithophile elements (B, 50% of total B; V, 58% of total V; Cr, 14% of total Cr and U, 17% of total U). The proportion of Cd (31% of total Cd) and Pb (28% of total Pb) among the chalcophile elements and Ni and Co from the siderophile (Ni, 48% of total Ni and Co, 19% of total Co) elements were also higher in the silicate phase. Rest of the phases such as carbonates, sulfides and organic matter in sediments had insignificant contribution to the total elemental concentrations in sediments (Figure 4-2).

4.3.3 Mineralogy of sediments

XRD analysis performed on selected high (11, 14 and 17) and low As sediments (1, 2 and 9) showed that FeS_2 was one of the dominant minerals in the high As sediments (Figure 4-3), particularly in sediments 11 (24.9±4.2 $\mu g\ g^{-1}$ As) and 17 (22.5±2.1 $\mu g\ g^{-1}$ As). In contrast, sediment 14 (12.4±0.8 $\mu g\ g^{-1}$ As) retrieved close to the top of core WEPA99-2 generated dominant goethite (FeOOH) peaks which supported our SEP results which showed more Fe released by the dissolution of amorphous and crystalline Fe oxyhydroxides than FeS_2 in that sediment (Figure 4-1 B). However, we did not identify phyllosilicate minerals in the high As sediments. In low As sediments, none of the FeS_2 and goethite peaks were identified. Peaks of kaolinite and muscovite clay minerals were identified in one of the sediments containing 3.5±0.1 $\mu g\ g^{-1}$ As (sediment 9; Figure 4-3); the other two sediments only showed quartz as a dominant mineral like other low and high As sediments. Because the detection limit of XRD (~4 wt% of mineral) was not enough to identify As minerals in the sediments, μ-XRD was employed to determine whether high As sediments had any As minerals or As was present within FeS_2. The μ-XRD results were presented as typical GADDS images showing diffracted cones (Figure C-5) integrated into diffractograms to reveal mineral contents at different 2-theta values (Figure 4-4). Some characteristic peaks of FeAsS appeared in the sediments containing high As (sediment 11; 24.9±4.2 μg g^{-1} As, and sediment 17; 22.5±2.1 μg g^{-1} As) indicating the presence of FeAsS.

XANES was performed to determine the oxidation state of As in sediment solid phase. The As K-edge XANES data acquired from the standards and selected low (sediments 1-9) and high As sediments (sediments 10-22) suggested that absorption peaks were easily distinguishable from one another by the white line energy positions (Figures 4-5, 4-6 and C-6). The white line energy positions of As^{V} and As^{III} in standard minerals acquired through XANES were in the following order: sodium arsenate (As^{V}-O, 11874.2 eV) > annabergite (As^{V}-O, 11874 eV) > arsenic oxide (As^{III}-O, 11871 eV) > sodium arsenite (As^{III}-O, 11870.5 eV) > orpiment (As^{III}-S 11868.4 eV) > arsenopyrite (As^{III}-S 11868 eV) (Figure 4-5); which were in agreement with the previously published literature (Xu et al., 2011). Most sediments generated white line energy positions close to 11868 eV that corresponded to As^{III} oxidation state possibly associated with sulfide minerals. The LCF results of XANES data from all the selected low and high As sediments (Figures C-6 and 4-6; Table C-1) showed that As was predominantly present in As^{III} form, except in sample 10, 12, 14 and 15 that were taken from oxidized till (Figures 1-2 and 2-2) where As^{V} ranged from 63 to 92 % of the total As (Figure 4-6). An example of the LCF of the standards spectra with an As XANES spectrum acquired from a high As sediment sample (~20 μg g^{-1} As) is shown in Figure C-7. Overall, XANES results suggested that As^{III} was the dominant As form in both low and high As sediments. Overall, our SEP and XANES findings suggested that most of As^{III} was associated with crystalline Fe, Al and Mn oxyhydroxides in low As sediments and with sulfide minerals in high As sediments.

4.3.4 Elemental mapping and micromorphology of sediments

One high As sediment (sediment 11; 24.9±4.2 $\mu g\ g^{-1}$ As) was used for XRF mapping for As and Fe. The results showed some spatial association (evident from matching hotspots) between both the elements (Figure 4-7 A and B). Though, we did not find good correlation ($r = 0.42$) between total As and total Fe in high As sediments, a significant positive correlation ($P < 0.05$; $r = 0.81$) between As and Fe associated with sulfide minerals (F8 of SEP for As and Fe, respectively) was found that suggested that high As concentration might not be spatially associated with all Fe phases but FeS might contain most of the As in sediments. To study the micromorphology of the sediments, SEM supported by EDX (LOD ~0.1 wt% of the element) was used to study high As sediment (Sediment 11). SEM image clearly showed single FeS_2 crystals associated with the quartz that was supported by the EDX where high Fe and S intensities suggested FeS_2 and high Si and O showed quartz in the sediment (Figure 4-7 C and D).

4.4 Discussion

Elevated As (> 10 $\mu g\ L^{-1}$) in domestic well water in the Cold Lake area of Alberta, Canada is a health concern that warrants detailed geochemical characterization of the glacial till sediments (surficial deposits) that feed the aquifers in the region. Arsenic-laden groundwater is attributed to the sediment's As through which the water passes (Wang and Mulligan, 2006). This study was conducted to comprehensively investigate the association of As with different solid constituents in sediments from 5 different locations (up to ~300 m depth) in the Cold Lake area to determine the potential source of As.

Arsenic fractionation in the selected high As (7 to 35 $\mu g\ g^{-1}$) sediments showed that ~32% of the total As (Average total As: 15 $\mu g\ g^{-1}$) was found adsorbed on the sediment solids. Xu et al., (2011) reported a significant proportion of As (~25% of 735 $\mu g\ g^{-1}$) strongly adsorbed on solids in sediments collected from a zinc (Zn) smelting site. In our study, analysis of Pearson correlation of the adsorbed As with different solid phases such as oxides of Fe, Al and Mn, sulfides and TOC showed significant correlation only between adsorbed As and sulfide minerals ($P < 0.05$; $r = 0.66$). In high As sediments, As coprecipitated with FeS_2 and As_2S_3 (11 to 34 %) was also one of the dominant fractions (Figure 4-1 A). XRD and μ-XRD analyses confirmed the presence of FeS_2 and FeAsS, respectively (Figures 4-3 and 4-4) and SEM-EDX showed the presence of single FeS_2 crystals (Figure 4-7 C and D). Fluorescence mapping revealed the spatial association of As and Fe in high As sediment (Figure 4-7 A and B). Smedley and Kinniburgh, (2002) also reported high As concentration (3-900 $\mu g\ g^{-1}$) under reduced conditions in FeS_2-containing sediments of marine shale in Canada.

In high As sediments after adsorbed and sulfide bound fractions, significant concentration of As (17% of the total As) was coprecipitated with crystalline Fe, Al and Mn oxyhydroxides and silicate minerals each. In the selected low As sediments (<7 µg g^{-1} As), As associated with crystalline Fe, Al and Mn oxyhydroxides constituted highest proportion of the total As (~40% of 1.8 µg g^{-1}). Fennell, (2008) also reported a significant proportion of As (~21% of 1.2 µg g^{-1}) bound with the crystalline Fe oxyhydroxides in aquifer sediments from the same region. Arsenic associated with amorphous Fe, Al and Mn oxyhydroxides was omnipresent in all the low and high As sediments due to high surface area of these oxides. Nonetheless, Fe oxyhydroxides content present in the soils and sediments is a good scavenger of As (Smedley and Kinniburgh, 2002; Gleyzes et al., 2002; Larios et al., 2012).

Overall, fractionation of other elements in the selected sediments showed that three major phases (amorphous and crystalline Fe oxides, exchangeable and specifically adsorbed, and silicate minerals) hosted most of the elemental concentrations in the sediments. Amorphous and crystalline Fe oxides contained the maximum (~36% of the total concentrations) elemental concentrations (Figure 4-2). Tessier et al., (1979) reported significant proportions of siderophile (~24% Ni and ~44% Co) and chalcophile elements (~20% Cu and ~26% Pb) associated with Fe oxides minerals in marine sediments. Around 27% of the total elemental concentrations were found sorbed (exchangeable and specifically adsorbed) on solid phase (mineral and organic phases) in the sediments. Tessier et al., (1979) also reported significant proportions of chalcophile elements (~17% Cu and ~

22% Pb) as surface bound on different solid phases in marine sediments. Silicate minerals also contained ~23% of the total elemental concentrations in the sediments. Okoro et al., (2012) performed sequential extraction of metals in sediments of different coastal systems and reported that a significant proportions of total concentrations of the lithophile (~82% Cr) and chalcophile elements (~43% Cu, ~16% Cd and ~42% Pb) were found with the primary and secondary minerals in the sediments. Rest of the phases such as carbonate minerals, amorphous Fe oxides, sulfide minerals and organic matter in sediments contained insignificant fractions of these elements.

We also determined the correlation of total elemental concentrations with Fe and Mn concentrations in amorphous- and crystalline-oxides of Fe and Mn, TOC, pH, redox zones and sulfides in the selected sediments (n = 22). Only Co concentration was found to be correlated with the amorphous- and crystalline-oxides of Fe ($r = 0.62$ and $r = 0.54$, respectively) and amorphous- and crystalline-oxides of Mn ($r = 0.60$ and $r = 0.58$, respectively) in sediments. Total concentration of Se in sediments were correlated with amorphous Mn oxides ($r = 0.54$). These Co and Se correlation results are in accordance with our SEP results where high Co and Se were associated with amorphous and crystalline Fe and Mn oxides. V, Rb, and Cu in the sediments showed correlation with TOC ($r = 0.60$, $r = 0.52$ and $r = 0.51$, respectively). Nickel was found to be correlated ($r = 0.53$) with sulfide minerals.

The results of As SEP and XANES suggested that whether the As was adsorbed or coprecipitated with different solid constituents (crystalline/amorphous oxides, silicates or sulfides), the dominant As form was As^{III} (~60 to 90 % of total As) in all the low (<7 µg g^{-1}) and high As (>7 µg g^{-1}) sediments. These results suggested that As might be initially existed in reduced minerals such as FeS_2 and FeAsS and further minerals transformation might have transferred or transported As to Fe oxide minerals. Elemental constituents of FeAsS oxidize at different rates. Yunmei et al., (2004) reported that ferrous (Fe^{II}) oxidized before the oxidation of As^{III} occurred, which indicated relatively low rate of As^{III} conversion to As^{V}. This might suggest the sequestration of As^{III} in newly formed Fe oxyhydroxides minerals. Different geochemical conditions such as presence of phosphate (PO_4^{3-}) and carbonates (CO_3^{2-}) in pore water that can desorb the surface bound As, and weathering of FeS_2 and FeAsS containing sediments that can release the minerals bound As into groundwater could be important processes in As groundwater contamination (Javed et al., 2013; Keon et al., 2001). Similar to As, different geochemical conditions such as presence of competing ions like phosphate (PO_4^{3-}) and carbonates (CO_3^{2-}) in the pore water for the anionic elements including V, Se and Cr, and presence of calcium (Ca^{2+}) and magnesium (Mg^{2+}) in pore water for cationic elements such as Cu, Pb and Cd can desorb the surface bound elements and make them bioavailable. Weathering of silicate minerals and reductive dissolution of the Fe oxides minerals in sediments that can also liberate the elements from the sediments to the surrounding pore water could be important processes that might contaminate the groundwater (Keon et al., 2001; Javed et al., 2013). In contrast, Meunier et al., (2010) reported very low As availability (<1%) in soils having a greater proportion of FeAsS minerals in mining-impacted area, and Tessier et al., (1979) reported that metals associated with silicate minerals are recalcitrant phase that cannot contaminate the groundwater under natural geochemical conditions. Though natural geochemical conditions cannot or slowly release metals through weathering, anthropogenic activities such as cyclic steam stimulation (CSS) that are currently operating in the Cold Lake region (Andriashek, 2003; Fennell, 2008) to extract the bitumen could enhance the metals release by the desorption of metals and/or breakdown of metals bearing minerals in sediments. The results of this study provide insights into the fractionation of elements in different solid phases in sediments that can be used to predict their availability and transport to groundwater.

Literature cited

Andriashek L. D. Quaternary geological setting of the Athabasca Oil Sands (in situ) area, Northeast Alberta. 2003. http://www.ags.gov.ab.ca/publications/ESR/PDF/ESR_2002_03.pdf

Boyle R. W., Jonasson I. R. The geochemistry of arsenic and its use as an indicatior element in geochemical prospecting. J Geochemical Explor 1973;2:251–296.

Feng R., Dolton W., Igarashi R., Wright G., Bradford M., McIntyre S. Commissioning of the VESPERS Beamline at the Canadian Light Source. 2010; CP1234, 10th Internation Conference on Synchrotron Radiation Instrumentation.

Fennell J. W. Effects of aquifer heating on groundwater chemistry with a review of arsenic and its mobility. PhD thesis 2008, Universiyt of Calgary.

Flemming R. L., Salzsauler K. A., Sherriff, B. L., Sidenko, N. V. Identification of scorodite in fine-grained, high-sulfide, arsenopyrite mine-waste using micro x-ray diffraction (μXrD). 2005;43:1243–1254.

Gleyzes C., Tellier S., Astruc M. Fractionation studies of trace elements in contaminated soils and sediments: a review of sequential extraction procedures. Trends Anal Chem 2002;21(6-7):451–467.

He Z. L., Yang X. E., Stoffella P. J. Trace elements in agroecosystems and impacts on the environment. J Trace Elem Med Biol. 2005;19(2-3):125–140.

Huang J-H., Kretzschmar R. Sequential extraction method for speciation of arsenate and arsenite in mineral soils. Anal Chem. 2010;82(13):5534–5540.

Javed M. B., Kachanoski G., Siddique T. A modified sequential extraction method for arsenic fractionation in sediments. Anal Chim Acta 2013;787:102–110.

Kachenko A. G., Grafe M., Singh B., Heald S. M. Arsenic speciation in tissues of the Hyperaccumulator P. calomelanos var. austroamericana using x-ray absorption spectroscopy. Envoron Sci Technol 2010;44(12):4735–4740.

Keon N. E., Swartz C. H., Brabander D. J., Harvey C., Hemond H. F. Validation of an arsenic sequential extraction method for evaluating mobility in sediments. Environ Sci Technol 2001;35(13):2778–2784.

Krauskopf K. B. Introduction to geochemistry. 1979; McGraw-Hill Book Company.

Larios R., Fernández-Martínez R., Rucandio I. Comparison of three sequential extraction procedures for fractionation of arsenic from highly polluted mining sediments. Anal Bioanal Chem 2012;402(9):2909–2921.

Manning B. Arsenic speciation in As(III)- and As(V)-treated soil using XANES spectroscopy. Microchim Acta 2005;151:181–188.

Meunier L., Walker S. R., Wragg J., Parsons M. B., Koch I., Jamieson H. E., Reimer K. J. Effects of soil composition and mineralogy on the bioaccessibility of arsenic from tailings and soil in gold mine districts of Nova Scotia. Environ Sci Technol 2010;44:2667–2674.

Muloin T., Dudas M. J. Aqueous phase arsenic in weathered shale enriched in native arsenic. J Environ Eng 2005;4:461–468.

Murphy A. P., Coudert M., Barker J. Plants as biomarkers for monitoring heavy metal contaminants on landfill sites using sequential extraction and inductively coupled plasma atomic emission spectrophotometry (ICP-AES). J Environ Monit. 2000;2(6):621–627.

Nickson R. T., McArthur J. M., Ravenscroft P., Burgess W. G., Ahmed K. M. Mechanism of arsenic release to groundwater, Bangladesh and West Bengal. Appl Geochem 2000;15:403–413.

Pradit S., Wattayakorn G., Angsupanich S., Baeyens W., Leermakers M. Distribution of trace elements in sediments and biota of Songkhla Lake, Southern Thailand. Water Air Soil Pollut 2010;206:155–174.

Sadiq M. Arsenic chemistry in soils: an overview of thermodynamic predictions and field observations. Water Air Soil Pollut 1997;93:117–136.

Shah P., Strezov V., Stevanov C., Nelson P. F. Speciation of arsenic and selenium in coal combustion products. Energy & fuels 2007;21:506–512.

Smedley P. L., Kinniburgh D. G. A review of the source, behaviour and distribution of arsenic in natural waters. Appl Geochem 2002;17:517–568.

Tessier A., Campbell P. G. C., Bisson M. Sequential extraction procedure for the speciation of particulate trace metals. Anal Chem 1979;51(7):844–851.

Wang S., Mulligan C. N. Occurrence of arsenic contamination in Canada: sources, behavior and distribution. Sci Total Environ 2006;366:701–721.

Xu L., Zhao Z., Wang S., Pan R., Jia Y. Transformation of arsenic in offshore sediment under the impact of anaerobic microbial activities. Water Res 2011;45(20):6781–6788.

Yunmei Y., Yongxuan Z., Williams-Jones A. E., Zhenmin G., Dexian L. A kinetic study of the oxidation of arsenopyrite in acidic solutions: implications for the environment. Appl Geochem 2004;19:435–444.

Figures

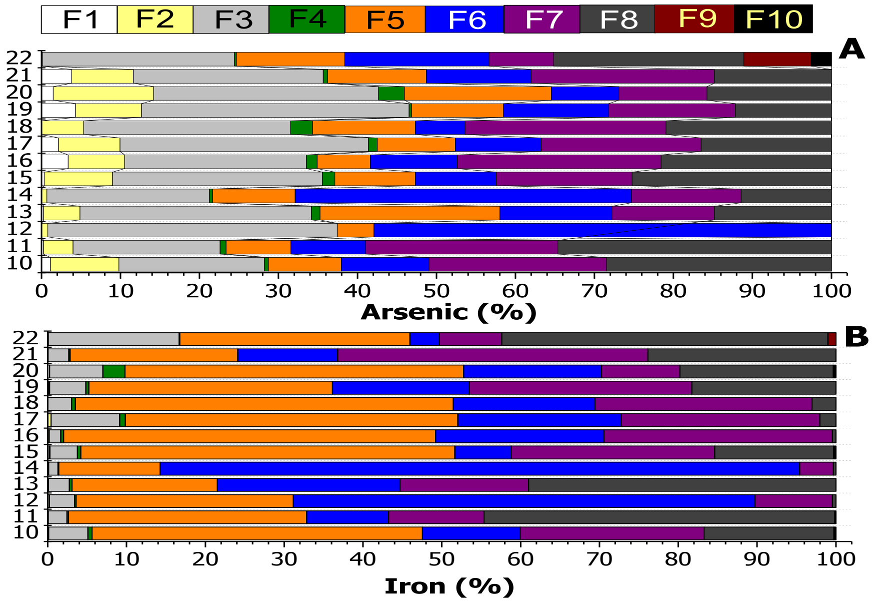

Figure 4- 1. Distribution of (A) arsenic and (B) iron in different sediment solid phases of the selected high As sediments (sample 10-22; As>7 µg g^{-1}).

Sequential extraction protocol (SEP; Javed et al., 2013) was used to determine the As and Fe fractionation in sediments. Arsenic and Fe concentrations were determined in the same aliquot of each extractant used in SEP. The results of As and Fe fractionation in low As sediments is given in Figure C-1. Legends are applicable for both panels and represent different fractions: F1, water soluble metals; F2, ionically bound/exchangeable metals; F3, strongly/specifically adsorbed metals; F4, metals bound in carbonates; F5, metals coprecipitated with amorphous Fe, Al and Mn oxyhydroxides; F6, metals coprecipitated with crystalline Fe, Al and Mn oxyhydroxides; F7, metals associated with their oxides and silicate clays; F8, metals coprecipitated with pyrite and amorphous orpiment; F9, metals associated with organic matter and recalcitrant sulfides; and F10, residual metals.

Actual concentration of As in different fractions is shown in Figure C-2.

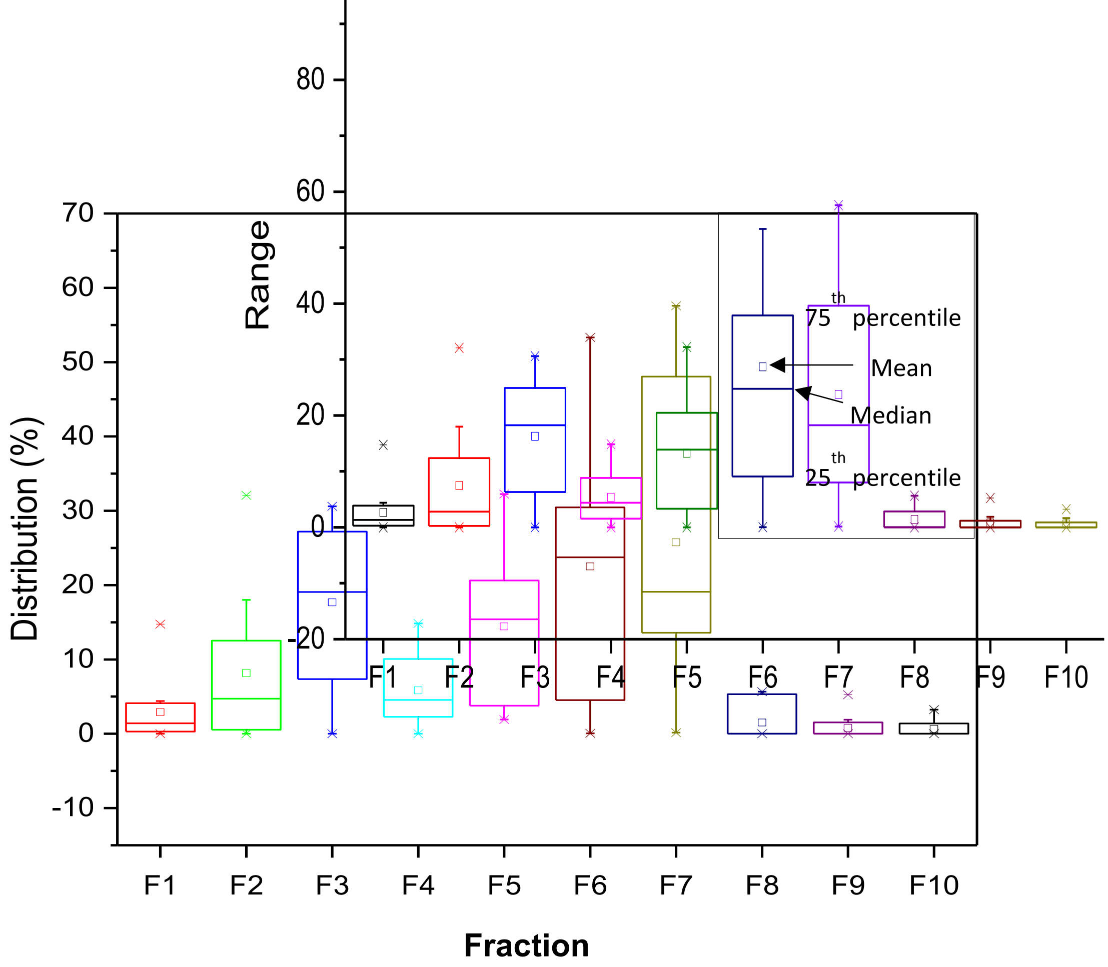

Figure 4- 2. Fractionation of other elements in 10 fractions (F1-F10) to determine their association with different solid phases in sediments to predict their potential to contaminate groundwater.

Sequential extraction protocol (Javed et al., 2013) was used to determine the metal fractionation in sediments. Legends represent different fractions: F1, water soluble metals; F2, ionically bound/exchangeable metals; F3, strongly/specifically adsorbed metals; F4, metals bound to carbonates; F5, metals coprecipitated with amorphous Fe, Al and Mn oxyhydroxides; F6, metals coprecipitated with crystalline Fe, Al and Mn oxyhydroxides; F7, metals associated with their oxides and silicate clays; F8, metals coprecipitated with pyrite and amorphous orpiment; F9, metals associated with organic matter and recalcitrant sulfides; F10, residual metals.

Detailed fractionation of the elements is provided in Figure C-4.

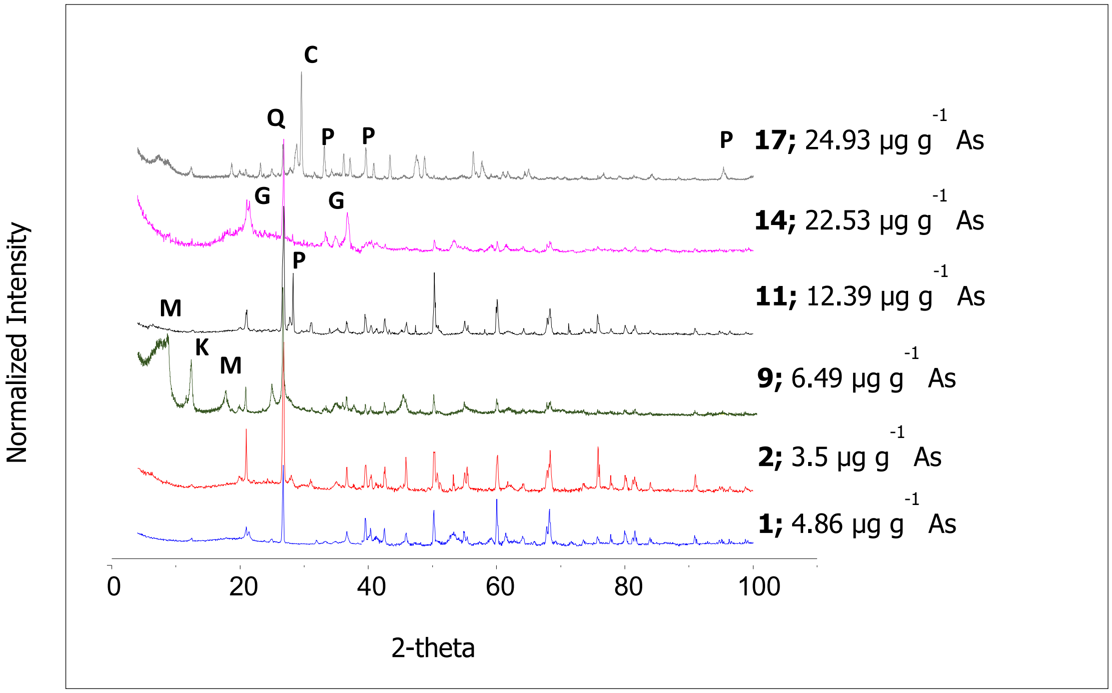

Figure 4- 3. XRD spectra of selected low (sample 1, 2 and 9) and high As sediments (sample 11, 14 and 17) show the dominance of pyrite in the high arsenic sediments.

Q, quartz; P, pyrite; C, calcite; G, goethite; M, muscovite; K, kaolinite; only primary peaks are labelled.

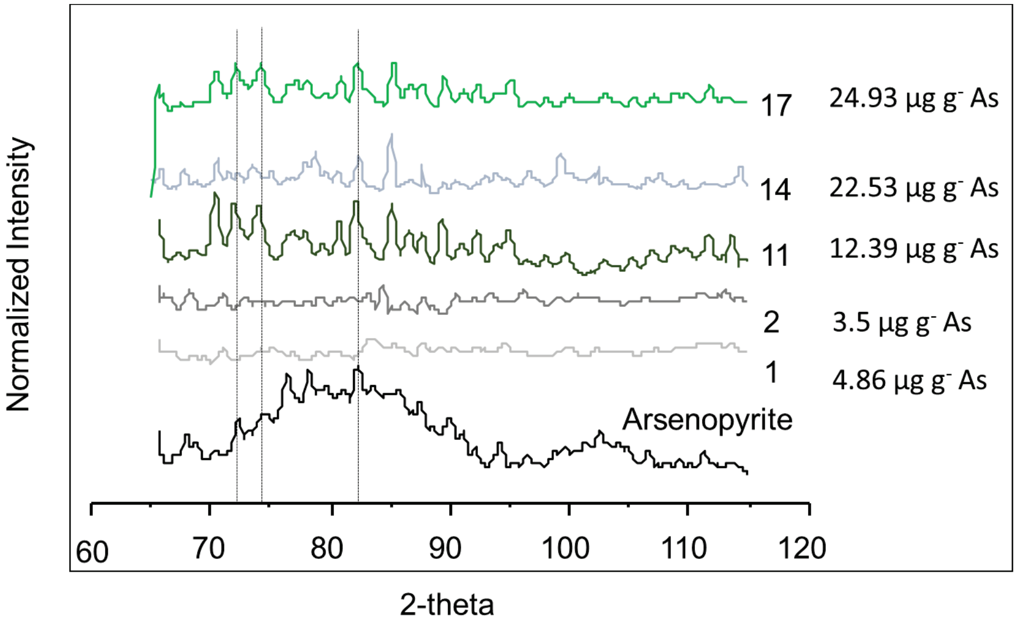

Figure 4- 4. µ-XRD spectrum of arsenopyrite pure phase shows that high arsenic sediments also contain some characteristics arsenopyrite peaks; dotted lines show the arsenopyrite peaks.

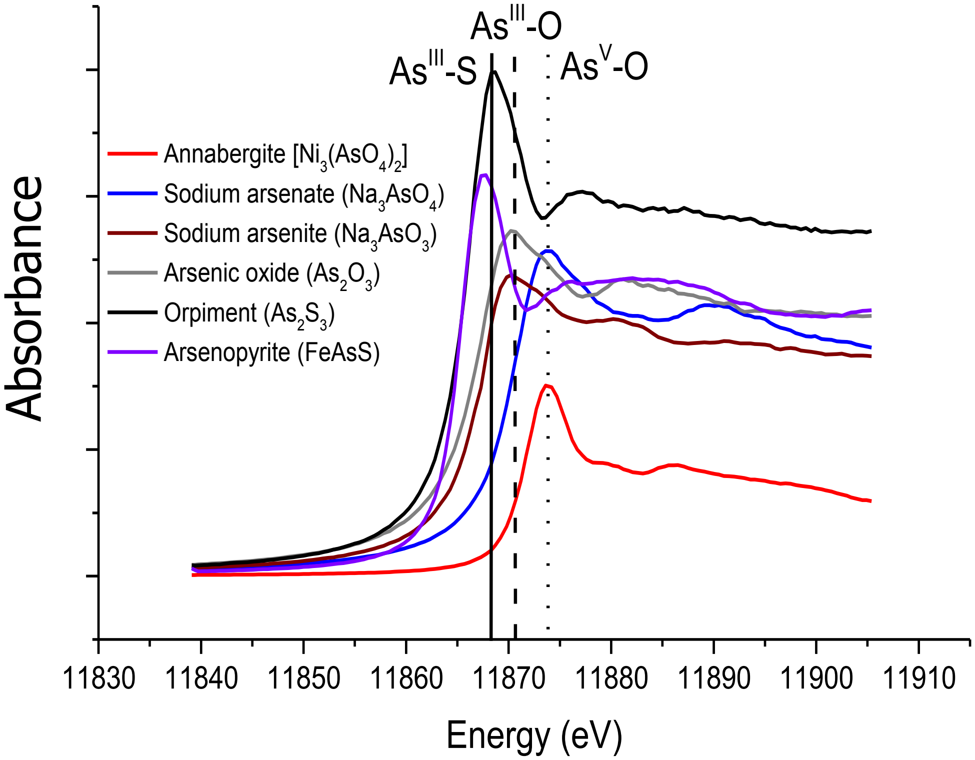

Figure 4- 5. Arsenic K-edge XANES spectra of reference minerals. Solid (-), dashed (---) and dotted (…) lines drawn at 11868 eV, 11870.7 eV and 11874 eV represent the position of white lines of As^{III}-S, As^{III}-O and As^{V}-O, respectively.

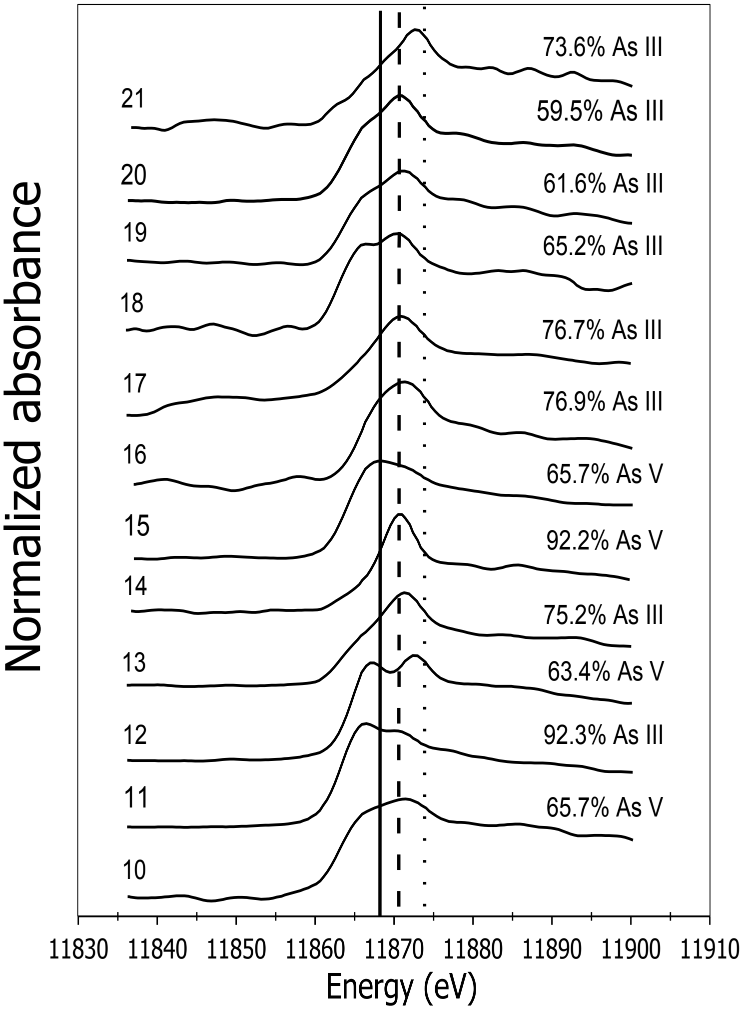

Figure 4- 6. XANES spectra of selected high arsenic sediments (>7 µg g^{-1} As). Liner combination fit (LCF) results show that arsenite (As^{III}) is the most dominant As form in the sediments as shown by the proportion of As^{III} or arsenate (As^{V}) beside each spectrum. Only that oxidation state of As is shown in the spectrum that was present >50% in the sediment. Detail of the LCF analysis is provided in Table C-1. XANES and LCF information about low As sediments are given in Figure C-6.

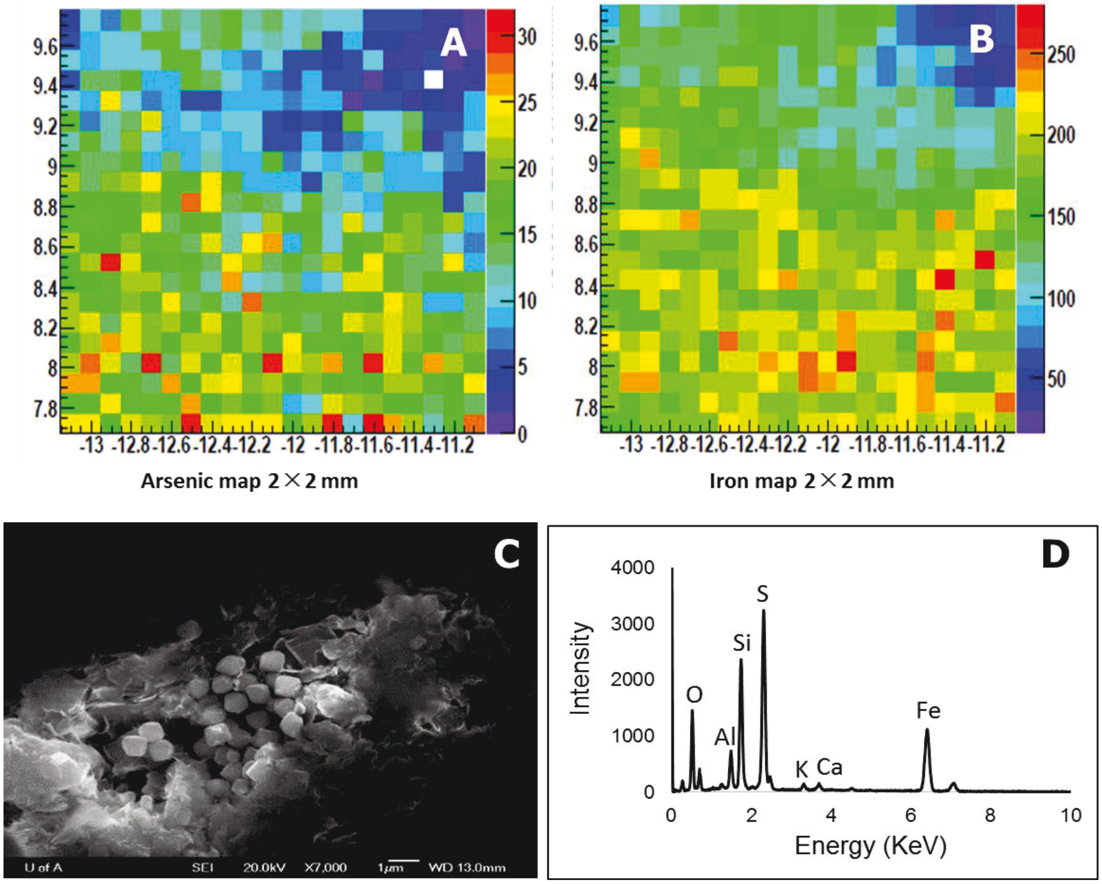

Figure 4- 7. Elemental mapping and micromorphology of a high arsenic sediment (sample 11; As: 24.9±4.2 μg g^{-1}).

XRF mapping of (A) As and (B) Fe; Both As and Fe maps show some spatial association between these elements (Pearson correlation, *r* = 0.42). (C) SEM image shows single pyrite crystals with quartz supported by (D) EDX that shows high intensities of S and Fe.

Chapter 5. Effect of heat on arsenic release from sediments[4]

5.1 Introduction

Arsenic (As) is one of the most abundant trace elements in the earth's crust with some of its chemical forms being extremely toxic to living organisms. In recent years, As groundwater contamination and its subsequent serious health effects have received global attention, where 40 to 100 million people in the world have been at risk of consuming As contaminated water (Páez-Espino et al., 2009; van Halem et al., 2009; de Mora et al., 2011). In the Cold Lake area of Alberta, relatively high concentrations of As (>10 µg L^{-1}; maximum acceptable concentration in drinking water in Canada; Health Canada, 2006) have been found in groundwater (Health Surveillance, 2000). The groundwater is extensively used for agricultural and household purposes in the area (Lemay et al., 2005). The rich source of bitumen in the area is attracting the growing industrial activity for bitumen extraction.

Significant oil sands deposits (80 to 85 %) are located at greater depth (~400 m deep), thus requiring the use of *in situ* techniques such as Cyclic Steam Stimulation (CSS) to enhance the bitumen recovery process (Alberta Environment; Imperial Oil, 2014). The bitumen is very viscous at normal temperature, therefore, heat is required to decrease the viscosity so that it can be brought to the surface. The CSS process consists of 3 phases: injection, soaking

---

[4] A version of this chapter is in preparation for publication.

and production. In the process, a vertical well is drilled in the surficial deposits through which high-pressure and high temperature (200-300°C) steam is injected into the oil sands deposits (injection phase). The high pressure steam creates fractured in the oil sands deposits that enhance the surface area of the deposits. As the steam soaks through the oil sands, the bitumen melts and flows (soaking phase). The melted bitumen is pumped to the surface during the production phase through the same well. Each cycle of this process can take from months to years (RAMP, 2014). The heat can be conducted away from the hot wellbores to the surrounding sediments and associated porewater (Fennell, 2008). A consequence of bitumen extraction activity at large scale in the area is the increasing risk of groundwater As contamination. The principal controlling factor of As release into groundwater is the distribution of As in different inorganic and organic phases (such as soluble, exchangeable, bound to carbonates, amorphous and crystalline Fe and Mn oxyhydroxides, and coprecipitated with sulfides and organic matter; see detail in Table 3-2) in sediments (Javed et al., 2013) that can be altered by localized heating of the sediments. These changes have the potential to deteriorate the groundwater quality by dissolving and mobilizing As from sediments to groundwater (Fennell, 2008).

The effect of localized heating of a fresh aquifer sediment on the quality of an aquifer water was studied by Fennel (2008) who reported As release from sediments at ~50^{o} C. But how the heat affects different sediment constituents or host phases of As in glacial till of the Cold Lake area has not been investigated yet. The As fractionation is important to investigate the changes in the distribution of As in different host phases in the sediments before and after thermal application so that it could be ascertained which sediment solid constituents contribute to As contamination in groundwater. Therefore, this study was initiated to study the effect of heat (~200^{o}C; simulating the conditions near the hot wells) on As distribution in sediments and release into porewater. In this study, sediments collected from Cold Lake area, Alberta were subjected to intense heat simulating CSS conditions. Arsenic fractionation in sediments was determined before and after thermal treatment to find contribution of different phases to As release into porewater. The results of this study will help understand the extent of As release during industrial processes so that management strategies could be developed to mitigate As contamination in the groundwater.

5.2 Methodology

5.2.1 Reagents

Trace metals grade calcium sulfate ($CaSO_4$; CAS # 7778-18-9) and sodium bicarbonate ($NaHCO_3$; CAS # 144-55-8) were purchased from Sigma-Aldrich (Ontario, Canada) to prepare the synthetic aquifer water that was used to moisten the sediments before heating. All the chemicals and reagents used for the preparation of extraction solutions for As fractionation were trace metal grade purchased from Sigma-Aldrich (Ontario, Canada), and all the solutions were prepared using nanopure water (Barnstead nanopure, Thermo Scientific). The detail of the reagents is provided in sections 2.2.1 and 3.2.2. The pH of the extraction solutions, if required, was adjusted to the desired level with either sodium hydroxide (NaOH) or appropriate acid (HOAc, $H_2C_2O_4$ or HNO_3). The reagent and experimental blanks of all the extraction solutions were also analyzed along with the experimental samples. The As concentration was lower than the detection limits (0.01 μg L^{-1} As) in all blank solutions as determined using quadrupole ICP-MS (iCap Q- Thermo scientific). All laboratory glass-and plastic-ware was cleaned by soaking in 5% (v/v) HNO_3 overnight and then repeatedly rinsed with nanopure water.

5.2.2 Sediment collection and physicochemical characterization

The Alberta Geological Survey-Alberta Energy Regulator (AGS-AER) drilled surficial deposits (~300 m deep) at eight different locations in the Cold Lake area (southeast part of the Athabasca Oil Sands) to explore the hydrogeology and hydro-geochemistry of the region. The cores were stored in wooden boxes at the Alberta Energy Regulator-Alberta Geological Survey (AER-AGS) Mineral Core Research Facility in Edmonton, Alberta, Canada under ambient conditions. More details of the cores are provided in section 2.2.2 in chapter 2. For this study, seven sediment samples (S1-S7) from different geological formations such as Marie Creek, Ethel Lake, Bonnyville, Empress and shale were selected (Table 5-1). The detail of the geological formation in the area is provided in Figure 1-1. Briefly, the pH of the seven sediments used in this study ranged between 6.2 $\pm$ 0.3 and 9.1 $\pm$ 0.3, but most sediments had pH ~7. Total organic carbon (TOC) contents in sediments were <1 % in most sediments but a few had TOC up to 2.8 ± 0.2 %. The information about lithology of the sediments was obtained from Andriashek, 2003. The particle size distribution of the sediments determined using laser particle size analyzer (Master sizer-Malvren

3000 Hydro®) are provided in Table D-1. To determine the total As concentration, sediment samples were digested using concentrated HNO_3 in a microwave digester. The detail of the digestion method is provided in section 2.2.3. The physicochemical properties of the sediments used in this experiment are provided in Table 5-1.

5.2.3 Heat treatment of sediments

Seven sediment samples (S1-S7) of varying As concentration (3.5 ± 0.1 $\mu g\ g^{-1}$ to 28.4 ± 1.8 $\mu g\ g^{-1}$) and geochemical characteristics (Table 5-1) were used to study the effect of heat on As fractionation in sediments. Synthetic aquifer water prepared using $CaSO_4$ and $NaHCO_3$ in the laboratory was used to moisten the sediments before heat to simulate conditions prevailing in the sediments during heat injection through wells. The synthetic aquifer water prepared in the laboratory had EC, 400 ± 10 $\mu S\ cm^{-1}$, TDS, 300 $mg\ L^{-1}$, Eh, 100 ± 10 and pH, 7 mimicking the aquifer porewater chemistry as described by Andriashek (2003). Sediment samples were moistened at 15 % (7.5 ml liquid: 50 g sediment) and 50% moisture (25 ml liquid: 50 g sediment) according to the natural moisture content in the sediments. In addition, to mimic the conditions in aquifer sediments 1.4:1 (70 ml liquid: 50 g sediment) and 3.7:1 (185 ml liquid: 50 g sediment) liquid to solid ratio were also used to moistened the sediments before heat to determine the As release. The 1.4:1 and 3.7:1 liquid to solid ratio to determine the As release from a fresh aquifer sediments was also used by Fennel (2008). A 480 cm^3 stainless steel autoclave reactor equipped with a stirrer and a heating jacket was used to heat the sediment under N_2 environment. Moist sediments were heated in a sealed vessel at 200 ± 6 ^{o}C temperature at ~20-30 bar pressure (simulating over burden pressure) for 1 h. The temperature of the reactor was controlled using Parr 4841 proportional controller. The experiment was conducted in the Canadian Centre for Clean Coal/Carbon and Mineral Processing Technologies (C^5MPT) laboratory at University of Alberta. After 1 hour heat treatment, the moistened sediments were removed from the reactor when the temperature decreased to ~100 ^{o}C temperature and immediately centrifuged (Sorvall® RC-5B Refrigerated Superspeed Centrifuge with Sorvall® HS-4 rotor) for 40 min at 6000*g* to separate the liquid and solid phases. The liquid phase was analyzed within 24 hours for As concentration to infer As release from the sediments after heat. The sequential extraction of As from sediments (solid phase) was also started within 24 hours of the heating of sediments to determine the effect of heat on distribution of As with different host phases in sediments. A separate experiment with similar experimental set up was also conducted using nanopure water to establish 15 % or 50 % moisture and 1.4:1 or 3.7:1 liquid to solid ratio in sediments. Nanopure water was used to determine the effect of low ionic strength porewater on As release under intense heat.

All the experiments were also repeated using microwave (MARS 6, CEM) unit where sediments were moistened with water in Teflon vials and heating was performed at 200^{o} C. Heating of the sediments using microwave was performed to compare the results of As release using stainless steel and Teflon containers. No significant ($P < 0.05$) difference was found in the As release using different vials.

5.2.4 Sequential extraction of arsenic

A sequential extraction of As was performed before and after the heat treatment of the sediments to determine the effect of heat on As distribution in different inorganic and organic phases such as soluble, exchangeable, bound to carbonates, associated with amorphous and crystalline Fe and Mn oxyhydroxides, sulfides and organic matter in sediments; see detail in Table 3-2, Chapter 3. Sequential extraction procedure (SEP; Javed et al., 2013) was applied for As fractionation in sediments. Briefly, sediments (0.4 g) were sequentially extracted with 40 mL of the extractants for appropriate period of time as given in Table 3-2. The sediment-extractant suspensions were shaken for the specified duration, and then centrifuged for 40 min at 6000*g* to separate the supernatants, which were decanted without removing any sediment particles. The sediments were washed with nanopure water for 30 min before adding the next extractant. After centrifugation, the washing solutions were pooled with their respective decanted solutions, filtered through 0.45-μm PTFE filters (033911C, Fisher Scientific), acidified (1% final concentration of HNO_3), and analyzed for As using quadrupole ICP-MS.

5.2.5 Inductively coupled plasma mass spectrometer (ICP-MS) analysis

To quantify As concentrations in liquid phase and different fractions of the sequential extraction, quadrupole ICP-MS was used with quality control / quality assurance analytical protocols. Arsenic external standards (CLMS-2N; SPEX Certi Prep) prepared in 1% HNO_3, and scandium (Sc) and yttrium (Y) as internal standards were used for quantitation and accounting for any instrumental drift over time. The limit of detection (LOD: determined using 3 × standard deviation (σ) of intensities of 7 blanks + average of the 7 blank intensities) of quadrupole ICP-MS for As was 0.01 μg L^{-1}. The detail of the ICP-MS analysis and QA/QC is provided in section 2.2.3.

5.2.6 Scanning electron microscopy (SEM) of sediments before and after heat treatment

To study the micromorphology of sediment before and after the heat treatment of sediments moisten with both synthetic aquifer and nanopure water, a high spatial resolution (~3 nm) JEOL scanning electron microscope (SEM; Field Emission) was used at the University of Alberta. JEOL SEM was used to get high-resolution digital images of surface textures and microstructures, at magnifications ranging from 20x to 250,000x with a resolution of approximately ~3 nm. Powdered sediment samples were mounted on an aluminum stub using a double-sided carbon tape, coated with carbon to prevent the charging on sample surface due to the electron beam and examined under SEM.

5.2.7 Statistical analysis

To compare As data before and after the heat treatment, analysis of variance (ANOVA) was applied to mean values of As in different sediment phases. After ANOVA, least significant difference (LSD) method was used to do the pair wise comparison of the means of As fractions. Statistical software SAS 9.3 was used to perform all the statistical analyses in this study.

5.3 Results and discussion

5.3.1 Effect of heat on Arsenic release from sediments

To determine the effect of heat (~200° C) on As release from sediments, seven sediment samples (S1-S7) collected from different geological formations such as Empress, Marie Creek, Ethel Lake, Bonnyville and shale were used in this study. The range of total As concentration in sediments was 3.5 ± 0.1 µg g^{-1} to 28.4 ± 1.8 µg g^{-1}.

After the heat treatment, liquid phase could not be separated for As analysis using centrifugation from sediments moistened at 15 % and 50 % moisture. However to determine change in the distribution of As with different host phases in sediments, sequential extraction of As before and after the heat treatment of sediments was performed. Results of As sequential extraction are described in section 5.3.2.

The results regarding the effect of heat on As release in aqueous phase from sediments moistened at 1.4:1 or 3.7:1 synthetic aquifer water or nanopure water to sediment ratio are shown in Table 5-2. After heating the sediment-water slurry, ~1320 µg L^{-1} and ~3148 µg L^{-1} As were released in the aquifer water from sediments moistened at 1.4:1 and 3.7:1 aquifer water to sediment ratio, respectively. Higher As (~3300 µg L^{-1} and ~4155 µg L^{-1} As from 1.4:1 and 3.7:1 nanopure water to sediment ratio, respectively) was released into the nanopure water from sediments after the heat treatment. These results suggested that thermal shock of ~200° C temperature to sediments could release As in the aqueous phase. The release of significant As from sediments into porewater by heat could be due to the high surface area of the sediments exposed to the heat because of the grinding the intact core sediments. The particle size distribution of the sediments is provided in Table D-1. The As release from sediments could significantly ($P < 0.05$) increase if the moisture would be high in sediments, and the As release from sediments could be further enhanced if the associated porewater of the sediments would be of less ionic strength. These results are in conformity with the findings of Fennell, (2008) who found a rapid increase (10 μg L^{-1} to 220 μg L^{-1}) in the aqueous As concentration at 200^{o} C heating of a sediment containing 1.4 ± 0.3 μg g^{-1} As. Tabelin et al., (2014) reported a significant increase in As release from sediments by increasing the liquid to solid ratio for As extraction.

5.3.2 Effect of heat on arsenic fractionation in sediments

To determine the effect of heat (~200^{o} C) on As distribution with different host phases in sediments, a detailed sequential extraction of As (Javed et al., 2013) was performed before and after heat treatment of sediments. To determine which As host phases in sediments contributed to As release into the porewater after the heat treatment, a high As sediment (S7: contained 28.4±1.8 μg g^{-1} total As that was partitioned in all the host phases in sediments) moistened with 1.4:1 or 3.7:1 aquifer or nanopure water to solid ratio was used. The results showed that As release from sediments after the heat treatment was caused by a significant ($P < 0.05$) decrease in exchangeable and specifically adsorbed As phases (Table 5-3).

The distribution of As with different solid phases such as crystalline Fe oxides, silicates and sulfides did not significantly change by the effect of heat.

The effect of heat on As fractionation in sediments moistened with 15 % and 50 % synthetic aquifer or nanopure water was also studied. Because of the insignificant ($P > 0.05$) difference in the As fractionation between the 15 % and 50 % moistened sediments (Tables D-2 and D-3), both results of As fractionation in sediments were averaged to avoid complexity in the presentation of results. The overall results of As fractionation in sediments (n = 7; average of each phase in 7 sediments) before heat treatment, As fractionation in sediments moistened with synthetic aquifer water after the heat treatment, and As fractionation in sediments moistened with nanopure water after the heat treatment are shown in Figure 5-1. The detailed As fractionation results in all the sediments before and after the heat treatment have been provided in Figure D-1 A-C.

The As fractionation in sediments before heat treatment (without adding water) showed that the dominant As containing phases were specifically adsorbed, sulfides, amorphous and crystalline Fe oxides, and silicates minerals in sediments. Other phases such as soluble, exchangeable, carbonate and organic matter contained insignificant As (< 10% of total As). Before heat, the maximum average As (2.5 ± 0.2 µg g^{-1}; ~21% of total As) was found in each of the specifically adsorbed and sulfide bound phases in sediments (Figures 5-1 and D-1 A). Around 16 % of the total As (~1.9 ± 0.2 µg g^{-1}) was associated with crystalline Fe oxides in sediments. Silicate minerals (1.6 ± 0.1 µg g^{-1}; ~14% of total As) and amorphous Fe oxides (1.4 ± 0.1 µg g^{-1}; ~12% of total As) also contained a significant proportion of total As in sediments. Rest of the sediment phases such as soluble, exchangeable, carbonate bound and organic matter bound As contained < 10 % of total As.

The detailed As fractionation results after heat (~200° C) treatment of the sediments moistened with synthetic aquifer water are shown in Figure D-1 B. After heat, a significant change was found in soluble and exchangeable phases in sediments. The average soluble As in all the sediments (n = 7) significantly ($P <$ 0.05) increased from 120 ± 6 μg kg^{-1} (soluble As in sediments before heat) to 663 ± 44 μg kg^{-1} (soluble As in sediments after heat) in the sediments. The increase in the soluble As in our sediments corresponded to the significant ($P < 0.05$) decrease of As from 858 ± 46 μg kg^{-1} to 509 ± 34 μg kg^{-1} in exchangeable phase. In addition to exchangeable As, slight decrease in As was also found in specifically adsorbed and amorphous Fe oxide phases, but the decrease was statistically insignificant ($P > 0.05$). Fennel (2008) reported a significant (~20 %) decrease in As associated with amorphous Fe and Al oxide by the effect of heat (~200° C). Rest of the As phases such as specifically adsorbed, crystalline Fe oxide, silicates, sulfides and organic matter bound As in the sediments moistened with aquifer water remained unchanged by the effect of heat.

The effect of heat treatment on As fractionation in sediments moistened with nanopure water is also shown in Figures 5-1 and D-1 C. After heat treatment, a significant increase in the concentration of soluble As from 120 ± 6 μg kg^{-1} to 987 ± 42 μg kg^{-1} ($P < 0.05$) was found in the sediments. The increase in the soluble As was accompanied with the significant decrease of As in exchangeable (from 858 ± 46 μg kg^{-1} to 391 ± 16 μg kg^{-1}; $P < 0.05$), specifically adsorbed (from 2.5 ± 0.1 μg g^{-1} to 2.2 ± 0.1 μg g^{-1}; $P < 0.05$) and amorphous Fe oxide phases (from 1.4 ± 0.1 μg g^{-1} to 1.1 ± 0.1 μg g^{-1}; $P < 0.05$). Rest of the As phases such as crystalline Fe oxides, silicates, sulfides and organic matter in the sediments moistened with nanopure water remained unchanged by the effect of heat. These results suggest that sediments moistened with nanopure water would liberate As from sorbed (exchangeable and specifically adsorbed) and amorphous Fe oxides phases after the heat treatment compared to the sediment moistened with aquifer water where As was released only from exchangeable phase. More release of As from sediments moistened with nanopure water was probably because of high activity of nanopure water as soluble salts (ionic strength) would decrease activity of water such as synthetic aquifer water.

Effect of heat on As fractionation in sediments from different geological formations such as Marie Creek, Ethel Lake, Bonnyville, Empress and shale was also investigated. The As fractionation results of all the sediments derived from different geological formations before the heat treatment are shown in Figure D-2 A. The results of As fractionation after the heat treatment of sediments moistened with synthetic aquifer water and nanopure water are shown in Figure D-2 B and C, respectively. After the heat treatment, a significant increase in the soluble As (F1 of SEP) was found in all the sediments (moistened with either of the waters) from different geological formations (Figure D-2 B and C). A clear difference in the effect of heat on exchangeable As was found among the sediments of different geological formations moistened with synthetic aquifer water. The sediments derived from Ethel Lake and shale showed significant ($P < 0.05$) decrease in the exchangeable As after heat. However, the exchangeable As in sediments derived from Marie Creek, Bonnyville and Empress formations did not significantly change after the heat treatment. On the other hand, a significant ($P < 0.05$) decrease in the exchangeable As in all the sediments moistened with nanopure water was found after heat treatment. Rest of the As phases such as specifically adsorbed, amorphous and crystalline Fe oxides, silicates and sulfides bound As in sediments moistened with aquifer or nanopure water did not significantly change after the heat treatment. These results suggest that sediments of Ethel Lake and shale are more prone to release As by the effect of heat, probably because of their high total As 10.5 $\mu g\ g^{-1}$ and 17.7 $\mu g\ g^{-1}$ (n =2), respectively and different lithology (texture). The Ethel Lake sediments had dominant clay and silt that attribute the high exchangeable As in sediments; which might be one of the reasons of more As release from sediments by the effect of heat. The lithology of the shale was not reported by Andriashek (2003).

5.3.3 Micromorphology of sediments before and after heat treatment

Scanning electron microscope (SEM) was used to study the micromorphology of the sediments before and after the heat treatment where sediments were moistened with 15% synthetic aquifer or nanopure water. Since only soluble, exchangeable and specifically adsorbed As phases were affected during thermal treatment and no As was released from mineral phases such as sulfides and silicates, we were not expecting any significant change in micromorphology. SEM backscattered image of the sediments before heat treatment clearly showed dominance of clays with some pyrite (FeS_2) mineral in the sediments (Figure 5-2 A). The intact crystal structures of both the clays and FeS_2 were found in both sediments moistened with aquifer and nanopure water after the heat treatment (Figure 5-2 B and C). These results supported our As fractionation results where we did not find any significant change in the As concentration associated with silicate and sulfide minerals after the heat treatment.

5.4 Conclusions

A laboratory experiment was conducted to determine the effect of intense heat (~200^o C) on As release into porewater from sediments collected from different geological formation in the Cold Lake area, Alberta. Before heat, the sediments were moistened with synthetic aquifer or nanopure water at 1.4:1 and 3.7:1 liquid to solid ratio to simulate the conditions in the aquifer sediments. After heat at 200^o C, a significant release of As was found in synthetic aquifer and nanopure water. To determine the As phases in sediments that release As by the effect of heat, As fractionation was performed. The results showed that release of As in the aqueous phase after the heat treatment was caused by significant ($P < 0.05$) decrease in exchangeable and specifically adsorbed As phases.

To determine the effect of heat on sediments with low moisture contents (non-aquifer sediments) that also remain in contact to the hot wells, the sediments were moistened with 15 % and 50 % (natural moisture contents) synthetic aquifer or nanopure water before heat. After heat treatment the liquid phase could not be recovered because of low moisture contents, therefore, As sequential extraction was applied to study the change in different As phase by the effect of heat. A significant ($P < 0.05$) increase in the soluble As in sediments moistened with aquifer or nanopure water was found by the effect of heat. The soluble As was significantly higher in the sediments moistened with nanopure water compared to the soluble As in sediment moistened with aquifer water. Overall, the As fractionation results after the heat treatment of the sediments showed that exchangeable, specifically adsorbed and amorphous Fe oxides phases contributed to the increase in soluble As. The results of this study will help understand the extent of As release during ongoing industrial processes in the Cold Lake area so that management strategies could be developed to mitigate groundwater As contamination.

Literature cited

Alberta Environment. Cold Lake – Beaver River Basin Groundwater Quality State of the Basin Report. 2006.

Andriashek L. D. Quaternary geological setting of the Athabasca Oil Sands (in situ) area, Northeast Alberta. 2003. http://www.ags.gov.ab.ca/publications/ESR/PDF/ESR_2002_03.pdf

Fennell J. W. Effects of aquifer heating on groundwater chemistry with a review of arsenic and its mobility. PhD thesis 2008, Universiyt of Calgary.

Imperial Oil, Cold Lake Operations. http://www.imperialoil.ca/Canada-English/operations_sands_cold.aspx (Accessed December 9, 2014).

Javed M. B., Kachanoski G., Siddique T. A modified sequential extraction method for arsenic fractionation in sediments. Anal Chim Acta 2013;787:102–110.

Javed M. B., Kachanoski G., Siddique T. Arsenic fractionation and mineralogical characterization in sediments in the Cold Lake Region of Alberta , Canada. Sci Total Environ 2014;500-501:181–190.

RAMP (Regional aquatics monitoring program). http://www.ramp-alberta.org/resources/development/history/insitu.aspx (Accessed December 18, 2014).

Tabelin C. B., Hashimoto A., Igarashi T., Yoneda T. Leaching of boron, arsenic and selenium from sedimentary rocks: I. effects of contact time, mixing speed and liquid-to-solid ratio. Science of the Total Environment 2014;47:620-629.

US EPA. Method 3050B acid digestion of sediments, sludges, and soils. Washington, D.C.: U.S. Environmental Protection Agency; 1996.

Tables and figures

Table 5- 1. Physicochemical properties of sediments used for arsenic release and fractionation in sediments by the effect of heat (~200° C).

Samples ID	**As $_{total}$**	**TOC**	**Sulfides**	**pH**	**Lithology**[a]	**Formation**[a]
	µg g^{-1}	%	%			
S1	3.5± 0.1	0.6 ± 0.1	0.1 ± 0	7.3± 0.3	Clay and silt	Empress
S2	4.2± 0.3	0.1 ± 0.0	0.1 ± 0	7.2± 0.3	Till	Marie Creek
S3	7.0 ± 0.7	0.6 ± 0.1	0.7 ± 0.1	9.1± 0.3	ND	Shale
S4	8.8± 0.9	0.3 ± 0.0	0.3 ± 0.1	7.4± 0.3	Mudstone	Bonnyville
S5	10.5± 1.1	0.7 ± 0.1	0.6 ± 0	6.6± 0.2	Clay and silt	Ethel Lake
S6	19.9± 1.8	2.8 ± 0.2	1.9 ± 0.1	6.2± 0.3	Till	Bonnyville
S7	28.4± 1.8	ND	2.2 ± 0.2	7.1± 0.2	ND	Shale

[a] The information about lithology and texture was obtained from Andraishek (2003).

Table 5- 2. Effect of heat (~200° C) on arsenic release in the porewater from sediments (S1 - S7) moistened with synthetic aquifer and nanopure water at 1.4:1 and 3.7:1 liquid to solid ratio to simulate the conditions in the aquifer.

	Synthetic aquifer water		Nanopure water	
Sample	1.4:1	3.7:1	1.4:1	3.7:1
	µg L^{-1}			
S1	565±23	1176±38	1106±26	1336±34
S2	489±28	1554±49	1324±30	1782±70
S3	1137±38	2123±65	2730±54	3038±34
S4	1735±52	4207±20	4557±39	5335±42
S5	1726±46	5029±47	5016±47	5993±28
S6	2199±69	4972±38	5191±57	6638±58
S7	1390±31	2975±35	3175±32	4965±37

Values represent the mean from analysis of triplicate ± 1 standard deviation.

After the heat treatment, the sediments were centrifuged (Sorvall® RC-5B Refrigerated Superspeed Centrifuge with Sorvall® HS-4 rotor) for 40 min at 6000*g* to separate the liquid phase for the analysis of release As.

Table 5- 3. Effect of heat (~200^{o} C) on arsenic fractionation in a high arsenic sediment (S7) moistened with synthetic aquifer or nanopure water at 1.4:1 and 3.7:1 liquid to solid ratios.

Fraction	Before heat	After heat			
		Sediment moistened with aquifer water		Sediment moistened with nanopure water	
		1.4:1	3.7:1	1.4:1	3.7:1
		Arsenic (µg g^{-1})			
F1	0.1±0	<LOD [a]	<LOD	<LOD	<LOD
F2	1.9±0.2	0.2±0	<LOD	<LOD	<LOD
F3	4.1±0.4	3.1±0.3	2.6±0.2	1.8±0.1	1.6±0.4
F4	0.1±0	<LOD	<LOD	<LOD	<LOD
F5	1.6±0.1	2.2±0.1	2.1±0.3	1.6±0.3	1.1±0.1
F6	5.5±0.5	6.2±0.5	6.1±0.6	6.1±0.6	5.9±0.5
F7	2.6±0.2	2.3±0.3	2.3±0.3	2.3±0.2	2.3±0.3
F8	8.4±0.6	8.1±0.7	8.1±0.7	8.1±0.8	8.1±0.7
F9	2.8±0.3	2.8±0.4	2.8±0.3	2.8±0.4	2.8±0.4
F10	0.8±0.2	<LOD	<LOD	<LOD	<LOD

Values represent the mean from analysis of duplicate ± 1 standard deviation.

[a] Limit of detection (LOD; determined using 3 × standard deviation (σ) of intensities of 7 blanks + average of the 7 blank intensities)

F1 to F10 represent As fractions: F1, water soluble As; F2, ionically bound/exchangeable As; F3, strongly/specifically adsorbed As; F4, As bound in carbonates; F5, As coprecipitated with amorphous Fe, Al and Mn oxyhydroxides; F6, As coprecipitated with crystalline Fe, Al and Mn oxyhydroxides; F7, As associated with its oxides and silicate clays; F8, As coprecipitated with pyrite and orpiment; F9, As associated with organic matter and recalcitrant sulfides; and F10, residual As.

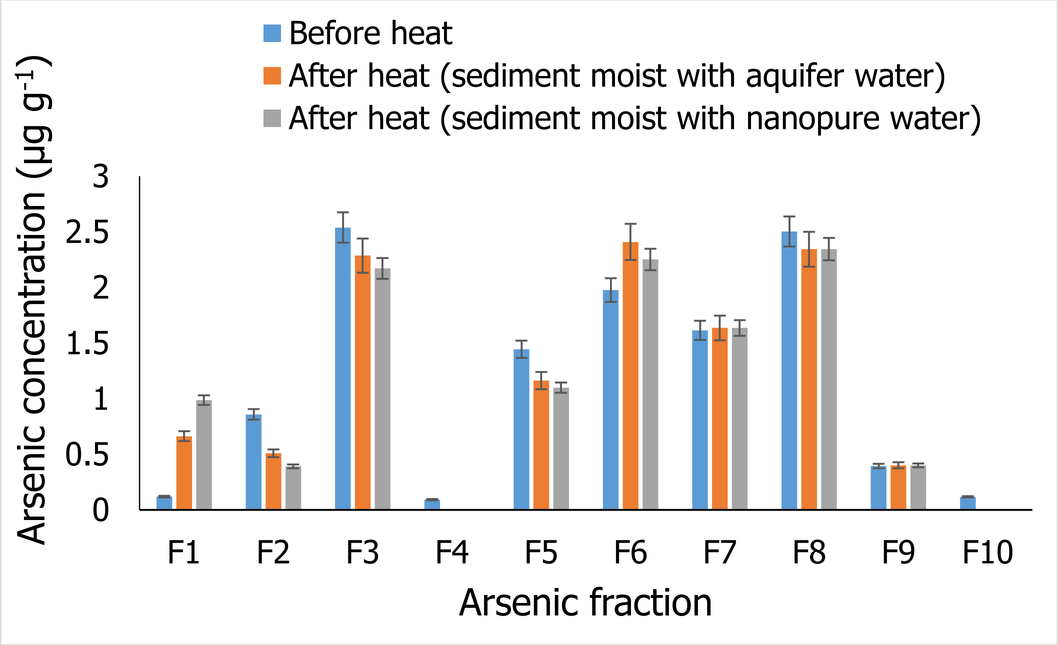

Figure 5- 1. Arsenic fractionation before and after (~200°C) heating the sediments moistened with synthetic aquifer or nanopure water to determine the effect of heat on arsenic fractionation in sediments.
Bars represent the mean of As fractions from analysis of 7 sediments ± standard error.

The sediments were moistened with 15% and 50% for either synthetic aquifer or nanopure water, however, due to insignificant difference in the fractionation results both the results of As fractionation were averaged to avoid complexity.

F1 to F10 on X-axis represent As fractions: F1, water soluble As; F2, ionically bound/exchangeable As; F3, strongly/specifically adsorbed As; F4, As bound in carbonates; F5, As coprecipitated with amorphous Fe, Al and Mn oxyhydroxides; F6, As coprecipitated with crystalline Fe, Al and Mn oxyhydroxides; F7, As associated with its oxides and silicate clays; F8, As coprecipitated with pyrite and orpiment; F9, As associated with organic matter and recalcitrant sulfides; and F10, residual As.

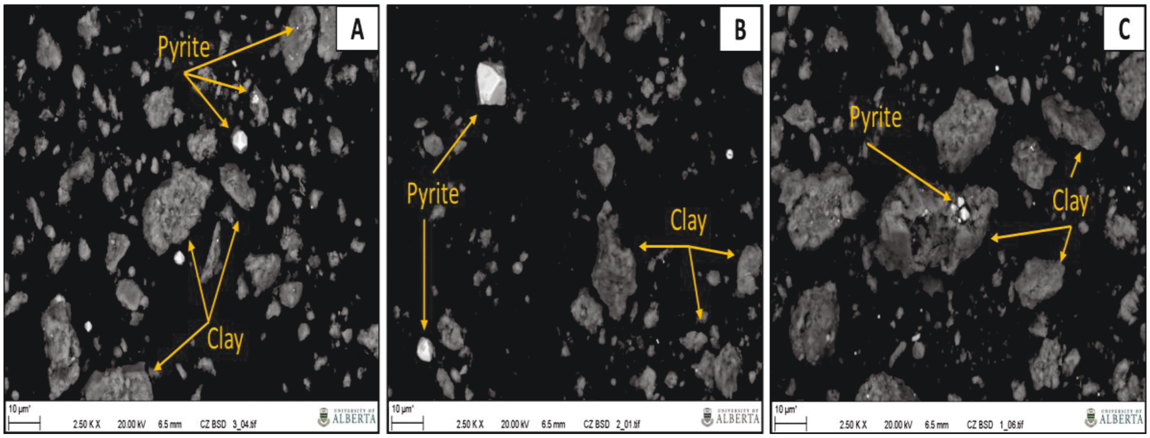

Figure 5- 2. Micromorphology of the (A) sediments before the heat treatment, (B) sediments moistened with synthetic aquifer water after the heat treatment, and (C) sediments moistened with nanopure water after the heat treatment.

Micrographs show the intact clay and pyrite minerals in the sediments before and after the heat treatment which do not show any significant change in their morphology during heat treatment.

Chapter 6. Development of method for arsenic speciation in river water and sediments[5]

6.1 Introduction

Arsenic (As) is one of the most abundant elements in the earth's crust that exists in many chemical species. It has long been established that study of the total As concentration in the natural ecosystems is not sufficient to predict the toxicity effect of As on environmental and human health (Gong et al., 2002; Wang et al., 2007). Bioavailability and toxicity of As depend on its chemical species. The dominant inorganic species of As are arsenate (H_3AsO_4; As^V) and arsenite (H_3AsO_3; As^{III}), which are most toxic As species and usually present in soil, sediments, and water (Cullen and Reimer, 1989). Between the inorganic As forms, arsenite is more toxic than arsenate (Wang and Mulligan, 2006). The dominant methylated species of As are monomethylarsonic acid [$CH_3AsO(OH)_2$; MMAA] and dimethylarsenic acid [$(CH_3)_2AsOOH$; DMAA], which are less toxic compared to the inorganic As forms. The methylated forms of As are important in As biogeochemical cycle, where inorganic As species are biologically converted to the volatile methylated forms of As that escape water and soil regimes to the atmosphere. Therefore, the methylated As species are present in much lower concentrations in soil, sediments and groundwater (Cullen and Reimer, 1989). The organic As compounds such as arsenobetaine (AsB) and arsenocholine (AsC) are relatively nontoxic and commonly found in seafood (Milstein et al., 2002).

---

[5] A version of this chapter is in preparation for publication.

Between the inorganic As species, arsenate species are dominant in environmental samples such as river water, soil and sediments under aerobic conditions, and their concentrations in natural waters are limited by adsorption onto hydrated ferric oxide (HFOs) phases, aluminium (Al) hydroxide, manganese (Mn) oxides or clays where these phases are present (Giles et al., 2011). Arsenite species are dominant in anaerobic environments, and may also adsorb onto these phases such as HFOs. In certain conditions such as high pH (>8.5), high As:Fe ratio and high total dissolved As, the adsorption of As^{III} onto Fe oxides may be more favoured than that of As^{V} (Pierce and Moore, 1982; Cheng et al., 2009). In sulfide-rich waters, only As^{III} is generally present and its solubility is limited by the formation of As sulfides such as orpiment (As_2S_3) and realgar (AsS) or As-bearing iron sulfides such as pyrite (FeS_2) (O'Day et al., 2004). Adsorption of arsenite and arsenate on solid phases in soil or sediment is of principal importance that regulates the fate and mobility of As species in natural environment, and the overall rate of adsorption relies mainly on pH of the system (Smedley and Kinniburgh, 2002).

Different techniques are used to determine the As speciation. Arsenic speciation in environmental samples can be determined using hydride generation-atomic absorption spectrometry (HG-AAS). In HG, all the As species must be reduced using suitable reducing agent such as sodium borohydride ($NaBH_4$) and concentrated hydrochloric acid (HCl) (Anawar, 2012) to produce volatile hydride form of As (AsH_3) that can be detected by AAS (Bora et al., 2014). Thus we can determine only hydride forming As species such as As^{III} using HG-AAS

(Georgiadis et al., 2006; Anawar 2012). To determine As^{V} using HG-AAS, it must be converted to As^{III} using potassium iodide (KI) or L-cysteine before the HG-AAS analysis so that total As (As^{III} + As^{V}) concentration can be measured in the form of As^{III}. Without pre-reduction of As^{V}, As^{III} concentration in the sample can be determined, and then subtracted from total As concentration to calculate As^{V}. In addition to the indirect quantification of As species, HG-AAS technique provides high procedure detection limits, a narrow linear calibration range, and interferences from transition elements for As quantification (Frank et al., 2006). In recent years, however, hyphenated techniques such as a combination of chromatography for separation of As species with inductively coupled plasma mass spectrometer (ICP-MS) for quantification of individual species are widely used for As speciation analysis. ICP-MS is commonly used for quantification of metal species with chromatography since it produces high sensitivity, large dynamic range and easy coupling with chromatographic instruments (Vassileva et al., 2001; Wang et al., 2007; Mar et al., 2009).

The quantitative determination of As species in environmental samples is very challenging task. In natural water, these species tend to be unstable, and the stability depends on the redox condition, pH, presence of precipitating metals such as Fe(II/III), presence of organic matter, and microbial activity (Samanta and Clifford, 2005). To determine the As species in soil or sediments, As species must be extracted from soil/sediments for chemical analysis. Many studies have quantified the inorganic As species in soil and sediment samples using different solvent extraction methods (Zagury et al., 2008; Frentiu et al., 2007; Garcia-

Manyes et al., 2002). These studies provide useful information on the release of As species from soil and sediments. However, Georgiadis et al., (2006) reported that most of the speciation studies did not produce the true As speciation in environmental samples. Transformation between As species, particularly oxidation of As^{III} to As^{V} have been found frequently during the extraction process (Ellwood and Maher, 2003). Therefore, this study was conducted to develop a comprehensive protocol for As^{III}, As^{V} and DMAA speciation; (1) to optimize parameters for As speciation using IC-ICP-MS; (2) to evaluate the effect of different pH values (2 to 10) under both aerobic and anaerobic conditions on stability of As species in solutions prepared with nanopure water; (3) to determine the stability of As species in river water using common preservation methods such as filtration (0.2 μm and 0.45 μm), acidification ($pH < 2$ using HCl) and complexation using EDTA (pH 3.2); and (4) to develop a method to extract the As species from sediments.

6.2 Experimental section

6.2.1 Reagents

Trace metal grade nitric acid (HNO_3) was purchased from Sigma-Aldrich (Ontario, Canada) to prepare the mobile phase in ion chromatograph (IC) for separation of As species. Trace metal grade arsenic trioxide (As_2O_3; As^{III}), arsenic pentaoxide (As_2O_5; As^{V}) and sodium cacodylate ($C_2H_6AsNaO_2.3H_2O$; DMAA) to prepare the standard solutions of As species and sodium phosphate (NaH_2PO_4) to prepare the extraction solution to extract the As species from sediments were also purchased from Sigma-Aldrich. To adjust the pH of the extraction solution, trace metal grade hydrochloric acid (HCl; Fluka, Oakville, Canada), phosphoric acid (H_3PO_4; Fluka, Oakville, Canada) and sodium hydroxide (NaOH; Sigma Aldrich) were used.

The mobile phase of IC and all the standard and extraction solutions were prepared using nanopure water (Barnstead nanopure, Thermo Scientific). The reagents and experimental blanks were also analyzed along with the experimental samples where the concentrations of As^{III}, As^{V} and DMAA species were below the limit of detection (LOD $\leq$ 47 ng L^{-1}: determined using 3 × standard deviation (σ) of intensities of 7 blanks + average of the 7 blank intensities).

6.2.2 Optimization of the chromatographic conditions for arsenic speciation

Chromatographic separation of As^{III}, As^{V} and DMAA species was carried out using ion chromatograph (IC; Thermo Scientific Dionex ICS-5000) with a 25 µL injection loop for sample introduction. An anion exchange column (Dionex IonPac™ AS7; 4 mm ID x 250 mm length) was used throughout this study to separate different As species. An HNO_3 mobile phase with a gradient from 2.5 to 50 mM and flow rate of 1 mL min^{-1} was used in IC. IC was connected with the quadrupole iCAP Q ICP-MS (Thermo Scientific) equipped with helium (He) pressurized QCell (collision cell) in Kinetic Energy Discrimination (KED) mode to reduce polyatomic interferences. IC-ICP-MS was used for quantification of the individual As species. Under these IC-ICP-MS conditions, complete elution of As^{III}, As^{V} and DMAA species was achieved in 4 min. Operating conditions for the IC and ICP-MS are summarized in Table 6-1, and a typical chromatogram showing As^{III}, As^{V} and DMAA peaks is shown in Figure 6-1. To determine the total As concentration in sediments, a closed vessel microwave digestion system (Mars 6; CEM, Matthews, NC) was used for the digestion of sediments followed by As quantification using quadrupole ICP-MS. The detail of the digestion method is provided in section 2.2.3.

To maintain quality assurance and quality control (QA/QC), external standard solutions containing all three As species (As^{III}, As^{V} and DMAA) in the range of 0.2 to 4 $\mu g\ L^{-1}$ prepared in nanopure water were used to calibrate the IC-ICP-MS. Immediately after calibration standards, three initial calibration blanks (ICB) were analyzed to ensure that instrument was clean. During the analysis of experimental samples, continuous calibration blanks (CCB) to check any metal contamination in the instrument and continuous calibration verification (CCV) standard of 2 $\mu g\ L^{-1}$ of all three As species to assure the validity of the initial calibration of the instrument were also included after every 10 samples. The concentrations of all the As species in blanks (ICB and CCB) were below the LOD while the concentrations of As species in the CCVs were within ±10% of the initial values of As species (2 $\mu g\ L^{-1}$). In addition, rhodium (Rh) was used as internal standard in the quantification of As in all the external standards, ICB, CCB, CCV and experimental samples to account for any instrumental drift. In addition, a standard reference material (SRM) of As^{III} (Fluka: 01969 contained 1000 ± 2 mg L^{-1} As^{III}) and two natural water reference materials for total trace metals (SLRS-5 contained 0.413 ± 0.039 $\mu g\ L^{-1}$ As, and SRM® 1640a contained 8.010 ± 0.067 $\mu g\ L^{-1}$ As) were also used to validate the speciation method. SLRS-

5 was analyzed without any dilution, however SRM of As^{III} and SRM 1640a were diluted to bring the concentration within 0.2 to 4 µg L^{-1} (our standards limit). Employing the developed IC-ICP-MS method for quantification of As species, the As^{III} concentration quantified was in excellent agreement ($\pm$ 5%) with the certified value of As^{III} in SRM of As^{III}. For SLRS-5 and SRM 1640a, all the As was found as As^{V} that was within $\pm$ 10% of the certified As concentration in the reference materials.

6.2.3 Preservation of arsenic species in nanopure and river water samples

6.2.3.1 Effect of pH and redox conditions over time on arsenic species in nanopure water

Before sampling the river water to test the effect of different preservatives, a laboratory study was conducted to evaluate the effect of pH (2 to 10) over time (12 and 24 h) on stability of As^{III}, As^{V} and DMAA species in nanopure water under both aerobic and anaerobic conditions. For this study, solutions of As^{III} (2.42 $\pm$ 0.12 µg L^{-1}; concentration was measured using IC-ICP-MS), As^{V} (3.26 $\pm$ 0.16 µg L^{-1}) and DMAA (1.77 $\pm$ 0.08 µg L^{-1}) were prepared using nanopure water in 125 mL Nalgene™ wide-mouth HDPE bottles (Thermo scientific; 312104-0004). Two sets of solutions were prepared; one was placed under anaerobic conditions [in nitrogen (N_2) filled disposable artificial atmosphere chamber (Fisher Scientific; catalogue # 19066549)] and other was placed at ambient (aerobic) conditions. The original pH of all the solutions was ~3.1 $\pm$ 0.2. The pH of the solutions in both aerobic and anaerobic conditions was adjusted at different levels (2, 4, 6, 8 and 10). To test the effect of HNO_3 and HCl [both acids are used to preserve the As species; (Kumar and Riyazuddin, 2010)] on the stability of As species, pH 2 was adjusted with both acids separately, and pH 4 to 10 was adjusted using 0.1 M NaOH. Immediately after adjusting the pH, aliquots of all the solutions were analyzed (time 0) and remaining solutions were kept under both aerobic and anaerobic conditions for 12 and 24 h.

6.2.3.2 River water sampling and preservation of the arsenic species

To preserve the As^{III}, As^{V} and DMAA species in river water, water samples were collected from the North Saskatchewan River (Edmonton) in 50 ml medical grade polypropylene (Corning, NY) tubes. Different preservation methods such as filtration (through 0.2 μm or 0.45 μm filters), acidification (using HCl to bring the pH <2) and complexation (using EDTA-HOAc, pH 3.2) were applied to the river water in field to preserve the natural distribution of As^{III}, As^{V} and DMAA species. The original concentrations of As^{III} and DMAA in river water were below their respective limit of detections (LODs), therefore river water sample was spiked with the known amount of As^{III} (0.53 ± 0.03 μg) and DMAA (0.48 ± 0.02 μg) in the field before preservation. The water samples were transported to the laboratory under cold (~ $4^{o}C$) conditions in dark to prevent any transformation of the species. In the laboratory, water samples were stored under cold (~ $4^{o}C$) and dark conditions and all the sample handling was done in the nitrogen (N_2) filled disposable artificial atmosphere chamber. Analysis of As^{III}, As^{V} and DMAA species in river water was performed at pre-determined time intervals (0, 12, 24, 48, 96 and 168 h). In addition to the preservation of As species in the river water, the distribution of As species in dissolved and colloidal phases in the river water was also tested. A river water sample was collected without any filtration or acidification, spiked at three different concentrations (0.5, 1 and 2 μg L^{-1}) of As^{III}, As^{V} and DMAA species and tested for the distribution of species in dissolved and colloidal phases. To separate the colloidal phase, the river water sample was centrifuged at 14000 rpm (18407 rcf) for 30 min using micro-centrifuge (Eppendorf) in the laboratory. After centrifugation, the concentration of dissolved As species were quantified using IC-ICP-MS. The concentration of the As species in colloidal phase was calculated by subtracting the dissolved As species from spiked concentration of As species.

6.2.4 Extraction of arsenic species from sediments

To optimize the extraction conditions such as pH of the extraction solution and extraction time to extract As^{III}, As^{V} and DMAA species from sediments, a large glacial till sediment already collected ~20 m below ground surface from the big bend river, Edmonton was used. The sediment sample was already grounded and sieved through 125 μm sieve. In this experiment, all the sample handling was performed under anaerobic conditions [(in nitrogen (N_2) filled disposable artificial atmosphere chamber (Fisher Scientific; catalogue # 19066549)].

To extract the most labile fraction of As^{III}, As^{V} and DMAA species from sediment, 0.1 M NaH_2PO_4 solution (original pH ~4.2 $\pm$ 0.3) was used for different extraction time (6, 12, 18 and 24 h). The labile fraction of As species are environmentally important that can impart the As to the surrounding porewater under natural conditions. Phosphate extractants are commonly used to extract the exchangeable and specifically adsorbed As (Javed et al., 2013; Georgiadis et al., 2006). Upon initial characterization of sediment, only small concentration of As^V (0.31 ± 0.03 μg g^{-1}) was found in sediment. Therefore, the sediment was spiked with known amount of As^{III} (0.53 ± 0.03 μg), As^V (0.46 ± 0.02 μg) and DMAA (0.48 ± 0.02 μg) species. The spiked As species could not completely recover without any transformation of the As species using the 0.1 M NaH_2PO_4 solution (pH ~4.2 ± 0.3). Therefore, to get the optimum recovery of the spiked As species in sediment, 0.1 M NaH_2PO_4 solution of different pH (2, adjusted with HNO_3, HCl or H_3PO_4; 5 and 7, adjusted with 0.1 M NaOH) and different extraction time (6, 12, 18, 24 h) were tested. For extraction of different As species, 1 g sediment was added into a 50 ml medical grade polypropylene (Corning, NY; Fisher Scientific, catalog no. 0553849) tube and extracted with 40 mL of 0.1 M NaH_2PO_4 solution. An orbital shaker was used to shake the sediment-extractant suspension at a speed of ~300 rpm for a pre-determined period of time (6, 12, 18 and 24 h). After extraction, sediment-extractant suspension was centrifuged at 6000*g* for 30 min. The supernatant was then transferred into a 1.5 mL polypropylene IC vial (Thermo scientific; catalogue # 079812) and immediately analyzed for As^{III}, As^V and DMAA species using IC-ICP-MS as described in section 6.2.2. The sediment extraction was conducted in triplicates for each of the experimental conditions tested.

6.2.5 Optimization of the chromatographic conditions for selenium and chromium speciation

In addition to As speciation, chromatographic conditions were also optimized for the speciation of inorganic selenium (selenite, Se^{IV} and selenate, Se^{VI}) and chromium species (trivalent Cr^{III} and hexavalent Cr^{VI}).

Chromatographic separation of Se^{IV} and Se^{VI} species was carried out using similar IC-ICP-MS setup used for As speciation. The only difference in the IC method was use of 50 to 400 mM HNO_3 gradient and a flow rate of 1.5 to 2 mL min^{-1}. Operating conditions of the IC and ICP-MS for Se^{IV} and Se^{VI} speciation are summarized in Table 6-2, and a typical chromatogram showing Se^{IV} and Se^{VI} peaks is shown in Figure 6-2. For QA/OC purpose, a standard reference material (SRM) of Se^{IV} (Fluka: 50002 contained 998 $\pm$ 2 mg L^{-1} Se^{IV}) and a natural water reference materials for total trace metals (SRM® 1640a contained 19.97 $\pm$ 0.16 µg L^{-1} Se) were also used to validate the speciation method. Both the reference materials were diluted to bring the concentrations within 0.2 to 4 µg L^{-1} (our standards limit). Employing the developed IC-ICP-MS method for quantification of Se species, the Se^{IV} concentration quantified was in excellent agreement with the certified value of Se^{IV} in SRM of Se^{IV}. For SRM 1640a, both Se^{IV} and Se^{VI} were found and the sum of species was within $\pm$ 10% of the certified Se concentration in the reference material.

Chromatographic conditions for the speciation of inorganic chromium species (Cr^{III} and Cr^{VI}) were also optimized. For chromatographic separation of Cr species, an anion exchange guard column (Dionex IonPac™ AG7; 4 mm ID x 50 mm length) was used instead of AS7 analytical column. This AG7 column has both cationic and anionic exchanger phases due to the presence of sulfonic and alkyl quaternary ammonium functional groups (Xing and Beauchemin, 2010). An HNO_3 mobile phase of 400 mM, and 0.6 to 1 mL min^{-1} flow rate were used in IC. Under these IC-ICP-MS conditions, complete elution of Cr^{III} and Cr^{VI} species was achieved in 5 min. Operating conditions of the IC and ICP-MS are summarized in Table 6-3, and a typical chromatogram showing Cr^{III} and Cr^{VI} peaks is shown in Figure 6-3. To maintain QA/QC, a standard reference material (SRM) of Cr^{III} (Fluka: 74582 contained 1002 $\pm$ 4 mg L^{-1} Cr^{III}) and two natural water reference materials for total trace metals (SLRS-5 contained 0.208 $\pm$ 0.023 µg L^{-1} Cr, and SRM® 1640a contained 40.22 $\pm$ 0.28 µg L^{-1} Cr) were also used to validate the speciation method. SLRS-5 was analyzed without any dilution, however SRM of Cr^{III} and SRM 1640a were diluted to bring the concentration within 0.2 to 4 µg L^{-1} (our standards limit). Employing the developed IC-ICP-MS method for quantification of Cr species, the Cr^{III} concentration quantified was in excellent agreement ($\pm$ 5%) with the certified value of Cr^{III} in SRM of Cr^{III}. For SLRS-5 and SRM 1640a, all the Cr was found as Cr^{III} that was within $\pm$ 10% of the certified Cr concentration in the reference materials.

6.3 Results and discussion

6.3.1 Chromatographic separation of arsenic species

The chromatographic separation of As^{III}, As^{V} and DMAA species was performed using IC followed by the determination and quantification of these species using quadrupole ICP-MS. The IC and ICP-MS operating parameters and a typical chromatogram of the As species are shown in Table 6-1 and Figure 6-1, respectively. In order to develop a chromatographic method that can effectively resolve the As^{III}, As^{V} and DMAA species, an anion-exchange column (Dionex IonPac™ AS7) was chosen that contained a strong anion exchanger with additional capacity for hydrophobic interactions. In combination with the strong anion exchange column, gradient elution of HNO_3 from 2.5 to 50 mM concentrations was used for better resolution of As^{III}, As^{V} and DMAA species within 5 min.

The AS7 analytical column has previously been used to separate the As^{III}, As^{V} and DMAA using NH_4BO_3, NH_4OH and $NH_4H_2PO_4$ in a gradient elution procedure (Jackson and Bertsch, 2001). However, the recommended eluent for AS7 column is HNO_3, and the separation of inorganic and organic As compounds has been demonstrated using HNO_3 (Mattusch and Wennrich, 1998). The ion exchange interactions between As species and exchanger phase in the column determine the elution order of the As^{III}, As^{V} and DMAA species. Due to their pK_a values such as As^{III} (pK_a^1 9.2), As^{V} (pK_a^1 2.2) and DMAA (pK_a^1 6.2), As^{III} eluted very quickly while As^{V} and DMAA strongly retained on the surface of the column (Figure 6-1). Due to the difference in the pK_a values, As^{V} and DMAA should resolved clearly in our chromatographic conditions where DMAA should elute before As^{V} because of the different apparent charges on As^{V} (-1) and DMAA (uncharged). The lipophilic/hydrophobic properties of DMAA might attribute to its strong retention in the column exchanger phase (Vassileva et al., 2001). Jackson and Bertsch (2001) also reported elution of DMAA after As^{V} similar to our observation. However, this observation is in contrast to the results obtained by Mattusch and Wennrich, (1998) who reported elution of DMAA before As^{V} using an AS7 column with HNO_3 as an eluent. This contrast is presumably due to the difference in the pH of the eluent, which in our method was 2.1 ± 0.3 (2.5 mM HNO_3) compared to a pH of 3.3 of the 0.5 mM HNO_3 used by Mattusch and

Wennrich (1998). The lower initial pH of the 2.5 mM HNO_3 in our method was nearer to the first pK_a of As^V (2.2), therefore As^V eluted earlier under our conditions compared to the chromatographic conditions used in Mattusch and Wennrich (1998). The later elution of DMAA was probably due to hydrophobic interactions with the column. The HNO_3 eluent used in our chromatographic separation is ideal for interfacing with quadrupole ICP-MS, because HNO_3 is generally used during sample analysis by quadrupole ICP-MS as the rinse solution and also in preserving samples prior to analysis.

The calibration curves of all three species based on the peak areas were linear in the range from 0.2 to 4 μg L^{-1} (Figure E-1). The percent relative standard deviation (RSD) of three replicates of all three species at 2 μg L^{-1} concentration were less than 5% and the analytical method was equally sensitive (1203 to 1252 cps ppb^{-1}) for all three species (Figure E-1). The LOD evaluated for each of the As species were 42 ng L^{-1} for As^{III}, 22 ng L^{-1} for As^V and 47 ng L^{-1} for DMAA.

6.3.2 Preservation of arsenic species in nanopure and river water

6.3.2.1 Stability of arsenic species in nanopure water at different pH and redox conditions

Before river water sampling and preservation of As species in river water sample, the stability of As^{III}, As^V and DMAA species in nanopure water was investigated at different pH values (2 to 10) under both aerobic and anaerobic laboratory conditions over time (12 and 24 h). The initial concentrations of As^{III} (2.42 $\pm$ 0.12 μg L^{-1}), As^V (3.26 $\pm$ 0.16 μg L^{-1}) and DMAA (1.77 $\pm$ 0.09 μg L^{-1}) measured using IC-ICP-MS in the solutions were same before they were incubated under aerobic and anaerobic conditions. Immediately after changing the pH of the solutions in both aerobic and anaerobic conditions, the speciation analysis of all the three species was performed (Figure 6-4; time 0). In As^{III} solutions with pH 2 adjusted with HNO_3 or pH 8 and 10 adjusted with 0.1 M NaOH, significant (>10 %) decrease in the concentration of As^{III} was found, possibly due to the oxidation of As^{III} (Figure 6-4). Oxidation of As^{III} by HNO_3 and at high (> 7) pH was also reported previously (McCleskey et al., 2004; Wang et al., 2014). However, the concentrations of As^{V} and DMAA species in all the solutions (n = 6) from pH 2 to 10 under both the conditions were within $\pm$ 10% of the concentrations of As^{V} and DMAA species in solutions where pH was not changed (Figure 6-4).

Effect of different pH levels on the stability of As^{III} solutions over time showed that As^{III} was found to be stable only in the solution of pH 2 adjusted with HCl under both aerobic and anaerobic conditions for 24 h. McCleskey et al., (2004) also reported that the distribution of As^{III} and As^{V} species remained unchanged for 45 days in standard solution of pH 2 with HCl. Under aerobic conditions over time (after 12 and 24 h), the concentrations of As^{III} in all the solutions at different pH levels remained within $\pm$10% of their initial As concentrations, except at pH 10 where As^{III} concentration was significantly (~26%; 0.47 ± 0.04 µg L^{-1}) decreased within 12 h and remained unchanged up to 24 h (Figure 6-4). The decrease in As^{III} concentration corresponded to the appearance of As^{V} in that solution suggesting the As^{III} oxidation at high pH. Wang et al., (2014) also reported the oxidation of As^{III} in the presence of OH^- that decrease the activation energy of As^{III} oxidation.

Under anaerobic conditions within first 12 h, As^{III} concentrations in all the As^{III} solutions of pH 2 to 10 remained unchanged except pH 10 where As^{III} decreased ~10% from its initial concentration (1.9 $\pm$ 0.1 μg L^{-1}). After 24 h, significant decrease (10 to 34%) in the As^{III} concentrations was found in all the As^{III} solutions except pH 2 adjusted with HCl, where change in As^{III} concentration was insignificant (~7% of the initial As^{III} concentration). However, the reason of the decrease in As^{III} concentration was not known.

Arsenate was found to be stable at all the pH levels (2 to 10) in both aerobic and anaerobic conditions up to 24 h. Effect of different pH levels on the stability of DMAA solutions over time showed that it remained stable under all the pH levels in anaerobic conditions up to 24 h. However in aerobic conditions at pH 10, ~16% decrease (1.77 μg L^{-1} to 1.48 μg L^{-1}) in the initial concentration of DMAA was found after 24 h (Figure 6-4). Both the acids (HCl and HNO_3) were found effective to preserve the DMAA species under both aerobic and anaerobic conditions up to 24 h. These results suggest that lowering the pH to 2 with HCl is an effective treatment to preserve As^{III}, As^{V} and DMAA species in nanopure water.

6.3.2.2 Preservation of arsenic species in river water

The effect of different preservation methods such as filtration (0.2 or 0.45), acidification (pH 2 using HCl) and complexation (EDTA pH 3.2) on As^{III}, As^{V} and DMAA preservation over time in river water sample is shown in Figure 6-5. The chemical characteristics of the river water were as follows: total organic C (32.4 $\pm$ 0.4 mg L^{-1}), Chloride (3.9 mg L^{-1}), nitrate (0.2 mg L^{-1}) and sulfate (12.8

mg L^{-1}). The total dissolved As concentration in river water was 0.4 ± 0.1 μg g^{-1} determined by quadrupole ICP-MS. Arsenic speciation analysis performed immediately after the sample collection showed that As^{V} was the only dominant As species (0.38 ± 0.04 μg L^{-1}; ~88 % of the total soluble As) in river water. Arsenite and DMAA were insignificant (< 5% of the total dissolved As) in the river water. Therefore, small amount of As^{III} (0.53 ± 0.03 μg) and DMAA (0.48 ± 0.02 μg) were spiked in the river water samples before applying the preservation techniques.

The distribution of As^{III}, As^{V} and DMAA species in the spiked river water remained unchanged in acidified (pH 2 with HCl), 0.2 μm filtered, and EDTA (pH 3.2) treated water for 7 days (Figure 6-5). Our results are in conformity with previous findings where acidification with HCl (pH 2) and complexation with EDTA (pH 3.2) were commonly used to preserve the As^{III} and As^{V} species in natural water (McCleskey et al., 2004; Samanta and Clifford, 2005). Our water sample filtered through 0.45 μm filter showed a gradual decrease in the concentrations of As^{V} with increase in As^{III} concentrations. McCleskey et al., (2004) also reported that filtration through 0.45 μm filter could not preserve the As^{III} and As^{V} distribution in natural water samples. The reduction of As^{V} in our 0.45 μm filtered and unpreserved (without any filtration, acidification and addition of EDTA) water sample might be due to the microbial activity because of high TOC (~32 mg L^{-1}) in our river water sample. Dissolved As^{V} is reduced rapidly only with either a strong inorganic reducing agent such as sulfides or by microbial activity through anaerobic dissimilatory respiration and detoxification mechanisms (Ahmann et al., 1994). Bednar et al., (2002) also reported rapid (within 100 h) reduction of >90 % of 10 μg L^{-1} As^{V} to As^{III} in groundwater and acid mine drainage samples because of microbial activity. Hall et al., (1999) monitored As^{III} and As^{V} distribution in deionized water spiked at two different concentrations (0.5 and 5 mg L^{-1}) of each species and kept under ambient conditions. He found nearly complete reduction of As^{V} to As^{III} within 2 days. A large number of microorganisms within the bacterial and archaeal domains have been identified that use As^{V} as a terminal electron acceptor for anaerobic respiration (Oremland and Stolz, 2003). Hence, a water sample that contains ~30 mg L^{-1} dissolved organic C and is kept under anaerobic conditions to avoid transformation of As species, may promote As^{V} reduction during storage if not properly preserved. Based on our results, it can be concluded that water samples that may contain concentration of As species ~1 μg L^{-1} and TOC ~30 mg L^{-1} can be preserved using HCl (pH < 2), 0.2 μm filter or EDTA (pH 3.2) and must be stored at 4°C in dark.

We also tested the distribution of As^{III}, As^{V} and DMAA in dissolved and colloidal phases in the river water to determine the partition of As species in both phases (Figure 6-6). For this study, the river water was used without any modification (no filtration, no acidification, and no addition of EDTA). We spiked the water sample with different concentrations (0.5, 1 and 2 μg L^{-1}) of each of the As species. The results showed that small concentrations of As^{III} (0.11 to 0.13 μg g^{-1}) and As^{V} (0.37 to 0.43 μg g^{-1}) were removed from the dissolved phase and adsorbed on the colloidal particles in all three solutions of 0.5 to 2 μg L^{-1}

concentrations of As^{III} and As^{V} tested in the river water. However, all the DMAA remained dissolved in all the solutions (Figure 6-6). These results suggested that colloidal particles could sequester/sorb only limited amount of As^{III} and As^{V} which did not depend on the concentrations of dissolved As species.

6.3.3 Optimization of extraction time and pH of 0.1 M NaH_2PO_4 solution to extract arsenic species from sediments

Arsenic species can be quantified chemically using IC-ICP-MS, however, to quantify the As species in sediments an extraction must be performed before quantification. During extraction, transformation between As species (particularly oxidation of As^{III} to As^{V}) has been found frequently (Ellwood and Maher, 2003). Therefore in this study, extraction time and pH of the extraction solution (0.1 M NaH_2PO_4) for extraction of As species from sediments was optimized to get the maximum recovery of As species without any transformation of As species. For our extraction method, 0.1 M NaH_2PO_4 solution (original pH 4.2) was used for the extraction of As^{III}, As^{V} and DMAA species from sediments. To extract the most labile fraction of As^{III}, As^{V} and DMAA species from sediments, phosphate solutions are commonly used that desorb the As species through ligand exchange reaction (Manning and Martens, 1997; Georgiadis et al., 2006). Ligand exchange process does not dissolve the adsorbent (solid phases) but actively competes with other metals or oxyanions such as As for exchange sites. Phosphate has many chemical properties similar to As^{V} such as ion size and acid dissociation constants, and the phosphate solution offers an extraction medium that is similar to environmental conditions that exist in soil and sediments (Georgiadis et al., 2006).

For initial characterization of the sediment sample used in this study, the sediment was extracted using 0.1 M NaH_2PO_4 (pH 4.2) for different extraction times (6, 12, 18 and 24 h). After extraction, only As^V (0.31 $\pm$ 0.03 µg g^{-1}) was found to be present in the sediment (Figure E-4) and there was no difference in the As^V concentration extracted for different extraction times. Because we did not have much As^{III} and DMAA in the sediment and As^V was also very low, we spiked the sediment with known amount of As^{III}, As^V and DMAA (0.53 $\pm$ 0.03, 0.46 $\pm$ 0.02 and 0.48 $\pm$ 0.02 µg, respectively) to test the recovery of these species using 0.1 M NaH_2PO_4 (pH 4.2) solution for 6, 12, 18 or 24 h extraction. All the spiked DMAA was recovered (> 90 % of spiked) after 6 h extraction (Figure 6-7 A). About 68% of the spiked As^{III} was recovered during 6 h extraction and no further significant increase in the recovery of As^{III} was achieved upon extending extraction time to 24 h. Regarding As^V, ~54% of the spiked As^V was recovered in the 6 h extraction, however, significant increase in the recovery of As^V was observed over extended period of extraction (Figure 6-7 A). After 24 h extraction, ~72% of the spiked As^V was recovered. Using 0.1 M NaH_2PO_4 (pH 4.2), all of the spiked As^{III} and As^V could not be recovered, even after 24 h extraction where ~70 % of the spiked amount of both As^{III} and As^V was recovered. However, we did not find any transformation between As^{III} and As^V species during the extraction, as the ratio of extracted As^{III} to As^V (1.11) was similar to the spiked As^{III} to As^V ratio (1.15).

To get the greater recovery of the spiked As species, pH of the 0.1 M NaH_2PO_4 solution was altered. We prepared the 0.1 M NaH_2PO_4 extraction solutions of pH 2 with HNO_3, HCl or H_3PO_4, and 5 and 7 with 0.1 M NaOH, and applied the extraction method on the un-spiked (Figure E-5) and spiked sediments (spiked in a similar way as described for earlier extraction method) for 6 h (Figure E-6).

Extraction of As^{III} and As^{V} with 0.1 M NaH_2PO_4 (pH 5) solution showed 66% and 72% recovery, respectively from the spiked sediment, and the species remained stable (As^{III}/As^{V}; 1.06, Figure E-6). Extraction of As^{III} and As^{V} using 0.1 M NaH_2PO_4 (pH 7) showed 60% and 80% recovery, respectively from the spiked sediment but significant (~25%) transformation of the species was found (As^{III}/As^{V}; 0.86). Extraction of As^{III} and As^{V} species using pH 2 extractants showed very low recovery of As^{III} (22 to 56 %) but recovery of As^{V} was very high in all three extractions performed using 0.1 M NaH_2PO_4 solutions adjusted at pH 2 (Figures E-5 and E-6). The high As^{V} might be due to the dissolution of some solid phases in sediments such as carbonates and acid volatile sulfides under strong acidic conditions. Therefore 0.1 M NaH_2PO_4 (pH 5) was selected to further test the optimum extraction time to recover the spiked As species. The results showed that the recovery of DMAA from the spiked sediment was >90 % in all the extraction solutions (Figure E-6).

Same spiked sediment sample was extracted with 0.1 M NaH_2PO_4 (pH 5) solution for 6, 12, 18 and 24 h to get the optimum recovery of As^{III}, As^{V} and DMAA. Extraction of As^{III} showed that ~70% of the spiked As^{III} was recovered in 6 h extraction, a significant further increase (around 22%) in As^{III} recovery was found in 12 h extraction that remained unchanged in the 18 h extraction (Figure 6-

7). However, in 24 h extraction, a decrease in the concentration of As^{III} was found, might be due to the oxidation of extracted As^{III}. Recovery of As^{V} was increased over time, after 18 h extraction all the spiked As^{V} (107%) was recovered. After 24 h extraction, the recovery of As^{V} was ~122%, probably due to the oxidation of As^{III}. All the spiked DMAA was extracted within 6 h extraction, and no significant change in the DMAA recovery was observed in 12 to 24 h extractions (Figure 6-7). These results of the As species extraction from sediments showed that 0.1 M NaH_2PO_4 (pH 5) solution for an extraction time of 18 h could be used to extract the As^{III}, As^{V} and DMAA species from sediments.

6.3.4 Chromatographic separation of selenium and chromium species

The chromatographic separation of selenium (Se^{IV} and Se^{VI}) and chromium (Cr^{III} and Cr^{VI}) species was performed using IC followed by the determination and quantification of these species using quadrupole ICP-MS.

In order to completely resolve the Se^{IV} and Se^{VI} species, an anion-exchange column (Dionex IonPac^{TM} AS7) was chosen that contained a strong anion exchanger interactions. In combination with the strong anion exchange column, gradient elution of HNO_3 from 50 to 400 mM concentrations was used for chromatographic separation of Se^{IV} and Se^{VI} species within 4 min. The IC and ICP-MS operating parameters and a typical chromatogram of the Se species are shown in Table 6-2 and Figure 6-2, respectively.

The AS7 analytical column has not been used previously to separate the Se^{IV} and Se^{VI} species. The ion exchange interactions between Se species and exchanger phase in the column determine the elution order of the Se^{IV} and Se^{VI}

species. Due to their pK_a values such as $\mathrm{Se^{IV}}$ (pK_a^1 2.35) and $\mathrm{Se^{VI}}$ (pK_a^1 <0), $\mathrm{Se^{IV}}$ eluted before $\mathrm{Se^{VI}}$, which strongly retained on the surface of the column (Figure 6-2). The use of HNO_3 eluent in our chromatographic separation is ideal for interfacing with quadrupole ICP-MS, because HNO_3 is normally used during sample analysis by quadrupole ICP-MS as the rinse solution.

The calibration curves of both Se species based on the peak areas were linear in the range from 0.2 to 4 μg L^{-1} (Figure E-2), and the percent relative standard deviation (RSD) of triplicates of $\mathrm{Se^{IV}}$ and $\mathrm{Se^{VI}}$ at all standard concentrations were less than 5%. The sensitivity of the method was almost double for $\mathrm{Se^{IV}}$ (1422 cps ppb^{-1}; Figure E-2A) compared to $\mathrm{Se^{VI}}$ (782 cps ppb^{-1}; Figure E-2B). The LOD evaluated for each of the Se species were 5 ng L^{-1} for $\mathrm{Se^{IV}}$ and 22 ng L^{-1} for $\mathrm{Se^{VI}}$.

To develop a rapid chromatographic separation of $\mathrm{Cr^{III}}$ and $\mathrm{Cr^{VI}}$ species, an anion-exchange guard column (Dionex IonPac^{TM} AG7; 2 x 50 mm) was chosen that contained both cationic and anionic exchanger phases due to the presence of sulfonic and alkyl quaternary ammonium functional groups (Xing and Beauchemin, 2010). Though the guard columns are generally designed to be used prior to analytical column to prevent contamination to analytical column, the highly effective separation medium in the AG7 column contains ability for the separation of both cationic ($\mathrm{Cr^{III}}$) and anionic ($\mathrm{Cr^{VI}}$) species (Dionex, 2014). A Thermo Scientific quadrupole iCAP Qc ICP-MS was used for the quantification of Cr species eluted from the ICS-5000. For $\mathrm{Cr^{III}}$ and $\mathrm{Cr^{VI}}$ speciation an isocratic elution of 400 mM HNO_3 was used with 0.6 to 1 mL min^{-1} flow rate of the 400 mM HNO_3. The IC and ICP-MS operating parameters and a typical chromatogram of the As species are shown in Table 6-3 and Figure 6-3, respectively.

The AS7 analytical column has been used to separate the Cr^{III} and Cr^{VI} using 50 mmol L^{-1} NH_4NO_3 (pH 8) in an isocratic elution procedure (Gurleyuk and Wallschlager, 2001). In their method, they made complex of the Cr^{III} with EDTA to make the $Cr(EDTA)^{-1}$ anion, and then resolve the $Cr(EDTA)^{-1}$ and Cr^{VI} anions. To avoid any pre-treatment of the sample for Cr^{III} and Cr^{VI} speciation, AG7 column was used with HNO_3 elution that is the recommended solution for the columns and quadrupole ICP-MS. In our chromatographic conditions where pH of the mobile phase was <2, Cr^{III} would be present as hexa-aqua chromium $[Cr(H2O)_6{}^{3+}]$ species, while Cr^{VI} would be present as $HCrO_4{}^{-1}$. Therefore, the anion interactions between Cr^{VI}, and cationic interaction between Cr^{III} species and exchanger phase in the column determine the elution order of the Cr^{III} and Cr^{VI} species (Xing and Beauchemin, 2010).

The calibration curves of both the species (Cr^{III} and Cr^{VI}) based on the peak areas were linear in the range from 0.2 to 4 μg L^{-1} (Figure E-3). The percent relative standard deviation (RSD) of triplicates of the species for all the standards concentrations were less than 5%. However, the analytical method was more sensitive for Cr^{VI} (78,189 cps ppb^{-1}; Figure E-3A) compared to the Cr^{III} (12,063 cps ppb^{-1}; Figure E-3B). The LOD evaluated for each of the Cr species were 37 ng L^{-1} for Cr^{VI} and 179 ng L^{-1} for Cr^{III}.

6.4 Conclusions

A very simple and robust modified method for arsenite (As^{III}), arsenate (As^{V}) and DMAA speciation was developed using ion chromatography coupled with quadrupole inductively coupled plasma mass spectrometer (IC-ICP-MS). The speciation method was equally sensitive (~1200 cps ppb^{-1}) for all three species with low detection limits ($\leq$ 47 ng L^{-1}). To preserve the As species in water, the effect of pH (2 to 10; pH 2 adjusted with both HNO_3 or HCl to determine the effect of acids, pH 4 to 10 adjusted with NaOH) on stability of As^{III}, As^{V} and DMAA species in nanopure water under both aerobic and anaerobic conditions over time (12 and 24 h) was studied. The results showed that lowering the pH of the solutions to 2 with HCl was a good preservative for all three As species in water samples under both aerobic and anaerobic conditions. Preservation of the As species in river water showed that pH 2 adjusted with HCl, 0.2 µm filtration or EDTA pH 3.2 (adjusted with acetic acid) were effective methods to preserve As^{III}, As^{V} and DMAA distribution in river water containing ~1 µg L^{-1} As and ~30 mg L^{-1} total organic carbon. In addition, to determine the As species in sediments an extraction method was also optimized. For the extraction of As^{III}, As^{V} and DMAA species from sediments, 0.1 M NaH_2PO_4 (pH 5) extraction for 18 h was found to be effective. This study provides a complete method for speciation of As^{III}, As^{V} and DMAA in river water and sediments without any transformation of the As species. In addition to As, detailed speciation methods for inorganic selenium (selenite, Se^{IV} and selenate, Se^{VI}) and chromium [trivalent (Cr^{III}) and hexavalent (Cr^{VI})] have been optimized. So far IC-

ICP-MS methods for Se^{IV}, Se^{VI}, Cr^{III} and Cr^{VI} have been optimized and work is in progress to optimize Se^{IV}, Se^{VI}, Cr^{III} and Cr^{VI} preservation method for water samples and extraction method for sediments.

Literature cited

Aggett J., Kriegman M. Preservation of arsenic (III) and arsenic (V) in samples of sediment interstitial water. Analyst. 1987;112:153–157.

Ahmann D., Roberts A. L., Krumholz L. R., Morel F. M. Microbe grows by reducing arsenic. Nature. 1994;371: 750.

Anawar H. M. Arsenic speciation in environmental samples by hydride generation and electrothermal atomic absorption spectrometry. Talanta. 2012;88:30–42.

Bednar A. J., Garbarino J. R., Ranville J. F., Wildeman T. R. Preserving the distribution of inorganic arsenic species in groundwater and acid mine drainage samples. Environ Sci Technol. 2002;36(10):2213–8.

Bora S., Aydin I., Kilinc E., Aydin F. Speciation of arsenic in soil, sediment and environmental samples. Speciat Stud soil, sediment Environ samples. Taylor & Francis Group, LLC. 2014.

Cheng H., Hu Y., Luo J., Xu B., Zhao J. Geochemical processes controlling fate and transport of arsenic in acid mine drainage (AMD) and natural systems. J Hazard Mater. 2009;165(1-3):13–26.

Cullen W. R., Reimer K. J. Arsenic speciation in the environment. Chem Rev. 1989;89(4):713–64.

Dionex homepage (http://www.dionex.com/en-us/products/columns/ic-rfic/specialty-packed/ionpac-as7/lp-73274.html) (Accessed December 9, 2014).

Ellwood M. J., Maher W. A. Measurement of arsenic species in marine sediments by high-performance liquid chromatography–inductively coupled plasma mass spectrometry. Anal Chim Acta. 2003;477(2):279–91.

Frank J., Krachler M., Shotyk W. Determination of arsenic in peat samples using HG-AFS and l-cysteine as pre-reductant. J Anal At Spectrom. 2006;21(2):204-207.

Frentiu T., Vlad S-N., Ponta M., Baciu C., Kasler I., Cordos E. Profile distribution of As(III) and As(V) species in soil and groundwater in Bozanta area. Chem Pap. 2007;61(3):186–93.

Garcia-Manyes S., Jiménez G., Padró A., Rubio R., Rauret G. Arsenic speciation in contaminated soils. Talanta. 2002;58(1):97–109.

Georgiadis M., Cai Y., Solo-Gabriele H. M. Extraction of arsenate and arsenite species from soils and sediments. Environ Pollut. 2006;141(1):22–9.

Giles D. E., Mohapatra M., Issa T. B., Anand S., Singh P. Iron and aluminium based adsorption strategies for removing arsenic from water. J. Enviro Manag. 2011;92:3011–3022.

Gong Z., Lu X., Ma M., Watt C., Le X. C. Arsenic speciation analysis. Talanta. 2002;58:77–96.

Gurleyuk H., Wallschlager D. Determination of chromium(III) and chromium(VI) using suppressed ion chromatography inductively coupled plasma mass spectrometry. J. Anal. At. Spectrum. 2001;16:926-930.

Hall G. E. M., Pelchat J. C., Gauthier G. Stability of inorganic arsenic (III) and arsenic (V) in water samples. J. Anal. At. Spectrum. 1999;14:205–213.

Jackson B. P., Bertsch P. M. Determination of arsenic speciation in poultry wastes by IC-ICP-MS. Environ Sci Technol. 2001;35(24):4868–73.

Javed M. B., Kachanoski G., Siddique T. A modified sequential extraction method for arsenic fractionation in sediments. Anal Chim Acta 2013;787:102–110.

Kumar A. R., Riyazuddin P. Preservation of inorganic arsenic species in environmental water samples for reliable speciation analysis. TrAC Trends Anal Chem. 2010;29(10):1212–23.

Manning B., Martens D. Speciation of arsenic (III) and arsenic (V) in sediment extracts by high-performance liquid chromatography-hydride generation atomic absorption spectrophotometry. Environ Sci Technol. 1997;31(1):171–7.

Mar J. L. G., Reyes L. H., Rahman G. M. M., Kingston H. M. S. Simultaneous extraction of arsenic and selenium species from rice products by microwave-assisted enzymatic extraction and analysis by ion chromatography-inductively coupled plasma-mass spectrometry. J Agric Food Chem. 2009 22;57(8):3005–13.

Mattusch J., Wennrich R. Determination of Anionic, Neutral, and Cationic Species of Arsenic by Ion Chromatography with ICPMS Detection in Environmental Samples. Anal Chem. 1998;70(17):3649–55.

McCleskey R. B., Nordstrom D. K., Maest A. S. Preservation of water samples for arsenic(III/V) determinations: an evaluation of the literature and new analytical results. Appl Geochemistry. 2004;19(7):995–1009.

Milstein L. S., Essader A., Pellizzari E. D., Fernando R. A., Raymer J. H., Levine K. E., Akinbo O. Development and Application of a Robust Speciation Method for Determination of Six Arsenic Compounds Present in Human Urine. Environ Health Perspect. 2002;111(3):293–6.

O’Day P. A., Vlassopoulos D., Root R., Rivera N. The influence of sulfur and iron on dissolved arsenic concentrations in the shallow subsurface under changing redox conditions. Proc Natl Acad Sci U S A. 2004;101(38):13703–8.

Oremland R. S., Stolz J. F. The ecology of arsenic. Science. 2003;300(5621):939–44.

Pierce M. L., Moore C. B. Adsorption of arsenite and arsenate on amorphous iron hydroxide. Water Res. 1982;16(7):1247–53.

Samanta G., Clifford D. A. Preservation of inorganic arsenic species in groundwater. Environ Sci Technol. 2005;39(22):8877–82.

Smedley P. L., Kinniburgh D. G. A review of the source, behaviour and distribution of arsenic in natural waters. 2002;17(5):517–568.

Vassileva E., Becker A., Broekaert J. A. C. Determination of arsenic and selenium species in groundwater and soil extracts by ion chromatography coupled to inductively coupled plasma mass spectrometry. Anal Chim Acta. 2001;441:135–46.

Wang R-Y., Hsu Y-L., Chang L-F., Jiang S-J. Speciation analysis of arsenic and selenium compounds in environmental and biological samples by ion chromatography-inductively coupled plasma dynamic reaction cell mass spectrometer. Anal Chim Acta. 2007;590(2):239–44.

Wang S., Mulligan C. N. Occurrence of arsenic contamination in Canada: sources, behavior and distribution. Sci Total Environ 2006;366:701–721.

Wang Z., Bush R. T., Sullivan L. A., Chen C., Liu J. Selective oxidation of arsenite by peroxymonosulfate with high utilization efficiency of oxidant. Environ Sci Technol. 2014;48(7):3978–85.

Xing L., Beauchemin D. Chromium speciation at trace level in potable water using hyphenated ion exchange chromatography and inductively coupled plasma mass spectrometry with collision/reaction interface. J. Anal. At. Spectrom., 2010, 25, 1046–1055

Zagury G. J., Dobran S., Estrela S., Deschênes L. Inorganic arsenic speciation in soil and groundwater near in-service chromated copper arsenate-treated wood poles. Environ Toxicol Chem. 2008;27(4):799–807.

Tables and figures

Table 6- 1. IC and ICP-MS operating parameters for arsenite (As^{III}), arsenate (As^{V}) and DMAA speciation.

Parameter	Value		
IC			
Column	Dionex AS-7 (4 mm I.D., 250 mm length)		
Elution	Gradient		
Injection volume	25 µL		
Mobile phases/Eluent	A: 2.5 mM HNO_3 B: 50 mM HNO_3		
Gradient	Time (min)	Eluent	Flow rate (mL min^{-1})
	0.00	A	1.0
	1.00	A	1.0
	1.01	B	1.0
	4.00	B	1.0
ICP-MS			
Nebulizer gas	0.80 L/min		
Injector	2 mm I.D., quartz		
Interface	Ni sampler and skimmer		
QCell He gas flow	5 mL/min		
75As dwell time	100 ms		

Table 6- 2. IC and ICP-MS operating parameters for selenite (Se^{IV}) and selenate (Se^{VI}) speciation.

Parameter	**Value**		
IC			
Column	Dionex AS-7 (4 mm I.D., 250 mm length)		
Elution	Gradient		
Injection volume	25 µL		
Mobile phases/Eluent	A: 50 mM HNO_3 B: 400 mM HNO_3		
Gradient	Time (min)	Eluent	Flow rate (mL min^{-1})
	0.00	A	1.5
	2.00	A	1.5
	2.01	B	2.0
	5.00	B	2.0
ICP-MS			
Nebulizer gas	0.80 L/min		
Injector	2 mm I.D., quartz		
Interface	Ni sampler and skimmer		
QCell He gas flow	5 mL/min		
78Se dwell time	100 ms		

Table 6- 3. IC and ICP-MS operating parameters for trivalent (Cr^{III}) and hexavalent (Cr^{VI}) chromium speciation.

Parameter	Value
IC	
Column	Dionex AG-7 (4 mm I.D., 50 mm length)
Elution	Isocratic
Injection volume	25 µL
Mobile phases/Eluent	400 mM HNO_3
Time (min)	Flow rate (mL min^{-1})
0.00	0.6
2.50	0.6
2.51	1.0
5.00	1.0
ICP-MS	
Nebulizer gas	0.80 L/min
Injector	2 mm I.D., quartz
Interface	Ni sampler and skimmer
QCell He gas flow	5 mL/min
52Cr dwell time	100 ms

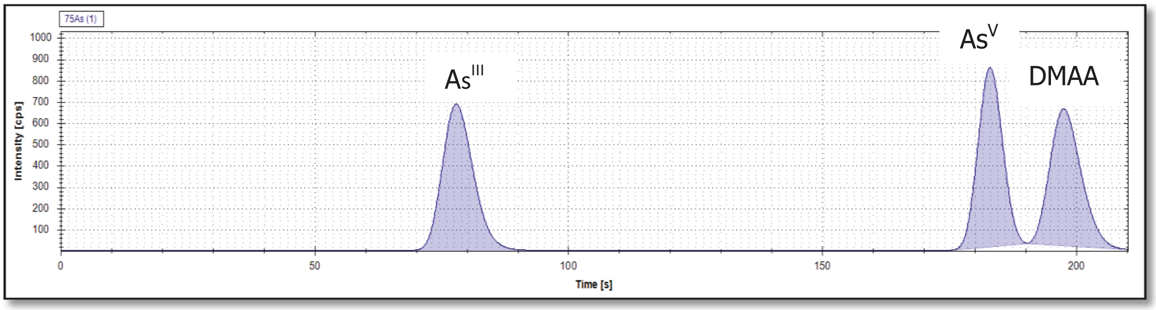

Figure 6- 1. A typical chromatogram of arsenite (As^{III}), arsenate (As^{V}) and DMAA species.

Each species was present at 2 μg L^{-1} in nanopure water; resolution and quantification of the species were achieved using IC-ICP-MS. The operating conditions of IC-ICP-MS for As^{III}, As^{V} and DMAA speciation are given in Table 6-1.

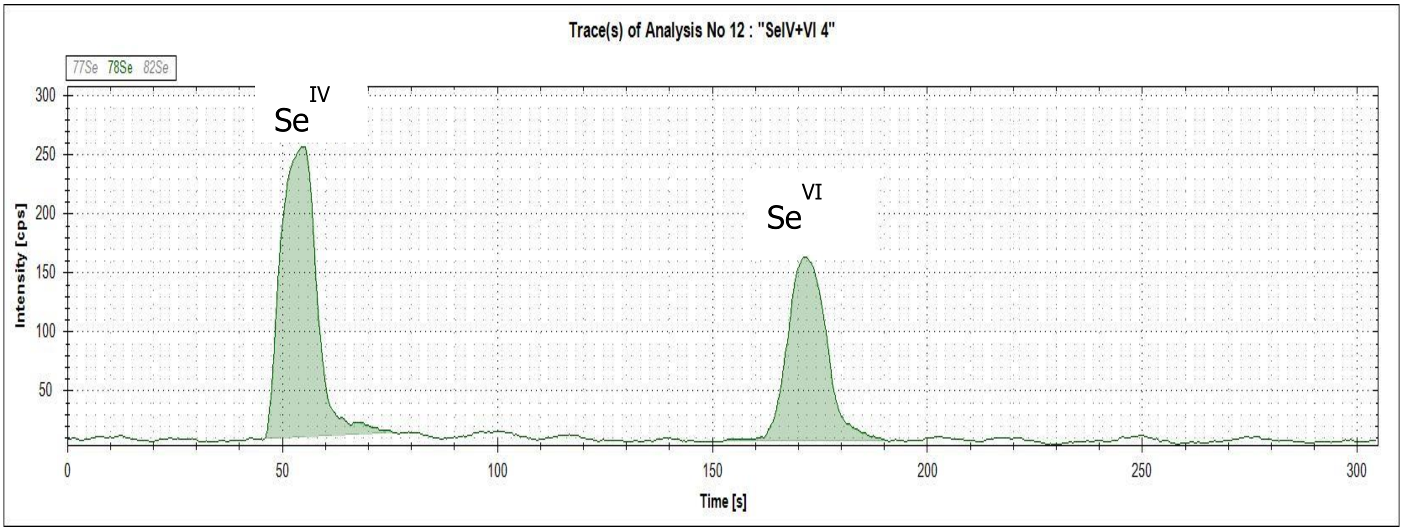

Figure 6- 2. A typical chromatogram of selenite (Se^{IV}) and selenate (Se^{VI}) species.

Each species was present at 4 μg L^{-1} in nanopure water; resolution and quantification of the species were achieved using IC-ICP-MS. The operating conditions of IC-ICP-MS for Se^{IV} and Se^{VI} speciation are given in Table 6-2.

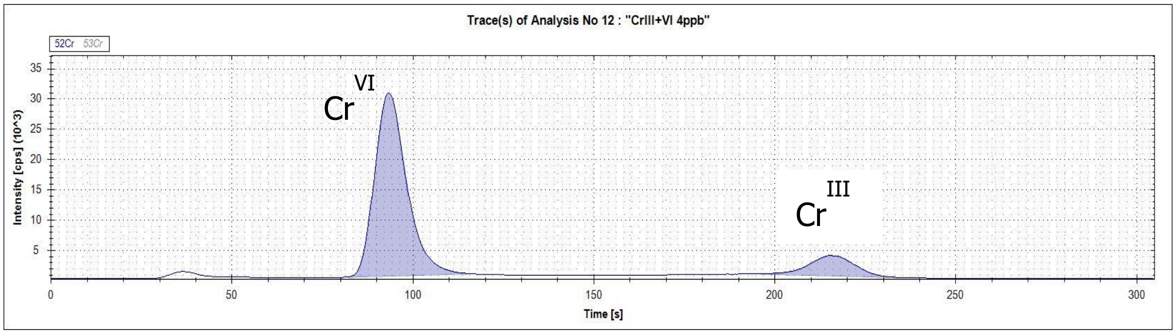

Figure 6- 3. A typical chromatogram of trivalent (Cr^{III}) and hexavalent chromium (Cr^{VI}) species.

Each species was present at 4 μg L^{-1} in nanopure water; resolution and quantification of the species were achieved using IC-ICP-MS. The operating conditions of IC-ICP-MS for Cr^{VI} and Cr^{III} speciation are given in Table 6-3.

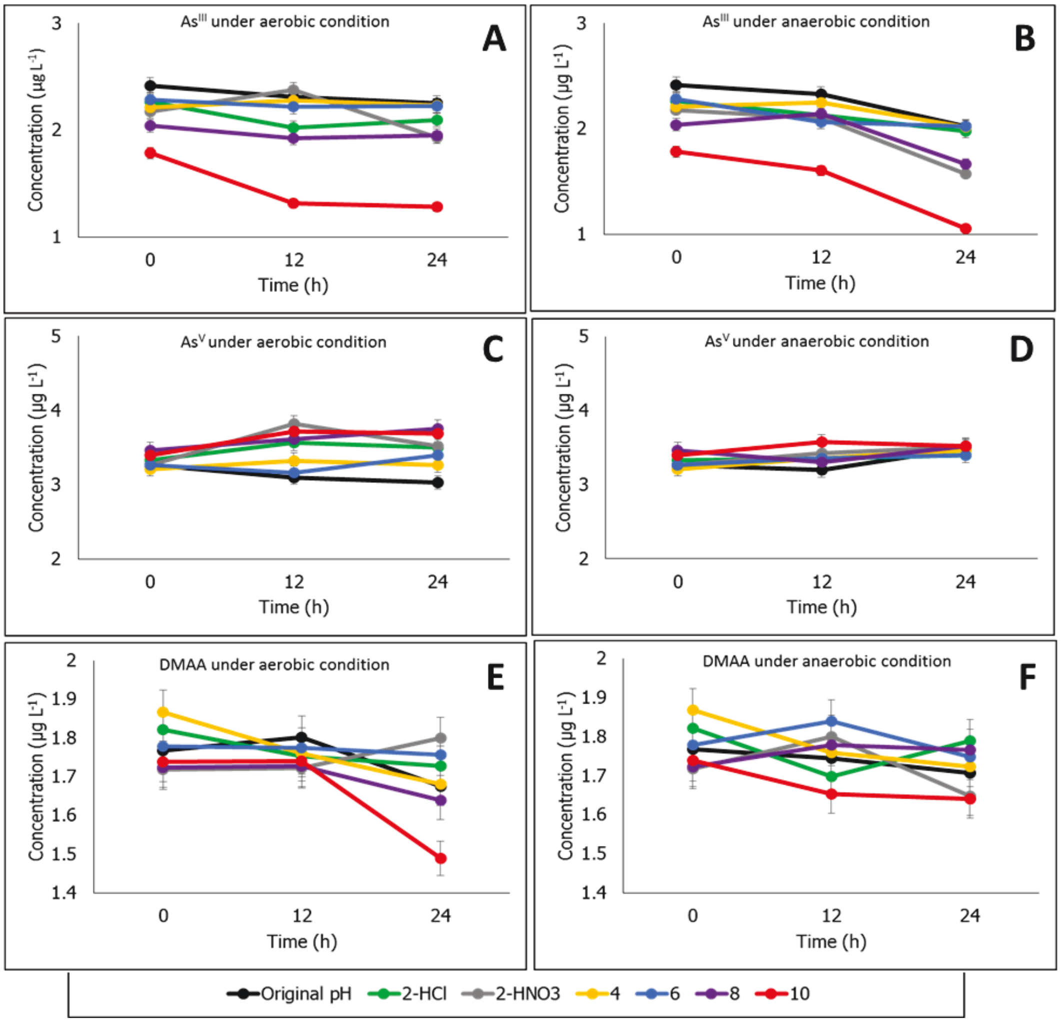

Figure 6- 4. Effect of pH (2 to 10) on stability of arsenite ($\mathrm{As^{III}}$), arsenate ($\mathrm{As^{V}}$) and DMAA speciation in nanopure water under aerobic and anaerobic conditions for 24 h.

The figure shows effect of pH on **A)** $\mathrm{As^{III}}$ speciation under aerobic conditions, **B)** $\mathrm{As^{III}}$ speciation under anaerobic conditions, **C)** $\mathrm{As^{V}}$ speciation under aerobic conditions, **D)** $\mathrm{As^{V}}$ speciation under anaerobic conditions, **E)** DMAA speciation under aerobic conditions, and **F)** DMAA speciation under anaerobic conditions.

The initial concentrations of $\mathrm{As^{III}}$ (2.42 + 0.12 µg L^{-1}), $\mathrm{As^{V}}$ (3.26 + 0.16 µg L^{-1}) and DMAA (1.77 + 0.09 µg L^{-1}) in the solutions were same before they were incubated under aerobic and anaerobic conditions. The original pH of all the solutions were ~3.1 ± 0.3.

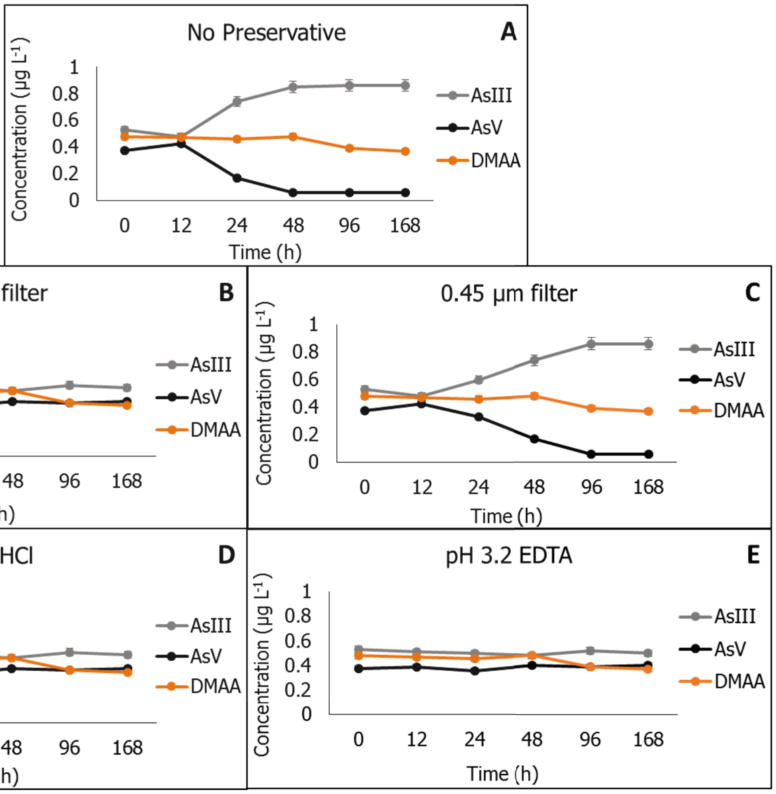

Figure 6- 5. Preservation of arsenite (As^{III}), arsenate (As^{V}) and DMAA species in river water (initial pH 7.1 ± 0.2) using filtration (0.2 µm and 0.45 µm), acidification (HCl to bring the pH <2), and complexation (EDTA-HAc pH 3.2) for 7 days.

The figure shows the As^{III}, As^{V} and DMAA speciation in river water **A)** without any preservation, **B)** after filtration through 0.2 µm filter, **C)** after filtration through 0.45 µm filter, **D)** after acidification using HCl to lower the pH to 2, and **E)** after complexation using EDTA-HOAc pH 3.2. Arsenic speciation analysis of the river water performed immediately after sample collection showed that As^{V} was the only dominant As species (0.38 ± 0.04 µg L^{-1}; ~88 % of the total dissolved As) in river water. Arsenite and DMAA were insignificant (< 5% of the total dissolved As) in the river water. Therefore, small amount of As^{III} (0.53 ± 0.03 µg) and DMAA (0.48 ± 0.02 µg) were spiked in the river water samples.

Samples were stored in transparent polypropylene bottles at 4°C, all the samples preparation and handling were performed under anaerobic conditions.

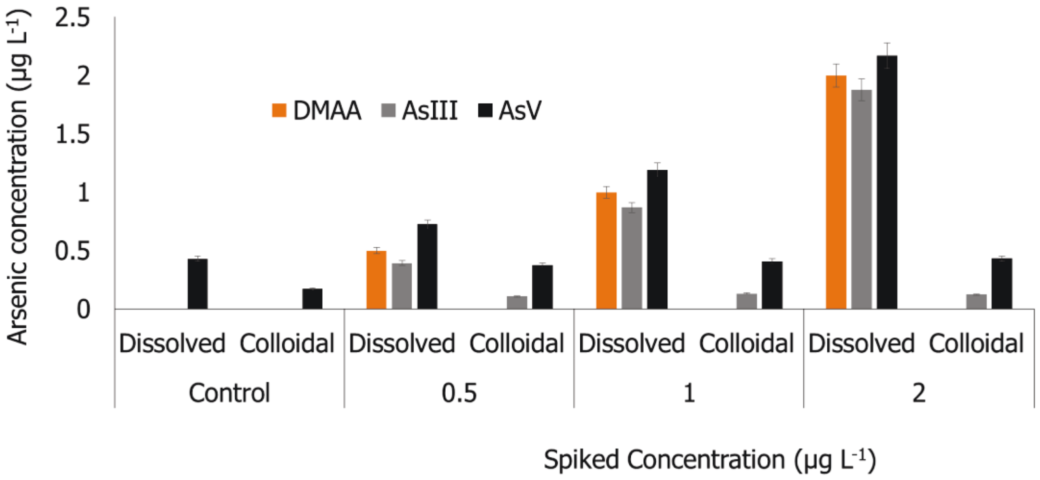

Figure 6- 6. Distribution of arsenite (As^{III}), arsenate (As^{V}) and DMAA species in dissolved and colloidal phases in the river water spiked at 0.5, 1 and 2 µg L^{-1} concentration of As^{III}, As^{V}, and DMAA species.

To separate the colloidal phase, the river water sample was centrifuged at 14000 rpm (18407 rcf) for 30 min using micro-centrifuge (Eppendorf).

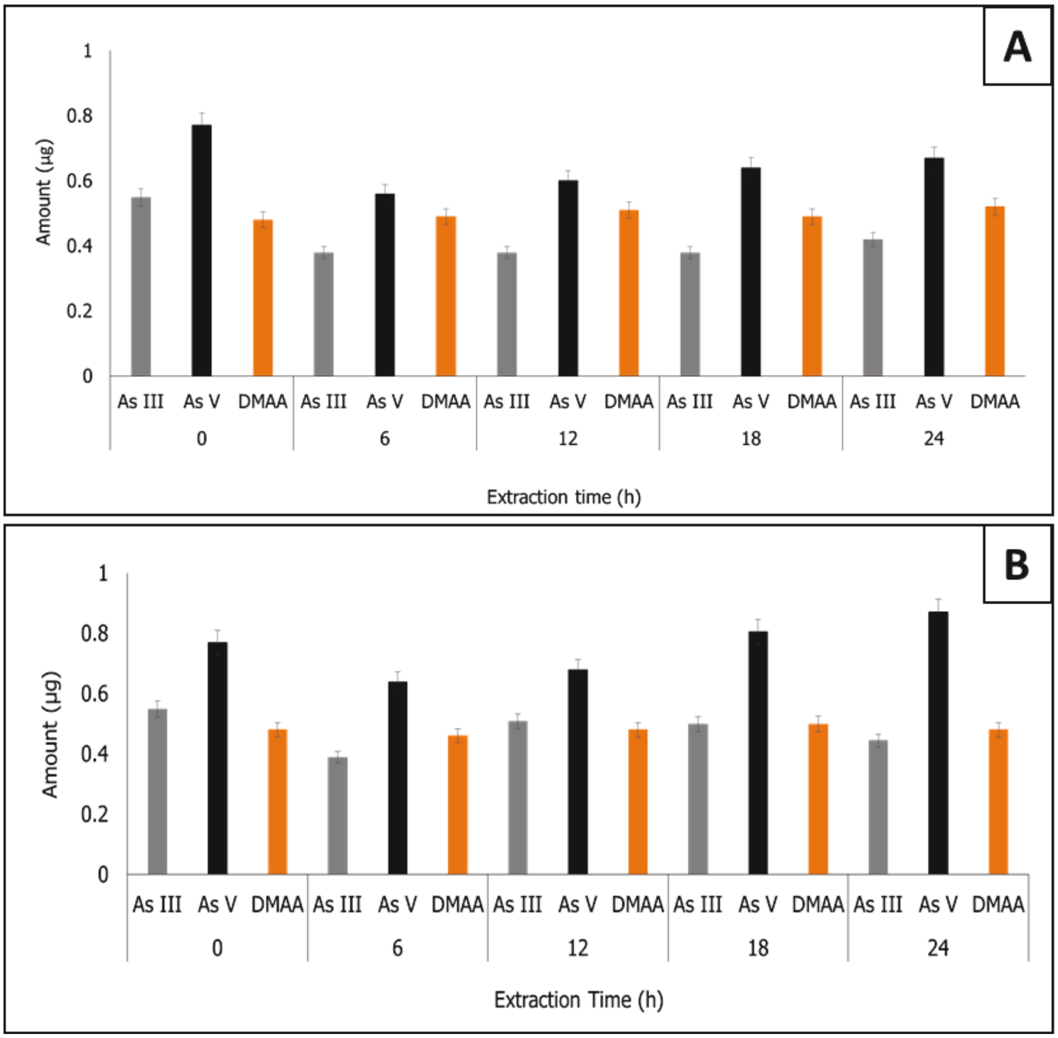

Figure 6- 7. Extraction of spiked arsenite (As^{III}), arsenate (As^{V}) and DMAA species from sediments using **A)** 0.1 M NaH_2PO_4 (pH 4.2) and **B)** 0.1 M NaH_2PO_4 (pH 5) for 6, 12, 18 and 24 h extraction time.

These results of the As species extraction from sediments showed that 0.1 M NaH_2PO_4 (pH 5) solution for an extraction time of 18 h could be used to extract the As^{III}, As^{V} and DMAA species from sediments.

Chapter 7. Summary and research limitations

7.1 Overall summary

High groundwater arsenic (As, >10 µg L^{-1}) in the Cold Lake area, Alberta is an issue of great concern for environmental and human health. The previous studies were pointing out that geological material might be the source of As but no study investigated detailed distribution of As in surficial deposits and identified host phases of As so that mechanisms of As release into groundwater could be understood. To determine the potential source of As, surficial deposits derived from different geological material were characterized to investigate the distribution of As in different geological formations, fractionation of As in different host phases in sediments and mineralogy of the sediments so that the potential source(s) of groundwater As could be inferred. To cover the larger extent of the area, sediment samples from different cores already drilled from five different locations up to ~300 m deep in the surficial deposits were collected from the mineral core research facility of Alberta Energy Regulator-Alberta Geological Survey (AER-AGS). These cores were selected based on stratigraphic units and their proximity to aquifers. The total As concentration in sediments (n = 135) ranged from ~0.8 to ~35 µg g^{-1}. High As concentration (~32 µg g^{-1}) was found in sediments derived from shale, particularly from the shale of Lea Park formation. In addition to shale, other high As concentrations (20 to 25 µg g^{-1}) were also found in Bonnyville, Grand Centre and Empress formations particularly at those depths where these formations were overlying the shale. Therefore, the high As might be due to the mixing of shale in the overlying geological formations during their deposition.

In addition to As, concentration of other chalcophile (Cd, Se, Pb and Cu), siderophile (Mo, Co and Ni) and lithophile (Be, U, Rb, Sr, Cr, B, V and Ba) elements were also quantified to determine their potential to contaminate the groundwater. Among the chalcophile elements, Cd, Se and Pb concentrations in our sediments were higher than their natural abundance in the earth crust and average concentrations in the shale sediments. Among the siderophile elements, only Mo concentration was higher than its natural abundance and average concentration in shale sediments. All the lithophile elements in our sediments were lower than their natural abundance in earth crust and average concentrations in shale sediments except Cr, V and B. The relationship between total As and other elements concentration were also studied to determine the association between their distribution in the sediments. A high positive correlation found between As and U, Mo, Pb and Ba in our sediments suggested that marine shale (enriched in pyrite, FeS_2) might be one of the potential sources of As in the area.

Since we observed variable concentrations of As in sediments, fractionation of As in sediments was performed to identify host phases of As in sediments. To study different labile and recalcitrant phases of As such as water soluble, exchangeable, bound to carbonates, Fe oxides and silicates, sequential extraction method is commonly used. However, recent methods target only few As phases and relegate the remaining As (~40-50% of total As) into unidentified residual fraction. In addition, these methods use chloride (Cl^-)-containing extractants such as magnesium chloride ($MgCl_2$), hydrochloric acid (HCl) and hydroxylamine hydrochloride (NH_2OH. HCl) that strongly interfere with As quantification using quadrupole ICP-MS. Chloride (Cl^-)-containing extractants produce polyatomic ions (argon chloride; $^{40}Ar^{35}Cl$) when Cl^- reacts with argon (Ar) in ICP plasma. Therefore to fractionate > 90% of total As in maximum possible meaningful fractions and avoid the Cl^- containing extractant for As fractionation, a modified sequential extraction method was developed. In the method only those extractants were used that could be analyzed by quadrupole ICP-MS without any polyatomic interference for ^{75}As quantification. The modified method was also tested for the fractionation of other elements such as copper (Cu), cobalt (Co), chromium (Cr), strontium (Sr). After optimization of the sequential extraction method, it was employed on the selected experimental sediments (n = 22) to fractionate the total As and other important elements into 9 fractions. We grouped the selected sediments in low As (<7 μg g^{-1} As; n = 9) and high As sediments (>7 μg g^{-1} As; n = 13) to find the difference in the host phases of As. The results of As fractionation showed that ~6 to 46 % of the total As was surface bound (exchangeable and specifically adsorbed) in all the sediments. In high As sediments (7 to 35 μg g^{-1} As; n = 13), significant amount of As (11 to 34 % of total As) was also found with the sulfide minerals. X-ray diffraction (XRD) and scanning electron microscope (SEM) analyses confirmed the presence of pyrite in high As sediments (~20 μg g^{-1} As). Micro-XRD analysis of the sediment containing ~20 μg g^{-1} As signaled the presence of arsenopyrite minerals in the sediment. X-ray absorption near edge structure (XANES) spectroscopy analysis showed dominance of arsenite (As^{III}; ~60 to 90 % of total As) in all the sediments. After surface bound and sulfide associated As, around 11-17 % of total As was associated with amorphous Fe, Al and Mn oxyhydroxides, crystalline Fe, Al and Mn oxyhydroxides and silicate minerals. Rest of the solid phases produced < 10 % of the total As. Overall a higher proportion of total As associated with sulfide minerals and a positive correlation of Pb, U, Mo and Ba with As in sediments suggested that shale sediments (enriched in pyrite, FeS_2) might be the potential source of As. Marine shale is 10 to 100 times enriched in As, U, Mo and Ba compared to other sedimentary rock (Mao et al., 2002; Orberger et al., 2005).

The results of the fractionation of other 10 important elements (other than As) such as chalcophile (Cd, Se, Pb and Cu), siderophile (Co and Ni) and lithophile (Cr, B, V and Ba) showed that three major phases including 1) amorphous and crystalline Fe and Mn oxides, 2) exchangeable and specifically adsorbed, and 3) silicate minerals contained the significant elemental concentrations.

In addition to naturally high level of As in groundwater, oil sands activity in the region also cause As mobilization in the groundwater. Therefore this project was further extend to study how high temperature used in cyclic steam stimulation (CSS) for bitumen extraction affect As release from sediments. A laboratory experiment was conducted to determine the effect of intense heat (~200^{o} C) on As release from sediments into porewater.

Before heating, the sediments were moistened with synthetic aquifer water or nanopure water with 15 % and 50 % moisture (according to the natural moisture contents in the sediments) and 1.4:1 and 3.7:1 liquid to solid ratio (to simulate the conditions in the aquifer sediments). Nanopure water was used to determine the effect of low ionic strength water on As release. The results showed significantly higher As release from sediments moistened with both type of water after the heat treatment as compared to the un-heated sediments. The release of As was significantly higher from the sediment moistened with nanopure water because of high activity compared to the As release from sediment moistened with aquifer water.

After heating liquid phase could not be recovered from both 15% and 50% moisture conditions, therefore sequential extraction of As was performed to determine any change in the As host phases in sediments. The fractionation results of 15% and 50% moistened sediment were not significantly ($P > 0.05$) different from each other, therefore both the results were averaged for simplicity. A significant ($P < 0.05$) increase in the soluble As was found by the effect of heat. The soluble As was significantly higher in the sediment moistened with nanopure water compared to the soluble As in sediment moistened with aquifer water. Overall, the fractionation results after the heat treatment of the sediments showed that exchangeable, specifically adsorbed and amorphous Fe oxides phases of As contributed to the increase in soluble As. The results of this study will help understand the extent of As release during industrial processes so that management strategies could be develop to mitigate groundwater As contamination.

In all our studies, total As concentration was quantified because the sediment cores were old and not preserved for As speciation. However, X-ray absorption near edge structure (XANES) spectroscopy was employed to infer the oxidation state of As in solid phase (minerals). Bioavailability and toxicity of As depend on its chemical species. Therefore for the future research, efforts will be made in collaboration with the AER-AGS to acquire a fresh core from the same area to perform speciation study. In this thesis research, a comprehensive method was also developed for river water and sediment sampling, their preservation for arsenite (As^{III}), arsenate (As^{V}) and dimethyl arsenic acid (DMAA) species and quantification of the species using ion chromatograph inductively coupled plasma mass spectrometer (IC-ICP-MS). The results showed that the distribution of As^{III}, As^{V} and DMAA species in the river water could be preserved in acidified (pH 2 with HCl), 0.2 μm filtered, or EDTA treated (pH 3.2) river water for 7 days. The results of the extraction of As species from sediments showed that 0.1 M NaH_2PO_4 (pH 5) solution for an extraction time of 18 h could be used to extract the As^{III}, As^{V} and DMAA species from sediments. In addition to the optimization of the As speciation method, IC-ICP-MS methods for the speciation of inorganic selenium (selenite, Se^{IV} and selenate, Se^{VI}) and chromium [trivalent (Cr^{III}) and hexavalent (Cr^{VI})] were also optimized.

7.2 Research limitations and future research

The sediment cores from sediments were taken for this study were old (four cores drilled in 1999-2000 namely WR99-1, WEPA99-1, WEPA99-2, and WEPA00-1, and one core drilled in 2009 namely 14-01w), and all the cores were stored in wooden boxes at the Alberta Energy Regulator-Alberta Geological Survey (AER-AGS) Mineral Core Research Facility in Edmonton, Alberta, Canada under ambient conditions. The sediment cores were already air dried when samples were taken in 2010. Therefore, chemical speciation of As was not performed using these sediments. However, to determine any environmental deposition or change in the total concentrations of As in the sediments, As concentrations determined in the sediments taken from outer and inner portions of the cores were compared to the As concentration determined at the time of cores collection by Andriashek, (2003). No significant difference ($P > 0.05$) was found in total As concentrations between outer and inner sediments and the As determined in sediments at the time of core collection. Nevertheless, sediments taken from the inner portion of the cores were used throughout in the study.

The results of all the studies reported in this thesis provide important base knowledge to develop strategies to investigate geochemical processes governing the As release into the groundwater. In future, a fresh sediment core could be collected from the area to perform the chemical speciation of As (and other elements such as selenium and chromium) in surficial deposits and associated porewater. In addition, effect of biotic and abiotic factors on As speciation and release into the groundwater could also be included in the future work.

Literature cited

Andriashek L. D. Quaternary geological setting of the Athabasca Oil Sands (in situ) area, Northeast Alberta. 2003. http://www.ags.gov.ab.ca/publications/ESR/PDF/ESR_2002_03.pdf

Mao J., Lehmann B., Du A., Zhang G., Ma D., Wang Y., Zeng M., Kerrich R. Re-Os Dating of Polymetallic Ni-Mo-PGE-Au Mineralization in Lower Cambrian Black Shales of South China and Its Geologic Significance. Econ Geol 2002;97:1051–1061.

Orberger B., Wagner C., Vymazalova A. Rare metal sequestration and mobility in mineralized black shales from the Zunyi region, South China. Mineral Deposit 2005: 167-170.

Bibliography

Aggett J., Kriegman M. Preservation of arsenic (III) and arsenic (V) in samples of sediment interstitial water. Analyst. 1987;112:153–157.

Ahmann D., Roberts A. L., Krumholz L. R., Morel F. M. Microbe grows by reducing arsenic. Nature. 1994;371: 750.

Alam M. B., Sattar M. A. Assessment of arsenic contamination in soils andwaters in some areas of Bangladesh. Water Sci Technol. 2000;42:185–193.

Alberta Environment. Cold Lake – Beaver River Basin Groundwater Quality State of the Basin Report. 2006.

Anawar H. M. Arsenic speciation in environmental samples by hydride generation and electrothermal atomic absorption spectrometry. Talanta. 2012;88:30–42.

Andriashek L. D., Fenton M. M. Quaternary stratigraphy and surficial geology of the Sand River area 73L. 1989. http://www.ags.gov.ab.ca/publications/BUL/PDF/BUL_057.pdf

Andriashek L. D. Geochemistry of selected glacial and bedrock geologic units, Cold Lake Area, Alberta. 2000. http://ags.gov.ab.ca/publications/ESR/PDF/ESR_2000_10.pdf

Andriashek L. D. Geochemistry of selected glacial and bedrock geological units, Cold Lake Area, Alberta. Alberta Geological Survey open file report. 1998.

Andriashek L. D. Quaternary geological setting of the Athabasca Oil Sands (in situ) area, Northeast Alberta. 2003. http://www.ags.gov.ab.ca/publications/ESR/PDF/ESR_2002_03.pdf

Ball D. F. Loss-on-ignition as an estimate of organic matter and organic carbon in non-calcareous soils. J soil Sci 1964;15(1):86-92.

Bednar A. J., Garbarino J. R., Ranville J. F., Wildeman T. R. Preserving the distribution of inorganic arsenic species in groundwater and acid mine drainage samples. Environ Sci Technol. 2002;36(10):2213–8.

Bora S., Aydin I., Kilinc E., Aydin F. Speciation of arsenic in soil, sediment and environmental samples. Speciat Stud soil, sediment Environ samples. Taylor & Francis Group, LLC. 2014.

Boyle R. W., Jonasson I. R. The geochemistry of arsenic and its use as an indicatior element in geochemical prospecting. J Geochemical Explor 1973;2:251–296.

Brost P. Redistribution of arsenic and iron in an acid sulphate soil, Alberta, Canada. MSc Thesis. University of Alberta. 2002.

Cheng H., Hu Y., Luo J., Xu B., Zhao J. Geochemical processes controlling fate and transport of arsenic in acid mine drainage (AMD) and natural systems. J Hazard Mater. 2009;165(1-3):13–26.

Cullen W. R., Reimer K. J. Arsenic speciation in the environment. Chem Rev. 1989;89(4):713–64.

Davidson C. M., Duncan A. L., Littlejohn D, Ure A. M., Garden L. M. A critical evaluation of the three-stage BCR sequential extraction procedure to assess the potential mobility and toxicity of heavy metals in industrially-contaminated land. Anal Chim Acta. 1998;363(1):45–55.

De Mora K., Joshi N., Balint B. L., Ward F. B., Elfick A., French C. E. A pH-based biosensor for detection of arsenic in drinking water. Anal Bioanal Chem 2011;400:1031–1039.

Dhar R. K., Zheng Y., Rubenstone J., Van-Geen A. A rapid colorimetric method for measuring arsenic concentrations in groundwater. Anal Chim Acta. 2004;526(2):203–209.

Dionex homepage (http://www.dionex.com/en-us/products/columns/ic-rfic/specialty-packed/ionpac-as7/lp-73274.html) (Accessed December 9, 2014).

Dudas M., Pawluk S. Natural abundances and mineralogical partitioning of trace elements in selected Alberta soils. Can J Soil Sci. 1980;60:763–71.

Dudas M. Accumulation of native arsenic in acid sulphate soils in Alberta. Can J soil Sci. 1987;67:317–31.

Eghbalnia M. Electrochemical and raman investigation of pyrite and chalcopyrite oxidation. Ph.D. Thesis. University of British Columbia. 2012.

Ellwood M. J., Maher W. A. Measurement of arsenic species in marine sediments by high-performance liquid chromatography–inductively coupled plasma mass spectrometry. Anal Chim Acta. 2003;477(2):279–91.

Feng R., Dolton W., Igarashi R., Wright G., Bradford M., McIntyre S. Commissioning of the VESPERS Beamline at the Canadian Light Source.

2010; CP1234, 10th Internation Conference on Synchrotron Radiation Instrumentation.

Fennell J. W. Effects of aquifer heating on groundwater chemistry with a review of arsenic and its mobility. PhD thesis 2008, Universiyt of Calgary.

Fitzgerald D., Chanasyk D. S., Neilson R. D., Kiely D., Audette R. Farm well water quality in Alberta. Water Qual Res 2001;36(3):565–588.

Flemming R. L., Salzsauler K. A., Sherriff, B. L., Sidenko, N. V. Identification of scorodite in fine-grained, high-sulfide, arsenopyrite mine-waste using micro x-ray diffraction (μXrD). 2005;43:1243–1254.

Frank J., Krachler M., Shotyk W. Determination of arsenic in peat samples using HG-AFS and l-cysteine as pre-reductant. J Anal At Spectrom. 2006;21(2):204-207.

Frentiu T., Vlad S-N., Ponta M., Baciu C., Kasler I., Cordos E. Profile distribution of As(III) and As(V) species in soil and groundwater in Bozanta area. Chem Pap. 2007;61(3):186–93.

Garcia-Manyes S., Jiménez G., Padró A., Rubio R., Rauret G. Arsenic speciation in contaminated soils. Talanta. 2002;58(1):97–109.

Georgiadis M., Cai Y., Solo-Gabriele H. M. Extraction of arsenate and arsenite species from soils and sediments. Environ Pollut. 2006;141(1):22–9.

Giles D. E., Mohapatra M., Issa T. B., Anand S., Singh P. Iron and aluminium based adsorption strategies for removing arsenic from water. J. Enviro Manag. 2011;92:3011–3022.

Gleyzes C., Tellier S., Astruc M. Fractionation studies of trace elements in contaminated soils and sediments: a review of sequential extraction procedures. TrAC Trends Anal Chem. 2002;21(6-7):451–67.

Goldberg S., Glaubig R. Anion sorption on a calcareous, montmorillonitic soil—arsenic. Soil Sci Soc Am. 1988;52:1297–300.

Gong Z., Lu X., Ma M., Watt C., Le X. C. Arsenic speciation analysis. Talanta. 2002;58:77–96.

Goossens J., Vanhaecke F., Moens L., Dams R. Elimination of interferences in the determination of arsenic and selenium in biological samples by inductively coupled plasma mass spectrometry. Anal Chim Acta. 1993;80:137–143.

Gurleyuk H., Wallschlager D. Determination of chromium(III) and chromium(VI) using suppressed ion chromatography inductively coupled plasma mass spectrometry. J. Anal. At. Spectrum. 2001;16:926-930.

Hall G. E. M., Pelchat J. C., Gauthier G. Stability of inorganic arsenic (III) and arsenic (V) in water samples. J. Anal. At. Spectrum. 1999;14:205–213.

Hall G. E. M., Vaive J. E., Beer R., Hoashi M. Selective leaches revisited, with emphasis on the amorphous Fe oxyhydroxide phase extraction. J Geochemical Explor. 1996;56(1):59–78.

He Z. L., Yang X. E., Stoffella P. J. Trace elements in agroecosystems and impacts on the environment. J Trace Elem Med Biol. 2005;19(2-3):125–140.

Health Canada (2006), Guidelines for Canadian drinking water quality: Guideline technical document-Arsenic. Water Quality and Health Bureau, Healthy Environments and Consumer Safety Branch, Health Canada, Ottawa, Ontario.

Health Surveillance, Alberta Health and Wellness. Arsenic in groundwaer from domestic wells in three areas of northern Alberta. 2000. http://www.health.alberta.ca/documents/Arsenic-Groundwater-Wells-2000.pdf

Hsieh Y. P., Shieh Y. N. Analysis of reduced inorganic sulfur by diffusion methods: improved apparatus and evaluation for sulfur isotopic studies. Chem Geol 1997;137(3-4):255–261.

Huang J-H., Kretzschmar R. Sequential extraction method for speciation of arsenate and arsenite in mineral soils. Anal Chem 2010;82(13):5534–5540.

Imperial Oil, Cold Lake Operations. http://www.imperialoil.ca/Canada-English/operations_sands_cold.aspx (Accessed December 9, 2014).

Jackson B. P., Bertsch P. M. Determination of arsenic speciation in poultry wastes by IC-ICP-MS. Environ Sci Technol. 2001;35(24):4868–73.

Javed M. B., Kachanoski G., Siddique T. A modified sequential extraction method for arsenic fractionation in sediments. Anal Chim Acta 2013;787:102–110.

Javed M. B., Kachanoski G., Siddique T. Arsenic fractionation and mineralogical characterization of sediments in the Cold Lake Region of Alberta , Canada. Sci Total Environ 2014;500-501:181–190.

Kachenko A. G., Grafe M., Singh B., Heald S. M. Arsenic Speciation in Tissues of the Hyperaccumulator P. calomelanos var. austroamericana using x-ray absorption spectroscopy. Envoron Sci Technol 2010;44(12):4735–4740.

Katsoyiannis I. A., Zouboulis A. I. Removal of arsenic from contaminated water sources by sorption onto iron-oxide-coated polymeric materials. Water Res. 2002; 36(20):5141–55.

Keon N. E., Swartz C. H., Brabander D. J., Harvey C., Hemond H. F. Validation of an arsenic sequential extraction method for evaluating mobility in sediments. Environ Sci Technol 2001;35(13):2778–2784.

Krauskopf K. B. Introduction to geochemistry. 1979; McGraw-Hill Book Company.

Kreidie N., Armiento G., Cibin G., Cinque G., Crovato C., Nardi E., Pacifico R., Cremisini C., Mottana, A. An integrated geochemical and mineralogical approach for the evaluation of arsenic mobility in mining soils. J Soils Sediments. 2010;11(1):37–52.

Kumar A. R., Riyazuddin P. Preservation of inorganic arsenic species in environmental water samples for reliable speciation analysis. TrAC Trends Anal Chem. 2010;29(10):1212–23.

Larios R., Fernández-Martínez R., Rucandio I. Comparison of three sequential extraction procedures for fractionation of arsenic from highly polluted mining sediments. Anal Bioanal Chem 2012;402(9):2909–2921.

Lemay T., Parks K., Andriashek L. D., Michael K., Jean G., Kempin E., Stewart S. Regional Groundwater Quality Appraisal , Cold Lake-Beaver River Drainage Basin , Alberta. 2005.

Lemay T. G., Parks K., Andriashek L. D., Michael K., Jean G. M., Stewart S. A., Kempin E. Regional groundwater quality appraisal , Cold Lake-Beaver River Drainage Basin , Alberta. 2005. http://www.ags.gov.ab.ca/publications/SPE/PDF/SPE_073.pdf

Lemay T. G. Arsenic concentration in quaternary drift and quaternary-tertiary buried channel aquifer in the Athabasca Oil Sands (In Situ) area, Alberta. 2003. http://www.ags.gov.ab.ca/publications/GEO/PDF/GEO_2002_04.pdf

Lombi E., Sletten R., Wenzel W. Sequentially extracted arsenic from different size fractions of contaminated soils. Water Air Soil Pollut. 2000;1:319–332.

Manning B., Martens D. Speciation of arsenic (III) and arsenic (V) in sediment extracts by high-performance liquid chromatography-hydride generation atomic absorption spectrophotometry. Environ Sci Technol. 1997;31(1):171–7.

Manning B. Arsenic speciation in As(III)- and As(V)-treated soil using XANES spectroscopy. Microchim Acta 2005;151:181–188.

Manning B., Goldberg S. Adsorption and stability of arsenic (III) at the clay mineral-water interface. Environ Sci Technol. 1997;31(7):2005–2011.

Mao J., Lehmann B., Du A., Zhang G., Ma D., Wang Y., Zeng M., Kerrich R. Re-Os Dating of Polymetallic Ni-Mo-PGE-Au Mineralization in Lower Cambrian Black Shales of South China and Its Geologic Significance. Econ Geol 2002;97:1051–1061.

Mar J. L. G., Reyes L. H., Rahman G. M. M., Kingston H. M. S. Simultaneous extraction of arsenic and selenium species from rice products by microwave-assisted enzymatic extraction and analysis by ion chromatography-inductively coupled plasma-mass spectrometry. J Agric Food Chem. 2009 22;57(8):3005–13.

Mattusch J., Wennrich R. Determination of Anionic, Neutral, and Cationic Species of Arsenic by Ion Chromatography with ICPMS Detection in Environmental Samples. Anal Chem. 1998;70(17):3649–55.

McCleskey R. B., Nordstrom D. K., Maest A. S. Preservation of water samples for arsenic(III/V) determinations: an evaluation of the literature and new analytical results. Appl Geochemistry. 2004;19(7):995–1009.

Mech. M. A Comprehensive Guide to the Alberta Oil Sands. 2011.

Meunier L., Walker S. R., Wragg J., Parsons M. B., Koch I., Jamieson H. E., Reimer K. J. Effects of soil composition and mineralogy on the bioaccessibility of arsenic from tailings and soil in gold mine districts of Nova Scotia. Environ Sci Technol 2010;44:2667–2674.

Mihaljevic M., Ponavic M., Ettler V., Sebek O. A comparison of sequential extraction techniques for determining arsenic fractionation in synthetic mineral mixtures. Anal Bioanal Chem. 2003;377(4):723–9.

Milstein L. S., Essader A., Pellizzari E. D., Fernando R. A., Raymer J. H., Levine K. E., Akinbo O. Development and Application of a Robust Speciation Method for Determination of Six Arsenic Compounds Present in Human Urine. Environ Health Perspect. 2002;111(3):293–6.

Mitchell P., Barre D. The nature and significance of public exposure to arsenic: a review of its relevance to South West England. Environ Geochem Health. 1995:57–82.

Moncur A. Uranium and Arsenic Sources in Shallow Groundwater Near Bonnyville , Alberta : A Mineralogy Study. Alberta Innovates Technology Futures 2011.

Müller K., Daus B., Morgenstern P., Wennrich R. Mobilization of Antimony and Arsenic in Soil and Sediment Samples – Evaluation of Different Leaching Procedures. Water Air Soil Pollut. 2007;183(1-4):427–36.

Muloin T., Dudas M. J. Aqueous phase arsenic in weathered shale enriched in native arsenic. J Environ Eng 2005;4(6):461–468.

Murphy A. P., Coudert M., Barker J. Plants as biomarkers for monitoring heavy metal contaminants on landfill sites using sequential extraction and inductively coupled plasma atomic emission spectrophotometry (ICP-AES). J Environ Monit. 2000;2(6):621–627.

Nickson R. T., McArthur J. M., Ravenscroft P., Burgess W. G., Ahmed K. M. Mechanism of arsenic release to groundwater, Bangladesh and West Bengal. Appl Geochem 2000;15:403–413.

Niemelä M., Perämäki P., Kola H., Piispanen J. Determination of arsenic, iron and selenium in moss samples using hexapole collision cell, inductively coupled plasma–mass spectrometry. Anal Chim Acta. 2003;493(1):3–12.

O'Day P. A., Vlassopoulos D., Root R., Rivera N. The influence of sulfur and iron on dissolved arsenic concentrations in the shallow subsurface under changing redox conditions. Proc Natl Acad Sci U S A. 2004;101(38):13703–8.

Orberger B., Wagner C., Vymazalova A. Rare metal sequestration and mobility in mineralized black shales from the Zunyi region, South China. Mineral Deposit 2005: 167-170.

Oremland R. S., Stolz J. F. The ecology of arsenic. Science. 2003;300(5621):939–44.

Páez-Espino D., Tamames J., De Lorenzo V., Cánovas D. Microbial responses to environmental arsenic. Biometals 2009;22:117–30.

Pierce M. L., Moore C. B. Adsorption of arsenite and arsenate on amorphous iron hydroxide. Water Res. 1982;16(7):1247–53.

Poulton S., Canfield D. Development of a sequential extraction procedure for iron: implications for iron partitioning in continentally derived particulates. Chem Geol. 2005;214(3-4):209–21.

Pradit S., Wattayakorn G., Angsupanich S., Baeyens W., Leermakers M. Distribution of trace elements in sediments and biota of Songkhla Lake, Southern Thailand. Water Air Soil Pollut 2010;206:155–174.

Raj S. M., Jayaprakash M. Distribution and enrichment of trace metals in marine sediments of Bay of Bengal, off Ennore, south-east coast of India. Environ Geol 2008;56:207–217.

RAMP (Regional aquatics monitoring program). http://www.ramp-alberta.org/resources/development/history/insitu.aspx (Accessed December 18, 2014).

Rodrigues M. L. K., Formoso M. L. A. Geochemical distribution of selected heavy metals in stream sediments affected by tannery activities. Water Air Soil Pollut 2006;169:167–184.

Rosen P. Theoretical significance of arsenic as a carcinogen. J Theor Biol. 1971;32(2):425–426.

Sadiq M. Arsenic chemistry in soils: an overview of thermodynamic predictions and field observations. Water Air Soil Pollut 1997;93:117–136.

Samanta G., Clifford D. A. Preservation of inorganic arsenic species in groundwater. Environ Sci Technol. 2005;39(22):8877–82.

Santona L., Castaldi P., Melis P. Evaluation of the interaction mechanisms between red muds and heavy metals. 2006;136(2):324–329.

Shah P., Strezov V., Stevanov C., Nelson P. F. Speciation of arsenic and selenium in coal combustion products. Energy & fuels 2007;21:506–512.

Smedley P. L., Kinniburgh D. G. A review of the source, behaviour and distribution of arsenic in natural waters. Appl Geochem 2002;17:517–568.

Smith A. H., Lingas E. O., Rahman M. Contamination of drinking-water by arsenic in Bangladesh: a public health emergency. Bull World Health Organ 2000;78(9):1093–1103.

Smith E., Naidu R., Alston A. Arsenic in the soil environment: a review. Adv Agron. 1998; 64: 149-195.

Steel K. M., Patrick J. W. The production of ultra clean coal by chemical demineralisation. Fuel. 2001;80(14):2019–23.

Stein R., Dudas M., Klebek M. Occurrence of arsenic in groundwater near Cold Lake, Alberta. 2000.

Stockdale A., Davison W., Zhang H., Hamilton-Taylor J. The association of cobalt with iron and manganese (Oxyhydr)oxides in marine sediment. Aquat Geochemistry. 2010;16(4):575–85.

Sumner M. E. Measurement of soil pH: Problems and solutions. Commun Soil Sci Plant Anal 1994; 25(7-8):859–879.

Tabelin C. B., Hashimoto A., Igarashi T., Yoneda T. Leaching of boron, arsenic and selenium from sedimentary rocks: I. effects of contact time, mixing speed and liquid-to-solid ratio. Science of the Total Environment 2014;47:620-629.

Tessier A., Campbell P. G. C., Bisson M. Sequential extraction procedure for the speciation of particulate trace metals. Anal Chem 1979;51(7):844–851.

Thomas R. Practical guide to ICP-MS: A tutorial for beginners. 2008.

US EPA. Method 3050B acid digestion of sediments, sludges, and soils. Washington, D.C.: U.S. Environmental Protection Agency; 1996.

Vassileva E., Becker A., Broekaert J. A. C. Determination of arsenic and selenium species in groundwater and soil extracts by ion chromatography coupled to inductively coupled plasma mass spectrometry. Anal Chim Acta. 2001;441:135–46.

Villanueva-Estrada R. E., Prol-Ledesma R. M., Rodríguez-Díaz A. A., Canet C., Armienta M. A. Arsenic in hot springs of Bahía Concepción, Baja California Peninsula, México. Chem Geol. 2013;348:27–36.

Wang R-Y., Hsu Y-L., Chang L-F., Jiang S-J. Speciation analysis of arsenic and selenium compounds in environmental and biological samples by ion chromatography-inductively coupled plasma dynamic reaction cell mass spectrometer. Anal Chim Acta. 2007;590(2):239–44.

Wang S., Mulligan C. N. Occurrence of arsenic contamination in Canada: sources, behavior and distribution. Sci Total Environ 2006;366:701–721.

Wang Z., Bush R. T., Sullivan L. A., Chen C., Liu J. Selective oxidation of arsenite by peroxymonosulfate with high utilization efficiency of oxidant. Environ Sci Technol. 2014;48(7):3978–85.

Wenzel W. W., Kirchbaumer N., Prohaska T., Stingeder G., Lombi E., Adriano D. C. Arsenic fractionation in soils using an improved sequential extraction procedure. Anal Chim Acta. 2001;436(2):309–323.

Wu S., Zhao Y., Feng X., Wittmeier A. Spectrometry for total metal determination in silicon-containing solid samples using the microwave-assisted nitric acid–hydrofluoric acid–hydrogen peroxide–boric acid. Anal At Spectrom. 1996;11:287–96.

Xing L., Beauchemin D. Chromium speciation at trace level in potable water using hyphenated ion exchange chromatography and inductively coupled plasma mass spectrometry with collision/reaction interface. J. Anal. At. Spectrom., 2010, 25, 1046–1055

Xu H., Allard B., Grimvall A. Effects of acidification and natural organic materials on the mobility of arsenic in the environment. Water Air Soil Pollut. 1991;57-58:269–78.

Xu L., Zhao Z., Wang S., Pan R., Jia Y. Transformation of arsenic in offshore sediment under the impact of anaerobic microbial activities. Water Res 2011;45(20):6781–6788.

Yunmei Y., Yongxuan Z., Williams-Jones A. E., Zhenmin G., Dexian L. A kinetic study of the oxidation of arsenopyrite in acidic solutions: implications for the environment. Appl Geochem 2004;19:435–444.

Zagury G. J., Dobran S., Estrela S., Deschênes L. Inorganic arsenic speciation in soil and groundwater near in-service chromated copper arsenate-treated wood poles. Environ Toxicol Chem. 2008;27(4):799–807.

Appendices

Appendix A

Table A- 1. Average elemental concentrations in sediments and average background values in earth crust and shale.

Element	Average abundance in earth crust	Average concentration in shale	Average concentration in sediments (n = 87)
		(μg g^{-1})	
Arsenic (As)	1.8	10	5 [a]
Nickel (Ni)	75	80	21
Selenium (Se)	0.05	0.6	1.4
Cadmium (Cd)	0.15	0.3	0.24
Lead (Pb)	12.5	20	9.46
Chromium (Cr)	100	100	45
Copper (Cu)	50	50	18.3
Beryllium (Be)	3	3	0.87
Vanadium (V)	110	130	60
Cobalt (Co)	22	20	8.5
Molybdenum (Mo)	1.5	2	1.2
Barium (Ba)	500	600	200
Uranium (U)	2.7	3.5	1.34
Boron (B)	10	100	119
Rubidium (Rb)	90	140	34
Strontium (Sr)	375	400	53

Average elemental concentrations in earth crust and shale were taken from Krauskopf (1979).

[a] For arsenic n = 135

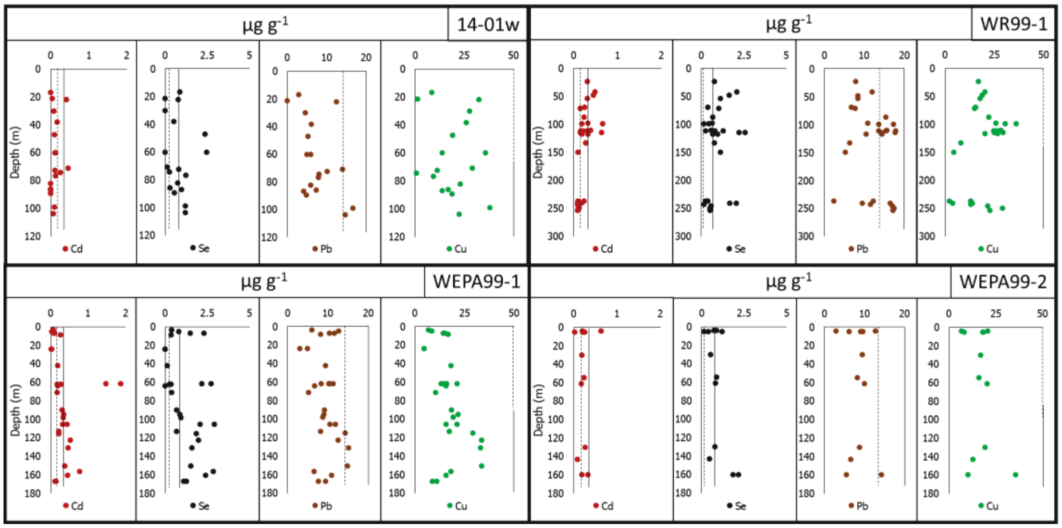

Figure A- 1. Distribution of the chlacophile elements in the sediment cores drilled from four different locations.

Dotted and solid lines are the average elemental concentrations in the earth crust and shale, respectively.

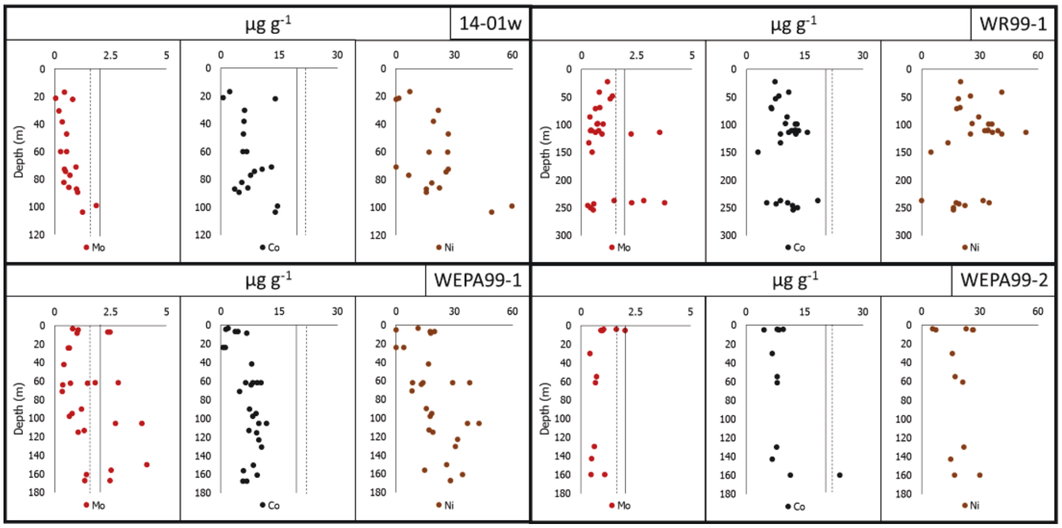

Figure A- 2. Distribution of the siderophile elements in the sediment cores drilled from four different locations.

Dotted and solid lines are the average elemental concentrations in the earth crust and shale, respectively.

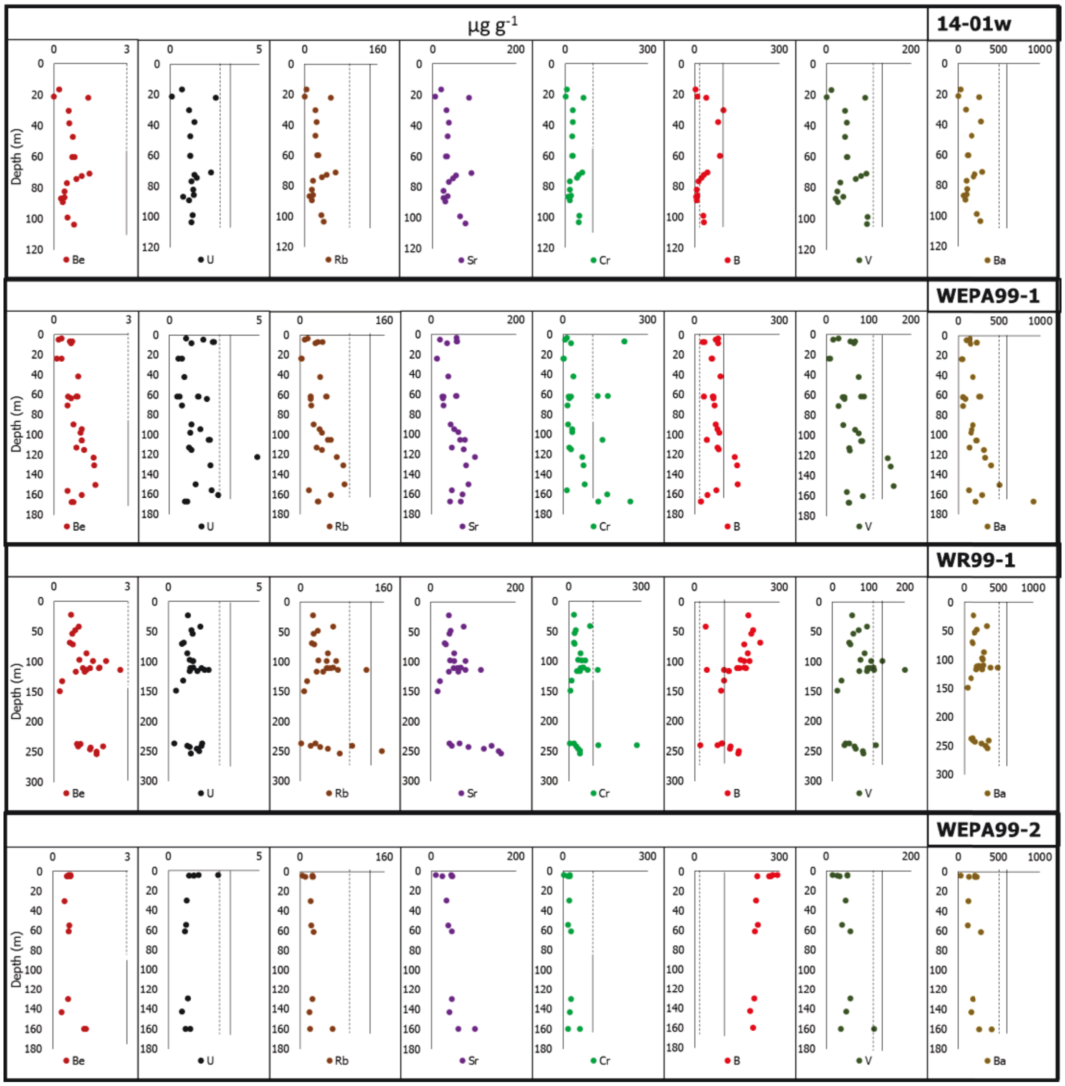

Figure A- 3. Distribution of the lithophile elements in the sediment cores drilled from four different locations.

Dotted and solid lines are the average elemental concentrations in the earth crust and shale, respectively.

Appendix B

Table B- 1. Particle size distribution of the sediments (S1-S8) used in the fractionation method development and the minerals used to test the specificity of the extractants.

Sample ID	Dx (10)	Dx (50)	Dx (90) [a]
		μm	
S1	6.02	57.45	115
S2	4.81	26.4	122.5
S3	7.09	47.15	94.5
S4	4.645	31.5	102
S5	6.06	36.95	119.5
S6	7.175	63.65	117
S7	7.28	26.75	86.3
S8	4.845	34.85	114.5
Calcite	5.53	17.65	50.3
Dolomite	4.13	22.8	66.6
Orpiment	4.545	32.8	119
Arsenopyrite	4.54	19.6	45.05

[a] Dx (10), Dx (50) and Dx (90) mean the distribution of 10%, 50% and 90% particles, respectively in the sample are less than the given sizes.

Table B- 2. Comparison of the sequential extraction of As (μg g^{-1}) from sediment S6 using four different methods.

Fraction [a]	Tessier	Wenzel	Keon	Developed
F1	- [b]	-	-	0.011
F2	0.037	0.031	2.16	0.022
F3	-	7.75	9.02	8.29
F4	0.21	-	1.37	0.08
F5	12.59	4.6	4.62	4.68
F6		8.3	6.97	6.22
F7	-	-	2.8	2.79
F8	-	-	7.72	8.21
F9	9.63	-	-	2.91
F10 (Residual)	12.32	16.24	3.35	0.87
Sum	34.78	36.92	38.01	34.07
% recovery [c]	98.24	104.27	107.34	96.22

[a] F1, water soluble As; F2, ionically bound/exchangeable As; F3, strongly/specifically adsorbed As; F4; arsenic bound to carbonate; F5, arsenic coprecipitated with amorphous Fe, Al and Mn oxyhydroxides; F6, arsenic coprecipitated with crystalline Fe, Al and Mn oxyhydroxides; F7, arsenic associated with As oxides and silicate clays; F8, arsenic coprecipitated with pyrite and orpiment; F9, arsenic associated with organic matter and recalcitrant sulfides; F10, residual As.

[b] Method does not have that extraction step

[c] Sum of all the As fractions extracted by the described methods ranged from 96-107% of the total As (35.4 μg g^{-1}) extracted by the acid digestion method.

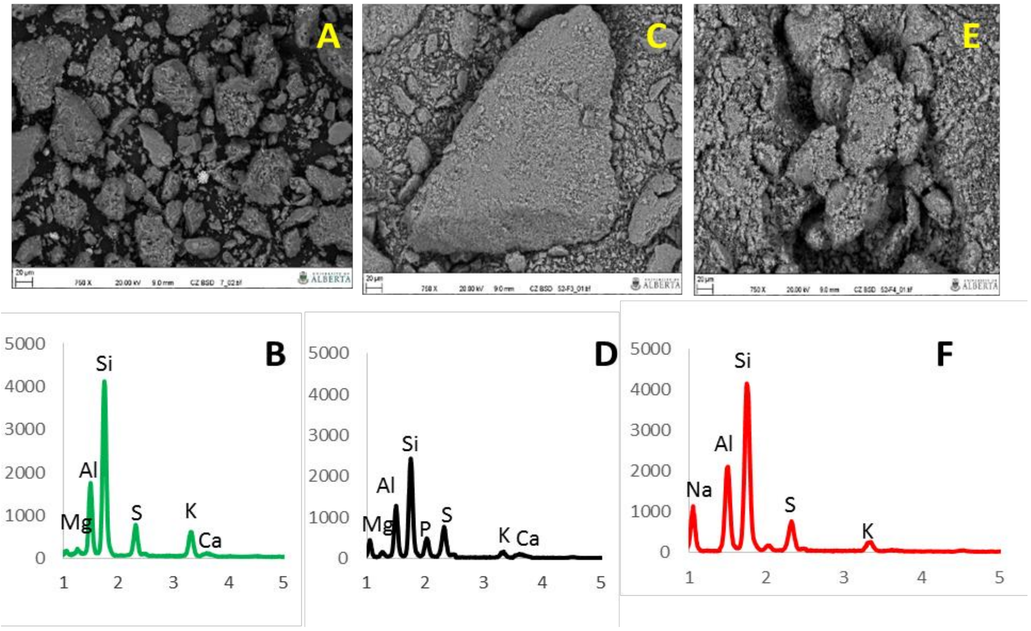

Figure B- 1. SEM-EDX analysis of sediment S6. (A) and (C) are SEM images of sediment before and after 1 M NaH_2PO_4 (pH 5) extraction, respectively with their corresponding EDX spectra (B and D) which show no evidence of carbonate minerals dissolution in F3, as Ca and Mg peaks are similar. (E) and (F) are the SEM image and EDX spectrum of sediment after 1 M NaOAc (pH 5) which suggest complete dissolution of Ca and Mg in F4.

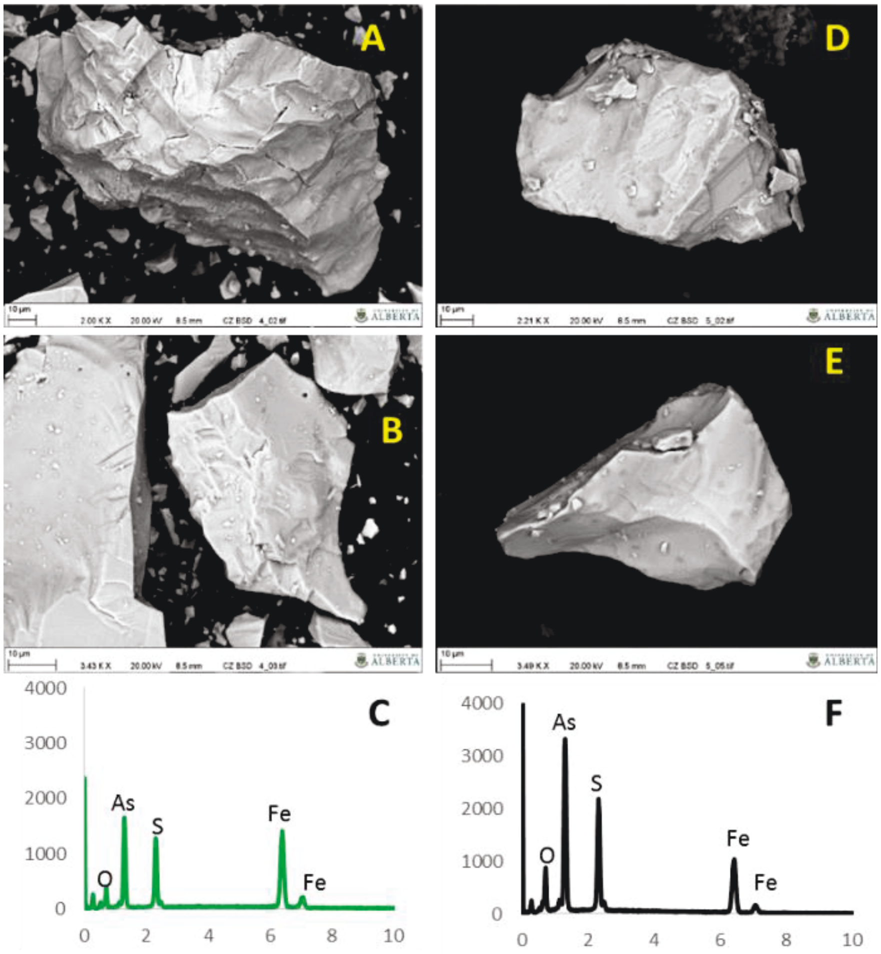

Figure B- 2. SEM-EDX analysis of arsenopyrite mineral. SEM images (A) and (B) show well crystal minerals of arsenopyrite along with EDX spectrum (C) before any extraction with 10 M HF. (D) and (E) are the equivalent SEM images with EDX (F) after 10 M HF extraction that show.the stability of arsenopyrite in 10 M HF. After F8, all the solid phase was dissolved and there was not enough material for SEM analysis.

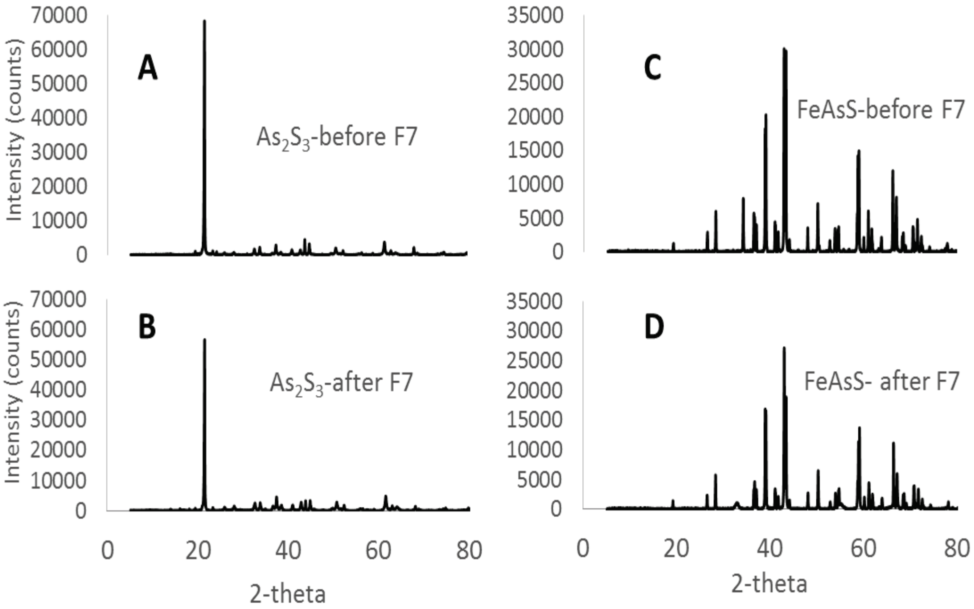

Figure B- 3. XRD analysis of orpiment and arsenopyrite minerals. XRD diffractograms of orpiment (A and B) and arsenopyrite (C and D) are obtained before and after 10 M HF extraction, respectively. Both the diffractograms before and after 10 M HF extraction of orpiment and arsenopyrite are similar which reveal the stability of both the minerals in 10 M HF. After F8, all the solid phase was dissolved and there was not enough material for XRD analysis.

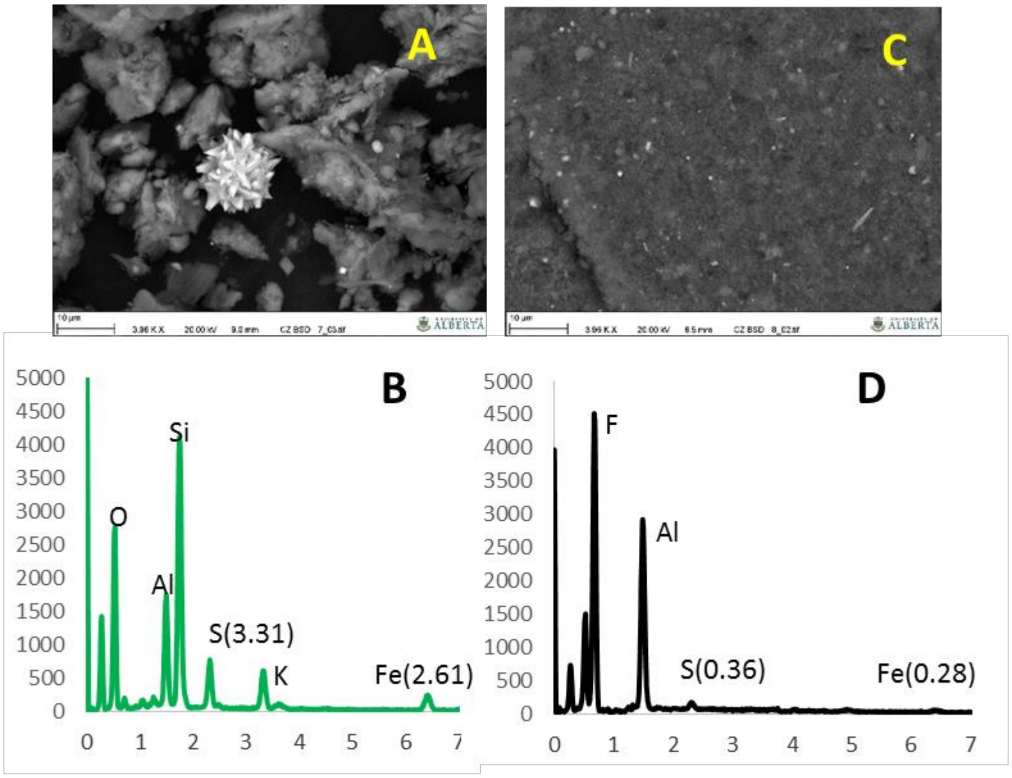

Figure B- 4. SEM-EDX analysis of sediment S6. SEM images of solid phase before (A) and after (C) 10 M HF extraction look different because of the removal of silicates. EDX spectra show Si removal after 10 M HF extraction (D) compared to solid phase before the extraction (B). Fe:S ratio is constant in both solid phases before (B) and after HF extraction (D) indicating the stability of sulfide minerals during HF extraction. Values in parentheses are the atomic % of the Fe and S.

Appendix C

Reference minerals (% weights)^{b}

Sample ID	Annabergite	Sodium arsenate	Arsenic oxide	Sodium arsenite	Orpiment	Arseno-pyrite	R-factor[c]
1	30.3	-	-	65.0	4.7	-	0.013
2	-	23.8	-	23.8	52.4	-	0.013
3	-	11.9	-	72.9	-	15.2	0.011
4	-	16.8	-	50.1	13.6	19.5	0.010
5	-	17.2	-	76.8	2.6	3.4	0.010
6	-	23.1	-	69.2	-	7.7	0.020
7	-	5.9	65.3	28.8	-	-	0.012
8	20	23.3	-	-	56.7	-	0.552
9	-	16.8	-	1.8	81.4	-	0.027
10	24.3	41.4	-	-	30.9	3.4	0.012
11	-	7.7	-	20.5	54.5	17.3	0.006
12	21.5	41.9	-	31.2	1.6	3.8	0.009
13	24.8	-	-	20.3	40.8	14.1	0.032
14	92.2	-	-	-	-	7.8	0.548
15	-	65.7	-	22.1	-	12.2	0.013
16	-	23.1	-	71.5	-	5.4	0.041
17	23.3	-	-	14.9	44.5	17.3	0.103
18	-	34.8	25.5	-	-	39.7	0.140
19	30.2	8.2	-	48.2	13.4	-	0.024
20	15.9	24.6	-	35.4	17.3	6.8	0.012
21	19.9	6.4	15.6	-	54.4	3.6	0.060
22	-	6.1	-	18.4	50.1	19.8	0.006

Table C- 1. Linear combination fits (LCF) of arsenic XANES spectra of reference compounds with the spectra of the selected sediments[a]

[a] detailed LCF results correspond to XANES spectra of the selected sediment samples plotted in Figures 4-5 and C6. [b] These results are presented with <±5% delta weights. [c] Normalized sum of the residuals (R-factor) is obtained by the following equation: R-factor = $\frac{\sum\{(data-fit)^2\}}{\sum(data^2)}$

Relatively high R-factor values show that quality of LCF may not be very good.

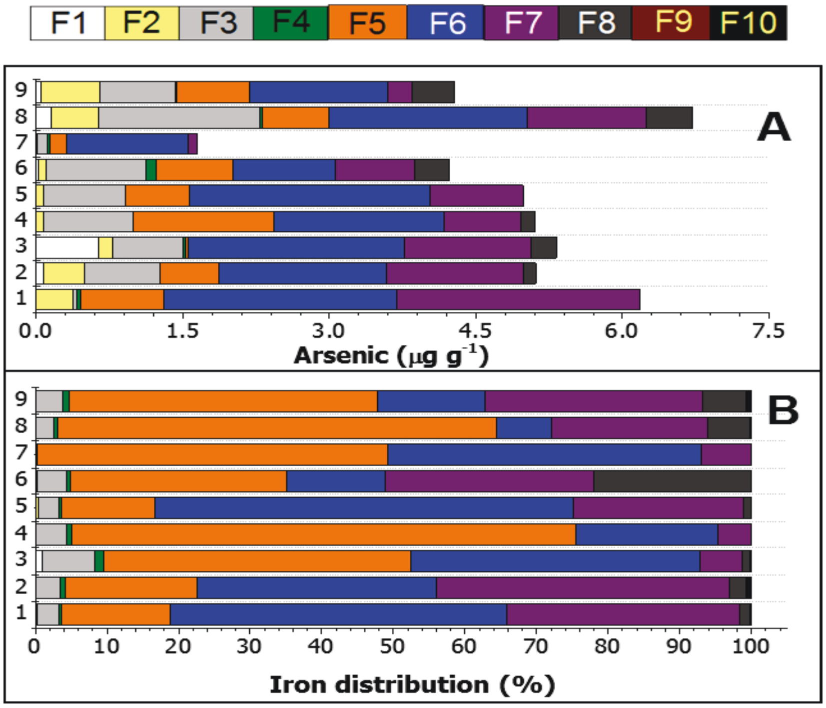

Figure C- 1. Distribution of **(A)** As and **(B)** Fe in different sediment solid phases of the selected low As sediments (sample 1-9; As <7 μg g^{-1}). Sequential extraction protocol (SEP; Javed et al., 2013) was used to determine the As and Fe fractionation in sediments. Arsenic and Fe concentrations were determined in the same aliquot of the extractants used in SEP. Legends are applicable for both panels and represent different fractions: F1, water soluble metals; F2, ionically bound/exchangeable metals; F3, strongly/specifically adsorbed metals; F4, metals bound in carbonates; F5, metals coprecipitated with amorphous Fe, Al and Mn oxyhydroxides; F6, metals coprecipitated with crystalline Fe, Al and Mn oxyhydroxides; F7, metals associated with their oxides and silicate clays; F8, metals coprecipitated with pyrite and orpiment; F9, metals associated with organic matter and recalcitrant sulfides; and F10, residual metals.

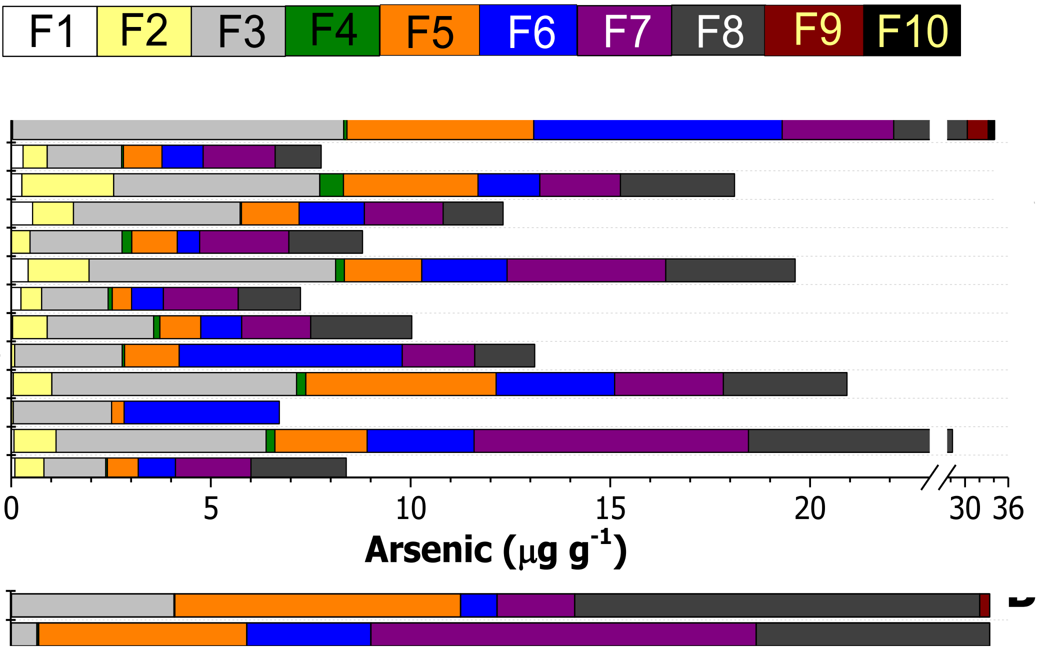

Figure C-2. Distribution of arsenic (As) in different sediment solid phases of the selected high As sediments (sample 10-22; As>7 μg g^{-1}). Sequential extraction protocol (SEP; Javed et al., 2013) was used to determine the As fractionation in sediments. Legends represent different fractions: F1, water soluble arsenic; F2, ionically bound/exchangeable arsenic; F3, strongly/specifically adsorbed arsenic; F4, metals bound in arsenic; F5, arsenic coprecipitated with amorphous Fe, Al and Mn oxyhydroxides; F6, arsenic coprecipitated with crystalline Fe, Al and Mn oxyhydroxides; F7, arsenic associated with their oxides and silicate clays; F8, arsenic coprecipitated with pyrite and amorphous orpiment; F9, arsenic associated with organic matter and recalcitrant sulfides; and F10, residual arsenic.

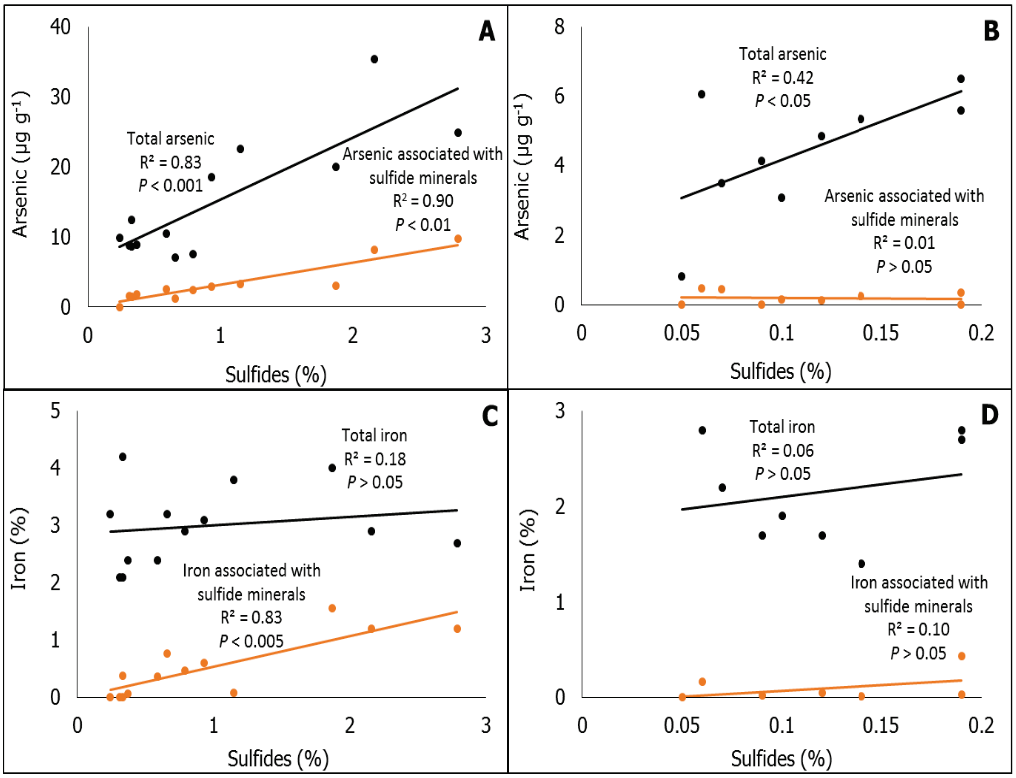

Figure C-3. Relationship of As and Fe with sulfide minerals in sediments. Association of sulfide minerals with As bound in sulfide minerals (F8 of As sequential extraction) and total As in (**A**) high and (**B**) low As sediments; and with Fe bound with sulfide minerals (F8) and total Fe in (**C**) high and (**D**) low As sediments. Arsenic bound in sulfide minerals and total As in high As sediments were highly correlated with sulfide minerals of the sediments, but in low As sediments total As showed some correlation with sulfide minerals but we did not find much As bound in sulfide minerals. Total Fe does not show good correlation with sulfide minerals in both low and high As sediments, but in high As sediments high correlation was found between sulfide minerals and Fe bound in the sulfide minerals compared to low As sediments. The results suggest that in high As sediments Fe might be present as Fe sulfide mineral but in low As samples Fe may be in the form of oxides.

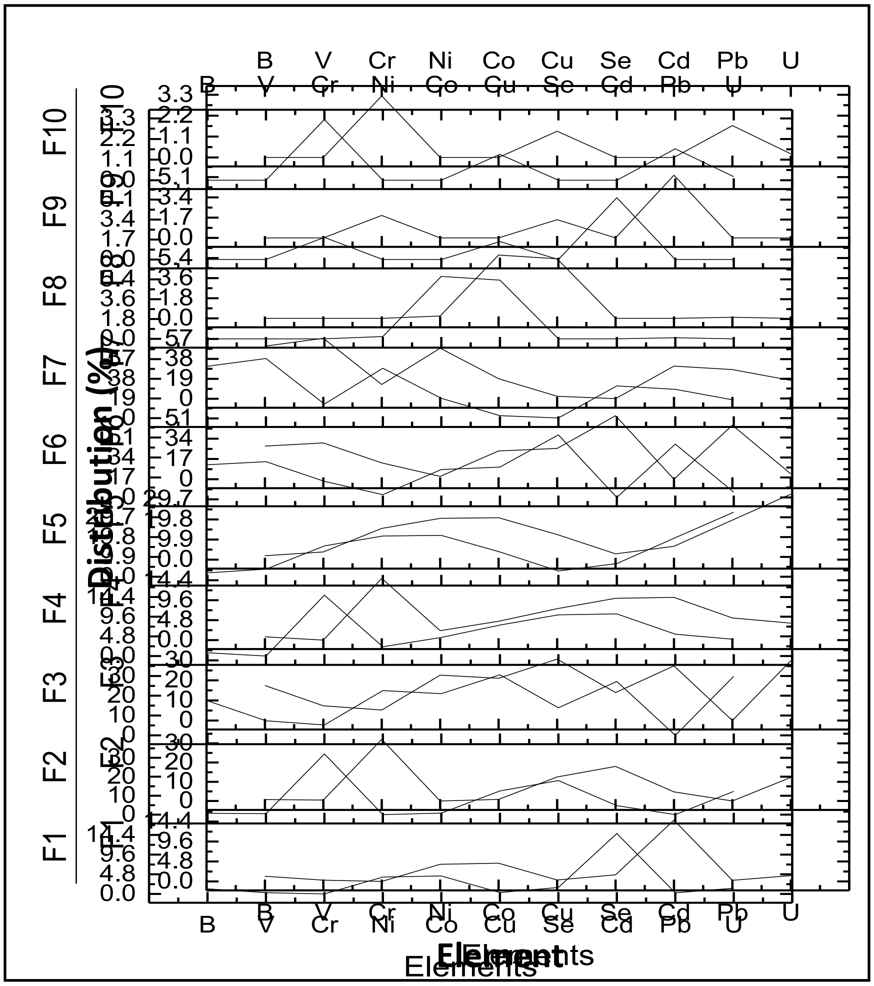

Figure C-4. Detailed sequential extraction of trace elements in 10 fractions (F1-F10) to determine their association with different solid phases in sediments to predict their potential to contaminate groundwater. Sequential extraction protocol (Javed et al., 2013) was used to determine the metal fractionation in sediments. Legends represent different fractions: F1, water soluble metals; F2, ionically bound/exchangeable metals; F3, strongly/specifically adsorbed metals; F4, metals bound to carbonates; F5, metals coprecipitated with amorphous Fe, Al and Mn oxyhydroxides; F6, metals coprecipitated with crystalline Fe, Al and Mn oxyhydroxides; F7, metals associated with their oxides and silicate clays; F8, metals coprecipitated with pyrite and orpiment; F9, metals associated with organic matter and recalcitrant sulfides; F10, residual metals.

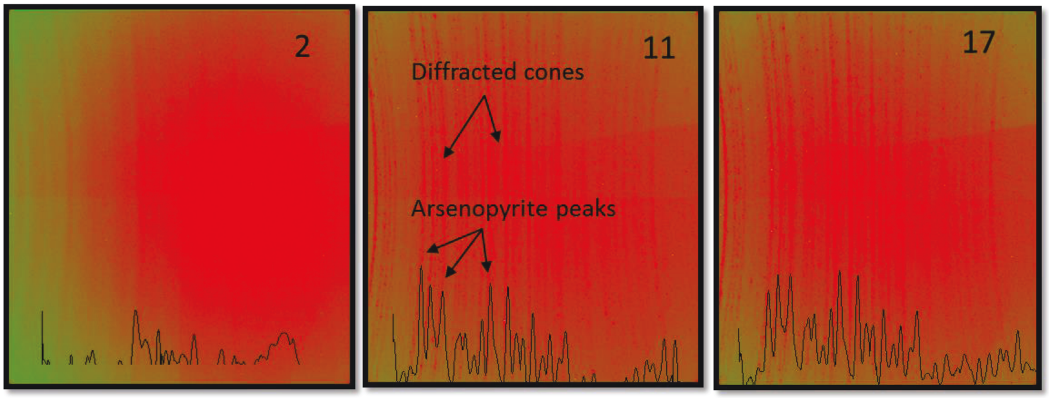

Figure C-5. Determination of arsenopyrite minerals in the selected high As (sample 11; 24.9±4.2 μg g^{-1} As and 17; 22.5±2.1 μg g^{-1} As) and low As sediments (sample 2; 4.9±0.7 μg g^{-1} As) using μ-XRD. General Area Diffraction Detector System (GADDS) images of sediments show diffraction cones. Diffractogrames are also shown on the images by the integration of cones pattern. Sediment 2 is a low As sediment where we could not find arsenopyrite peaks using high energy synchrotron radiation at ~11.867 KeV, whereas in sediments 11 and 17 clear arsenopyrite peaks were detected.

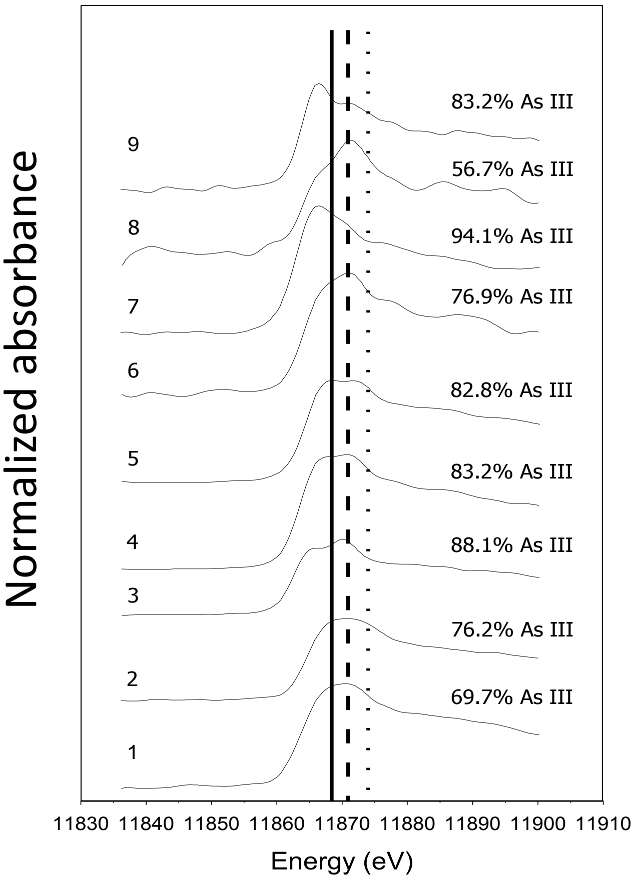

Figure C-6. Determination of dominant oxidation state of As using As K-edge XANES spectroscopy in the selected low As sediments (sample 1-9; <7 µg g^{-1} As). Solid (-), dashed (---) and dotted (…) lines drawn at 11868 eV, 11870.7 eV and 11874 eV represent the position of white lines of As^{III}-S, As^{III}-O and As^{V}-O, respectively. Liner combination fit (LCF) results show that arsenite (As^{III}) is the most dominant As form in the sediments as shown by the proportion of As^{III} beside each spectrum. Only that oxidation state of As is shown in the spectrum that was present >50% in the sediment. Detail of the LCF analysis is provided in Table C-1.

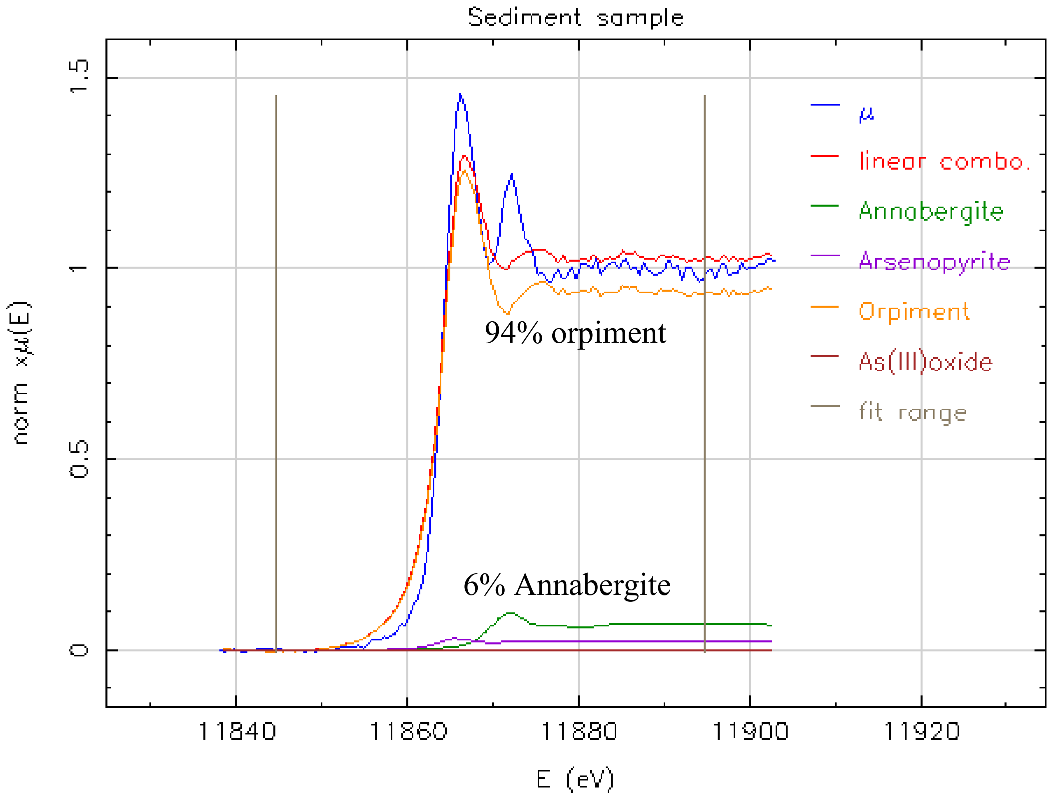

Figure C-7. A linear combination fit (LCF) of the standards spectra with an As XANES spectrum acquired from a high As sediment (~20 µg g^{-1} As). All six standards [sodium arsenate (As^{V}), annabergite (As^{V}), arsenic oxide (As^{III}), sodium arsenite (As^{III}), orpiment (As^{III}), and arsenopyrite (As^{III}) were used to perform the LCF. A complete range of the As XANES spectra (pre-edge, edge, and post-edge) was used to get the best fit. The goodness of the fit was determined by the R-factor value (normalized sum of the residuals = $\frac{\sum\{(data-fit)^2\}}{\sum(data^2)}$) that was 0.007 in the fit. The result shows that the sediment As 94% resemble with the As in orpiment (As_2S_3) mineral.

Appendix D

Table D- 1. Particle size distribution of the sediments (S1-S7) used to study the effect of heat on As release into the porewater from sediments.

Sample ID	Dx (10)	Dx (50)	Dx (90) [a]
		μm	
S1	7.18	52.83	120.8
S2	3.85	25.48	118
S3	6.36	39.72	101.7
S4	5.03	32.32	112
S5	6.12	35.79	117.4
S6	7.72	65.90	114.9
S7	7.82	27.48	89.65

[a] Dx (10), Dx (50) and Dx (90) mean the distribution of 10%, 50% and 90% particles, respectively in the sample are less than the given sizes.

Table D-2. Detailed fractionation of arsenic (As) after the heat treatment of sediments moistened with 15% and 50% synthetic aquifer water. The results show the average As concentration in different fractions (µg kg^{-1}) ± standard deviation.

Fraction	S1		S2		S3		S4		S5		S6		S7	
	Moisture content													
	15%	50%	15%	50%	15%	50%	15%	50%	15%	50%	15%	50%	15%	50%
	µg kg^{-1}													
F1	186±24	212±37	281±28	320±32	489±48	526±39	889±64	910±79	920±88	1138±73	1059±109	1103±136	570±63	638±91
F2	375±50	438±68	482±48	531±57	301±41	339±30	872±72	1061±109	105±34	138±21	674±57	786±69	489±42	521±48
F3	573±61	648±52	579±45	640±68	1392±221	1429±96	1198±356	2109±472	1681±238	1742±307	5581±169	5608±225	3909±247	3937±274
F4	ND	ND	ND	ND	ND	ND	ND	ND	ND	ND	ND	ND	ND	ND
F5	292±58	327±41	291±38	309±29	681±75	742±94	675±118	761±85	1207±107	1250±132	2457±386	2539±275	2360±254	2418±317
F6	860±148	937±125	1082±102	1159±85	1109±75	1139±92	1206±119	1251±148	2491±315	2509±363	3891±290	3944±362	6158±421	6205±212
F7	186±48	206±72	182±39	205±52	1576±116	1649±182	1692±182	1701±202	1860±382	2063±401	3359±277	3408±362	2307±174	2283±199
F8	281±65	326±81	365±72	435±81	1190±114	1209±102	1260±69	1298±84	2471±270	2536±298	2571±188	2648±239	8068±491	8135±303
F9	ND	ND	ND	ND	ND	ND	ND	ND	ND	ND	ND	ND	2764±280	2808±170
F10	ND	ND	ND	ND	ND	ND	ND	ND	ND	ND	ND	ND	ND	ND

No significant difference was found between the As fractions in sediments moistened with 15% and 50% synthetic aquifer water after heat.

ND: not detected

Legends (F1 – F10) represent different As fractions: F1, water soluble As; F2, ionically bound/exchangeable As; F3, strongly/specifically adsorbed As; F4, As bound in carbonates; F5, As coprecipitated with amorphous Fe, Al and Mn oxyhydroxides; F6, As coprecipitated with crystalline Fe, Al and Mn oxyhydroxides; F7, As associated with its oxides and silicate clays; F8, As coprecipitated with pyrite and orpiment; F9, As associated with organic matter and recalcitrant sulfides; and F10, residual As.

Table D-3. Detailed fractionation of arsenic (As) after the heat treatment of sediments moistened with 15% and 50% nanopure water.

The results show the average As concentration in different fractions (µg kg^{-1}) ± standard deviation.

Fraction	S1		S2		S3		S4		S5		S6		S7	
	Moisture content													
	15%	50%	15%	50%	15%	50%	15%	50%	15%	50%	15%	50%	15%	50%
	µg kg^{-1}													
F1	302+36	328+29	288+24	315+31	1172+76	1227+59	1295+68	1309+73	1669+106	1758+183	126+27	137+17	743+46	784+5234
F2	286+57	340+66	516+48	542+56	201+38	237+26	625+31	651+48	ND	ND	577+76	649+58	381+30	409+32
F3	588+48	629+53	565+34	538+29	1067+105	1106+92	2066+163	2140+12	1202+85	1239+103	5470+126	5581+140	3880+228	3706+171
F4	ND	ND	ND	ND	ND	ND	ND	ND	ND	ND	ND	ND	ND	ND
F5	289+42	307+27	309+19	327+24	691+40	737+53	686+97	744+82	1084+138	1129+146	2359+268	2396+209	2185+164	2224+190
F6	866+71	917+77	1083+69	1129+87	1061+127	941+84	1185+64	1209+77	1465+150	1544+126	3855+146	3896+131	6194+99	6222+76
F7	197+31	229+35	201+33	226+27	1573+41	1608+50	1694+66	1733+79	1943+164	2060+201	3356+254	2450+277	2265+215	2290+177
F8	334+40	361+31	391+27	416+33	1176+116	1198+88	1280+86	1307+72	2468+241	2494+183	2568+184	2594+140	8064+259	8142+231
F9	ND	ND	ND	ND	ND	ND	ND	ND	ND	ND	ND	ND	2795+143	2839+162
F10	ND	ND	ND	ND	ND	ND	ND	ND	ND	ND	ND	ND	ND	ND

No significant difference was found between the As fractions in sediments moistened with 15% and 50% nanopure water after heat.

ND: not detected

Legends (F1 – F10) represent different As fractions: F1, water soluble As; F2, ionically bound/exchangeable As; F3, strongly/specifically adsorbed As; F4, As bound in carbonates; F5, As coprecipitated with amorphous Fe, Al and Mn oxyhydroxides; F6, As coprecipitated with crystalline Fe, Al and Mn oxyhydroxides; F7, As associated with its oxides and silicate clays; F8, As coprecipitated with pyrite and orpiment; F9, As associated with organic matter and recalcitrant sulfides; and F10, residual As.

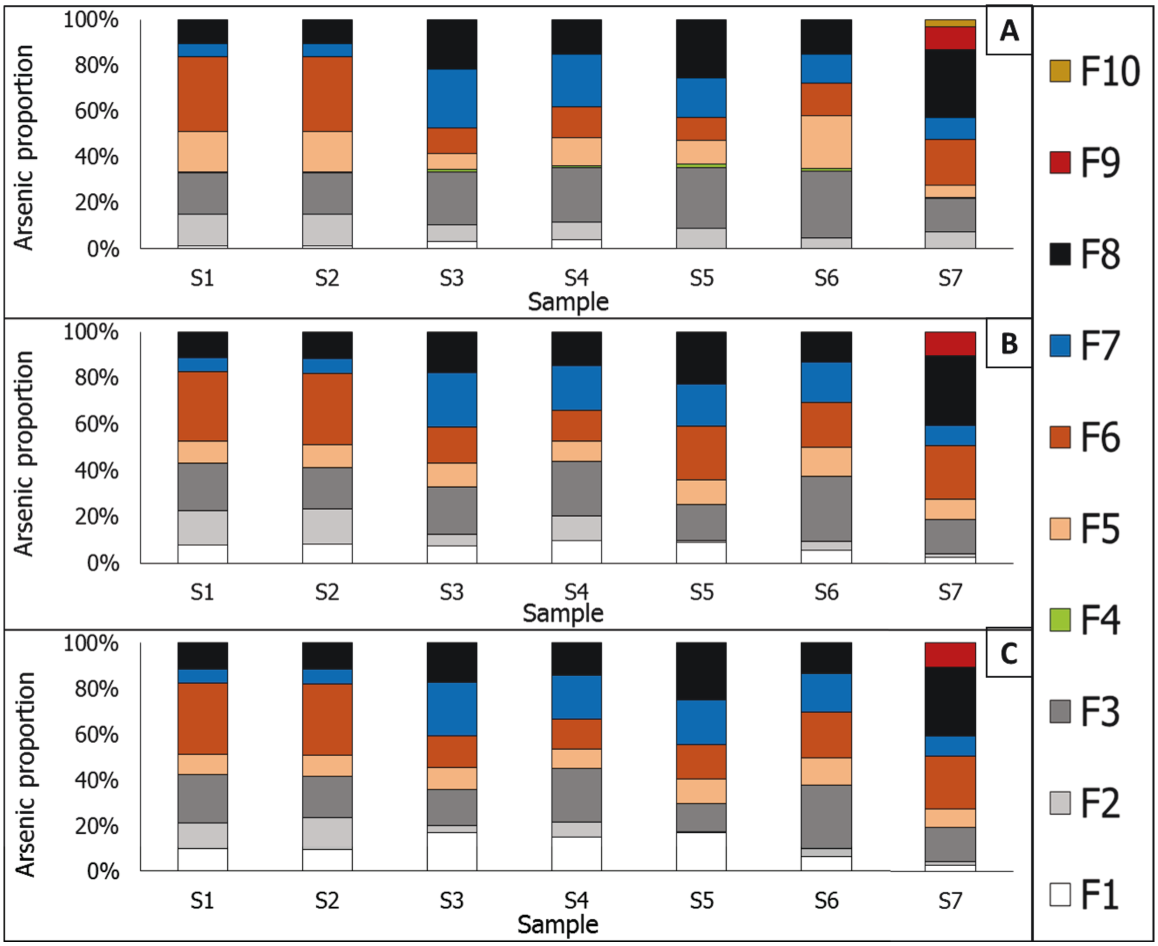

Figure D- 1. Detailed fractionation of arsenic (As) in sediments. The figure shows the As fractionation in **(A)** sediments before heat, and **(B)** sediments moistened with synthetic aquifer after the heat treatment, and **(C)** sediments moistened with nanopure water after the heat treatment.

The sediments were moistened with 15% and 50% for both synthetic aquifer and nanopure water, however, due to insignificant difference in the fractionation results both the results were averaged to avoid complexity. The results show that there is a significant increase in the soluble As (F1) after the heat treatment in both sediments moistened with aquifer and nanopure water.

Legends represent different As fractions: F1, water soluble As; F2, ionically bound/exchangeable As; F3, strongly/specifically adsorbed As; F4, As bound in carbonates; F5, As coprecipitated with amorphous Fe, Al and Mn oxyhydroxides;

F6, As coprecipitated with crystalline Fe, Al and Mn oxyhydroxides; F7, As associated with its oxides and silicate clays; F8, As coprecipitated with pyrite and orpiment; F9, As associated with organic matter and recalcitrant sulfides; and F10, residual As.

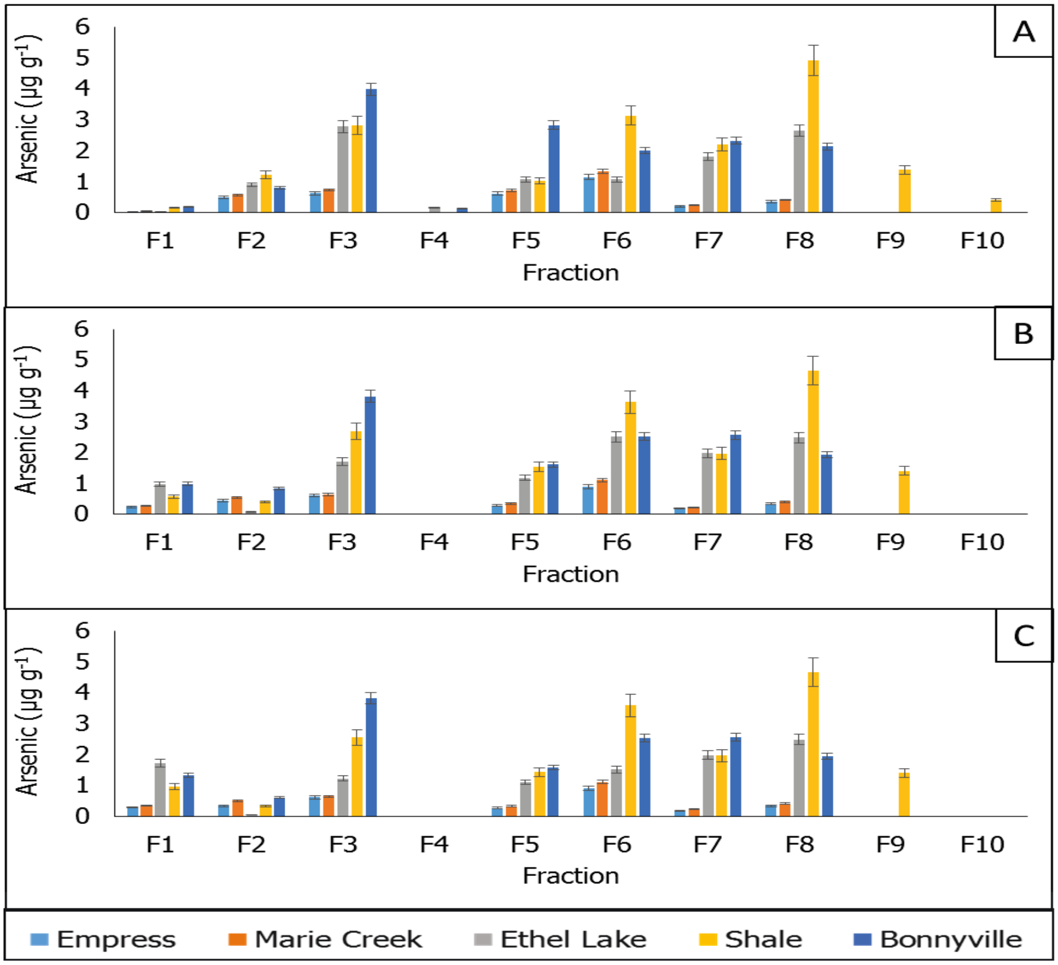

Figure D- 2. Arsenic (As) fractionation in sediments derived from different geological formations such as Empress (n = 1), Marie Creek (n = 1), Ethel Lake (n = 1), Shale (n = 2) and Bonnyville (n = 2). The figure shows the As fractionation in **(A)** sediments before heat, and **(B)** sediments moistened with synthetic aquifer after the heat treatment, and **(C)** sediments moistened with nanopure water after the heat treatment. The results show that there is a significant increase in the soluble As (F1) in all the sediments moistened with aquifer and nanopure water after the heat treatment.

Legends represent different As fractions: F1, water soluble As; F2, ionically bound/exchangeable As; F3, strongly/specifically adsorbed As; F4, As bound in carbonates; F5, As coprecipitated with amorphous Fe, Al and Mn oxyhydroxides; F6, As coprecipitated with crystalline Fe, Al and Mn oxyhydroxides; F7, As associated with its oxides and silicate clays; F8, As coprecipitated with pyrite and orpiment; F9, As associated with organic matter and recalcitrant sulfides; and F10, residual As.

Appendix E

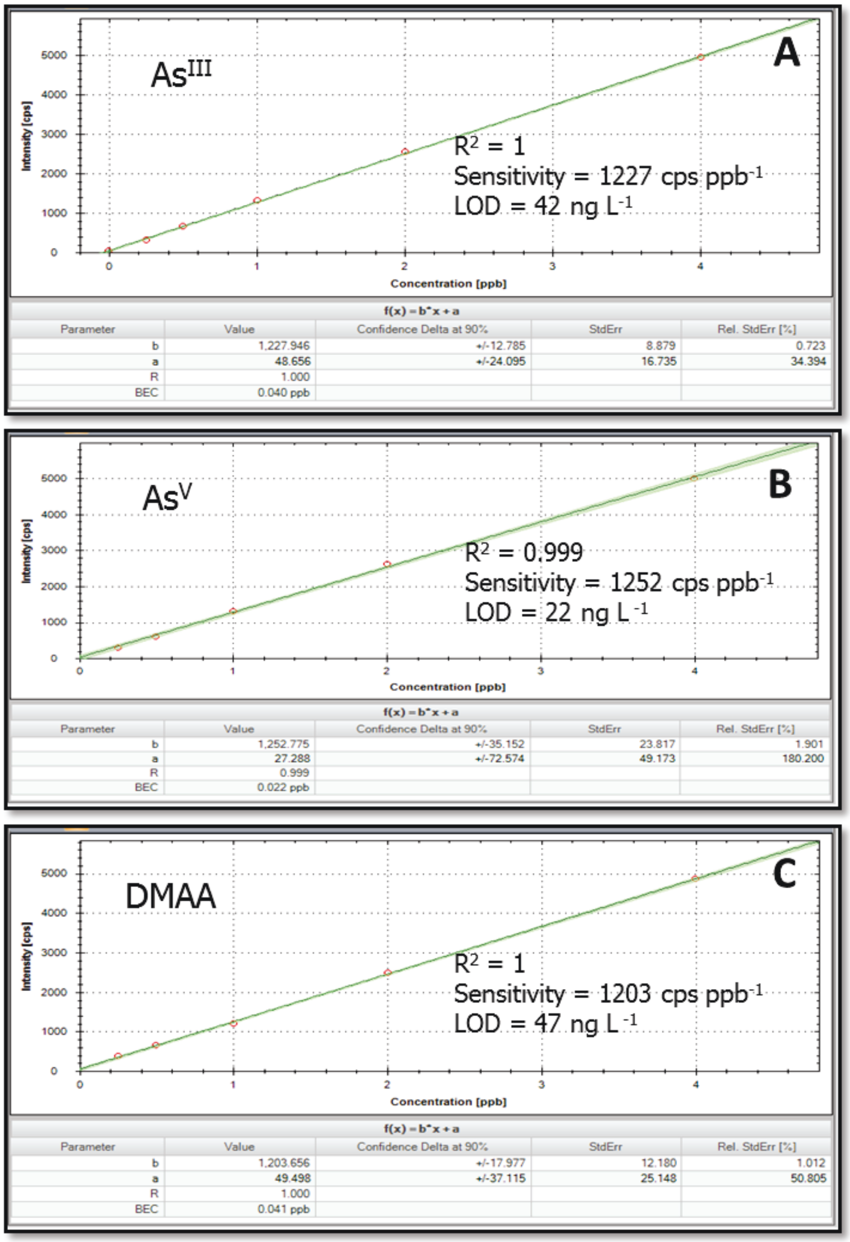

$f(x) = b^*x + a$

Parameter	Value	Confidence Delta at 90%	StdErr	Rel. StdErr [%]
b	1,227.946	+/-12.785	8.879	0.723
a	48.656	+/-24.095	16.735	34.394
R	1.000			
BEC	0.040 ppb			

$f(x) = b^*x + a$

Parameter	Value	Confidence Delta at 90%	StdErr	Rel. StdErr [%]
b	1,252.775	+/-35.152	23.817	1.901
a	27.288	+/-72.574	49.173	180.200
R	0.999			
BEC	0.022 ppb			

$f(x) = b^*x + a$

Parameter	Value	Confidence Delta at 90%	StdErr	Rel. StdErr [%]
b	1,203.656	+/-17.977	12.180	1.012
a	49.498	+/-37.115	25.148	50.805
R	1.000			
BEC	0.041 ppb			

Figure E- 1. Calibration curves of **A)** As^{III}, **B)** As^{V} and **C)** DMAA standards in the range of 0.2 to 4 µg L^{-1}. These curves show that the speciation method is equally sensitive (~1200 cps ppb^{-1}) for all the species with very low limit of detection (LOD; 22 to 47 ng L^{-1}). LOD was determined using 3 × standard deviation (σ) of intensities of 7 blanks + average of the 7 blank intensities).

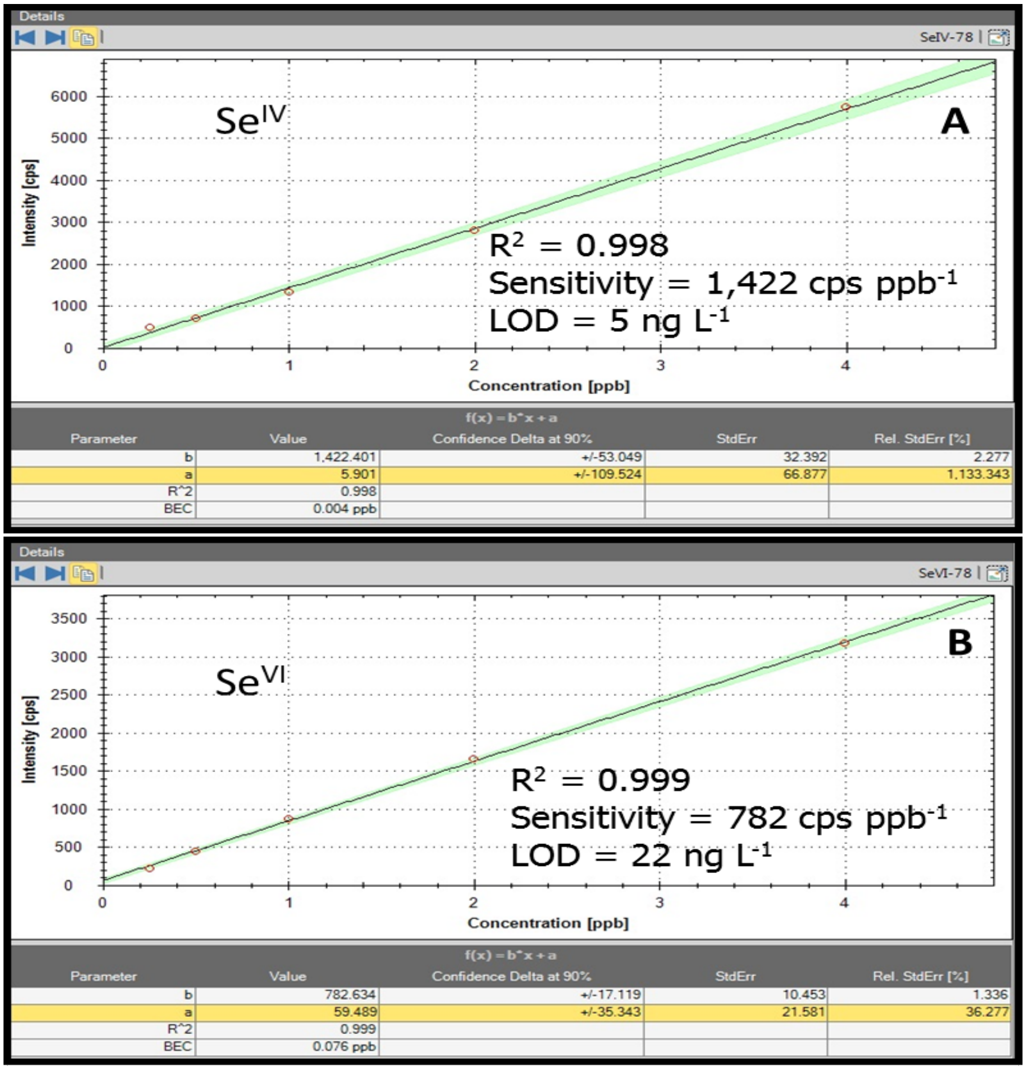

f(x) = b*x + a

Parameter	Value	Confidence Delta at 90%	StdErr	Rel. StdErr [%]
b	1,422.401	+/-53.049	32.392	2.277
a	5.901	+/-109.524	66.877	1,133.343
R^2	0.998			
BEC	0.004 ppb			

f(x) = b*x + a

Parameter	Value	Confidence Delta at 90%	StdErr	Rel. StdErr [%]
b	782.634	+/-17.119	10.453	1.336
a	59.489	+/-35.343	21.581	36.277
R^2	0.999			
BEC	0.076 ppb			

Figure E- 2. Calibration curves of **A)** Se^{IV} and **B)** Se^{V} in the range of 0.2 to 4 µg L^{-1}. These curves show that the speciation method is more sensitive for Se^{IV} (1,422 cps ppb^{-1}) compared to Se^{VI} (782 cps ppb^{-1}). The limit of detection (LOD: determined using 3 × standard deviation (σ) of intensities of 7 blanks + average of the 7 blank intensities) of Se^{IV} was also lower (5 ng L^{-1}) than Se^{VI} (22 ng L^{-1}).

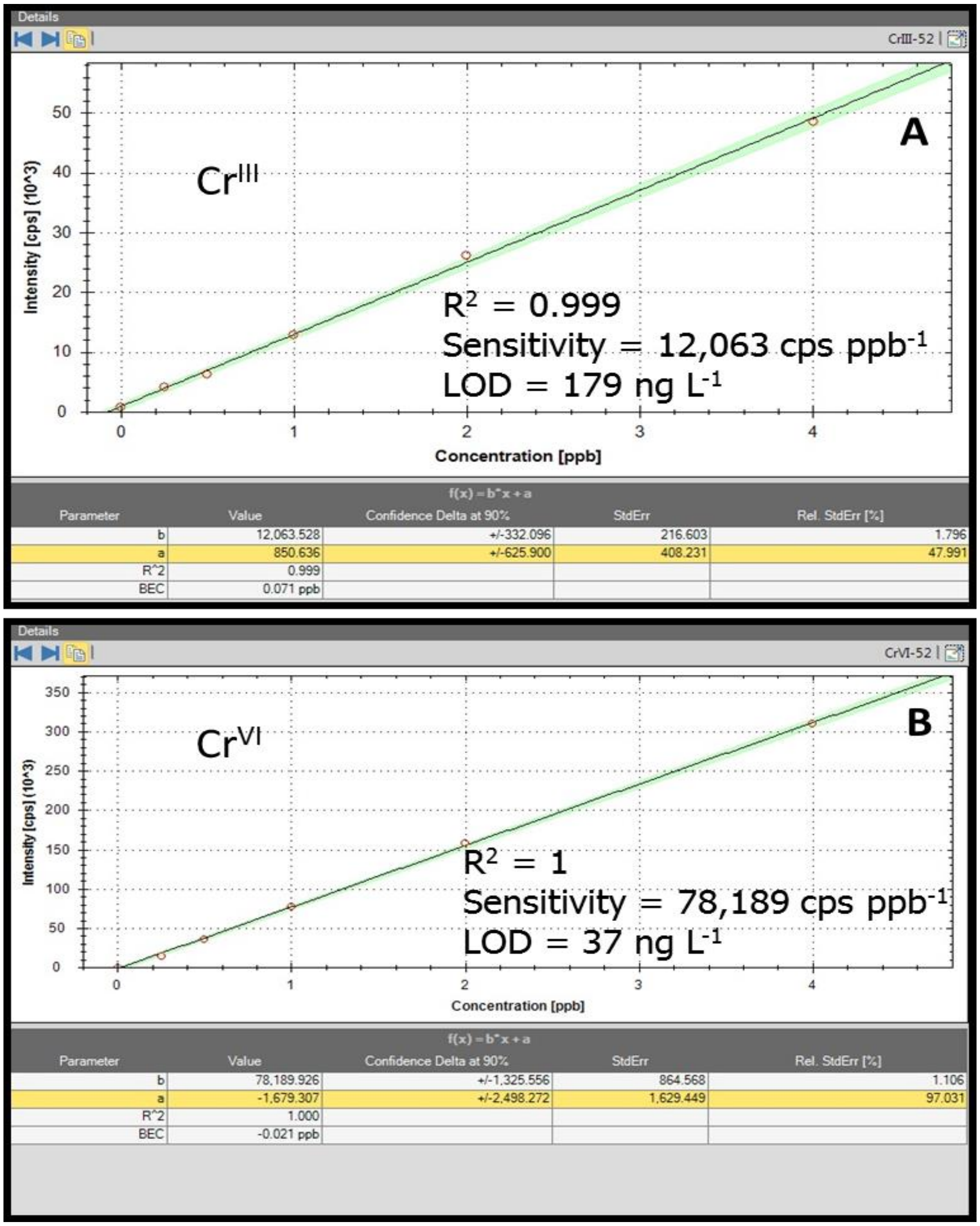

f(x) = b*x + a

Parameter	Value	Confidence Delta at 90%	StdErr	Rel. StdErr [%]
b	12,063.528	+/-332.096	216.603	1.796
a	850.636	+/-625.900	408.231	47.991
R^2	0.999			
BEC	0.071 ppb			

f(x) = b*x + a

Parameter	Value	Confidence Delta at 90%	StdErr	Rel. StdErr [%]
b	78,189.926	+/-1,325.556	864.568	1.106
a	-1,679.307	+/-2,498.272	1,629.449	97.031
R^2	1.000			
BEC	-0.021 ppb			

Figure E- 3. Calibration curves of **A)** Cr^{III} and **B)** Cr^{VI} in the range of 0.2 to 4 µg L^{-1}. These curves show that the speciation method is more sensitive for Cr^{VI} (78,189 cps ppb^{-1}) compared to Cr^{III} (12,063 cps ppb^{-1}). The limit of detection (LOD: determined using 3 × standard deviation (σ) of intensities of 7 blanks + average of the 7 blank intensities) of Cr^{VI} was also lower (37 ng L^{-1}) than Cr^{III} (179 ng L^{-1}).

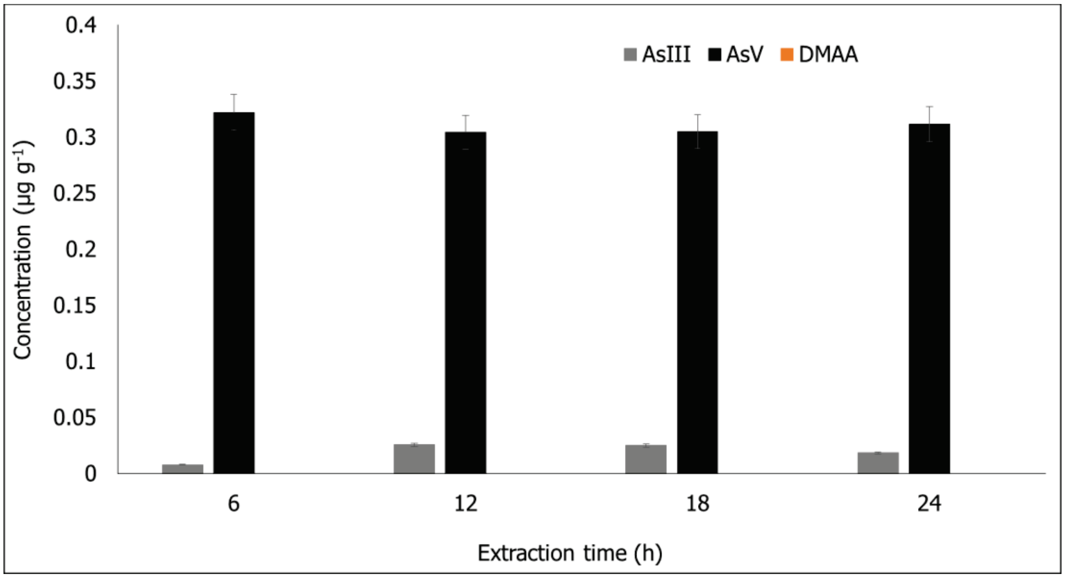

Figure E- 4. Initial concentrations of As^{III}, As^{V} and DMAA in the sediment extracted using 0.1 M NaH_2PO_4 (pH 4.2) at different extraction times. These results show that As^{V} is the only dominant species present in the sediment, and there is no significant difference in different extraction times. All the As^{V} in sediment was extracted in 6 h extraction.

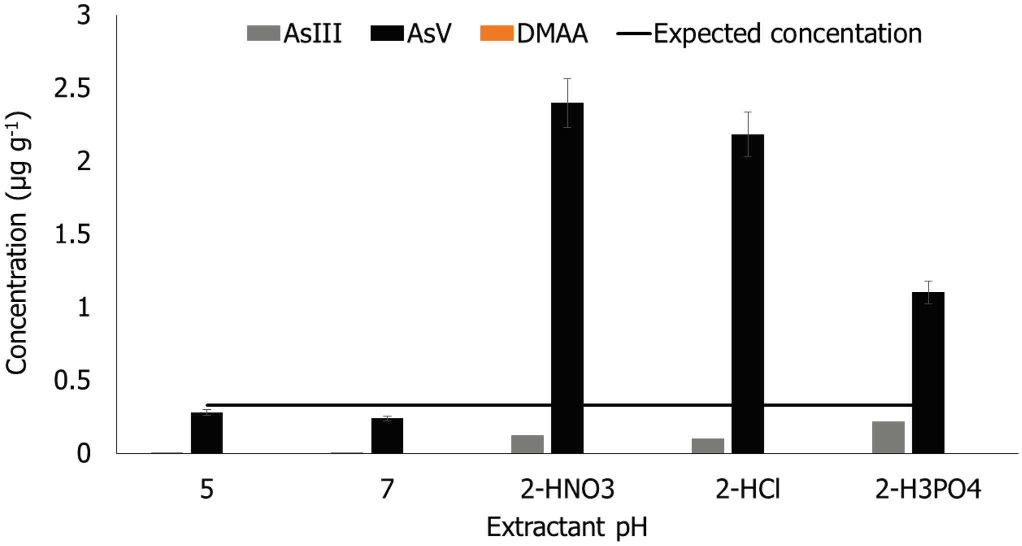

Figure E- 5. Determination of initial concentrations of As^{III}, As^{V} and DMAA species in sediment extracted using 0.1 M NaH_2PO_4 solution of different pH values for 6 h to determine the specificity and efficiency of the extractant.

It was already known (because of initial characterisation) that the concentration of As^{V} in the sediment was ~0.31 $\pm$ 0.03 µg g^{-1}, and it was the only dominant species present in the sediment. Thus, the expected concentration of As^{V} was ~0.31 µg g^{-1}. However, the figure shows that the extractants having pH 2 produce significantly high As^{V}, probably due to the release of mineral bound As because of dissolution of carbonates and acid volatile sulfides. Extractant of pH 5 produced the optimum recovery of As^{V}.

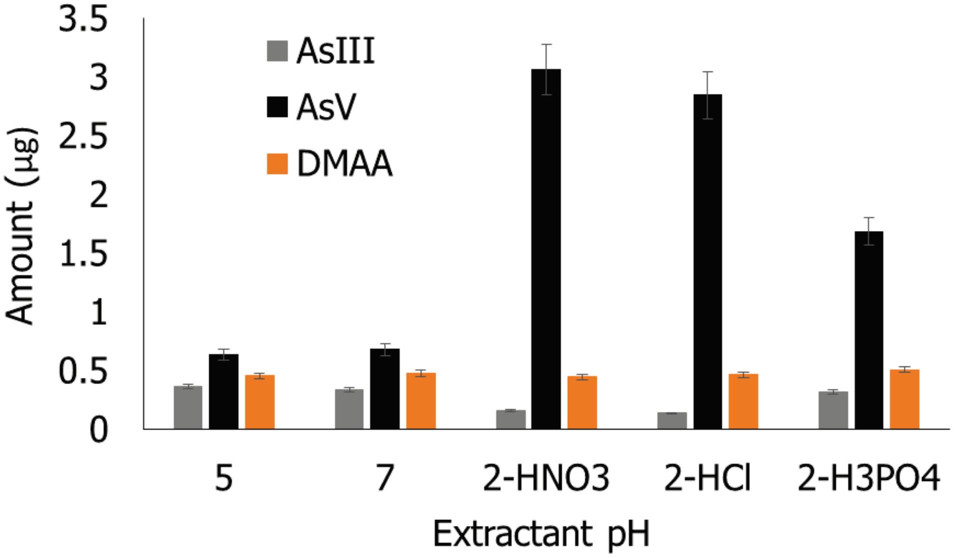

Figure E- 6. Extraction of the spiked As^{III} (0.53 µg), As^{V} (0.46 µg) and DMAA (0.48 µg) species from sediment for 6 h using 0.1 M NaH_2PO_4 solution of different pH (pH 2 was adjusted with different acids).

Before spiking, the sediment contained only small concentration of As^{V} (~0.31 µg g^{-1}), thus the expected amount of As^{V} was ~0.77 µg, and for As^{III} and DMAA species spiked amount (0.53 µg and 0.48 µg, respectively) were expected to be recovered after extraction. 0.1 M NaH_2PO_4 solution of pH 5 produced the optimum recovery of all the species.

Copyright Clearance Center RightsLink®

Home | Account Info | Help | Live Chat

Title: A modified sequential extraction method for arsenic fractionation in sediments

Author: Muhammad Babar Javed,Gary Kachanoski,Tariq Siddique

Publication: Analytica Chimica Acta

Publisher: Elsevier

Date: 17 July 2013

Logged in as:
Muhammad Javed
Account #:
3000772809

LOGOUT

Order Completed

Thank you very much for your order.

This is a License Agreement between Muhammad B Javed ("You") and Elsevier ("Elsevier"). The license consists of your order details, the terms and conditions provided by Elsevier, and the payment terms and conditions.

Get the printable license.

License Number	3512080258585
License date	Nov 18, 2014
Licensed content publisher	Elsevier
Licensed content publication	Analytica Chimica Acta
Licensed content title	A modified sequential extraction method for arsenic fractionation in sediments
Licensed content author	Muhammad Babar Javed,Gary Kachanoski,Tariq Siddique
Licensed content date	17 July 2013
Licensed content volume number	787
Licensed content issue number	n/a
Number of pages	9
Type of Use	reuse in a thesis/dissertation
Portion	full article
Format	both print and electronic
Are you the author of this Elsevier article?	Yes
Will you be translating?	No
Title of your thesis/dissertation	Distribution of arsenic in surficial deposits in the Cold Lake area of Alberta, Canada
Expected completion date	Dec 2014
Estimated size (number of pages)	200
Elsevier VAT number	GB 494 6272 12
Permissions price	0.00 CAD
VAT/Local Sales Tax	0.00 CAD / 0.00 GBP
Total	0.00 CAD

ORDER MORE... | CLOSE WINDOW

Analytica Chimica Acta 787 (2013) 102–110

Contents lists available at SciVerse ScienceDirect

Analytica Chimica Acta

journal homepage: www.elsevier.com/locate/aca

A modified sequential extraction method for arsenic fractionation in sediments

Muhammad Babar Javed, Gary Kachanoski[1], Tariq Siddique*

Department of Renewable Resources, University of Alberta, Edmonton, AB T6G 2E3, Canada

HIGHLIGHTS

- A sequential extraction method was developed to characterize As in sediment.
- The method can predict ~97% distribution of total As in 9 meaningful fractions.
- Extractants used are compatible with ICP-MS eliminating interference for As.
- This scheme can also be employed for fractionation of Cu, Co, Cr and Sr.

GRAPHICAL ABSTRACT

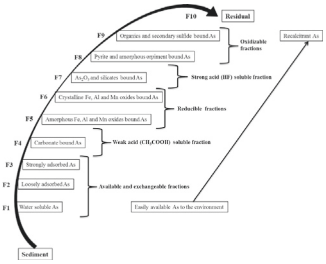

ARTICLE INFO

Article history:
Received 6 February 2013
Received in revised form 22 May 2013
Accepted 28 May 2013
Available online 4 June 2013

Keywords:
Sequential extraction
Arsenic fractionation
Inductively coupled plasma mass spectroscopy
Polyatomic ion interference

ABSTRACT

A modified sequential extraction method was developed to characterize arsenic (As) associated with different solid constituents in surficial deposits (sediments), which are unconsolidated glacial deposits overlying bedrock. Current sequential extraction methods produce a significant amount of unresolved As in the residual fraction, but our proposed scheme can fractionate >90% of the As present in sediments. Sediment samples containing different As concentrations (3–35 $\mu g\, g^{-1}$) were used to assess the developed method. The pooled amount of As recovered from all the fractions using the developed method was similar (83–122%) to the total As extracted by acid digestion. The concentrations of As in different fractions using the developed scheme were comparable (89–106%) to the As fractions obtained by other existing methods. The developed method was also evaluated for the sequential extraction of other metals such as copper (Cu), cobalt (Co), chromium (Cr) and strontium (Sr) in the sediment samples. The pooled concentrations of these four individual metals from all the fractions were similar (96–104%) to their total concentrations extracted by acid digestion. During method development, we used extractants that did not contain chloride to eliminate formation of polyatomic ions of argon chloride ($^{40}Ar^{35}Cl$) that interfered with ^{75}As when analyzed using inductively coupled plasma mass spectrometer (ICP-MS). The results suggest that the developed method can reliably be employed for complete As and other metals' fractionation in sediments using ICP-MS.

1. Introduction

Arsenic (As) is a toxic trace element and its crustal abundance is ~0.0001% [1]. However through geogenic processing of crustal materials, As can concentrate in soils up to 57–110 $\mu g\, g^{-1}$ causing high concentrations of As in pore or surface water through desorption or dissolution [2,3]. High As concentration (>10 $\mu g\, L^{-1}$) in groundwater is of increasing concern due to its implications in human and ecological health [4,5]. Arsenic mobility is principally controlled by adsorption–desorption and solid phase precipitation–dissolution reactions. Important geochemical factors affecting these reactions in soils and sediments are porewater chemistry, pH, redox conditions, soil solid composition and As-bearing minerals [6]. To predict the fate of As in soils

---

* Corresponding author. Tel.: +1 780 492 2899; fax: +1 780 492 1767.
E-mail address: tariq.siddique@ualberta.ca (T. Siddique).

[1] Present address: Memorial University of Newfoundland, St John's, NL A1C 5S7, Canada.

0003-2670/$ – see front matter © 2013 Elsevier B.V. All rights reserved.
http://dx.doi.org/10.1016/j.aca.2013.05.050

or sediments and its transport to ground or surface water, it is important to understand nature of As association with different solid constituents.

Distribution and chemical association of As with various solid constituents, rather than its total concentration, affect As mobility in sediment and its transport to water bodies. Sorption of As on solid particles is one of the most important processes that immobilizes As [6]. Arsenic can adsorb on the surfaces of a variety of materials, especially oxides of iron (Fe), aluminum (Al) and manganese (Mn) [7]. Coprecipitation of As with Fe oxyhydroxides has also been defined as the major mechanism that strongly retains As in sediments [8] but As-bearing Fe oxyhydroxides may act as a source of As during reductive dissolution of both amorphous and crystalline oxyhydroxides [6]. Arsenic associated with hydrous Mn oxides (easily reducible oxides) is relatively more labile than Fe oxyhydroxides [9]. Arsenic adsorption on the edges of clay minerals and on the surface of calcite has also been observed [8]. Other more stable forms of As are naturally occurring As-bearing sulfide ores and silicate minerals; but weathering of these sulfides and silicate minerals can release As into the environment and/or may cause formation of other thermodynamically metastable new secondary minerals [6].

Arsenic distribution in different solid constituents can be studied by sequential extraction procedure (SEP). Several SEP schemes have been developed by previous researchers to fractionate As in sediments [9–12]. These schemes vary in terms of number of fractions, extraction solutions and conditions and the sequence of extraction steps but the common feature is that the fractions are operationally defined. Different methods target different As phases in sediments and yield ∼40–50% of the total As in their final residual fractions. These unresolved residual fractions might contain As bound in silicates, pyrite and orpiment such as in Tessier, Hall and Wenzel methods [9,10,12] or As associated with organic and recalcitrant sulfides in Keon method [11]. Characterization of these residual fractions is important for comprehensive understanding of As fate in soils and sediments. Secondly, the common extractants used in the existing SEPs create interference during As determination if those extractants are analyzed by inductively coupled plasma mass spectrometry (ICP-MS). Chloride (Cl^-)-containing extractants produce polyatomic ions (argon chloride; $^{40}Ar^{35}Cl$) when Cl^- reacts with argon (Ar) in ICP plasma. These polyatomic ions can interfere with ^{75}As due to same mass to charge ratio (m/z) [13,14] even if the ICP-MS is equipped with a collision cell [15]. Therefore, we developed a sequential extraction scheme by modifying the existing methods to (1) quantify As in maximum possible meaningful fractions and (2) choose only those extractants that can be analyzed by ICP-MS without any polyatomic interference for As quantification. To check the applicability of the developed method, we compared it with the three existing sequential extraction methods described by Tessier et al. [9], Keon et al. [11] and Wenzel et al. [12] using sediment samples. We also used the new scheme to test the specificity of the extractants to target pure minerals such as calcite ($CaCO_3$), dolomite [$CaMg(CO_3)_2$], arsenopyrite (FeAsS) and orpiment (As_2S_3), which are dominant minerals in the sediments. In addition, the developed method was also evaluated for the fractionation of other metals such as copper (Cu), cobalt (Co), chromium (Cr) and strontium (Sr).

2. Experimental

2.1. Description of sediment samples used in sequential extraction protocol development

Sediment (surficial desposits) core samples used in the protocol development were obtained from Alberta Geological Survey (AGS) collected at 100–300 m depths from the Cold Lake region in Alberta, Canada, which is one of the As affected areas in northern Alberta. The air dried sediment samples were ground with agate mortar and pestle and passed through 2 mm sieve. The pH of the samples was determined by preparing a sediment slurry (sediment:0.05 M $CaCl_2$; 1:5) [16] and measuring pH using Accumet® AR20 pH meter. Total organic carbon content of the sediments was determined by the loss on ignition (LOI) method [17]. The information about the texture of the sediments was obtained from the report published by the Energy Resource Conservation Board-Alberta Geological Survey (ERCB-AGS) [18]. To determine the reduced inorganic sulfur, chromium reduction method [19] was employed that was based on the conversion of reduced inorganic sulfur to H_2S by a hot acidic $CrCl_2$ solution. The evolved H_2S was trapped in a zinc acetate solution as ZnS. This ZnS was quantified by iodometric titration. The reduced inorganic sulfur compounds determined by this method were: (1) pyrite and other metal sulfides, (2) elemental sulfur, and (3) acid volatile sulfides. The sediments were also subjected to total metal analysis particularly for Fe, calcium (Ca) and As. The samples were digested with nitric acid (trace metal grade HNO_3) in the microwave digestion unit [20] and analyzed using ICP-MS.

The total As concentrations in the core sediments ranged from 3 to 200 $\mu g\, g^{-1}$. Five samples with low As concentration (3.49–6.07 $\mu g\, g^{-1}$) and three samples with high As concentration (19.99–35.4 $\mu g\, g^{-1}$) were selected for the development of sequential extraction method. Physicochemical properties of the sediment samples used in this study are provided in Table 1.

2.2. Chemicals and minerals

To prepare the extraction solutions for As fractionation, trace metal grade hydrofluoric acid (HF), nitric acid (HNO_3), sodium acetate (CH_3COONa; abbreviated as NaOAc), sodium phosphate (NaH_2PO_4), ammonium oxalate [$(NH_4)_2C_2O_4\cdot H_2O$], oxalic acid ($H_2C_2O_4$), titanium (Ti), sodium citrate ($Na_3C_6H_5O_7\cdot 2H_2O$), sodium bicarbonate ($NaHCO_3$), acetic acid (CH_3COOH; abbreviated as HOAc) and EDTA ($C_{10}H_{14}N_2Na_2O_2\cdot 2H_2O$) were purchased from Sigma–Aldrich. The extraction solutions were prepared using nanopure water (Barnstead nanopure, Thermo Scientific). The pH of the extractants, if required, was adjusted with either sodium hydroxide (NaOH) or appropriate acid (CH_3COOH, $H_2C_2O_4$, or HNO_3) to bring the pH to the desired values listed in Table 2. The reagent blanks from all the extraction solutions were also analyzed along with the experimental samples. To test the specificity of the extractants, pure minerals of calcite and dolomite were purchased from the Ward's scientific, and orpiment and arsenopyrite were collected from the Mineralogy Petrology Museum from the Department of Earth and Atmospheric Sciences, University of Alberta, Canada.

2.3. Development and use of sequential extraction protocol

A modified sequential extraction scheme was developed by combining the fractions reported in the existing methods [9,11,21]. We substituted Cl^--containing extractants by those solvents that eliminated formation of polyatomic ions ($^{40}Ar^{35}Cl$) and yielded same extraction efficiency in targeting As in different solid phase constituents. Table 2 summarizes the fractions, target solid phases, extractants, possible mechanisms to liberate the As and the source references for the extractants used in this proposed modified sequential extraction method.

In the sequential extraction, the sediment samples were treated with different extraction solutions in a sequence to collect the individual fraction from each extractant for As analysis. For the extraction of soluble fraction of As (F1), 0.4 g sediment was added to a 50-mL Nalgene (3118-0050, Fisher Scientific) centrifuge tube along with 40 mL of nanopure water. The sediment-extractant

Table 1
Selected physico-chemical properties of the sediment samples used in this study.

Sample	S1	S2	S3	S4	S5	S6	S7	S8
As ($\mu g\, g^{-1}$)	4.91 ± 0.74	5.37 ± 0.52	4.15 ± 0.13	6.13 ± 0.59	3.59 ± 0.83	35.46 ± 5.81	20.01 ± 4.18	24.4 ± 6.21
Fe (%)	2.44 ± 0.38	1.46 ± 0.20	1.92 ± 0.48	2.84 ± 0.81	2.20 ± 0.27	2.99 ± 0.53	4.04 ± 0.51	2.94 ± 0.36
Ca (%)	1.87 ± 0.45	0.05 ± 0.03	0.28 ± 0.24	1.08 ± 0.15	0.86 ± 0.39	0.85 ± 0.21	0.85 ± 0.42	0.41 ± 0.12
Sulfide (%)	0.12 ± 0.06	0.11 ± 0.03	0.09 ± 0.03	0.33 ± 0.27	0.66 ± 0.15	1.37 ± 0.30	1.11 ± 0.06	1.79 ± 0.39
Texture[a]	Sandy clay	Till	Oxidized till	Silty clay	Silty clay	Shale	Clayey till	Clayey till
Sand (%)	–[b]	40	29	5	4	–	30	33
Silt (%)	–	42	46	75	77	–	43	45
Clay (%)	–	18	25	20	19	–	27	22
pH[c]	7.02	4.67	7.15	7.2	7.33	7.07	6.15	6.75
TOC (%)	0.28	0.11	ND	0.64	0.6	ND	0.75	0.57

Values represent the mean from analysis of triplicate ± 1 standard deviation. TOC: total organic carbon; ND: not detected.

[a] Information about texture was obtained from a report ESR 2002-03 [18].

[b] Texture analysis was not performed.

[c] pH was measured in suspension of sediment:0.05 M $CaCl_2$ (1:5).

suspension was shaken for 30 min and then centrifuged to separate the supernatant. After that 1 M NaOAc (pH 8.2, adjusted with NaOH) was added and shaken for 2 h for the extraction of loosely adsorbed As (fraction F2). For strongly adsorbed As fraction (F3), 1 M NaH_2PO_4 (pH 5, adjusted with NaOH) was used and sediment suspension was shaken for 16 h, centrifuges to separate supernatant. After that the same solid phase was subjected to second extraction for 24 h. Both the supernatants were pooled for As analysis. For the extraction of As bound to carbonate minerals (fraction F4), the sediment recovered from F3 was extracted with 1 M NaOAc (pH 5, adjusted with HOAc) for 5 h and supernatant was separated after centrifugation. The As coprecipitated with amorphous Fe, Al and Mn oxyhydroxides (fraction F5) was extracted with Tamm's reagent (0.2 M ammonium oxalate at pH 3 adjusted with oxalic acid) in the dark (tubes were wrapped with aluminum foil) for 2 h. Extractant 0.05 M Ti–citrate–EDTA–bicarbonate (pH 7, adjusted with NaOH) was used for the removal of As coprecipitated with crystalline Fe, Al and Mn oxyhydroxides (fraction F6). The suspension was shaken for 2 h and repeated twice to completely extract the As from crystalline oxides. The As associated with As oxides and silicate clays (fraction F7) was extracted using 10 M HF for 1 and 24 h (5 g boric acid (H_3BO_3) was added at 16th h of 24 h extraction). By adding H_3BO_3, HF reacts with boron (B) to produce fluoroboric acid (HBF_4), which is equivalent to HNO_3 in strength and keep the liberated As in soluble form [22]. For the extraction of pyrite and amorphous orpiment coprecipitated As (fraction F8), 16 N HNO_3 was used for 2 h extraction and the process was repeated twice. To determine the organic matter- and secondary sulfide-bound As (fraction F9), the recovered sediment from previous step was extracted with 30% H_2O_2 + 1 M NH_4OAc (1:2) (pH 2, adjusted with HNO_3) for 16 h. Finally, the remaining sediment sample was digested with concentrated HNO_3 in a microwave assisted digestion unit to find the residual fraction of As.

In all the extraction steps, the sediment to extractant ratio (SER) of 1:100 as reported by Keon et al. [11] was used to ensure complete reactivity of extractant with the solid phase. A minimum SER of 1:25 was recommended by Gleyzes et al. [23] in the extraction process. The sediment–extractant suspensions were shaken for the specified duration, and then centrifuged (Sorvall® RC-5B Refrigerated Superspeed Centrifuge with Sorvall® HS-4 rotor) for 40 min at 6000 × g to separate the supernatant. The supernatant was decanted without removing any sediment particles and filtered through 0.45-μm PTFE filters (033911C, Fisher Scientific). The sediment sample was washed with nanopure water for 30 min after completion of each extraction and before the addition of the next extractant to the sediment sample. The washing solution after centrifugation was pooled with the decanted solution of the preceding fraction. The decanted extractants were acidified (at 1% final concentration of HNO_3) to prevent any precipitation before ICP-MS analysis. In addition to As, the developed extraction method was also evaluated for the sequential extraction of Cu, Co, Cr and Sr from all the eight sediment samples.

Table 2
Modified sequential extraction procedure for As fractionation.

Fraction	Target phase	Extractant[a]	Possible mechanism	Source Ref.
F1	Soluble As	D.I. water	dissolution with water	[b]
F2	Loosely adsorbed As	1 M NaOAc, pH 8.2	anion exchange of acetate for As	[c]
F3	Strongly adsorbed As	1 M NaH_2PO_4, pH 5	anion exchange of $PO_4{}^{3-}$ for $AsO_4{}^{3-}$ and $AsO_3{}^{3-}$	[d]
F4	Carbonate bound As	1 M NaOAc, pH 5	dissolution of carbonate minerals to liberate As	[c]
F5	As co-precipitated with amorphous Fe, Al and Mn oxyhydroxide	Tamm's reagent (ammonium oxalate/oxalic acid, pH 3)	ligand promoted complexation and dissolution of Fe, Al and Mn oxyhydroxide	[d]
F6	As co-precipitated with crystalline Fe, Al and Mn oxyhydroxide	Ti-citrate-EDTA-bicarbonate, pH 7	Ti induced reduction of Fe^{3+} to Fe^{2+}	[d]
F7	As associated with As oxides and silicate clays	10 M HF	dissolution of silicate clays and As oxides	[d]
F8	As coprecipitated with pyrite and amorphous orpiment	16 N HNO_3	oxidation of pyrite and amorphous sulfides	[d]
F9	organic matter and secondary sulfides	30% H_2O_2 + 1 M NH_4OAc (1:2), pH 2	Oxidation of organic matter and secondary sulfides bound As	[b]
F10	Residual As	concentrated HNO_3	microwave assisted digestion	[e]

[a] Extractants were added to sediments in sequential order (F1–10) and the supernatant was removed after extraction and centrifugation. Sediments were washed with nano pure water by extraction for 30 min after removing each extractant. The water was separated by centrifugation and pooled with the decanted supernatant of the each preceding extractant.

[b] Kreidie et al. [21].

[c] Tessier et al. [9].

[d] Keon et al. [11].

[e] US EPA [20].

2.4. ICP-MS analysis

The aliquot from each fraction was analyzed for As, Cu, Co, Cr and Sr determination using ICP-MS (Perkin-Elmer ELAN 9000). For the quantification of these elements, calibration curves were developed using multi-elemental external standards (CLMS-2N, SPEX Certi Prep) in the range from 0.2 to 500 μg L^{-1} in 1% HNO_3 that represented the matrix of extraction solutions. Scandium (Sc), yttrium (Y) and terbium (Tb) were used as internal standards to account for any instrumental drift over time. The limit of detection (LOD) of ICP-MS for As was 0.05 μg L^{-1}.

2.5. Method verification and reproducibility

To compare the efficiency of the developed method to the existing source methods for the determination of As associated with different fractions of sediments, one sediment sample (S6; Table 1) was subjected to extraction using our proposed developed scheme as well as the existing source methods [9,11,12]. From now onward, we will be calling those methods by their first author names. This sample was chosen for the comparison because it was the only sample that contained As in all the fractions. Some extractants used in the source methods were replaced with their own alternatives mentioned in those methods to make the extractants compatible with ICP-MS. For Tessier method, [8] we used sodium acetate (NaOAc) and citrate-dithionite ($C_6H_5O_7{}^{3-}$-$S_2O_4{}^{2-}$) solutions instead of $MgCl_2$ and hydroxylamine hydrochloric acid ($NH_2OH{\cdot}HCl$), respectively. This replacement of extractants was done to avoid the interference of ArCl with As using ICP-MS. The Keon [11] and Wenzel [12] extraction methods were carried out exactly according to their original work. The supernatant solutions derived from this comparative study were analyzed using ICP-MS.

To facilitate the comparison of different extraction steps among four sequential extraction methods, the extraction steps in the developed method were categorized into eight groups: G1, loosely adsorbed As (sum of fractions 1 and 2); G2, strongly adsorbed As; G3, arsenic bound to carbonates; G4, arsenic coprecipitated with Fe, Al and Mn oxyhydroxide (sum of fractions 5 and 6); G5, arsenic in As oxides (As_2O_3) and silicate clays; G6, arsenic coprecipitated with pyrite (FeS_2) and amorphous orpiment (As_2S_3); G7, arsenic bound to organic matter and secondary sulfides; and G8, residual As.

We also tested the specificity of the extractants used in our developed scheme to dissolve four pure minerals such as calcite, dolomite, orpiment and arsenopyrite. The dissolution of calcite and dolomite was assessed using 1 M NaOAc (pH 5) in fraction F4 and orpiment and arsenopyrite using 16 N HNO_3 in fraction F8. After the extraction, the resulting solutions were subjected to ICP-MS analysis to determine elemental composition, and the solid phase was examined using scanning electron microscope equipped with energy dispersive X-ray spectrometer (SEM-EDX) and X-ray diffractometer (XRD). We oven dried the solid phase of pure minerals after F3 and F7 and of S6 sample after F3, F4, F7 and F8 at 105 °C. For SEM-EDX analysis, samples were mounted on a double sided carbon tape attached on the aluminum stub and then coated with carbon to prevent charging on sample surface. Zeiss EVO MA 15 SEM with LaB6 crystal source was used to get highly magnified (20–100,000×) micromorphology images at ~5 nm resolution. SEM was also equipped with a Bruker silicon drift detector for EDX analysis with a peak resolution of ~125 eV. For XRD, oven dried solid phase were directly mounted on zero-background plates and analyzed via Rigaku Geigerflex powder diffractometer equipped with a cobalt X-ray source, graphite monochromator and scintillator detector. Samples were scanned using X-ray (Co Kα) from 5 to 80 2θ in continuous mode. Rest of the sequential extraction steps for amorphous and crystalline oxides of Fe and Mn were already verified and used in the previous method [11]. To analyze the difference among means while comparing different methods, *t*-test at 95% confidence interval was performed. SAS 9.3 was used for statistical comparisons and Pearson correlation analyses.

3. Results and discussion

3.1. Arsenic fractionation

To evaluate the performance of the developed sequential extraction method for As fractionation in sediment samples, eight samples (S1–S8) of different textures (till to silty clay) and As concentrations (3.5–35 μg g^{-1}) were used in this study (Table 1).

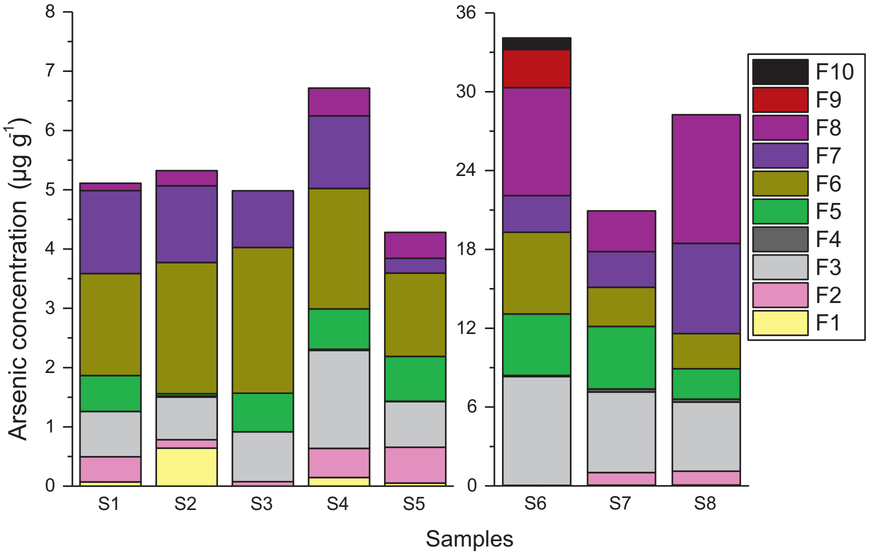

Fig. 1. Application of the developed sequential extraction method for As fractionation in sediments. F1, water soluble As; F2, ionically bound As; F3, strongly adsorbed As; F4; arsenic bound to carbonates; F5, arsenic coprecipitated with amorphous Fe, Al and Mn oxyhydroxides; F6, arsenic coprecipitated with crystalline Fe, Al and Mn oxyhydroxides; F7, arsenic associated with As oxides and silicate clays; F8, arsenic coprecipitated with pyrite and amorphous orpiment; F9, arsenic associated with organic matter and recalcitrant sulfides; F10, residual As. Sum of As fractions extracted by the developed method varied from 83 to 122% of the total As extracted by the acid digestion in the sediments used in this study.

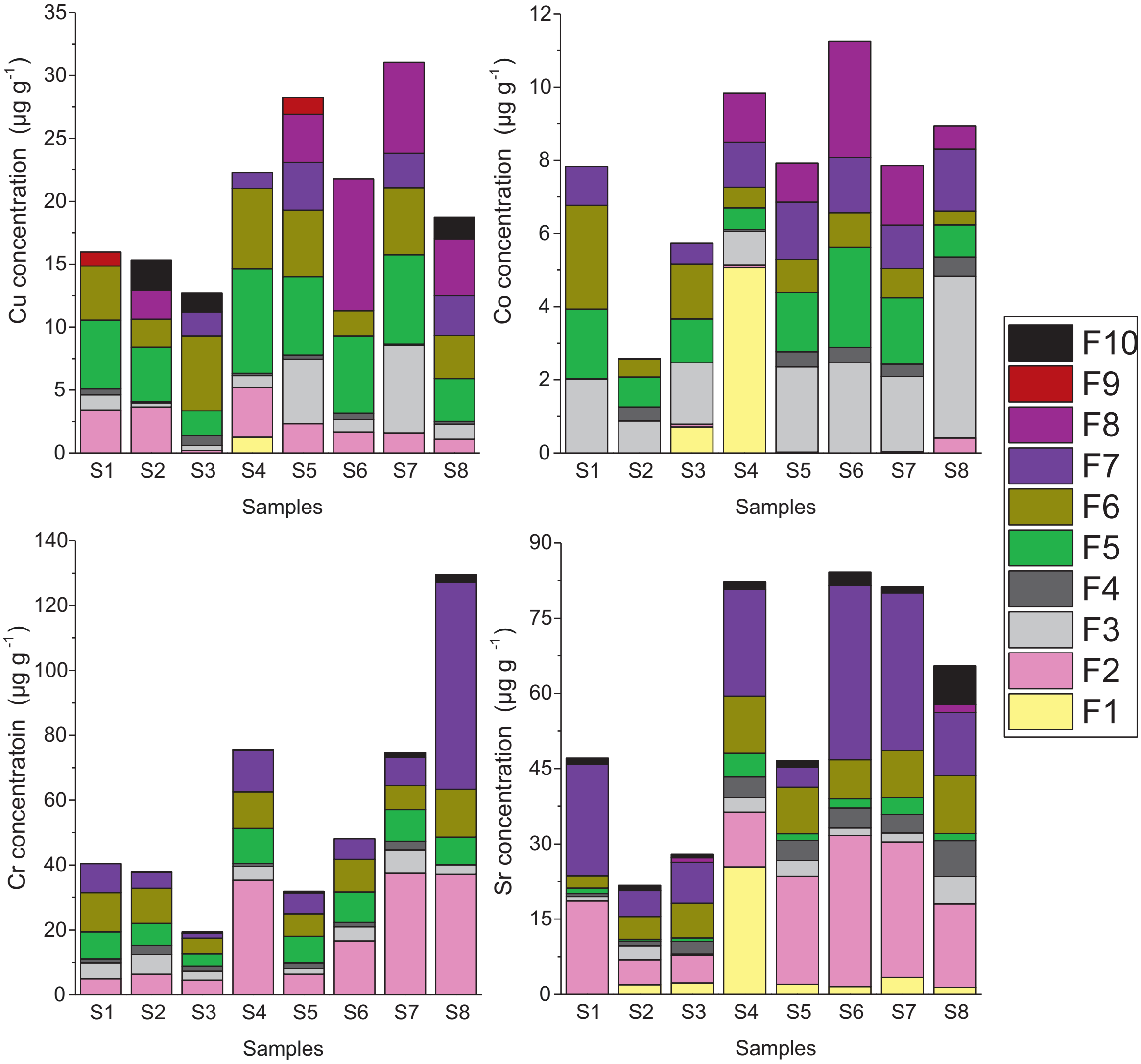

Fig. 2. Fractionation of Cu, Co, Cr and Sr by the developed method. F1, water soluble metals; F2, ionically bound metals; F3, strongly adsorbed metals; F4; metals bound to carbonates; F5, metals coprecipitated with amorphous Fe, Al and Mn oxyhydroxides; F6, metals coprecipitated with crystalline Fe, Al and Mn oxyhydroxides; F7, metals associated with metal oxides and silicate clays; F8, metals coprecipitated with pyrite and amorphous orpiment; F9, metals associated with organic matter and recalcitrant sulfides; F10, residual metals. Sum of all the sequential extraction fractions of all four elements in sediments varied from 96 to 104% as compared to the total elemental concentrations determined by the acid digestion.

Arsenic fractionation (Fig. 1) revealed that soluble fraction (F1) of As was very low (~2% of the total As) in fine-textured sediment whereas ~12% of the total As was extracted in the soluble fraction from coarse sediment (S2). This finding was in agreement with the observation of Lombi et al. [24] who found that sand- and silt-sized particles released typically equal or larger amounts of As in soluble fraction than the clay-sized particles. Also, the pH of the sample (S2) was low (pH 4.67) which suggested the probable dominance of the soluble $H_2AsO_4^-$ and H_3AsO_3 forms of As at low pH as compared to other sparingly soluble forms of As ($HAsO_4^{2-}$, AsO_4^{3-}, $H_2AsO_3^-$ and $HAsO_3^{2-}$) [6].

In ionically bound fraction (F2) where As is usually loosely adsorbed on the solid particles through outer-sphere complexes, relatively higher concentrations of As (7–14% of the total As) in samples S1, S4 and S5 are probably due to medium to fine textures. Third fraction (F3) represents strongly adsorbed (inner-sphere complexation) As in sediments. The amount of As in the analyzed samples varied from 13 to 29% of the total As in F3 fraction. Keon [11] also found this fraction dominant (~50% of the total As) in samples having diverse chemical characteristics. After the first three fractions (F1–F3), it was assumed that the entire surface adsorbed As from all solid constituents (oxides of Fe, Al and Mn, carbonates, sulfides and silicates clays) was removed and only mineral coprecipitated As remained in the sediments. A little amount of carbonate bound As (~1% of the total As) was extracted in fraction F4 because we did not find appreciable amount of carbonates in the sediments. The results of fraction F5 showed clear relationship between As coprecipitated with amorphous Fe, Al and Mn oxyhydroxides and Fe content in the sediments. The least amount of As (<1% of the total As) was extracted from sediment S2 where total Fe concentration (1.36%) was minimum. Maximum As (22% of the total As) was extracted from sediment S7 that contained maximum total Fe (Table 1).

Arsenic coprecipitated with crystalline Fe, Al and Mn oxyhydroxides (F6) was the most dominant As pool (30–49% of the total As) in all the low-As sediments (S1–S5). Arsenic in F6 fraction ranged between 9 and 18% of the total As in high-As sediments containing higher sulfide minerals (Fig. 1 and Table 1). A wide range of As (6–27% of the total As) associated with As oxides and silicate clays (fraction F7) was found in the sediments. In fraction F8, As coprecipitated with pyrite and amorphous orpiment significantly correlated ($r = 0.93$, $P < 0.05$) with sulfide minerals in the sediments. Maximum As (34% of the total As) was observed in sediment S8 that

Table 3
Total concentrations of Cu, Co, Cr and Sr in all the sediment samples. Values represent the mean from analysis of triplicate ± 1 standard deviation.

Sample	Cu ($\mu g\,g^{-1}$)	Co ($\mu g\,g^{-1}$)	Cr ($\mu g\,g^{-1}$)	Sr ($\mu g\,g^{-1}$)
S1	15.64 ± 0.83	8.14 ± 0.31	41.98 ± 2.72	45.97 ± 1.63
S2	14.98 ± 0.39	2.64 ± 0.14	38.63 ± 1.75	20.98 ± 1.04
S3	13.10 ± 0.08	5.91 ± 0.37	20.10 ± 0.72	28.95 ± 0.84
S4	23.06 ± 0.74	9.91 ± 0.13	74.69 ± 4.93	79.03 ± 2.05
S5	26.99 ± 0.28	7.68 ± 0.29	32.85 ± 1.83	44.98 ± 1.37
S6	22.32 ± 5.06	11.56 ± 0.42	46.80 ± 0.96	81.05 ± 3.18
S7	32.16 ± 1.05	7.53 ± 0.09	71.75 ± 2.92	79.83 ± 2.42
S8	17.94 ± 0.74	9.08 ± 0.15	127.39 ± 6.53	63.97 ± 1.85

contained highest sulfide content (1.8%). Organic matter and secondary sulfide bound As (fraction F9) was low in all the sediments due to low (<1%) total organic carbon, except in sediment S6 where 9% of total As was extracted in F9 probably due to shale, which was a rich source of sulfide. Finally, the residual fraction (F10) contained less than 1% of the total As in all the sediments except S6 that contained ~3% As in F10 fraction.

The pooled amount of As recovered from all the fractions using the developed method matched (~83–122%) the total As in sediments extracted by acid digestion. These results are in conformity with As recoveries of 80–120% [25] and 72–111% [26] when sum of As from all the fractions was compared to total As concentrations. Percent distribution of As among different fractions in the sediments using the developed method (Fig. 1) was also supported by the physicochemical properties of the sediments reported in Table 1.

3.2. Applicability of the developed method to other metals' fractionation

The developed method was also evaluated for the fractionation of Cu, Cr, Co and Sr (Fig. 2). In the sequential extraction of Cu, amorphous and crystalline Fe, Al and Mn oxyhydroxides bound Cu (F5 and F6) were the dominant fractions in most of the sediments (Fig. 2). Pyrite and amorphous orpiment bound Cu fraction (F8) was also dominant in S5–S8 where higher concentration of sulfides were determined (Table 1). Similar results about Cu distribution were reported by Tessier [9] who found dominant fraction of Cu associated with sulfides, and Fe and Al oxides. For the sequential extraction of Co, ~50% of total Co was released in soluble fraction (F1) from sediment S4, while strongly adsorbed fraction (F3) of Co was dominant (21–49% of the total Co) in rest of the samples. Amorphous Fe, Al and Mn oxides bound (F5) Co (6–31% of total Co) was also found in all the samples whereas pyrite bound (F8) Co (7–20% of total Co) was only observed in sediments S4–S8 that contained higher sulfides. The results are in accordance with the findings of Tessier [9] who found that maximum Co was bound to Fe oxides. Chromium (Cr) and Strontium (Sr) were dominantly present in the available forms (F1 and F2) and with silicates (F7). Overall, sum of all the fractions of sequential extraction for Cu, Co, Cr and Sr (Fig. 2) showed 96–104% recoveries compared to the total concentrations of Cu, Co, Cr and Sr in sediments obtained by acid digestion (Table 3), which suggested the applicability of the proposed extraction method for the fractionation of these metals.

3.3. Comparison of the developed method to the existing fractionation methods

To compare the developed method to other extraction methods described by Tessier et al. [9], Keon et al. [11] and Wenzel et al. [12], one sediment sample (S6) was sequentially extracted with all the methods (Fig. 3 and Supplemental Table S1). A few previous sequential extraction methods [8,21] separated soluble As as first fraction, but most commonly used sequential extraction schemes [9,11,12] skipped this first step and defined their first fractions as loosely adsorbed or exchangeable As fraction. Therefore for comparing our developed method to the other methods, we pooled the data of our first two fractions (water soluble and ionically adsorbed) and defined this pooled fraction as G1 (Fig. 3). The concentration of As in G1 ($0.033 \pm 0.009\,\mu g\,g^{-1}$) of our developed method was similar to the As extracted in the first fractions obtained using Tessier [9] ($0.037 \pm 0.011\,\mu g\,g^{-1}$) and Wenzel [12] ($0.031 \pm 0.007\,\mu g\,g^{-1}$) methods (Supplemental Table S1). Therefore, the application of the proposed method is advantageous because it differentiates between the immediately available As fraction (soluble As) and a fraction potentially available as a result of desorption processes (loosely adsorbed As on mineral surfaces). In our scheme, we used 1 M NaOAc (pH 8.2) for loosely adsorbed fraction of As similar to the Tessier [9] method but in Wenzel method [12], 0.05 M $(NH_4)_2SO_4$ was used, which showed almost the same extraction efficiency (90% of the developed method).

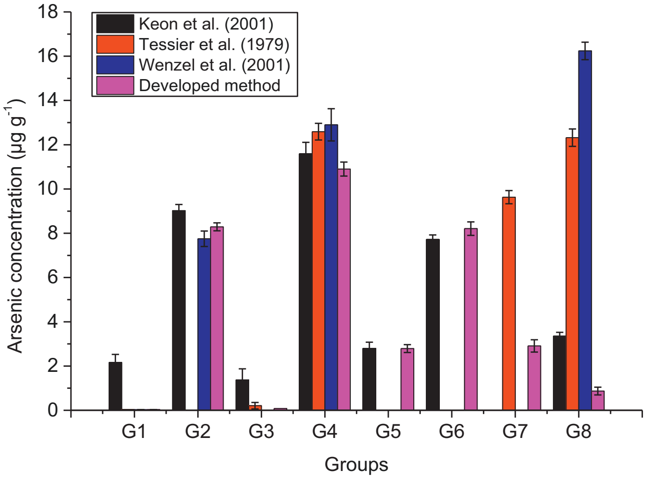

Fig. 3. Comparison of the developed sequential extraction method to the existing Keon et al. [11], Tesseir et al. [9] and Wenzel et al. [12] methods for As fractionation in sediment S6. To facilitate the comparison of different extraction steps among four sequential extraction methods, the extraction steps were presented in eight groups: G1, loosely adsorbed As; G2, strongly adsorbed As; G3, arsenic bound to carbonates; G4, arsenic coprecipitated with Fe, Al and Mn oxyhydroxides; G5, arsenic associated with As oxides and silicate clays; G6, arsenic coprecipitated with pyrite and amorphous orpiment; G7, arsenic associated with organic matter and recalcitrant sulfides; G8, residual As. For detailed comparison of the sequential extraction methods, see Supplemental Table S1.

For the extraction of strongly adsorbed As fraction (G2, Fig. 3), we used 1 M NaH_2PO_4 extraction solution (used in the Keon method) while 0.05 M $(NH_4)H_2PO_4$ was used in the Wenzel method. Strongly adsorbed As extracted using the developed ($8.29 \pm 0.82\,\mu g\,g^{-1}$) and Keon ($9.02 \pm 0.97\,\mu g\,g^{-1}$) methods were similar ($P > 0.05$) due to the same extractant and extraction conditions. Wenzel method extracted slightly less As in this fraction due to weak extractant (0.05 M versus 1 M) and less extraction time (16 h versus 40 h). Tessier method [9] did not describe extraction of strongly adsorbed As fraction.

For the determination of carbonate bound As fraction (G3, Fig. 3 and Supplemental Table S1), we used 1 M NaOAc (pH 5) for carbonate dissolution according to the Tessier method with the only modification of using SER of 1:100 to ensure the extractant availability to target all the carbonate minerals. Wenzel method did not describe carbonate bound As fraction. Keon method used HCl but that extractant overestimated the carbonate bound As due to Cl^- contribution to polyatomic ion interference (Fig. 3). Further, specificity of HCl for carbonate minerals is not very appropriate because it also dissolves some sulfides and overestimates

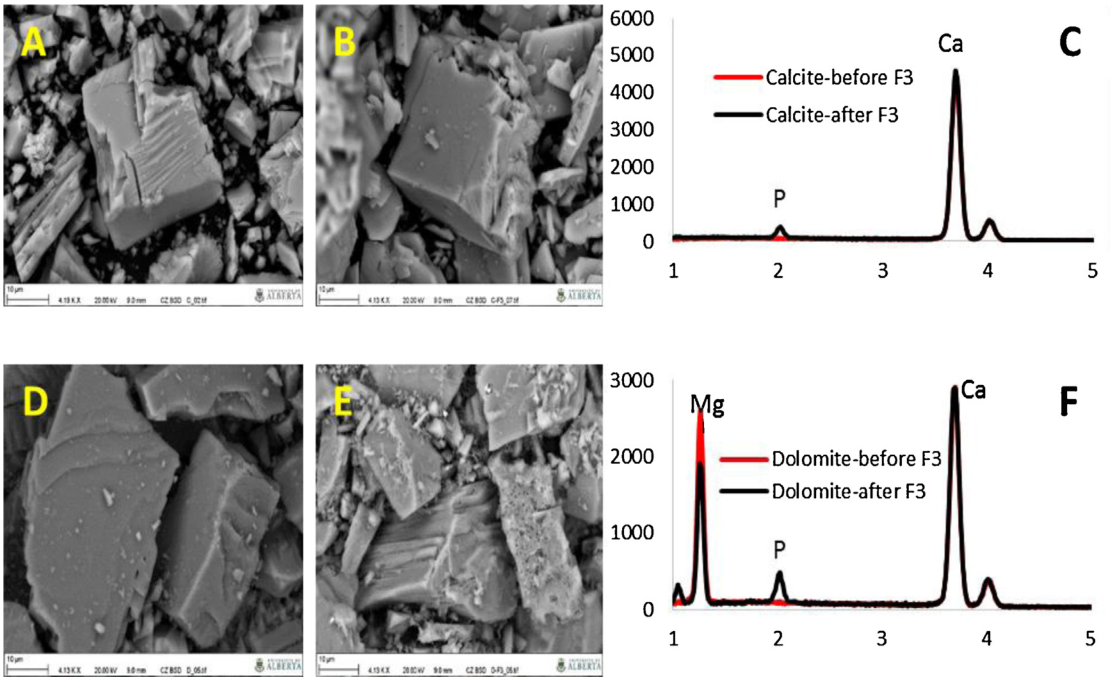

Fig. 4. SEM-EDX analysis of calcite (A–C) and dolomite (D–F) minerals. (A) and (B) are SEM images of calcite mineral before and after 1 M NaH_2PO_4 (pH 5) extraction, respectively, along with EDX spectrum (C) where Ca peaks are superimposed which show no evidence of calcite dissolution in F3. (D) and (E) are SEM images of dolomite mineral before and after 1 M NaH_2PO_4 (pH 5) extraction, respectively, along with EDX spectrum (F). These images show sign of NaH_2PO_4 attack on dolomite mineral as Mg peak decreases after F3.

carbonate bound fraction of As [11]. Using the developed and Tessier methods, we extracted <1% carbonate bound As (of the total As) because carbonates in the sediments were ~1% (LOD ~ 0.1%). Extraction of As specifically bound to carbonates is also expected to occur in F3 fraction (strongly adsorbed As extracted by 1 M NaH_2PO_4) by competitive desorption with phosphate anions [6,7].

To extract As coprecipitated with amorphous and crystalline oxyhydroxides of Fe, Al and Mn, $NH_2OH{\cdot}HCl$ with reducing properties is one of the most frequently used extraction solutions. The amount of As released by this reagent depends primarily on reaction temperature and acid concentration in $NH_2OH{\cdot}HCl$ solution that helps to release As in the solution [23]. Tessier method used this reagent but Cl^- can interfere with As if samples are analyzed using ICP-MS. Mihaljevič et al. [27] also showed that the recovery of As was five times higher from the extraction of synthetic minerals by using $NH_2OH{\cdot}HCl$ than the expected As concentrations due to the dissolution of non-targeted minerals. Therefore for comparing G4 fraction, a solution (commonly known as citrate-dithionite) containing 0.03 M sodium dithionite ($Na_2S_2O_4$), 0.175 M sodium citrate and 0.025 M citric acid ($C_6H_8O_7$) was used for Tessier method replacing $NH_2OH{\cdot}HCl$ for the extraction of (amorphous and crystalline) oxyhydroxides of Fe, Al and Mn bound As in a single fraction. Both extraction solutions have been suggested in Tessier method. Additionally, Poulton and Canfield [28] compared the efficiency of $NH_2OH{\cdot}HCl$ and citrate-dithionite for selective dissolution of iron oxyhydroxides and demonstrated that the citrate-dithionite extraction provided the most complete dissolution of iron minerals (ferrihydrite, lepidocrocite, goethite, and hematite), whereas $NH_2OH{\cdot}HCl$ dissolved only (ferrihydrite, lepidocrocite). For Wenzel method, ammonium oxalate buffer was used for amorphous (fraction F5), and ammonium oxalate buffer and ascorbic acid ($C_6H_8O_6$) were used for crystalline oxyhydroxides of Fe, Al and Mn (fraction F6). We used Tamm's reagent (ammonium oxalate/oxalic acid buffer) and Ti–citrate–EDTA–bicarbonate in our developed method according to the Keon method for the extraction of amorphous (fraction F5) and crystalline (fraction F6) Fe oxyhydroxides coprecipitated As, respectively. Fractions F5 and F6 were combined into fraction G4 for comparison. In the Tamm's reagent, ammonium (NH_4^+) induces processes of protonation and oxalate causes complexation and reduction. In Ti–citrate–EDTA–bicarbonate, Ti causes reduction; citrate and EDTA are used for complexation; and bicarbonate maintains the pH around 7. In fraction G4, we found similar As extracted (10.89 ± 1.26–$12.76 \pm 1.57\ \mu g\ g^{-1}$; $P > 0.05$) using all the four methods (Fig. 3), which also supported the accuracy of our developed method till this fraction. Arsenic co-precipitated with amorphous and crystalline iron oxyhydroxides (fractions F5 and F6, respectively, Supplemental Table S1) was dominant in sediments extracted with either of the methods used in this study. But in Tessier method, co-precipitated As was extracted from both amorphous and crystalline oxyhydroxides as a single fraction unable to differentiate between amorphous or crystalline Fe bound As. In the developed method, presence of higher amount of crystalline oxyhydroxides bound As (18% of the total As) signifies importance of separating crystalline oxyhydroxides bound As as a single fraction. Müller et al. [29] reported a significant contribution of the crystalline Fe oxides to retain As (>45%) in river sediments. Similar observation was reported by Larios et al. [8] where >20% of As was associated with crystalline Fe oxides in an industrially polluted damping site. Because these minerals (Fe, Al and Mn oxides) are regarded as important As scavengers in soils and sediments, sequential extraction of As from amorphous and crystalline Fe oxides is suggested [30].

Though Fe oxyhydroxides appear to dominate in As sorption process in soils, other constituents such as silicate clay minerals (kaolinite and montmorillonite) are also capable of retaining or complexing As species [31]. The type and quantity of silicate minerals present in soils or sediments also influence the retention of As. The degree of As sorption onto silicate minerals decreases in the order of kaolinite > vermiculite > montmorillonite [31,32]. Besides silicates bound As, arsenic oxides are also one of the major secondary As minerals formed by oxidation of arsenopyrite and native arsenic [33]. For the extraction of As associated with As

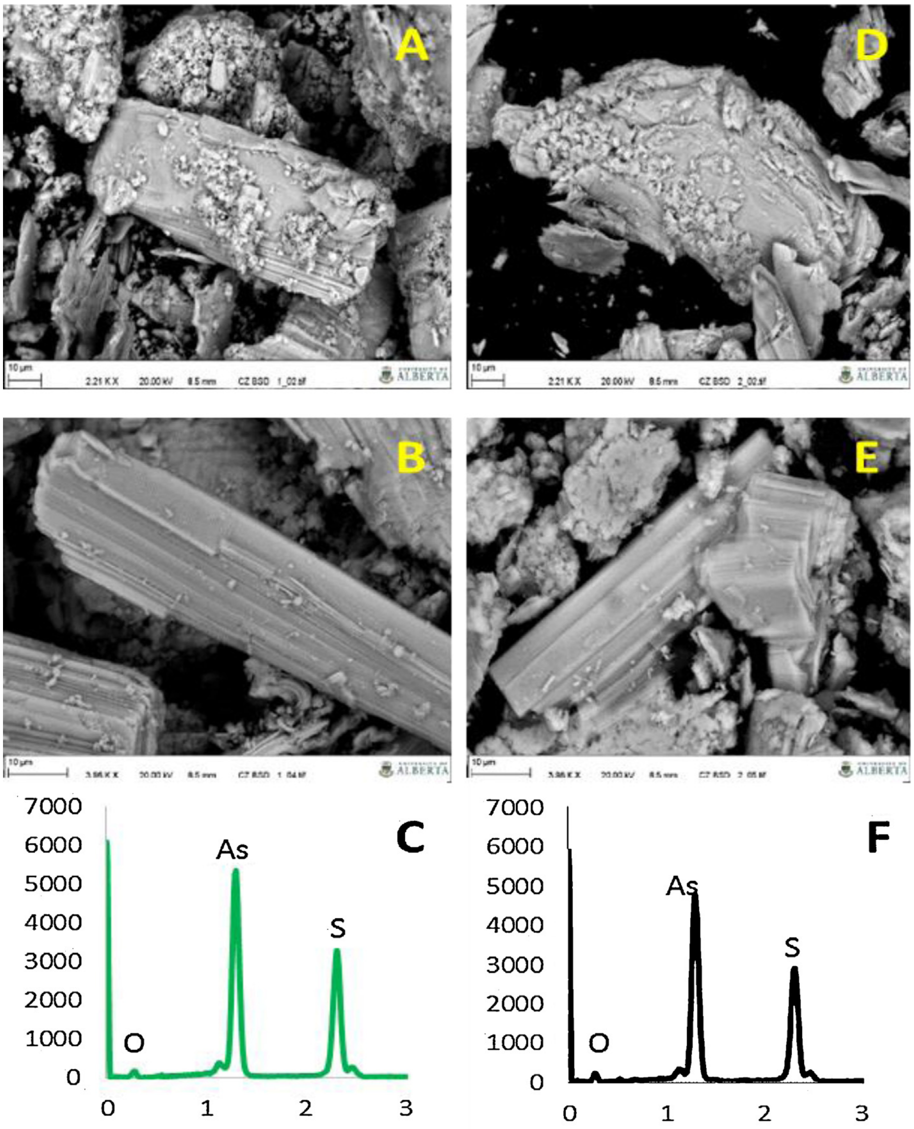

Fig. 5. SEM-EDX analysis of orpiment mineral. In orpiment, two types of mineral phases were observed. SEM images (A) and (B) reveal two different phases in orpiment minerals along with EDX spectrum (C) before any extraction with 10 M HF. (D) and (E) are corresponding SEM images of those two phases (A) and (B), respectively after HF extraction. (F) shows EDX of 10 M HF extracted orpiment mineral. Both the phases were found after 10 M HF extraction, which showed the stability of orpiment in 10 M HF. After F8, all the solid phase was dissolved and there was not enough material for SEM analysis.

oxides and silicate clays (G5, Fig. 3) in the developed method, 10 M HF was adopted as an extraction solution from the Keon method. HF has the ability to dissolve silicate minerals but it does not react with pyrite [34]. Thus, it is appropriate to have 10 M HF extraction step before the extraction of pyrite and amorphous sulfide bound As. Arsenic extracted in this fraction by the developed ($2.79 \pm 0.07\ \mu g\ g^{-1}$) and Keon method ($2.8 \pm 0.11\ \mu g\ g^{-1}$) was in agreement. This fraction was not described in the Tessier and Wenzel methods (Supplemental Table S1).

Sulfide minerals are very insoluble and most of the methods [8–10] relegate sulfide bound As to the residual fraction. But biogeochemical redox processes can release sulfide bound As [35]. Therefore, As coprecipitated with pyrite and amorphous orpiment (fraction G6) was also extracted using 16 N HNO_3 according to Keon method. The results (Fig. 3) reported similar As concentrations in G6 using both the developed ($8.21 \pm 0.47\ \mu g\ g^{-1}$) and Keon ($7.72 \pm 0.29\ \mu g\ g^{-1}$) methods due to similar extraction conditions. Other methods did not describe this fraction. HNO_3 has the ability to react with uncoated or available pyrite only. If there is any recalcitrant sulfide covered with organic matter, HNO_3 cannot dissolve that sulfide minerals [34]. For this reason, arsenic coprecipitated with pyrite and amorphous orpiment was extracted first and then organic matter and secondary sulfide bound As was extracted in a separate fraction afterward.

For the extraction of organic matter and recalcitrant sulfide bound As (fraction G7), we used $H_2O_2 + NH_4OAc$ (pH 2) adopted from the method described by Kreidie et al. [21] while Tessier method used $H_2O_2 + HNO_3$ (pH 2) for the extraction of organic matter associated As. The strong oxidizing action of H_2O_2 in acidic medium is frequently employed for oxidation of organic material and refractory sulfides in sequential extraction. Arsenic extracted in this fraction was low in the developed method ($2.91 \pm 0.62\ \mu g\ g^{-1}$) compared to the Tessier method ($9.63 \pm 1.06\ \mu g\ g^{-1}$) because Tessier methods skipped some previous extraction steps (G2, G5 and G6, Fig. 3). Tessier et al. [9] also suggested separation of pyrite bound metals before the application of organic matter extraction step. Hall et al. [10] used a combination of H_2O_2, NaOAc and HNO_3 for the extraction of As associated with sulfides and organic matter in spiked samples. They also compared their results with Tessier method which overestimated As due to the dissolution of sulfide minerals.

High concentrations of As were determined in the residual fractions extracted using Tessier ($12.32 \pm 1.58\ \mu g\ g^{-1}$) and Wenzel ($16.24 \pm 0.82\ \mu g\ g^{-1}$) methods compared to our developed method ($0.9 \pm 0.2\ \mu g\ g^{-1}$) (G8, Fig. 3). Because Tessier and Wenzel methods skipped previous extraction steps for silicate clay (G5) and sulfide bound (G6) As, the residual fractions in these methods might contain silicate and sulfide bound As. Tessier et al. [9] defined their residual fraction as primary and secondary minerals including silicates and recalcitrant sulfides. The sum of G5 and G6 ($\sim 11.0 \pm 0.4\ \mu g\ g^{-1}$) in our method corresponds to the As in residual fraction of Tessier method showing the advantage of our proposed scheme. Similarly, Mihaljevič et al. [27] found elevated As concentrations in the residual fraction of spiked samples using Tessier method and attributed this higher concentration to arsenopyrite that was insufficiently extracted (oxidized) before As extraction in the residual fraction.

3.4. Assessment of the developed method for the dissolution of targeted minerals in pure phase and sediment

Four pure minerals such as calcite, dolomite, arsenopyrite and orpiment were sequentially extracted by applying the developed method. The dissolution of carbonate minerals (calcite and dolomite) were expected in fraction F4. Chemical analysis (data not shown) of the extraction solution revealed complete dissolution (~94%) of pure calcite in F4 using 1 M NaOAc (pH 5) as an extractant and no dissolution occurred in F3 (strongly adsorbed As). The SEM-EDX images (Fig. 4A–C) substantiated the persistence of calcite in F3. But F3 fraction might include some carbonate bound As particularly from dolomite because ~50% of the pure dolomite was dissolved in F3 fraction. Evidence of dolomite dissolution was also observed by SEM-EDX (Fig. 4D–F), where magnesium (Mg) intensity decreased after extraction with 1 M NaH_2PO_4 (F3). But in the S6 sediment, similar Ca and Mg intensities of EDX (Supplemental Fig. S1B and D) were observed whether or not the sediment was extracted with 1 M NaH_2PO_4 though the intensities of these peaks were very small probably due to very low (<1%) carbonate minerals. These peaks were not detected after 1 M NaOAc (pH 5) extraction (Supplemental Fig. S1F) suggesting dissolution of carbonates in F4.

Fraction F8 in sequential extraction scheme determines As bound in sulfide minerals using 16 N HNO_3 as extractant. To evaluate if any dissolution of sulfide minerals (amorphous orpiment and arsenopyrite) occurs in F7, pure minerals (orpiment and pyrite) were extracted using 10 M HF. The SEM-EDX (Fig. 5 and Supplemental Fig. S2) results suggested that these minerals were not dissolved in F7. SEM analysis revealed two mineral phases in untreated orpiment (Fig. 5A and B). Both the phases remained unaffected during 10 M HF extraction (Fig. 5C–F) which showed the stability of orpiment in 10 M HF. XRD diffractograms also showed the existence of these minerals when solid phase was analyzed by XRD before and after the extraction with 10 M HF (Supplemental Fig. S3). Arsenopyrite did not dissolve in F7 as evident from SEM-EDX (Supplemental Fig. S3) and XRD (Supplemental Figs. S3C and D) analyses. However, ~99% amorphous orpiment and ~96% arsenopyrite (determined by chemical analysis; data not shown) were only dissolved by 16 N HNO_3 in F8. Similar results were found in S6 sediment (Supplemental Fig. S4), where no change in Fe:S ratio was observed before and after 10 M HF extraction.

4. Conclusions

The developed sequential extraction method can predict ~97% distribution or partitioning of total As in nine different meaningful pools associated with different solid constituents. The extractants used in the developed method are compatible with ICP-MS eliminating interference from polyatomic ions during As analysis. This extraction scheme can also be employed for the fractionation of other metals such as Cu, Co, Cr and Sr. The applicability and utility of this method can further be augmented by testing this developed protocol for metal characterization in samples collected from different geo-environmental conditions.

Acknowledgements

We gratefully acknowledge funding from NSERC (Discovery Grants to TS), Canadian Water Network (GK) and School of Energy and the Environment (TS). We also thank Dr. Laurence Andriashek (Geologist, Energy Resource Conservation Board) for providing samples of surficial deposits and technical assistance. We also acknowledge Ph.D. scholarship award from Islamia, University, Bahawalpur, Pakistan (MBJ).

Appendix A. Supplementary data

Supplementary data associated with this article can be found, in the online version, at http://dx.doi.org/10.1016/j.aca.2013.05.050.

References

[1] R.S. Oremland, J.F. Stolz, Science 300 (2003) 939–944.
[2] M.B. Alam, M.A. Sattar, Water Sci. Technol. 42 (2000) 185–192.
[3] P. Mitchell, D. Barr, Environ. Geochem. Health 17 (1995) 57–82.
[4] R.K. Dhar, Y. Zheng, J. Rubenstone, A. Van-Green, Anal. Chim. Acta 526 (2004) 203–209.
[5] Health Canada, Guidelines for Canadian Drinking Water Quality, 2006, Ottawa, Ontario.
[6] M. Sadiq, Water Air Soil Pollut. 93 (1997) 117–136.
[7] E. Smith, R. Naidu, A.N. Alston, Adv. Agron. 64 (1998) 149–195.
[8] R. Larios, R.F. Martínez, I. Rucandio, Anal. Bioanal. Chem. 402 (2012) 2909–2921.
[9] A. Tessier, P.G.C. Campbell, M. Bisson, Anal. Chem. 51 (1979) 844–851.
[10] G.E.M. Hall, J.E. Vaive, R. Beer, M. Hoashi, J. Geochem. Explor. 56 (1996) 59–78.
[11] N.E. Keon, C.H. Swartz, D.J. Brabander, C. Harvey, H.F. Hemond, Environ. Sci. Technol. 35 (2001) 2778–2784.
[12] W.W. Wenzel, N. Kirchbaumer, T. Prohaska, G. Stingeder, E. Lombi, D.C. Adriano, Anal. Chim. Acta 436 (2001) 309–323.
[13] J. Goossens, F. Vanhaecke, L. Moens, R. Dams, Anal. Chim. Acta 280 (1993) 137–143.
[14] R. Thomas, Practical Guide to ICP-MS: A Tutorial for Beginners, 2nd ed., Taylor & Francis Group, Boca Raton, FL, 2008.
[15] M. Niemelä, P. Perämäki, H. Kola, J. Piispanen, Anal. Chim. Acta 493 (2003) 3–12.
[16] M.E. Sumner, Commun. Soil Sci. Plant Anal. 25 (1994) 859–879.
[17] D.F. Ball, J. Soil Sci. 15 (1964) 84–92.
[18] L.D. Andriashek, EUB/AGS Earth Sciences Report, 2003.
[19] N.N. Zhabina, I.I. Volkov, Environ. Biogeochem. 3 (1978) 735–745.
[20] US EPA, Method 3050B, US Environmental Protection Agency, Washington, DC, 1996.
[21] N. Kreidie, G. Armiento, G. Cibin, G. Cinque, C. Crovato, E. Nardi, R. Pacifico, C. Cremisini, A. Mottana, J. Soils Sediments 11 (2011) 37–52.
[22] W.U. Shaole, Z. Yu-Hui, F. Xinbang, W. Adolph, J. Anal. Atom. Spectrom. 11 (1996) 287–296.
[23] C. Gleyzes, S. Tellier, M. Astruc, Trends Anal. Chem. 21 (2002) 451–467.
[24] E. Lombi, R.S. Sletten, W.W. Wenzel, Water Air Soil Pollut. 124 (2000) 319–332.
[25] C.M. Davidson, A.L. Duncan, D. Littlejohn, A.M. Ure, L.M. Garden, Anal. Chim. Acta 363 (1998) 45–55.
[26] R.E. Villanueva-Estrada, R.M. Prol-Ledesma, A.A. Rodríguez-Díaz, C. Canet, M.A. Armienta, Chem. Geol. 348 (2013) 27–36.
[27] M. Mihaljevič, M. Poňavič, V. Ettler, O. Šebek, Anal. Bioanal. Chem. 377 (2003) 723–729.
[28] S.W. Poulton, D.E. Canfield, Chem. Geol. 214 (2005) 209–221.
[29] K. Müller, B. Daus, P. Morgenstern, R. Wennrich, Water Air Soil Pollut. 183 (2007) 427–436.
[30] H. Xu, B. Allard, A. Grimvall, Water Air Soil Pollut. 40 (1991) 269–278.
[31] S. Goldberg, R.A. Glaubig, Soil Sci. Soc. Am. J. 2 (1988) 1297–1300.
[32] B.A. Manning, S. Goldberg, Environ. Sci. Technol. 31 (1997) 2005–2011.
[33] P.L. Smedley, D.G. Kinniburgh, Appl. Geochem. 17 (2002) 517–568.
[34] K.M. Steel, J.W. Patrick, Fuel 80 (2001) 2019–2023.
[35] M. Eghbalnia, Electrochemical and raman investigation of pyrite and chalcopyrite oxidation. Ph.D. Thesis, University of British Columbia (2012).

Appendix A:

The following are the supplementary data for “A modified sequential extraction method for arsenic fractionation in sediments”.

Muhammad Babar Javed, Gary Kachanoski[1], Tariq Siddique[*]
Department of Renewable Resources, University of Alberta, Edmonton, AB, T6G 2E3, Canada

[1] Present address:

Memorial University of Newfoundland, St John’s, NL A1C 5S7, Canada

[*]Corresponding author address:

Department of Renewable Resources, University of Alberta, 338A Earth Sciences Building, Edmonton, AB, T6G 2E3, Canada

Table S1

Comparison of the sequential extraction of As (μg g^{-1}) from sediment S6 using four different methods.

Fraction [a]	Tessier	Wenzel	Keon	Developed
F1	- [b]	-	-	0.011
F2	0.037	0.031	2.16	0.022
F3	-	7.75	9.02	8.29
F4	0.21	-	1.37	0.08
F5	12.59	4.6	4.62	4.68
F6		8.3	6.97	6.22
F7	-	-	2.8	2.79
F8	-	-	7.72	8.21
F9	9.63	-	-	2.91
F10 (Residual)	12.32	16.24	3.35	0.87
Sum	34.78	36.92	38.01	34.07
% recovery [c]	98.24	104.27	107.34	96.22

[a] F1, water soluble As; F2, ionically bound As; F3, strongly adsorbed As; F4; arsenic bound to carbonate; F5, arsenic coprecipitated with amorphous Fe, Al and Mn oxyhydroxides; F6, arsenic coprecipitated with crystalline Fe, Al and Mn oxyhydroxides; F7, arsenic associated with As oxides and silicate clays; F8, arsenic coprecipitated with pyrite and amorphous orpiment; F9, arsenic associated with organic matter and recalcitrant sulfides; F10, residual As.

[b] Method does not have that extraction step

[c] Sum of all the As fractions extracted by the described methods ranged from 96-107% of the total As (35.4 μg g^{-1}) extracted by the acid digestion method.

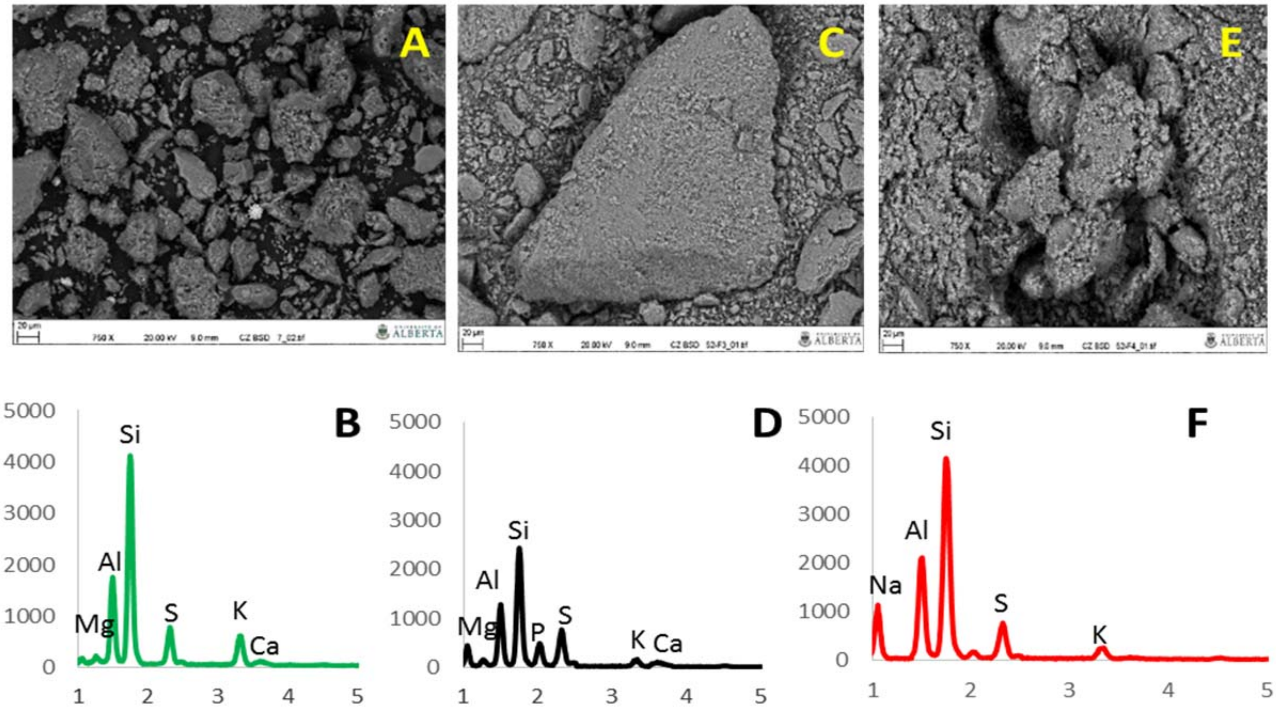

Fig. S1. SEM-EDX analysis of sediment S6. (A) and (C) are SEM images of sediment before and after 1 M NaH_2PO_4 (pH 5) extraction, respectively with their corresponding EDX spectra (B and D) which show no evidence of carbonate minerals dissolution in F3, as Ca and Mg peaks are similar. (E) and (F) are the SEM image and EDX spectrum of sediment after 1 M NaOAc (pH 5) which suggest complete dissolution of Ca and Mg in F4.

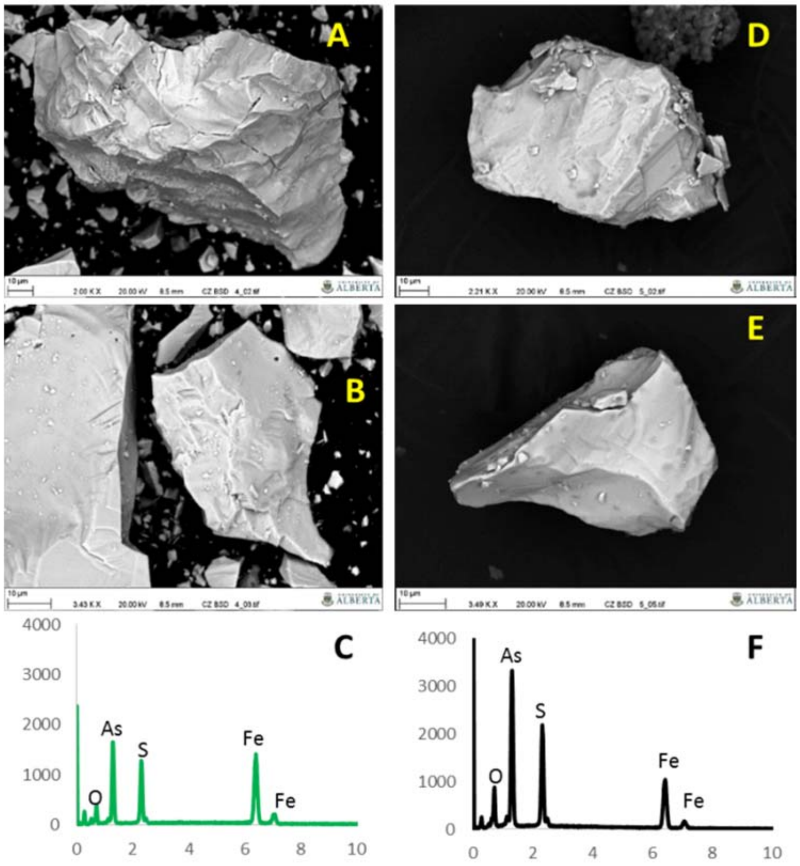

Fig. S2. SEM-EDX analysis of arsenopyrite mineral. SEM images (A) and (B) show well crystal minerals of arsenopyrite along with EDX spectrum (C) before any extraction with 10 M HF. (D) and (E) are the equivalent SEM images with EDX (F) after 10 M HF extraction that show.the stability of arsenopyrite in 10 M HF. After F8, all the solid phase was dissolved and there was not enough material for SEM analysis.

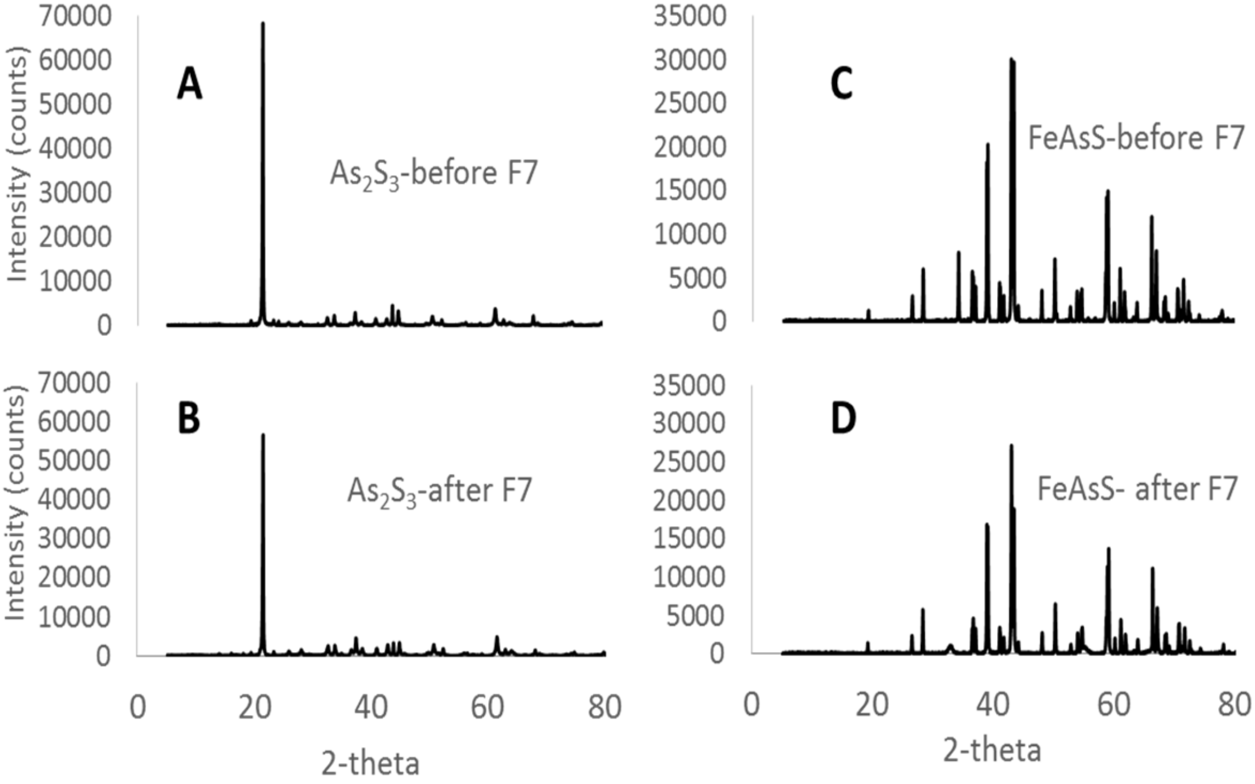

Fig. S3. XRD analysis of orpiment and arsenopyrite minerals. XRD diffractograms of orpiment (A and B) and arsenopyrite (C and D) are obtained before and after 10 M HF extraction, respectively. Both the diffractograms before and after 10 M HF extraction of orpiment and arsenopyrite are similar which reveal the stability of both the minerals in 10 M HF. After F8, all the solid phase was dissolved and there was not enough material for XRD analysis.

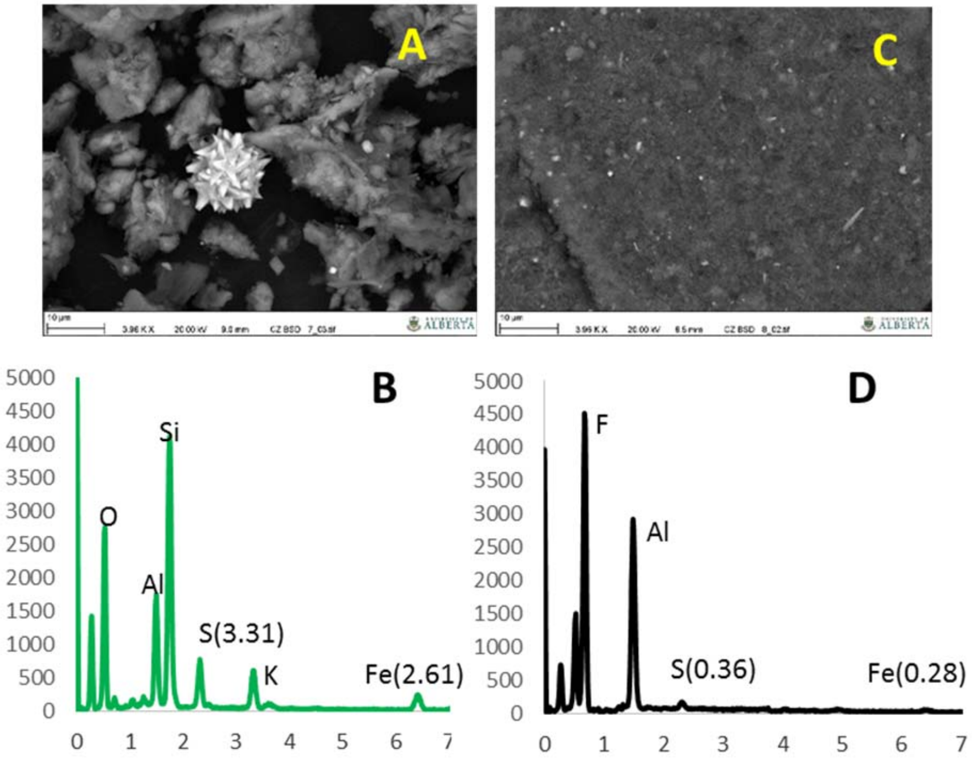

Fig. S4. SEM-EDX analysis of sediment S6. SEM images of solid phase before (A) and after (C) 10 M HF extraction look different because of the removal of silicates. EDX spectra show Si removal after 10 M HF extraction (D) compared to solid phase before the extraction (B). Fe:S ratio is constant in both solid phases before (B) and after HF extraction (D) indicating the stability of sulfide minerals during HF extraction. Values in parentheses are the atomic % of the Fe and S.

Copyright Clearance Center RightsLink®

Home | Account Info | Help | Live Chat

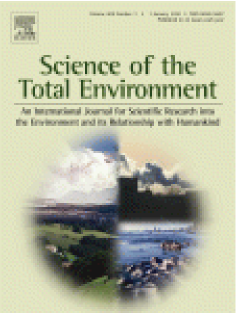

Title:	Arsenic fractionation and mineralogical characterization of sediments in the Cold Lake area of Alberta, Canada
Author:	Muhammad Babar Javed,Gary Kachanoski,Tariq Siddique
Publication:	Science of The Total Environment
Publisher:	Elsevier
Date:	1 December 2014

Logged in as:
Muhammad Javed
Account #:
3000772809

LOGOUT

Order Completed

Thank you very much for your order.

This is a License Agreement between Muhammad B Javed ("You") and Elsevier ("Elsevier"). The license consists of your order details, the terms and conditions provided by Elsevier, and the payment terms and conditions.

Get the printable license.

License Number	3512080532383
License date	Nov 18, 2014
Licensed content publisher	Elsevier
Licensed content publication	Science of The Total Environment
Licensed content title	Arsenic fractionation and mineralogical characterization of sediments in the Cold Lake area of Alberta, Canada
Licensed content author	Muhammad Babar Javed,Gary Kachanoski,Tariq Siddique
Licensed content date	1 December 2014
Licensed content volume number	500
Licensed content issue number	n/a
Number of pages	10
Type of Use	reuse in a thesis/dissertation
Portion	full article
Format	both print and electronic
Are you the author of this Elsevier article?	Yes
Will you be translating?	No
Title of your thesis/dissertation	Distribution of arsenic in surficial deposits in the Cold Lake area of Alberta, Canada
Expected completion date	Dec 2014
Estimated size (number of pages)	200
Elsevier VAT number	GB 494 6272 12
Permissions price	0.00 USD
VAT/Local Sales Tax	0.00 USD / 0.00 GBP
Total	0.00 USD

ORDER MORE... | CLOSE WINDOW

Science of the Total Environment 500–501 (2014) 181–190

Contents lists available at ScienceDirect

Science of the Total Environment

journal homepage: www.elsevier.com/locate/scitotenv

Arsenic fractionation and mineralogical characterization of sediments in the Cold Lake area of Alberta, Canada

Muhammad Babar Javed [1], Gary Kachanoski [2], Tariq Siddique *

Department of Renewable Resources, University of Alberta, Edmonton, AB T6G 2E3, Canada

HIGHLIGHTS

- High arsenic was found in sediments derived from shale.
- Arsenic was mainly found in exchangeable and sulfide bound phases.
- Pyrite and arsenopyrite minerals were found in high arsenic sediments.
- Sulfide minerals in the sediments could be the potential source of groundwater As.

GRAPHICAL ABSTRACT

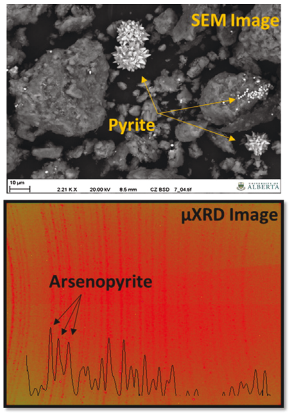

ARTICLE INFO

Article history:
Received 29 May 2014
Received in revised form 31 July 2014
Accepted 23 August 2014
Available online xxxx

Editor: F.M. Tack

Keywords:
Arsenic distribution
Fractionation
Mineralogy
XANES spectroscopy
Geological formation
Surficial deposits

ABSTRACT

Elevated arsenic (As >0.01 mg L^{-1}) in some domestic well water in the Cold Lake area of Alberta, Canada is of great concern for public health. To determine possible sources of groundwater As, sediments ($n = 135$) collected from five different locations (up to ~300 m depth) in the area were characterized. Total As concentrations in the sediments varied from ~1 to 35 mg kg^{-1}. Sediments derived from shale contained high As (~13 mg kg^{-1}; $n = 14$), particularly the shale of Lea Park formation where maximum average As was ~32 mg kg^{-1} ($n = 2$). Unoxidized sediments of Grand Centre (24.9 ± 4.2 mg kg^{-1} As) and Bonnyville (19.9 ± 1.8 mg kg^{-1} As) formations also contained high As. Sequential extraction procedure (SEP) revealed the dominance of exchangeable and specifically adsorbed As (6 to 46% of total As) in the sediments of varying As concentrations (0.8 to 35.4 mg kg^{-1} As). The high As sediments (>7 mg kg^{-1} As) also contained significant amount of sulfide bound As (11 to 34% of total As), while low As (<7 mg kg^{-1} As) sediments had crystalline oxide minerals bound As (25 to 75% of total As) as major phases. X-ray diffraction (XRD) and scanning electron microscopy (SEM) analyses confirmed the presence of pyrite, and µ-XRD analysis signaled the presence of arsenopyrite in sediments containing ~20 mg kg^{-1} As. X-ray absorption near edge structure (XANES) spectroscopy analysis suggested dominance of arsenite (AsIII; ~60 to 90% of total As) in all the sediments. These findings may help to devise strategies to investigate mechanisms of As release into the groundwater.

---

* Corresponding author. Tel.: +1 780 492 2899; fax: +1 780 492 1767.
E-mail addresses: mjaved@ualberta.ca (M.B. Javed), gary.kachanoski@mun.ca (G. Kachanoski), tariq.siddique@ualberta.ca (T. Siddique).

[1] Tel: +1 780 492 4422.

[2] Present address: Memorial University of Newfoundland, St John's, NL A1C 5S7, Canada.

http://dx.doi.org/10.1016/j.scitotenv.2014.08.083
0048-9697/

1. Introduction

Arsenic (As) is a ubiquitous metalloid with some of its chemical forms being extremely toxic. It has received global attention in recent years for its groundwater contamination and subsequent serious health effects. It is estimated that 40 to 100 million people in the world are at risk of consuming As contaminated water (Páez-Espino et al., 2009; van Halem et al., 2009; de Mora et al., 2011). The biggest poisoning outbreak of the 20th century is also attributed to As contaminated groundwater in Bangladesh, where 30 to 77 million people are at risk due to excessive As in drinking water (Smith et al., 2000; van Halem et al., 2009). In Alberta (Canada), relatively high As concentrations have been found in the groundwater particularly in the Lakeland health region including Cold Lake area (Health Surveillance, 2000; Fitzgerald et al., 2001) where ~50% of drinking water wells contained As that exceeded the maximum acceptable concentration (As 0.01 mg L^{-1}; Health Canada, 2006). Generally, high levels of As in groundwater (a source of drinking water) are attributed to the sulfide-rich high As aquifers (Wang and Mulligan, 2006).

It is agreed that As in groundwater usually originates geogenically from sediments (Nickson et al., 2000). Arsenic is naturally enriched in shale containing pyrite (FeS_2, which is considered the principal carrier of As in rocks) and other minerals such as arsenopyrite (FeAsS), enargite (Cu_3AsS_4), scorodite ($FeAsO_4.2H_2O$) and annabergite [$(Ni)_3(AsO_4)_2$] (Boyle and Jonasson, 1973). Weathering and biological transformation of these As containing minerals under natural conditions can mobilize As from soil and sediment to the aquatic environment (Smedley and Kinniburgh, 2002; Muloin and Dudas, 2005). Alberta Health and Wellness (Health Surveillance, 2000) and Alberta Environment and Water Communications (Moncur, 2011) conducted studies in eastern Alberta and correlated naturally occurring higher groundwater As concentration with bedrock geological formations containing marine shale. Marine shale inclusions or enrichment within Quaternary (glacial) sediments are one of the important sources of groundwater As (Andriashek, 2000).

The distribution and chemical association of As with different sediment constituents affect As mobility in sediment pore water and its transport to groundwater depending on the prevailing geochemical conditions. Arsenic sequestration (sorption/coprecipitation) in solid constituents, especially oxyhydroxides of iron (Fe), aluminum (Al) and manganese (Mn) is one of the most important processes that immobilize As under oxidizing conditions (Smith et al., 1998; Larios et al., 2012). Arsenic-bearing Fe oxyhydroxides may also act as a source of As during reductive dissolution under reducing conditions (Larios et al., 2012). Arsenic associated with Mn oxyhydroxides (easily reducible oxides) is relatively more labile than Fe oxyhydroxides (Tessier et al., 1979). One other major form of As is naturally occurring As-bearing sulfide minerals that are stable under reducing conditions but oxidative breakdown of these minerals can release As into the environment (Larios et al., 2012). Anthropogenic activities such as mining and smelting can enhance As release by exposing these unoxidized minerals to the atmosphere and making them vulnerable to weathering (Smedley and Kinniburgh, 2002). However, part or all of the released As may occlude in the resulting metastable secondary minerals such as $FeAsO_4.2H_2O$ (Sadiq, 1997) and diminish the danger of groundwater contamination.

Because the source(s) responsible for As-laden groundwater in the Cold Lake area of Alberta are still unknown, this study combines sequential extraction procedure (SEP), mineralogical and spectroscopic techniques to comprehensively investigate the As distribution in surficial deposits (sediments) in the Cold Lake area. This study will provide base knowledge to further investigate geochemical processes governing As release into the groundwater.

2. Material and methods

2.1. Reagents and minerals

Trace metal grade nitric acid (HNO_3), sodium acetate (CH_3COONa; abbreviated as NaOAc), sodium phosphate (NaH_2PO_4), calcium chloride ($CaCl_2$), ammonium oxalate [$(NH_4)_2C_2O_4.H_2O$], oxalic acid ($H_2C_2O_4$), titanium (Ti) powder, sodium citrate ($Na_3C_6H_5O_7.2H_2O$), sodium bicarbonate ($NaHCO_3$), ethylene-diamine-tetra-acetic acid ($C_{10}H_{14}N_2Na_2O_2.2H_2O$; abbreviated as EDTA), acetic acid (CH_3COOH; abbreviated as HOAc) and hydrofluoric acid (HF) were purchased from Sigma-Aldrich (Ontario, Canada) to prepare the extraction solutions. All solutions were prepared using nanopure water (Barnstead nanopure, Thermo Scientific), and the pH of the extractant solution, if required, was adjusted to the desired level (as reported in Table S1) with either sodium hydroxide (NaOH) or appropriate acid (HOAc, $H_2C_2O_4$ or HNO_3). The reagent blanks from all the extraction solutions were also analyzed along with the experimental samples. Negligible concentrations of trace elements (As was undetectable) were found in all the blank solutions that were accounted for during calculations. All laboratory glass-and plastic-ware was cleaned by soaking in 5% (v/v) HNO_3 overnight and then repeatedly rinsed with nanopure water.

Pure phases of sodium arsenate [$Na_3As(V)O_4$], sodium arsenite [$Na_3As(III)O_3$] and arsenic oxide [$As_2(III)O_3$] were purchased from Sigma-Aldrich (Ontario, Canada). Natural minerals such as annabergite [$Ni_3(As(V)O_4)_2$], orpiment [$As_2(III)S_3$] and arsenopyrite [$FeAs(III)S$] were collected from the Mineralogy Petrology Museum in the Department of Earth and Atmospheric Sciences at the University of Alberta, Canada. These salts and minerals were used to obtain X-ray diffraction (XRD) patterns and X-ray absorption near edge structure (XANES) white line energy positions (As absorption edge energy) of arsenite (As^{III}) and arsenate (As^{V}) for comparison with the sediment As.

2.2. Sediment collection and their physicochemical characterization

The Alberta Geological Survey, Alberta Energy Regulator (AGS-AER) drilled surficial deposits (105 to ~300 m-thick sediments above bedrock) at eight different locations in the Cold Lake area (southeast part of the Athabasca Oil Sands) to explore the hydrogeology and hydrogeochemistry of the region. The cores were stored in wooden boxes at the AGS Mineral Core Research Facility in Edmonton, Alberta, Canada under ambient conditions. To cover a large area in the region, these already drilled cores were used for As distribution in sediments. For this study, five sediment cores (four cores drilled in 1999–2000 namely WR99-1, WEPA99-1, WEPA99-2, and WEPA00-1, and one core drilled in 2009 namely 14-01w) were selected based on stratigraphic units and their proximity to buried channel aquifers (Fig. S1A). The stratigraphy of the area consists of eight glacial and non-glacial formations (Fig. S1B), and the nature and distribution of geological sediments are well described by Andriashek (2003). Because of the lithological heterogeneity in each sediment core, sub-samples were taken along the whole core depth to represent each stratum (based on visual observation) in the cores. In addition, sub-samples were also collected from the depths that represent oxidized (brownish sediment due to Fe oxyhydroxide) and reduced [grayish sediment due to high iron sulfide (FeS)] zones as well as the zones of surficial (<75 m deep) and buried (75–150 m deep) channel aquifers to correlate sediment redox conditions with groundwater As concentration.

Sediment cores were air dried when sub-samples were taken in 2010, which might have changed the oxidation state of As in the sediments. Therefore, chemical speciation of As was not performed using these sediments. Total As concentrations determined in the sediments taken from the outer and inner portions of the cores were compared to the As concentration determined at the time of core collection by Andriashek (2003). No significant difference was found in As concentrations between the outer and inner sediments and the As determined in sediments at the time of core collection. However, sediments taken from the inner portion of the cores were used in this study. Sediment samples were ground with agate mortar and pestle to pass through a 125 μm sieve before all chemical, mineralogical and spectroscopic analyses. The pH of sediment slurry prepared with 0.05 M $CaCl_2$ solution (1:5 ratio; Sumner, 1994) was measured using accumet® AR20 pH meter. The pH ranged between 4.7 and 9.1, but most sediments had pH ~7. Total organic carbon (TOC) contents in sediments determined by the loss on ignition (LOI) method (Ball, 1964) were <1% in most sediments but a few had TOC up to 2.8 ± 0.2%. The information about particle size distribution (PSD) and lithology of the sediments was obtained from Andriashek (2003). In general, ~50% of the PSD was in the range of 50 to 63 μm size. The redox potential (E_h) of the surficial and buried channel aquifer water of the study area ranged between 80 and 100 mV (Lemay, 2003). Total As and Fe concentrations were determined using the methods described in Section 2.3. The chromium reducible sulfur method (Hsieh and Shieh, 1997) was employed to determine the reduced inorganic sulfur. The physicochemical properties of selected ($n = 22$) sediments are provided in Table 1.

2.3. Total and sequentially extracted As from sediments

For total As, sediments were digested with concentrated HNO_3 (1:20 sediment:acid ratio) in a microwave digestion unit (MARS6, CEM) at 180 ± 10 °C for 10 min using a modified EPA method (3050B, 1996) After cooling, the digested samples were diluted with nanopure water (final HNO_3 concentration ~1% in solution), filtered through 0.45-μm PTFE filters (033911C, Fisher Scientific) and analyzed by inductively coupled plasma mass spectrometry (ICP-MS; Perkin-Elmer ELAN 9000). After total As determination, 22 sediment samples were chosen from different cores representing different lithologies and grouped under low (As <7 mg kg^{-1}; samples 1 to 9) and high As sediments (As >7 mg kg^{-1}; samples 10 to 22) for further chemical, mineralogical and spectroscopic investigations (Table 1). Shale is considered a source of high As in sediments that contain an average of 10 to 15 mg kg^{-1} As (Krauskopf, 1979; Boyle and Jonasson, 1973). The lowest As concentration (~7 mg kg^{-1}) found in our shale sediments was used for demarcation between designated low and high As sediments. To study different phases (soluble, exchangeable, specifically adsorbed, bound to carbonates, amorphous and crystalline oxides/oxyhydroxides, sulfides and organic matter; see detail in Table S1) of As in sediments, a modified SEP (Javed et al., 2013) was applied to the selected sediments. Briefly, sediments (0.4 g) were sequentially extracted with 40 mL of the extractants for the appropriate period of time as given in Table S1. The sediment–extractant suspensions were shaken for the specified duration, and then centrifuged (Sorvall® RC-5B Refrigerated Superspeed Centrifuge with Sorvall® HS-4 rotor) for 40 min at 6000 g to separate the supernatants, which were decanted without removing any sediment particles and filtered through 0.45-μm PTFE filters. The sediments were washed with nanopure water for 30 min before adding the next extractant. After centrifugation, the washing solutions were pooled with their respective decanted solutions, acidified (1% final concentration of HNO_3), and analyzed for As and Fe using ICP-MS. Pearson correlation of As with other elements in different sediment phases was performed using SAS 9.3.

To maintain quality assurance and quality control (QA/QC) for experimental procedure and equipment operation, duplicate experimental blanks and duplicate sediments ($n = 6$) were included in microwave digestion for the determination of total As from 135 sediment samples. For As fractionation in 22 sediments using sequential extraction method, again duplicate extraction blanks were included and the data of 8 (out of 22) sediments from a previous study (Javed et al., 2013) was used as reference data to verify QA/QC measures. The variation in duplicate samples ranges between 2 and 9% for both total As and As fractionation. In all the experimental blanks, As was below the limit of detection (LOD; 5×10^{-5} mg L^{-1} As) using ICP-MS. Multi-elemental external standards (CLMS-2N, SPEX Certi Prep) in the range of 0.002 to 0.05 mg L^{-1} prepared in 1% HNO_3 were used to calibrate the ICP-MS. Immediately after calibration standards, six initial calibration blanks (ICB) were analyzed to ensure that the instrument was clean. During the analysis of experimental samples, continuous calibration blanks (CCB) to check any metal contamination in the instrument and continuous calibration verification (CCV) standards of 0.002 and 0.02 mg L^{-1} As to assure the validity of the initial calibration of the instrument were also included after every 10 samples. All the blanks (ICB and CCB) showed As concentrations lower than the LOD, and As concentrations in all the CCVs were within ±10% of the actual values of As (0.002 and 0.02 mg L^{-1}). In addition, scandium (Sc), yttrium (Y) and terbium (Tb) internal standards were used in all the external standards, ICB, CCB, CCV and experimental samples to account for any instrumental drift.

2.4. X-ray diffraction (XRD) of sediments

To determine the As minerals in the sediments, random powder XRD analysis was performed. XRD (RIGAKU RU-200B) coupled with Cu X-ray source and scintillator detector was used to determine the bulk (silicate and non-silicate) mineralogy of the sediments. Fine powdered samples of high (samples 11, 14 and 17) and low As sediments (samples 1, 2 and 9) were mounted on the holder and scanned using Cu Kα X-ray from 4 to 100 2θ with a 0.05 2θ step-size and 4 second count-time per step. Because most As minerals such as FeAsS are very fine-grained (30–50 μm) and less abundant (<1 wt.%) in natural sediments making them difficult to be detected using conventional XRD (Flemming et al., 2005), high energy synchrotron radiation (VESPER beam-line) at Canadian Light Source (CLS), University of Saskatchewan (Feng et al., 2010) was used to detect As minerals by applying micro (μ) XRD. For μ-XRD, standard minerals and sediments in Kapton tape were scanned under high energy radiation (~11.867 KeV). Diffracted X-rays were detected by 2D detector (GADDS) positioned at a distance of ~45 cm from the sample intersecting a 45° segment of diffraction space. Diffracted lines and spots from each lattice plane (*hkl*) of minerals produced an arc of radius 2θ (*hkl*) on GADDS image, and the intensity of diffracted lines and spots along each arc was integrated to create a plot of intensity versus 2θ. Jade and XMAS software were used for the analyses of XRD and μ-XRD data, respectively to identify the minerals.

2.5. X-ray absorption near edge structure (XANES) spectroscopy of sediments

To determine the dominant oxidation state of As in the sediments, As K-edge XANES data were collected at the CLS. All the low (samples 1 to 9) and high As sediments (samples 10 to 22) were prepared in the same way as described for μ-XRD analysis. Six standards including sodium arsenate (As^{V}; absorption edge at 11874.2 eV), annabergite (As^{V}; 11874 eV), arsenic oxide (As^{III}; 11871 eV), sodium arsenite (As^{III}; 11870.5 eV), orpiment (As^{III}; 11868.4 eV) and arsenopyrite (As^{III}; 11868 eV) were analyzed to generate white line energy positions of As^{V} and As^{III} to compare with the sediment As white lines to determine the oxidation state of As in sediments. Most sediments generated white line energy position close to 11868 eV that corresponded well to As^{III} (Kachenko et al., 2010). Five scans from each standard and sediment sample were collected in the XANES region using a 4-element detector in fluorescence mode. Analysis of standard and sediment XANES spectra including smoothing, normalization and averaging the five raw spectra was carried out using Athena (Ifeffit, v.1.3) software. Athena was also used for linear combination fit (LCF) analysis (Shah et al., 2007) of sediments XANES spectra to determine the proportion of As^{V} and As^{III} present in the sediments. The goodness and quality of LCF of sediment among possible combinations of standards were assessed calculating the R-factor value that was equivalent to the normalized sum of the residuals (Manning, 2005).

Table 1
Physicochemical characteristics of the selected sediments used for detailed As investigation.

Sediment ID[a]	Core name	Texture[b]	Geological formation	pH[c]	TOC (%)	As_{total} (μg g^{-1})	Sulfide (%)	Fe_{total} (%)
Low as samples (<7 μg g^{-1})								
1	14–01w	Sandy Clay	Bonnyville	7.2	0.48 ± 0.07	6.5 ± 0.8	0.19 ± 0.03	2.8 ± 0.4
2	14–01w	Sandy Clay	Bonnyville	7.0	0.28 ± 0.03	4.7 ± 0.7	0.12 ± 0.05	1.7 ± 0.2
3	WEPA99–1	Sand	Grand Centre	4. 7	0.11 ± 0.03	5.3 ± 0.5	0.14 ± 0.02	1.4 ± 0.2
4	WEPA99–1	Sand	Grand Centre	6.3	0.05 ± 0.01	3.1 ± 0.1	0.10 ± 0.02	1.9 ± 0.5
5	WEPA99–1	Till	Marie Creek	7. 2	0.09 ± 0.04	4.2 ± 0.3	0.09 ± 0.04	1.7 ± 0.3
6	WEPA99–2	Till	Grand Centre	6.3	0.72 ± 0.13	5.6 ± 0.8	0.19 ± 0.07	2.7 ± 0.8
7	WEPA99–2	Mudstone	Bonnyville	7.3	1.18 ± 0.09	0.8 ± 0	0.05 ± 0.04	ND
8	WR99–1	Clay	Empress	7.2	0.64 ± 0.11	6.1 ± 0.7	0.06 ± 0.01	2.8 ± 0.9
9	WR99–1	Clay and silt	Empress	7.3	0.60 ± 0.07	3.5 ± 0.1	0.07 ± 0.01	2.2 ± 0.5
High as samples (>7 μg g^{-1})								
10	WEPA99–1	Till	Grand Centre	7.5	0.55 ± 0.08	7.5 ± 0.1	0.79 ± 0.04	2.9 ± 0.7
11	WEPA99-1	Till	Grand Centre	6.8	0.57 ± 0.03	24.9 ± 4.2	2.79 ± 0.17	2.7 ± 0.4
12	WEPA99–1	Till	Marie Creek	7.1	0.11 ± 0.01	9.9 ± 0.4	0.24 ± 0.02	3.2 ± 0.2
13	WEPA99-1	Till	Bonnyville	6.2	2.75 ± 0.19	19.9 ± 1.8	1.87 ± 0.14	4.0 ± 0.2
14	WEPA99–2	Till	Grand Centre	6.3	0.50 ± 0.05	12.4 ± 0.8	0.33 ± 0.08	4.2 ± 0.9
15	WEPA99–2	Silt and clay	Ethel Lake	6.6	0.66 ± 0.11	10.5 ± 1.1	0.59 ± 0.04	2.4 ± 0.7
16	WEPA99–2	Mudstone	Bonnyville	7.4	0.34 ± 0.04	8.8 ± 0.9	0.31 ± 0.07	2.1± 0.6
17	WR99-1	Clay and silt	Empress	6.8	1.27 ± 0.37	22.5 ± 2.1	1.15 ± 0.03	3.8 ± 0.3
18	WR99-1	Clay and silt	Empress	6.2	1.13 ± 0.19	8.9 ± 0.9	0.37 ± 0.01	2.4 ± 0.8
19	WR99–1	–	Marine shale	8.9	0.64 ± 0.20	8.6 ± 0.4	0.33 ± 0.07	2.1 ± 0.4
20	WR99–1	–	Marine shale	5.4	0.04 ± 0.01	18.6 ± 1.8	0.93 ± 0.12	3.1 ± 0.7
21	WR99–1	–	Marine shale	9.1	0.60 ± 0.09	7.0 ± 0.7	0.66 ± 0.07	3.2 ± 0.9
22	14–01w	–	Marine shale	7.1	ND	35.4 ± 2.3	2.16 ± 0.24	2.9 ± 0.4

Values represent the mean from analysis of triplicate ± 1 standard deviation.

[a] Sample ID refers to the numbers in Fig. 1, [b] information about texture was obtained from Andriashek (2003), texture analysis was not performed for samples 19 to 22, [c] pH was measured in suspension of sediment:0.05 M $CaCl_2$ (1:5).

TOC: total organic carbon; ND: not detected.

Shaded areas: Sediments taken from unoxidized zones/layers, samples 17 and 18 were taken from the localized reduced layers.

2.6. X-ray fluorescence (XRF) and scanning electron microscopy (SEM) of sediments

To determine the spatial association of As and Fe, a 2 × 2 mm sample area of high As sediment (sediment 11; 24.9 ± 4.2 μg g^{-1} As) prepared for μ-XRD was used for XRF mapping at VESPER beam-line using 0.2 mm step size and 5 second scan-time per step. To study the micromorphology of selected high As sediments, a high spatial resolution (~3 nm) JEOL (Field Emission) SEM equipped with energy dispersive X-ray spectrometer (EDX) was used at the University of Alberta. Powdered sediment samples were mounted on Al stub using a double-sided carbon tape, coated with carbon to prevent the charging on sample surface due to the electron beam and examined under SEM.

3. Results

3.1. Arsenic distribution in sediments

Arsenic distribution in sediments with respect to depth, geological formations, lithology, TOC, pH and redox conditions is shown in Fig. 1 and Table 1. Generally, arsenic concentrations in sediments at different depths did not significantly ($p > 0.05$) vary with geological formations, lithologies, pH and TOC of sediments. ICP-MS analysis showed that As was present in all the sediments ranging from ~1 to 35 mg kg^{-1}. However, higher As concentrations were detected in unoxidized clayey zones in the Grand Centre (24.9 ± 4.2 mg kg^{-1} As) and Bonnyville (19.9 ± 1.8 mg kg^{-1} As) formations, particularly in core WEPA99-1 compared to the average As concentration (~5 mg kg^{-1}) measured in all sediments (n = 135) collected from all the geological formations with different lithologies and redox zones (Fig. S1B). High As concentration (22.5 ± 2.1 mg kg^{-1} As) was also found in localized unoxidized sediment in the Empress formation (core WR99-1). The marine shale sediments clearly exhibited higher concentrations of As (~13 mg kg^{-1}; n = 14) in the cores (WR99-1, WEPA99-1 and 14-01w). Among all the sediments, the highest average concentration of As (32 mg kg^{-1}; n = 2) was also determined in shale from Lea Park formation (core 14-01w).

3.2. Arsenic fractionation in sediments

Different As phases in selected low (samples 1 to 9; Fig. S2A) and high As sediments (samples 10 to 22; Fig. 2A) were determined using sequential extraction procedure. In high As sediments, greater As was found in exchangeable and specifically adsorbed fractions (F2 + F3: ~4.5 mg kg^{-1} As; 32% of total As) on the solid phase (mineral and organic solid phases). Higher concentrations of As were also found coprecipitated with sulfide minerals such as FeS_2 and As_2S_3 (F8: ~3.4 mg kg^{-1} As; 19% of total As). About 17% of total As was extracted from each of the crystalline Fe, Al and Mn oxyhydroxides (F6), and silicate minerals and As oxides (F7). Arsenic associated with the amorphous Fe, Al and Mn oxyhydroxides (F5) contributed ~11% to the total As, and the rest of the As phases produced <10% of the total As (Fig. 2A). In the low As sediments, a significant proportion of total As was associated with the crystalline Fe, Al and Mn oxyhydroxides (F6: ~1.8 mg kg^{-1} As; 40% of total As) and adsorbed on different solid phases (F2 + F3: ~1 mg kg^{-1} As; ~20% of total As; Fig. S2A). Arsenic associated with FeS_2 and As_2S_3 (F8) was only 0.2 mg kg^{-1} (3.9% of total As), and rest of the sediment solid phases contained As similar to the high As sediments.

Total Fe concentrations and sulfide minerals also varied in sediments. In high As sediments, total Fe concentrations ranged from 2.1 to 4.2%. Fractionation of Fe revealed that ~60% of total Fe was associated with amorphous and crystalline Fe oxides. Silicate and sulfide minerals also contained significant amounts of Fe (21 and 12% of total Fe, respectively; Table 1; Fig. 2B). In low As samples, total Fe ranged between 1.4 and 2.8%, and ~80% of total Fe was associated with amorphous and

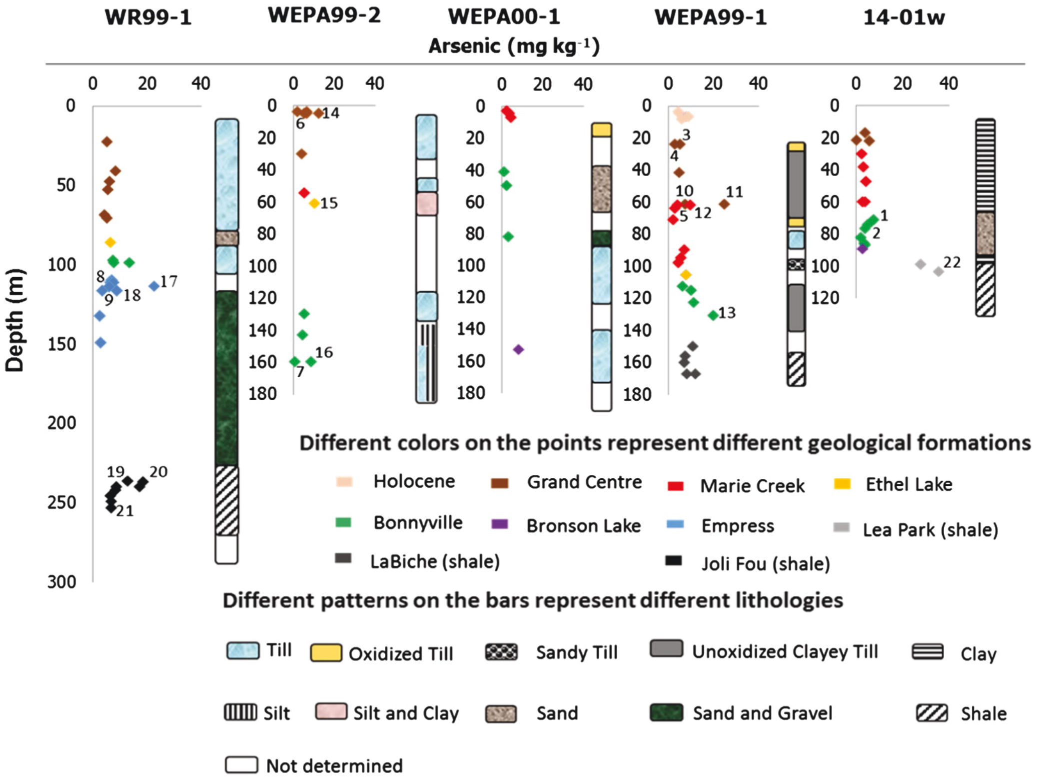

Fig. 1. Arsenic (As) distribution in sediment cores collected from five different locations in the Cold Lake area of Alberta. The numbers (1 to 22) displayed on the data in the figure are the sediment samples selected for further As characterization. The information about the sediment texture and formation was obtained from Andriashek (2003).

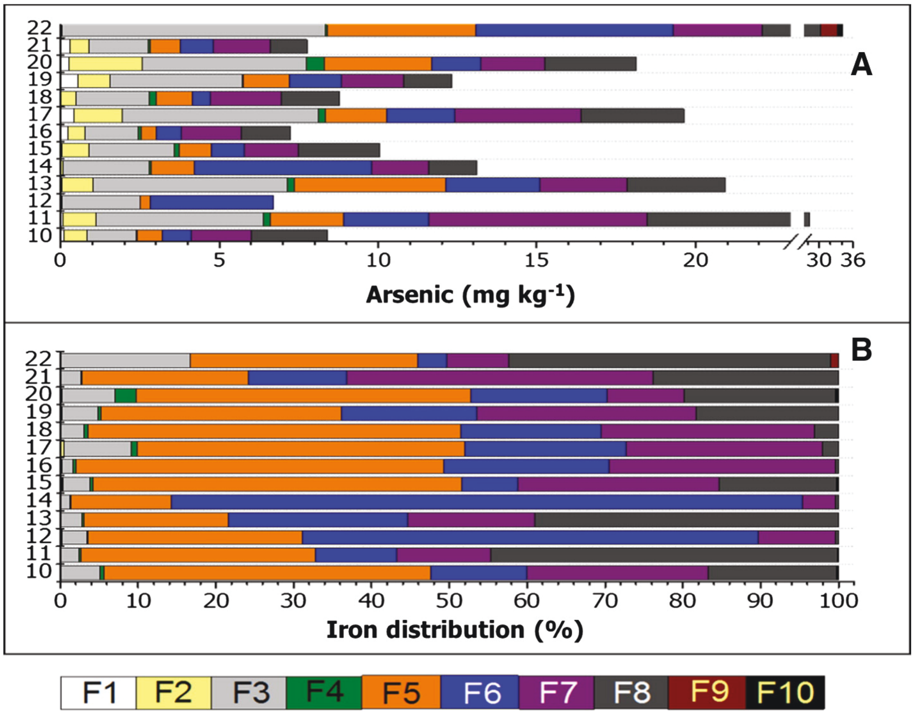

Fig. 2. Distribution of (A) As and (B) Fe in different sediment phases of the selected high As sediments (samples 10 to 22; As > 7 mg kg^{-1}). Sequential extraction procedure (SEP; Javed et al., 2013) was used to determine the As and Fe fractionations in sediments. Arsenic and Fe concentrations were determined in the same aliquot of each extractant used in SEP. The results of As and Fe fractionations in low As sediments are given in Fig. S2. Legends are applicable to both panels and represent different fractions: F1, water soluble metals; F2, exchangeable metals; F3, specifically adsorbed metals; F4, metals bound in carbonates; F5, metals coprecipitated with amorphous Fe, Al and Mn oxyhydroxides; F6, metals coprecipitated with crystalline Fe, Al and Mn oxyhydroxides; F7, metals associated with their oxides and silicate clays; F8, metals coprecipitated with pyrite and orpiment; F9, metals associated with organic matter and recalcitrant sulfides; and F10, residual metals.

crystalline Fe oxides. Around 12% of total Fe was associated with silicate minerals and only 1% of total Fe was found with sulfide minerals (Table 1; Fig. S2B); because low As sediments contained small quantities of sulfide minerals (0.05 to 0.19%) as compared to high As sediments (0.24 to 2.79% sulfide minerals; Table 1). Generally, higher concentrations of As were found in the unoxidized sediments enriched in FeS minerals. In high As sediments, a significant positive correlation of sulfide minerals was found with total As ($p < 0.001$; $r = 0.83$) and As associated with sulfide minerals ($p < 0.01$; $r = 0.90$; Fig. S3A) as compared to the low As sediments where we could not find good correlation between As (total and sulfide bound) and sulfide minerals (Fig. S3B). As far as correlation between sulfide minerals and Fe concentrations in sediments is concerned, sulfide minerals in high As sediments showed higher correlation ($r = 0.83$; $p < 0.005$) with Fe associated with sulfide minerals, but did not correlate well with total Fe in sediments ($r = 0.18$; Fig. S3C). Fe and sulfide minerals did not show any correlation in low As sediments at all (Fig. S3D).

3.3. Mineralogy of sediments

XRD analysis performed on selected high (11, 14 and 17) and low As sediments (1, 2 and 9) showed that FeS_2 was one of the dominant minerals in the high As sediments (Fig. 3A), particularly in sediments 11 (24.9 ± 4.2 mg kg^{-1} As) and 17 (22.5 ± 2.1 mg kg^{-1} As). In contrast, sediment 14 (12.4 ± 0.8 mg kg^{-1} As) retrieved close to the top of core WEPA99-2 generated dominant goethite [FeO(OH)] peaks which supported our SEP results that showed more Fe released by the dissolution of amorphous and crystalline Fe oxyhydroxides than FeS_2 in that sediment (Fig. 2B). However, we could not identify phyllosilicate minerals in the high As sediments. In low As sediments, none of the FeS_2 and goethite peaks were identified. Peaks of kaolinite and muscovite clay minerals were identified in one of the sediments containing 3.5 ± 0.1 mg kg^{-1} As (sediment 9; Fig. 3A); the other two sediments only showed quartz as a dominant mineral like other low and high As sediments. Because the detection limit of XRD (~4 wt.% of mineral) was not enough to identify As minerals in the sediments, μ-XRD was employed to determine whether high As sediments had any As minerals or As was present within FeS_2. The μ-XRD results were presented as typical GADDS images showing diffracted cones (Fig. S4) that were integrated into diffractograms to reveal mineral contents at different 2-theta values (Fig. 3B). Some characteristic peaks of FeAsS appeared in the sediments containing high As (sediment 11; 24.9 ± 4.2 mg kg^{-1} As, and sediment 17; 22.5 ± 2.1 mg kg^{-1} As) indicating the presence of FeAsS.

XANES spectroscopy analysis was performed to determine the oxidation state of As in sediment solid phase. The As K-edge XANES data acquired from the standards and selected low (sediments 1 to 9) and high As sediments (sediments 10 to 22) suggested that absorption peaks were easily distinguishable from one another by the white line energy positions (Figs. 3C, D and S5). The white line energy positions of As^{V} and As^{III} in standard minerals acquired through XANES were in the following order: sodium arsenate (As^{V}-O, 11874.2 eV) > annabergite (As^{V}-O, 11874 eV) > arsenic oxide (As^{III}-O, 11871 eV) > sodium arsenite (As^{III}-O, 11870.5 eV) > orpiment (As^{III}-S 11868.4 eV) > arsenopyrite (As^{III}-S 11868 eV) (Fig. 3C); which were in agreement with the previously published literature (Xu et al., 2011). Most of our sediments generated white line energy positions close to 11868 eV that corresponded to As^{III} oxidation state possibly associated with sulfide minerals. The LCF results of XANES data from all the selected low and high As sediments (Figs. 3D and S5; Table S2) showed that As was predominantly present in As^{III} form, except in samples 10, 12, 14 and 15 that were taken from the oxidized till (Fig. S6) where As^{V}

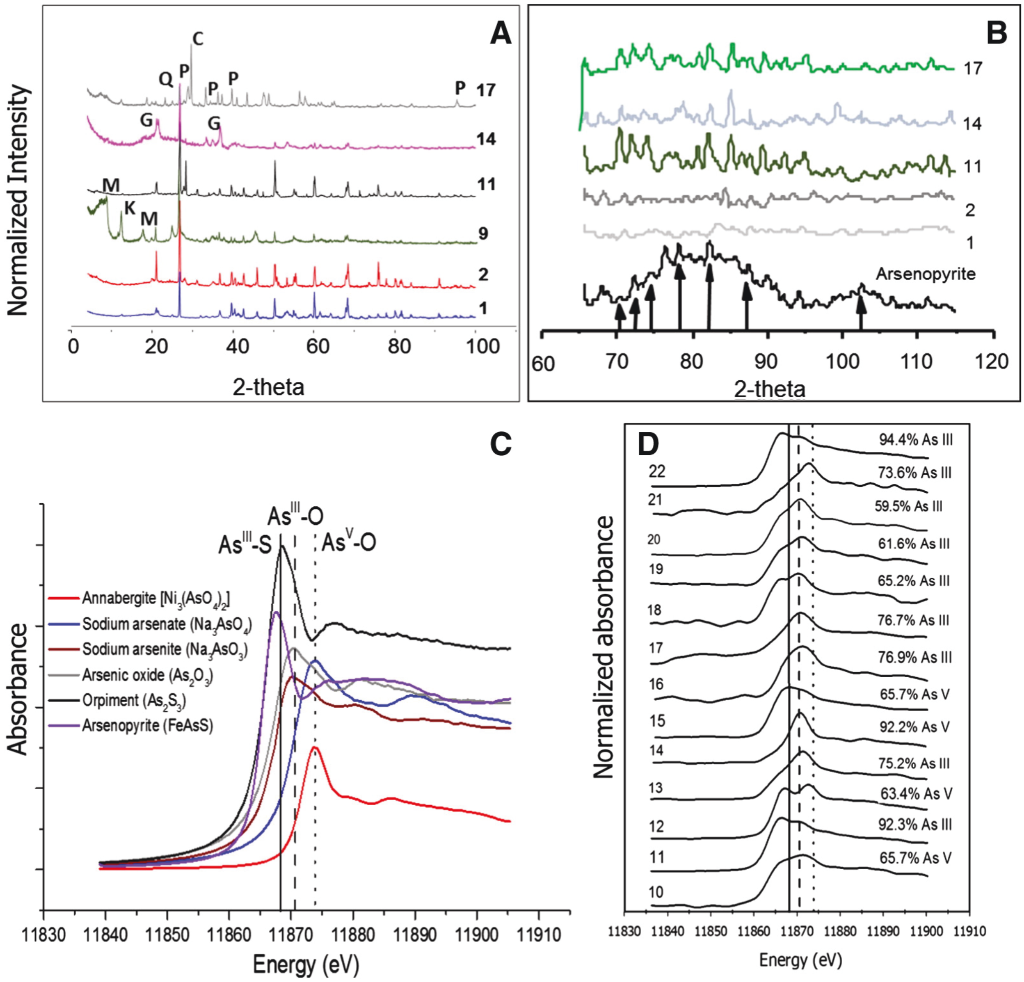

Fig. 3. Mineralogical characterization of host phases of As in sediments. (A) XRD spectra of selected low (samples 1, 2 and 9) and high As sediments (samples 11, 14 and 17) show the dominance of pyrite in the high As sediments. Q, quartz; P, pyrite; C, calcite; G, goethite; M, muscovite; K, kaolinite; only primary peaks are labeled. (B) µ-XRD spectrum of arsenopyrite pure phase shows that high As sediments also contain some characteristic arsenopyrite peaks; all arrows show the arsenopyrite peaks. (C) As K-edge XANES spectra of reference compounds. Solid (-), dashed (—) and dotted (…) lines drawn at 11868 eV, 11870.7 eV and 11874 eV represent the position of white lines of As^{III}-S, As^{III}-O and As^{V}-O, respectively. (D) XANES spectra of selected high As sediments (>7 mg kg^{-1} As). Linear combination fit (LCF) results show that arsenite (As^{III}) is the most dominant As form in the sediments as shown by the proportion of As^{III} or arsenate (As^{V}) beside each spectrum. Only that oxidation state of As is shown in the spectrum that was present >50% in the sediment. Details of the LCF analysis are provided in Table S2. XANES and LCF information about low As sediments is given in Fig. S5.

ranged from 63 to 92% of the total As (Fig. 3D). Overall, XANES results suggested that As^{III} was the dominant As form in both low and high As sediments. If we interpret SEP and XANES result together, we can say that most of the As^{III} was associated with crystalline Fe, Al and Mn oxyhydroxides in low As sediments and with sulfide minerals in high As sediments.

3.4. Elemental mapping and micromorphology of sediments

One high As sediment (sediment 11; 24.9 ± 4.2 mg kg^{-1} As) was used for XRF mapping for As and Fe. The results showed some spatial association (evident from matching hotspots) between both the elements (Fig. 4A and B), but we did not find good correlation ($r = 0.42$) between total As and total Fe in high As sediments. However, a significant positive correlation ($p < 0.01$; $r = 0.81$) was found between As and Fe associated with sulfide minerals (F8 of SEP for As and Fe, respectively). These results suggested that high As concentration might not be spatially associated with all Fe phases but FeS might contain most of the As. To study the micromorphology of the sediments, SEM supported by EDX (LOD ~0.1 wt.% of the element) was used to observe high As sediment (Sediment 11). SEM image clearly showed single FeS_2 crystals associated with the quartz that was supported by the EDX where high Fe and S intensities suggested FeS_2 and high Si and O showed quartz in the sediment (Fig. 4C and D).

4. Discussion

Elevated As in domestic well water in the Cold Lake area of Alberta, Canada is a health concern that warrants detailed geochemical characterization of the surficial deposits (sediments) that feed the aquifers in the region. Arsenic-laden groundwater is attributed to the sediment's As concentration through which the water passes (Wang and Mulligan, 2006). This study was conducted to comprehensively investigate As in sediments from 5 different locations (up to ~300 m depth) in the Cold Lake area and correlate it with As in surficial (<75 m deep) and buried (75 to 150 m deep) aquifer water to determine the potential source of As. Arsenic concentrations in aquifer water from the same study area was reported by Lemay (2003).

In our study, we observed that As concentrations varied from ~1 to 35 mg kg^{-1} in sediments without exhibiting any significant relationship with geochemical parameters such as lithology, pH, TOC and redox zones along the depth profiles of collected sediment cores. However, some pattern of As distribution in different geological formations could be established (Figs. 1 and S1B). Higher As concentrations (7 to

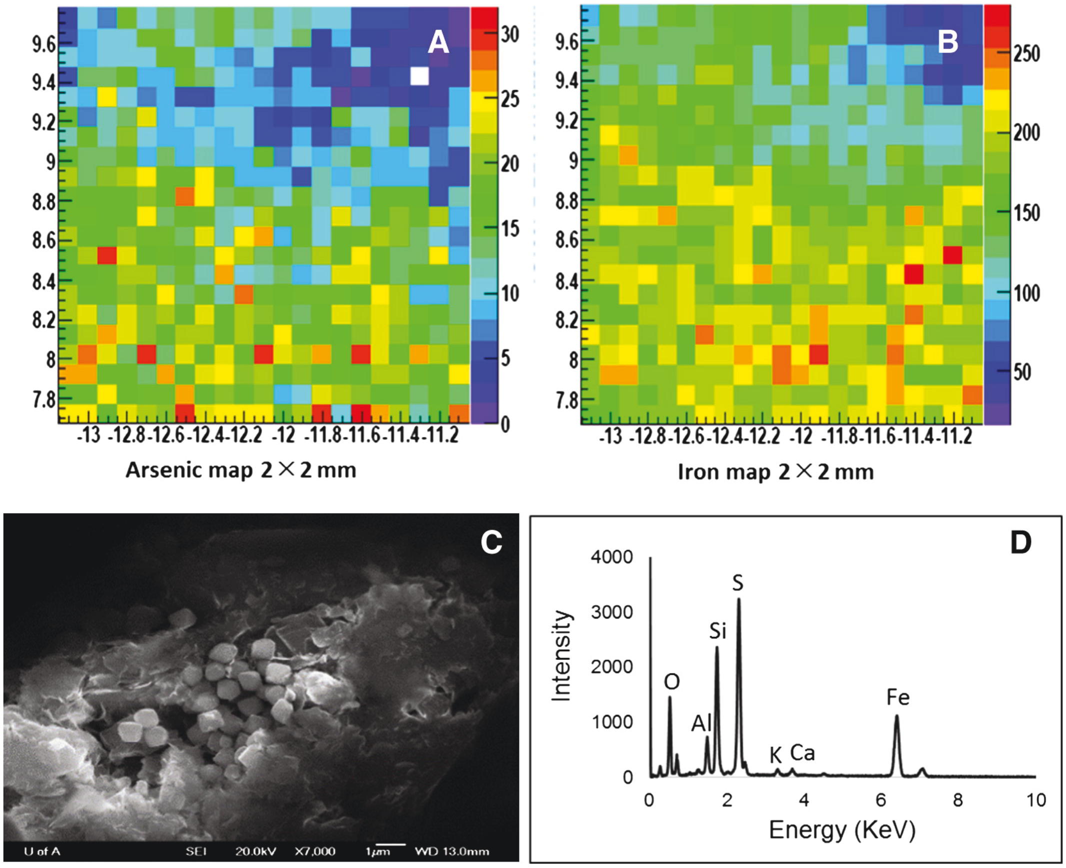

Fig. 4. Elemental mapping and micromorphology of high As sediment (sample 11; As: 24.9 ± 4.2 mg kg^{-1}). XRF mapping of (A) As and (B) Fe; both As and Fe maps show some spatial association between these elements (Pearson correlation, $r = 0.42$). (C) SEM image shows single pyrite crystals with quartz supported by (D) EDX that shows high intensities of S and Fe.

35 mg kg^{-1}; average: ~13 mg kg^{-1}; $n = 14$) were found in samples of marine shale that constituted the bottom portions of core holes WR99-1, WEPA99-1 and 14-01w. These As concentrations were similar to the average As concentration (~15 mg kg^{-1}) in the shale reported by Boyle and Jonasson (1973), which is commonly found in various parts of Canada including east- and west-central Alberta (Muloin and Dudas, 2005). Shale of marine origin often contains elevated levels of As that is concentrated in sulfide minerals such as FeS_2 and FeAsS (Muloin and Dudas, 2005). In general, the average As concentration in shale is an order of magnitude greater than other geological materials such as carbonates (Smedley and Kinniburgh, 2002). High As concentrations were also found in some sediments taken from the Grand Centre (24.9 ± 4.2 mg kg^{-1} As), Bonnyville (19.9 ± 1.8 mg kg^{-1} As) and Empress formations (~15 mg kg^{-1} average As; $n = 2$). If we see the locations of collected cores with respect to the geological setting of all the formations present in the region (Fig. S1B), the Bonnyville and Empress formations were directly overlying the marine shale that might be mixed with these formations during deposition (Andriashek and Fenton, 1989), and high As concentrations in these formations were found mostly in unoxidized horizons. Though the Grand Centre formation did not have any direct contact with shale (core WEPA99-1), a higher spike of As was probably due to the ice thrust that displaced and mixed older deposits (such as shale) during the deposition of Grand Centre formation (Andriashek and Fenton, 1989; Andriashek, 2000). Our results are in conformity with the findings of Andriashek (2000), who studied As in glacial till farther to the south in the Cold Lake area and reported high As in Grand Center and Bonnyville formations. In our study, other formations in the region such as Marie Creek, Ethel Lake, and Bronson Lake as well as Holocene (recently deposited material) showed lower concentrations of As at different depths in the collected cores. In contrast to our results, Andriashek (2003) reported a high As concentration in the oxidized zone of the Marie Creek formation in the core WEPA99-1. However in our study, higher As concentrations were found in the unoxidized sediments from the Grand Center, Bonnyville and Empress formations. A few brown Fe oxide mottles were found within the unoxidized Grand Center formation but upon analysis lower As concentrations were found in these mottles compared to the adjacent unoxidized sediments. The high As in unoxidized sediments could be due to the inclusion of marine shale.

Total As determined at various depths did not provide much information about its association with different solid constituents (phases) to predict its availability and potential transport to groundwater. Arsenic fractionation in the selected high As sediments showed that ~32% of the total As (Average total As: 15 mg kg^{-1}; $n = 13$) was exchangeable and specifically adsorbed on the sediment solids. Xu et al. (2011) reported a significant proportion of As (~25% of 735 mg kg^{-1}) strongly adsorbed on solids in sediments collected from a zinc (Zn) smelting site. In our study, analysis of Pearson correlation of the adsorbed As with different solid phases such as oxides of Fe, Al and Mn, sulfide minerals and TOC showed significant correlation only between adsorbed As and sulfide minerals ($p < 0.05$; $r = 0.66$). In high As sediments, As coprecipitated with FeS_2 and As_2S_3 was also one of the dominant fractions (Fig. 2A).

High As sediments were relatively darker (unoxidized) in color than low As sediments. For example in core WEPA99-1, a few occurrences of brown-colored Fe oxides were observed within the unoxidized dark gray sediments taken from the Grand Center formation (Fig. S6). We separated the oxidized sediment (sample 10) from the unoxidized sediment (sample 11) for As determination. High As concentration (24.9 ± 4.2 mg kg^{-1} As) was found in unoxidized sediment, which also contained high sulfide minerals (2.79 ± 0.17%), as compared to the oxidized sediment (7.5 ± 0.1 mg kg^{-1} As) in which only 0.79 ± 0.04%

sulfide minerals were present. Sediments obtained from the Bonnyville formation in core WEPA99-1 showed a darker gray color with depth and corresponding increase in As concentrations. We found ~20 mg kg^{-1} As in sediment 13 at deepest depth in the Bonnyville formation where sulfide minerals were ~2%. Another high As sediment (sample 17; 22.5 ± 2.1 mg kg^{-1} As) sampled from Empress formation, was also very dark gray to black colored and it too contained relatively high sulfide minerals (1.2%). Overall, sediments (11, 13 and 17) containing higher As (20 to 25 mg kg^{-1}) among all the high As sediments (10 to 22) from different formations also contained relatively higher sulfide minerals (1.2–2.8%) (Table 1). XRD and μ-XRD analyses confirmed the presence of FeS_2 and FeAsS, respectively (Fig. 3A and B) and SEM-EDX showed the presence of single FeS_2 crystals (Fig. 4C and D). Fluorescence mapping revealed the spatial association of As and Fe in high As sediment (Fig. 4A and B). Smedley and Kinniburgh (2002) also reported high As concentration (3 to 900 mg kg^{-1}) under reduced conditions in FeS_2-containing sediments of marine shale in Canada.

In high As sediments after adsorbed and sulfide bound fractions, a significant concentration of As (17% of the total As) was coprecipitated with crystalline Fe, Al and Mn oxyhydroxides and silicate minerals each. In the selected low As sediments, As associated with crystalline Fe, Al and Mn oxyhydroxides constituted the highest proportion of the total As (~40% of 1.8 mg kg^{-1}). Fennell (2008) also reported a significant proportion of As (~21% of 1.2 mg kg^{-1}) bound with the crystalline Fe oxyhydroxides in aquifer sediments from the same area. Arsenic associated with amorphous Fe, Al and Mn oxyhydroxides was omnipresent in all the low and high As sediments due to the high surface area of these oxides. Nonetheless, Fe oxyhydroxide content present in the soils and sediments is a good scavenger of As (Gleyzes et al., 2002; Smedley and Kinniburgh, 2002; Larios et al., 2012).

Overall, whether the As would adsorbed or coprecipitated with different solid constituents (crystalline/amorphous oxides, silicates or sulfides) in the sediments, our XANES results revealed the dominance (~60 to 90% of total As) of As^{III}, the reduced form of As, in all the low and high As sediments. We can speculate from these results that As initially existed in reduced minerals such as FeS_2 and FeAsS, and mineral transformation might have transferred or transported As to Fe oxide minerals. Elemental constituents of FeAsS oxidize at different rates. Yunmei et al. (2004) reported that ferrous (Fe^{II}) oxidized before the oxidation of As^{III} occurred, which indicated a relatively low rate of As^{III} conversion to As^{V}. This might suggest sequestration of As^{III} in newly formed Fe oxyhydroxide minerals in prevailing redox conditions (Eh ~80 to 100 mV of the aquifer water; Lemay, 2003). However, efforts will be made to get a fresh core from the same area for further research on As release mechanisms, microbial community involved in As release, As mobility in the pore water and chemical speciation of As.

Lemay reported water As concentrations in different Quaternary drift and Quaternary–Tertiary buried channel aquifers from the same locations where our sediment cores were taken (Lemay, 2003). Comparing our sediment As concentrations to the aquifer-water As, we found that generally sediment total As concentrations were lower than the average As concentration (5 mg kg^{-1}) in all the sediments where aquifer As was <0.01 mg L^{-1}. For example in core WEPA00-1, two surficial aquifers at 39.5 m and 74 m depths were present (Lemay, 2003). The As concentrations in these aquifer waters were <0.01 mg L^{-1}, and the surrounding sediments had ~3 mg kg^{-1} As. On the other hand in core WR99-1, a sand and gravel aquifer in the drift sediments at ~229 m depth with ~0.02 mg L^{-1} As (Lemay, 2003) corresponded to relatively higher As concentration (average ~11 mg kg^{-1}) in the sediments at that depth. This might suggest that the source of high As in aquifers is of localized origin, and proximity of the As-bearing sediment to aquifer water might be one of the possible causes of high As in the groundwater. Presence of competing anions such as phosphate (PO_4^{3-}) and carbonate (CO_3^{2-}) in pore water can desorb exchangeable As, and oxidative breakdown of FeS_2 and FeAsS in sediments can release As into groundwater (Keon et al., 2001).

In summary, high As concentration was found in the sediments derived from shale. Fractionation of As showed that exchangeable and specifically adsorbed As were the dominant phases in all the sediments, whereas sulfide minerals also constituted the major phase of As in the high As sediments. Chemical and micro-spectroscopic studies substantiated the association of As with Fe and S and mineralogical investigation revealed the presence of pyrite and arsenopyrite in high As sediments. These findings provide important knowledge about As distribution in sediments that can lead to further investigation of mechanisms responsible for As release into the groundwater.

Conflict of interest

The authors declare no competing financial interest.

Acknowledgments

We gratefully acknowledge the funding from NSERC (Discovery Grant to TS: G121211199), Canadian Water Network (GK: G119990371) and the School of Energy and the Environment (TS: RES0008628). We appreciate Laurence Andriashek (Alberta Geological Survey, Alberta Energy Regulator) for providing geological core sediments, technical assistance for result interpretation and reviewing the manuscript. We also acknowledge graduate scholarship award from Islamia University, Bahawalpur, Pakistan (MBJ).

Appendix A. Supplementary data

Supplementary data (Tables S1 and S2, and Figures S1-S6) to this article can be found online at http://dx.doi.org/10.1016/j.scitotenv.2014.08.083.

References

Andriashek LD. Geochemistry of selected glacial and bedrock geologic units, Cold Lake Area, Alberta. http://ags.gov.ab.ca/publications/ESR/PDF/ESR_2000_10.pdf, 2000.

Andriashek LD. Quaternary geological setting of the Athabasca Oil Sands (in situ) area, Northeast Alberta. http://www.ags.gov.ab.ca/publications/ESR/PDF/ESR_2002_03.pdf, 2003.

Andriashek LD, Fenton MM. Quaternary stratigraphy and surficial geology of the Sand River area 73 L. http://www.ags.gov.ab.ca/publications/BUL/PDF/BUL_057.pdf, 1989.

Ball DF. Loss-on-ignition as an estimate of organic matter and organic carbon in non-calcareous soils. J Soil Sci 1964;15(1):86–92.

Boyle RW, Jonasson IR. The geochemistry of arsenic and its use as an indicator element in geochemical prospecting. J Geochem Explor 1973;2:251–96.

De Mora K, Joshi N, Balint BL, Ward FB, Elfick A, French CE. A pH-based biosensor for detection of arsenic in drinking water. Anal Bioanal Chem 2011;400:1031–9.

Feng R, Dolton W, Igarashi R, Wright G, Bradford M, McIntyre S. Commissioning of the VESPERS Beamline at the Canadian Light Source. CP1234, 10th International Conference on Synchrotron Radiation Instrumentation; 2010.

Fennell JW. Effects of aquifer heating on groundwater chemistry with a review of arsenic and its mobility [PhD thesis] University of Calgary; 2008.

Fitzgerald D, Chanasyk DS, Neilson RD, Kiely D, Audette R. Farm well water quality in Alberta. Water Qual Res 2001;36(3):565–88.

Flemming RL, Salzsauler KA, Sherriff BL, Sidenko NV. Identification of scorodite in fine-grained, high-sulfide, arsenopyrite mine-waste using micro X-ray diffraction (μXrD), 43; 2005. p. 1243–54.

Gleyzes C, Tellier S, Astruc M. Fractionation studies of trace elements in contaminated soils and sediments: a review of sequential extraction procedures. Trends Anal Chem 2002;21(6–7):451–67.

Health Canada. Guidelines for Canadian drinking water quality: guideline technical document—arsenic. Ottawa, Ontario: Water Quality and Health Bureau, Healthy Environments and Consumer Safety Branch, Health Canada; 2006.

Health Surveillance, Alberta Health and Wellness. Arsenic in groundwater from domestic wells in three areas of northern Alberta. http://www.health.alberta.ca/documents/Arsenic-Groundwater-Wells-2000.pdf, 2000.

Hsieh YP, Shieh YN. Analysis of reduced inorganic sulfur by diffusion methods: improved apparatus and evaluation for sulfur isotopic studies. Chem Geol 1997;137(3–4):255–61.

Javed MB, Kachanoski G, Siddique T. A modified sequential extraction method for arsenic fractionation in sediments. Anal Chim Acta 2013;787:102–10.

Kachenko AG, Grafe M, Singh B, Heald SM. Arsenic speciation in tissues of the hyperaccumulator *P. calomelanos* var. *austroamericana* using X-ray absorption spectroscopy. Environ Sci Technol 2010;44(12):4735–40.

Keon NE, Swartz CH, Brabander DJ, Harvey C, Hemond HF. Validation of an arsenic sequential extraction method for evaluating mobility in sediments. Environ Sci Technol 2001;35(13):2778–84.

Krauskopf KB. Introduction to geochemistry. McGraw-Hill Book Company; 1979.

Larios R, Fernández-Martínez R, Rucandio I. Comparison of three sequential extraction procedures for fractionation of arsenic from highly polluted mining sediments. Anal Bioanal Chem 2012;402(9):2909–21.

Lemay TG. Arsenic concentration in quaternary drift and Quaternary–Tertiary buried channel aquifer in the Athabasca Oil Sands (in situ) area, Alberta. http://www.ags.gov.ab.ca/publications/GEO/PDF/GEO_2002_04.pdf, 2003.

Manning B. Arsenic speciation in As(III)- and As(V)-treated soil using XANES spectroscopy. Microchim Acta 2005;151:181–8.

Moncur A. Uranium and arsenic sources in shallow groundwater near Bonnyville, Alberta: a mineralogy study. Alberta Innovates Technology Futures; 2011.

Muloin T, Dudas MJ. Aqueous phase arsenic in weathered shale enriched in native arsenic. J Environ Eng 2005;4:461–8.

Nickson RT, McArthur JM, Ravenscroft P, Burgess WG, Ahmed KM. Mechanism of arsenic release to groundwater, Bangladesh and West Bengal. Appl Geochem 2000;15:403–13.

Páez-Espino D, Tamames J, de Lorenzo V, Cánovas D. Microbial responses to environmental arsenic. Biometals 2009;22:117–30.

Sadiq M. Arsenic chemistry in soils: an overview of thermodynamic predictions and field observations. Water Air Soil Pollut 1997;93:117–36.

Shah P, Strezov V, Stevanov C, Nelson PF. Speciation of arsenic and selenium in coal combustion products. Energy Fuel 2007;21:506–12.

Smedley PL, Kinniburgh DG. A review of the source, behaviour and distribution of arsenic in natural waters. Appl Geochem 2002;17:517–68.

Smith E, Naidu R, Alston A. Arsenic in the soil environment: a review. Adv Agron 1998;64:149–95.

Smith AH, Lingas EO, Rahman M. Contamination of drinking-water by arsenic in Bangladesh: a public health emergency. Bull World Health Organ 2000;78(9):1093–103.

Sumner ME. Measurement of soil pH: problems and solutions. Commun Soil Sci Plant Anal 1994;25(7–8):859–79.

Tessier A, Campbell PGC, Bisson M. Sequential extraction procedure for the speciation of particulate trace metals. Anal Chem 1979;51(7):844–51.

US EPA. Method 3050B acid digestion of sediments, sludges, and soils. Washington, D.C.: U.S. Environmental Protection Agency; 1996

Van Halem D, Bakker SA, Amy GL, Van Dijk JC. Arsenic in drinking water: a worldwide water quality concern for water supply companies. Drink Water Eng Sci 2009;29(2):29–34.

Wang S, Mulligan CN. Occurrence of arsenic contamination in Canada: sources, behavior and distribution. Sci Total Environ 2006;366:701–21.

Xu L, Zhao Z, Wang S, Pan R, Jia Y. Transformation of arsenic in offshore sediment under the impact of anaerobic microbial activities. Water Res 2011;45(20):6781–8.

Yunmei Y, Yongxuan Z, Williams-Jones AE, Zhenmin G, Dexian L. A kinetic study of the oxidation of arsenopyrite in acidic solutions: implications for the environment. Appl Geochem 2004;19:435–44.

Appendix A.

Supplementary information (SI) for

Arsenic fractionation and mineralogical characterization of sediments in the Cold Lake area of Alberta, Canada

Muhammad Babar. Javed [1], Gary Kachanoski [2], Tariq Siddique [1,*]

[1] Department of Renewable Resources, University of Alberta, Edmonton, AB T6G 2E3, Canada

[2] Memorial University of Newfoundland, St John's, NL A1C 5S7, Canada

* Corresponding Author E-mail: tariq.siddique@ualberta.ca

The supplementary information contains two tables (Tables S1 and S2) and six figures (Figs. S1 to S6) on nine pages including this cover page.

Table S1.

A modified sequential extraction procedure used for As fractionation in sediments.

Fraction	Target phase	Extractant [a]
F1	Soluble As	Nanopure water, 30 min
F2	Exchangeable As	1 M NaOAc, pH 8.2, 2 h
F3	Specifically adsorbed As	1 M NaH_2PO_4, pH 5, 16 and 24 h
F4	Carbonate bound As	1 M NaOAc, pH 5, 5 h
F5	As co-precipitated with amorphous Fe, Al and Mn oxyhydroxides	0.2 M Ammonium oxalate, pH 3, 2 h
F6	As co-precipitated with crystalline Fe, Al and Mn oxyhydroxides	0.05 M Ti-citrate-EDTA-bicarbonate, pH 7, 2 h
F7	As associated with As oxides and silicate clays	10 M HF, 1 and 24 h
F8	As coprecipitated with pyrite and orpiment	16 N HNO_3, 2 h twice
F9	As associated with organic matter and recalcitrant sulfides	30% H_2O_2 + 1 M NH_4OAc (1:2), pH 2, 16 h
F10	Residual As	Concentrated HNO_3, microwave digestion

[a] Extractants were added to sediments in sequential order (F1-F10) and the supernatant was removed after extraction and centrifugation. Sediments were washed with nanopure water for 30 min after each extractant. The water was separated by centrifugation and pooled with the decanted supernatant of each preceding extractant.

Table S2.

Linear combination fits (LCF) of As XANES spectra of reference compounds with the spectra of the selected sediments [a]

Sample ID	Reference minerals (% weights)[b]						R-factor[c]
	Annabergite	Sodium arsenate	Arsenic oxide	Sodium arsenite	Orpiment	Arseno-pyrite	
1	30.3	-	-	65.0	4.7	-	0.013
2	-	23.8	-	23.8	52.4	-	0.013
3	-	11.9	-	72.9	-	15.2	0.011
4	-	16.8	-	50.1	13.6	19.5	0.010
5	-	17.2	-	76.8	2.6	3.4	0.010
6	-	23.1	-	69.2	-	7.7	0.020
7	-	5.9	65.3	28.8	-	-	0.012
8	20	23.3	-	-	56.7	-	0.552
9	-	16.8	-	1.8	81.4	-	0.027
10	24.3	41.4	-	-	30.9	3.4	0.012
11	-	7.7	-	20.5	54.5	17.3	0.006
12	21.5	41.9	-	31.2	1.6	3.8	0.009
13	24.8	-	-	20.3	40.8	14.1	0.032
14	92.2	-	-	-	-	7.8	0.548
15	-	65.7	-	22.1	-	12.2	0.013
16	-	23.1	-	71.5	-	5.4	0.041
17	23.3	-	-	14.9	44.5	17.3	0.103
18	-	34.8	25.5	-	-	39.7	0.140
19	30.2	8.2	-	48.2	13.4	-	0.024
20	15.9	24.6	-	35.4	17.3	6.8	0.012
21	20.0	6.4	15.6	-	54.4	3.6	0.060
22	-	6.1	-	18.4	50.1	19.8	0.006

[a] detailed LCF results correspond to XANES spectra of the selected sediment samples plotted in Figures 3D and S5. [b] These results are presented with <±5% delta weights. [c] Normalized sum of the residuals (R-factor) is obtained by the following equation:

$$\text{R-factor} = \frac{\sum\{(data - fit)^2\}}{\sum(data^2)}$$

Relatively high R-factor values show that quality of LCF may not be very good.

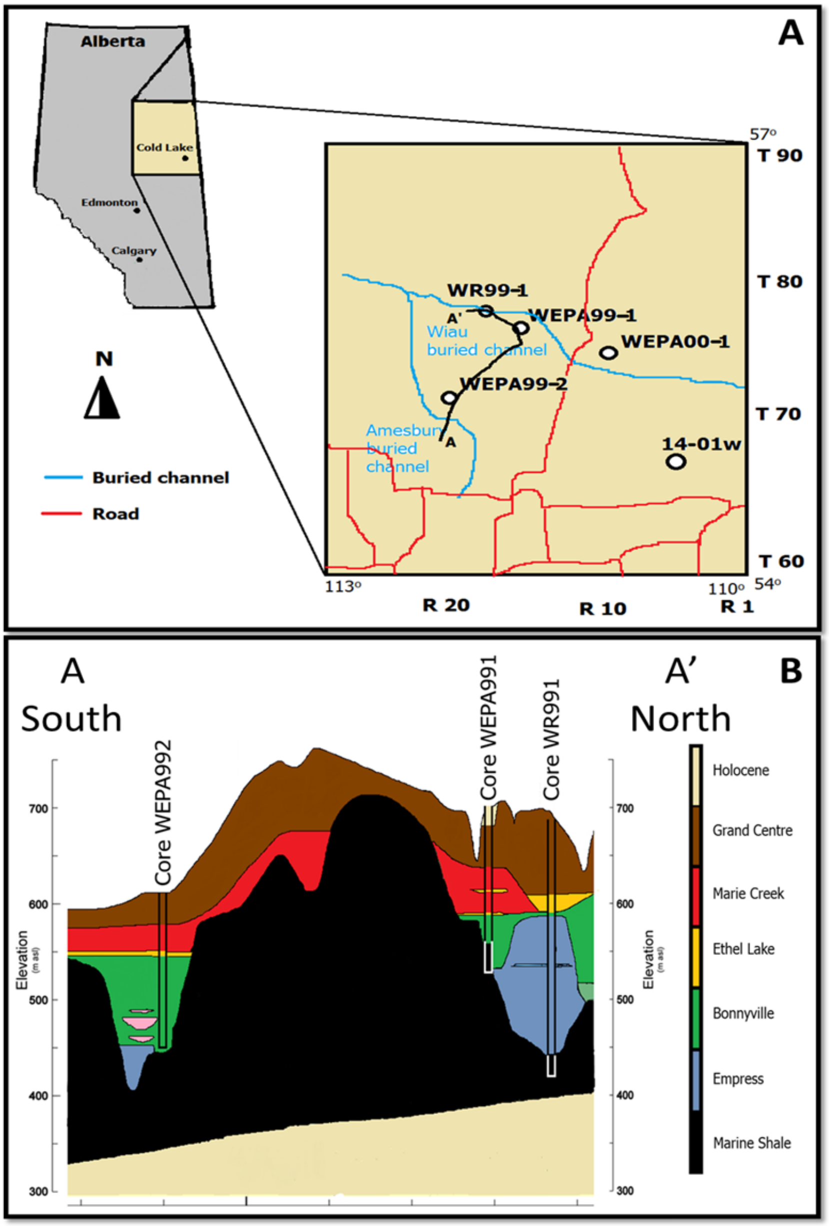

Fig. S1. Sample location and stratigraphy of surficial geological formations in study area. **(A)** Location of the five sediment cores taken for this study and two buried channel aquifers within the study area. **(B)** Geological cross section of part (A-A´) of study area that is showing three cores taken for our study and stratification of different formations within the cores. In this cross section Bronson Lake formation is not present. The information to construct these figures were obtained from Andriashek, 2002.[19]

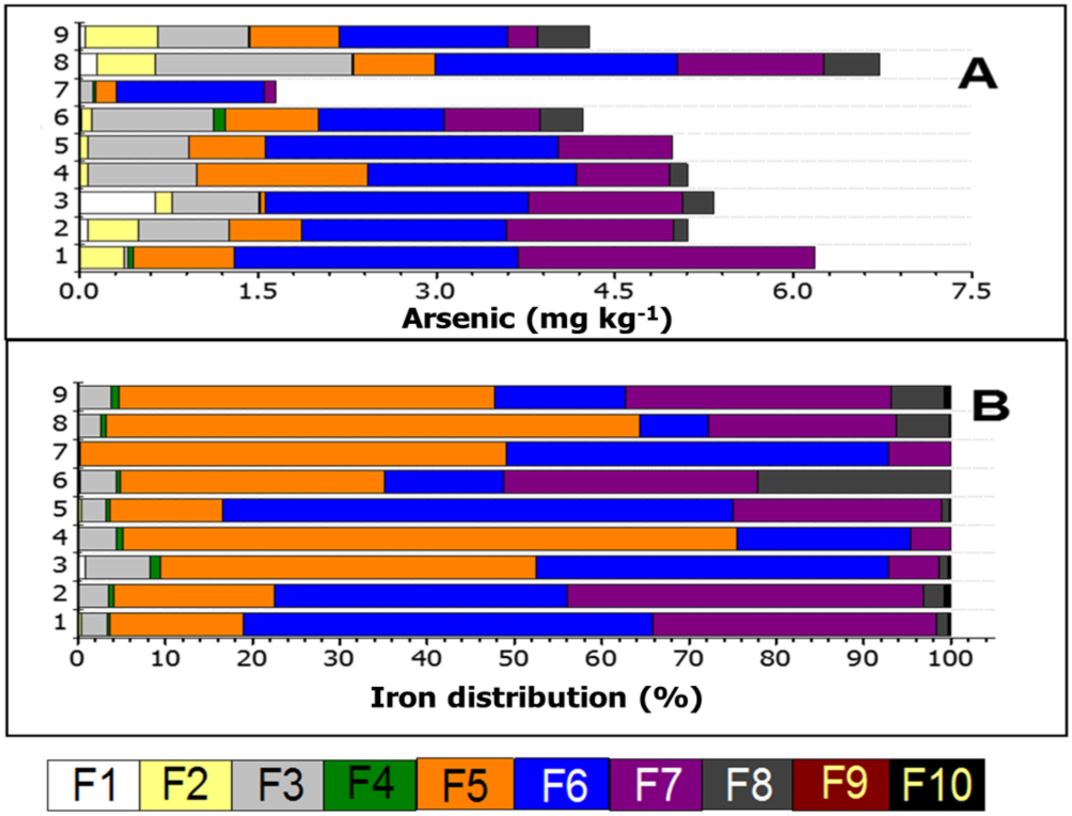

Fig. S2. Distribution of **(A)** As and **(B)** Fe in different sediment solid phases of the selected low As sediments (sample 1-9; As <7 mg kg^{-1}). Sequential extraction protocol (SEP, Javed et al., 2013) was used to determine the As and Fe fractionation in sediments. Arsenic and Fe concentrations were determined in the same aliquot of the each extractants used in SEP. Legends are applicable for both panels and represent different fractions: F1, water soluble metals; F2, exchangeable metals; F3, specifically adsorbed metals; F4, metals bound in carbonates; F5, metals coprecipitated with amorphous Fe, Al and Mn oxyhydroxides; F6, metals coprecipitated with crystalline Fe, Al and Mn oxyhydroxides; F7, metals associated with their oxides and silicate clays; F8, metals coprecipitated with pyrite and orpiment; F9, metals associated with organic matter and recalcitrant sulfides; and F10, residual metals.

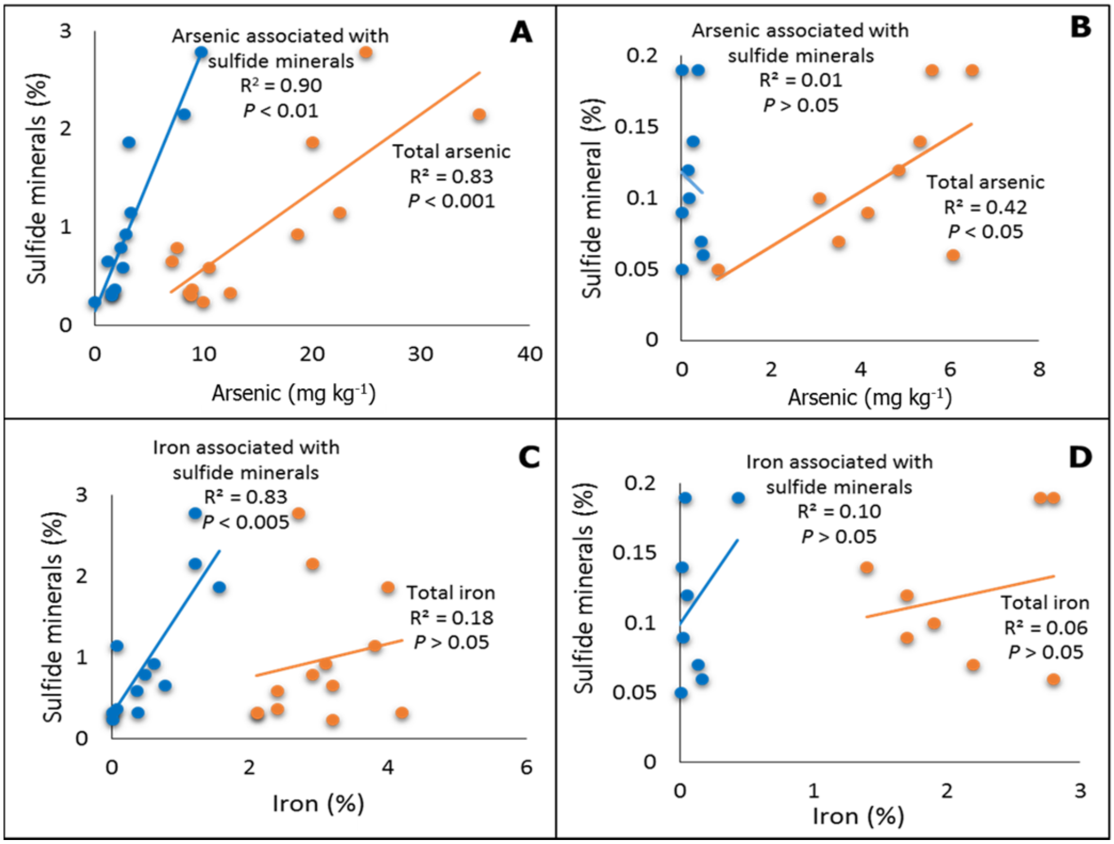

Fig. S3. Relationship of As and Fe with sulfide minerals in sediments. Association of sulfide minerals with As bound in sulfide minerals (F8 of As sequential extraction) and total As in (**A**) high and (**B**) low As sediments; and with Fe bound with sulfide minerals (F8) and total Fe in (**C**) high and (**D**) low As sediments. Arsenic bound in sulfide minerals and total As in high As sediments were highly correlated with sulfide minerals of the sediments, but in low As sediments total As showed some correlation with sulfide minerals but we did not find much As bound in sulfide minerals. Total Fe does not show good correlation with sulfide minerals in both low and high As sediments, but in high As sediments high correlation was found between sulfide minerals and Fe bound in the sulfide minerals compared to low As sediments. The results suggest that in high As sediments Fe might be present as Fe sulfide mineral but in low As samples Fe may be in the form of oxides.

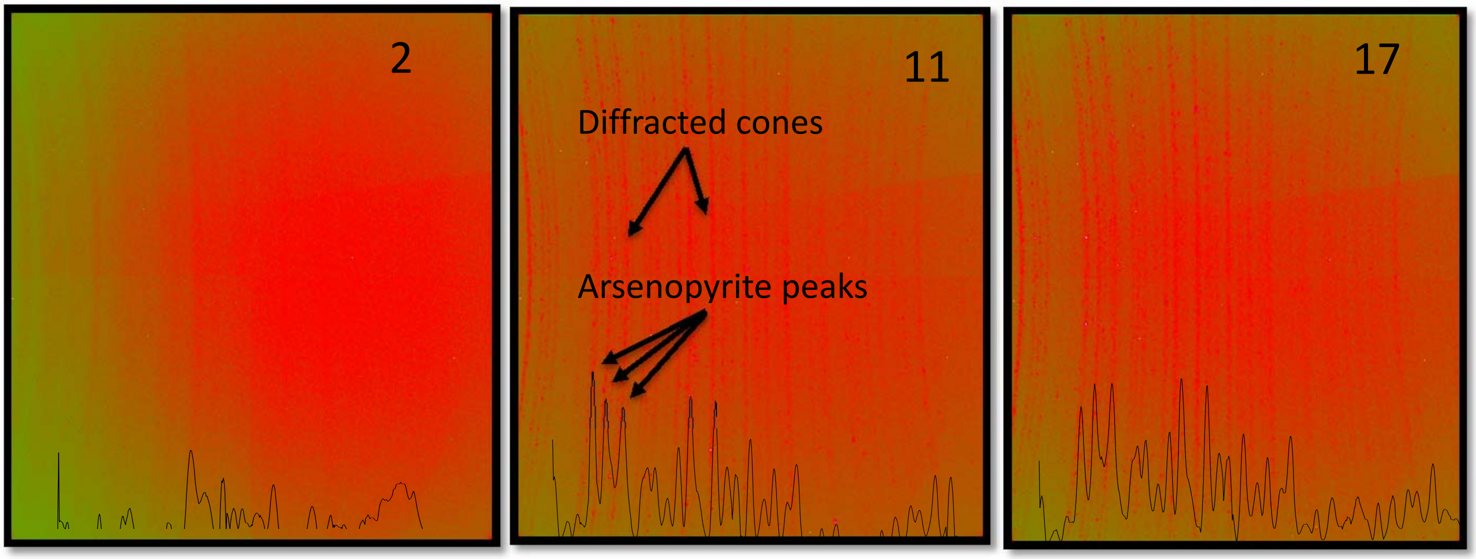

Fig. S4. Determination of arsenopyrite minerals in the selected high As (sample 11; 24.9±4.2 mg kg^{-1} As and 17; 22.5±2.1 mg kg^{-1} As) and low As sediments (sample 2; 4.9±0.7 mg kg^{-1} As) using µXRD. General Area Diffraction Detector System (GADDS) images of sediments show diffraction cones. Diffractogrames are also shown on the images by the integration of cones pattern. Sediment 2 is a low As sediment where we could not find arsenopyrite peaks using high energy synchrotron radiation at ~11.867 KeV, whereas in sediments 11 and 17 clear arsenopyrite peaks were detected.

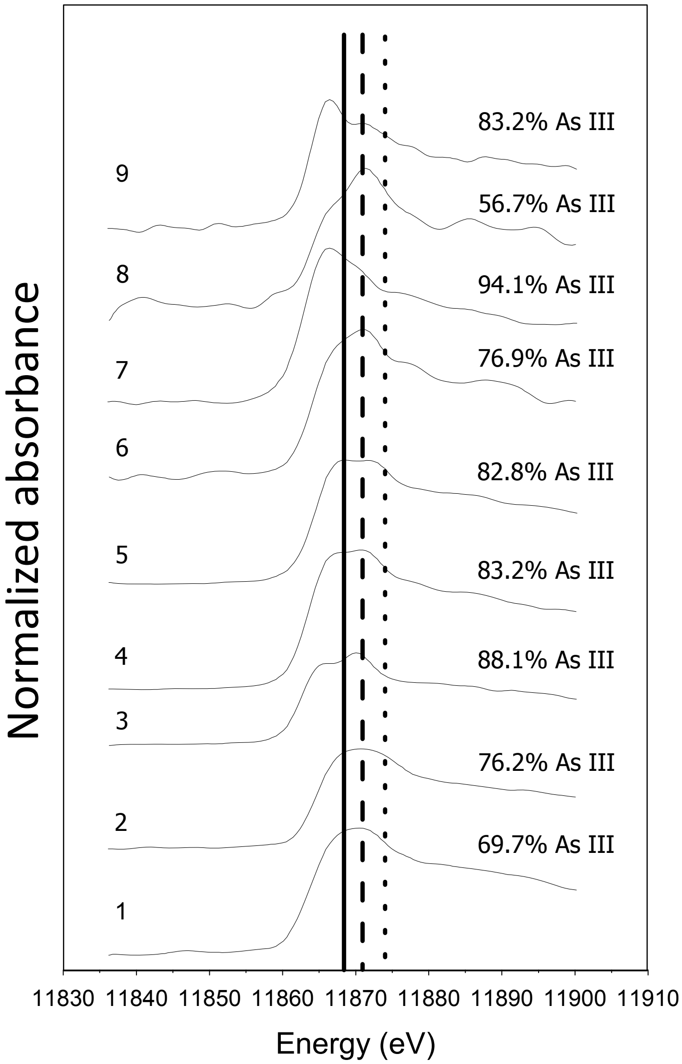

Fig. S5. Determination of dominant oxidation state of As using As K-edge XANES spectroscopy in the selected low As sediments (sample 1-9; <7 mg kg^{-1} As). Solid (–), dashed (---) and dotted (…) lines drawn at 11868 eV, 11870.7 eV and 11874 eV represent the position of white lines of As^{III}-S, As^{III}-O and As^{V}-O, respectively. Liner combination fit (LCF) results show that arsenite (As^{III}) is the most dominant As form in the sediments as shown by the proportion of As^{III} beside each spectrum. Only that oxidation state of As is shown in the spectrum that was present >50% in the sediment. Detail of the LCF analysis is provided in Table S2.

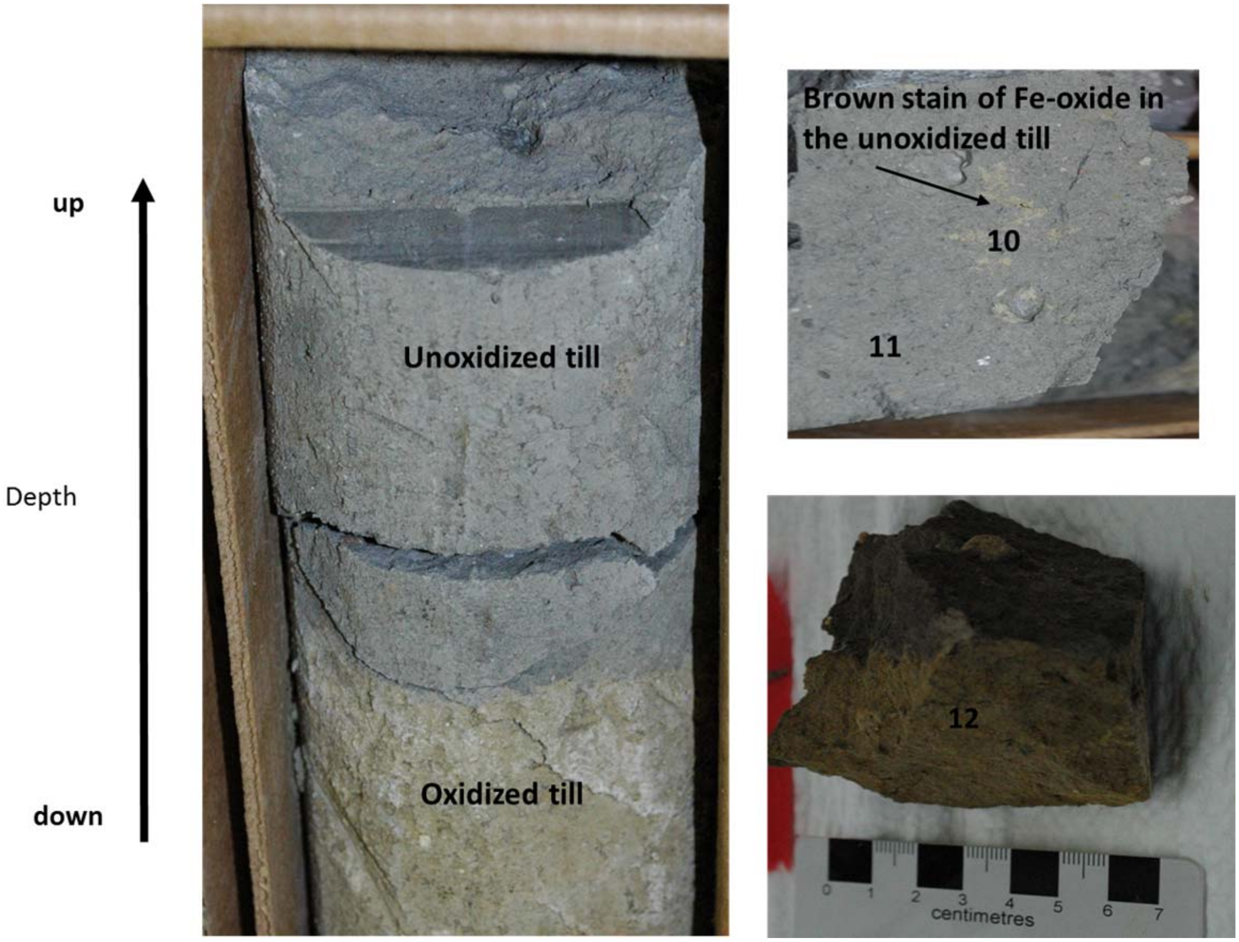

Fig. S6. Photos of sediments taken from core WEPA99-1 at 62 m depth from surface which show oxidized till underlying unoxidized till. Subsamples of Fe oxides within the unoxidized till were also taken for As analysis. Different numbers correspond to the sample numbers shown in Fig 1.